

Birla Central Library

PILANI (Jaipur State)

Engg College Branch

Class No :- 624.6

Book No :- H452 R

Accession No :- 32115

THE RIGID-FRAME BRIDGE



Frontispiece

EAST THIRD STREET BRIDGE—MT. VERNON.
Hutchinson River Parkway—Westchester County Park System.

THE RIGID-FRAME BRIDGE

BY

ARTHUR G. HAYDEN, M.Am.Soc.C.E.

Consulting Civil Engineer

Formerly Designing Engineer, Westchester County Park Commission

SECOND EDITION

NEW YORK

JOHN WILEY & SONS, INC.

LONDON: CHAPMAN & HALL, LIMITED

1940

COPYRIGHT, 1931, 1940

BY

ARTHUR G. HAYDEN

All Rights Reserved

*This book or any part thereof must not
be reproduced in any form without
the written permission of the publisher.*

PRINTED IN U. S. A.

PRESS OF
BRAUNWORTH & CO., INC.
BUILDERS OF BOOKS
BRIDGEPORT CONN.

THIS BOOK IS DEDICATED TO

CHARLES M. SPOFFORD

HAYWARD PROFESSOR OF CIVIL ENGINEERING

MASSACHUSETTS INSTITUTE OF TECHNOLOGY

MY INSTRUCTOR AND FRIEND

PREFACE TO SECOND EDITION

THE method of analysis used in the first edition of this book has been retained in the revised edition, although several other methods applying to rigid-frame bridges have been brought forward in the past few years. All were given fair trial in the office of the Westchester County Park Commission when the author was in charge of the design division, and the consensus of opinion of the designers was that the process explained in this book is simpler, more flexible, and, for the type of structure under consideration, at least as rapid as any other, particularly if the suggestions made at the end of Chapter IV are followed. Furthermore, the process is just as susceptible of abbreviation by a designer who has had experience with it and developed good judgment as is any other.

The moment-distribution method, incomparable for the analysis of frames composed of many members, each of constant moment of inertia, is applicable to the structures illustrated in this book only with the aid of diagrams from which fixed-end moments for members of various shapes must be obtained preliminary to analysis. If independent calculation of the fixed-end moments for members of variable section not covered by the diagrams is necessary, more work is involved by the moment-distribution method.

A convention of algebraic signs is more clearly explained in the new edition than in the old.

Calculations for the double-span frame bridge have been shortened by selecting a different "transformed system" to begin with. At the end of Chapter IX, recommendations are made with respect to the design of rigid-frame bridges restrained at the footings.

A simpler and apparently a more logical method for proportioning the steel reinforcement in a skewed arch or frame bridge is explained and used in the new edition.

Recommendations are made in Chapter X relative to the design of rigid-frame bridges of small skew.

A procedure is outlined in Chapter X for designing double-span skew arch or frame bridges.

Secondary effects, such as shrinkage, plastic yield, and side-sway, as elements of design, are discussed in Chapter XI.

Some important tests and research work relating directly to rigid-frame bridges have recently been carried out. Professor Harold E. Wessman, formerly of the University of Illinois, now of New York University, has re-edited the Chapter on research to cover recent developments.

It was not deemed necessary to change the tabulated calculations that were carried over from the first edition so as to conform to the current specifications of the American Association of State Highway Officials. The specifications followed in the book are given in the Appendix, but the designer of a new bridge should follow current practice. For this purpose a diagram for proportioning steel reinforcement, based upon a value of $n = 10$, is given in this book, although the calculations for reinforcement shown in the book are based upon the diagram for $n = 15$.

A number of errors made in the calculations shown in the old edition have been corrected in the new.

ARTHUR G. HAYDEN

June, 1940

INTRODUCTION TO FIRST EDITION

THIS book treats of the application of rigid-frame construction to short-span reinforced-concrete and structural steel bridges. The building of the magnificent system of parkways in Westchester County, leading from New York City, demanded the construction of many short-span bridges up to 120 ft., over and under intersecting highways and over numerous streams. The rigid-frame type of bridge has been developed to a high degree of perfection to meet the conditions imposed by restricted headroom between intersecting roads, and its economy and extreme adaptability to architectural expression as compared with ordinary types of construction have been completely demonstrated.

The theory of design of this type of indeterminate structure is fully explained in this volume, although it involves principles that are not new. The method of presentation of these principles is, however, so simplified and illustrated by examples that designers in Mr. Hayden's office have been able to grasp their meaning and apply them without having had previous training in higher structural analysis. Higher mathematics and the calculus have been excluded from the argument. Few authors seem to recognize the fact that, in the mathematical line, a knowledge of simple arithmetic, proportion and the solution of algebraic equations is all that is necessary for a comprehension of indeterminate structural analysis. Mr. Hayden has also included in this volume the results of his six years' experience in the design of rigid-frame bridges in order to meet the demand of many engineers and state highway officials for more complete information.

The rigid-frame bridge is not an offshoot. It has its proper place in the scheme of structural engineering practice and is in the direct line of modern structural development; hence the timeliness of the present volume. In this respect an editorial in *Engineering News-Record*, April 29, 1926, says in part:

In recent years structural engineering practice has turned unmistakably toward fuller use of the continuous form of structure. . . . One phase of this departure from precedent is represented in the adaptation of continuous construction to concrete bridges in Westchester County, with results so impressive in increased efficiency and esthetic range as to forecast an important influence on future short-span practice. . . . The planning of these bridges is an important contribution to the present stage of development and directs attention to the fact that many structures are inherently integral from footing to hand rail, and that no great gain is realized from dissecting it into the elements of abutment and span. The gain in economy, simplicity, and freedom from many common bridge troubles that can be realized by planning the structure as an integral unit, is brought clearly into view. . . . No less stimulating are the esthetic phases of the subject; for the continuity of the structure necessarily demands also a representation of this continuity in the external aspect and involves abandoning the simple form of arch, girder, abutment and wing wall. In this particular it is evident that extensive possibilities lie before us. . . . The proven possibilities and advantages of the continuous type are sufficiently important to claim its consideration for the many structures that will have to be built in the years immediately ahead.

The advantages of rigid-frame construction are, however, not limited to bridges. The beauty of structural form that has been realized in these structures can be extended to many other applications. Large areas for industrial buildings, hangars, etc., can be roofed with economy by the use of indeterminate portals of reinforced concrete or steel as the main structural element; the omission of trusses adding beauty to the structure, improving lighting, and eliminating waste space. Great opportunities lie ahead in this direction and undoubtedly this volume will facilitate such development. G. A. HOOL

CONTENTS

CHAPTER	PAGE
I. PRINCIPLE OF THE RIGID-FRAME BRIDGE..... Inherent Economy—Incidental Economies—Economic Limits.	I
II. INDETERMINACY..... Degrees of Indeterminacy—Fundamentals of Indeterminate Analysis.	5
III. THEORY OF INDETERMINATE ANALYSIS..... Symmetrical Two-Hinged Arch—Symmetrical Single-Span Frame Bridge, Fixed Ends—Unsymmetrical Single-Span Frame Bridge, Free Ends.	10
IV. CALCULATIONS..... Convention of Algebraic Signs—Denomination of Units of Calculation—Free-End Conditions—Restraint at Footings—Effects of Earth Pressure—Selection of Coordinate System—Moments of Inertia—Division of Axis—Influence Load—Proportioning Steel Reinforcement—Adjustment of Calculations.	33
V. CALCULATIONS FOR SYMMETRICAL SINGLE-SPAN CONCRETE FRAME BRIDGE—FREE-END CONDITIONS.....	45
VI. CALCULATIONS FOR SYMMETRICAL SINGLE-SPAN CONCRETE FRAME BRIDGE—FIXED-END CONDITIONS.....	61
VII. CALCULATIONS FOR UNSYMMETRICAL SINGLE-SPAN CONCRETE-FRAME BRIDGE—FREE-END CONDITIONS.....	75
VIII. CALCULATIONS FOR SYMMETRICAL SINGLE-SPAN STEEL GIRDER FRAME BRIDGE.....	87

CHAPTER	PAGE
IX. THEORY AND DESIGN OF DOUBLE-SPAN FRAME BRIDGE....	107
X. THE THEORY AND DESIGN OF CONCRETE SKEW-FRAME BRIDGE—FREE-END CONDITIONS.....	137
XI. PRACTICAL POINTS ON DESIGN AND CONSTRUCTION.....	183
Design of Rigid-Frame Bridges Restrained at the Foot- ings—Secondary Effects in Design—Proportions for Analysis—Construction Joints—Expansion Joints—An- choring of Stone Arch Facing—Secondary Reinforcement.	
XII. GENERAL NOTES ON RIGID-FRAME BRIDGES.....	197
XIII. DEFORMETER ANALYSIS FOR FRAME BRIDGES OF HIGH INDE- TERMINACY	206
XIV. RESEARCH IN CONNECTION WITH DEVELOPMENT OF DESIGN	212
XV. ARCHITECTURE OF SHORT-SPAN BRIDGES.....	238
APPENDIX. LIVE LOADS* AND UNIT STRESSES.....	279

THE RIGID-FRAME BRIDGE

CHAPTER I

PRINCIPLE OF THE RIGID-FRAME BRIDGE

Figures 1 and 2 illustrate the mechanical principle of this type of structure. These figures are photographs of toy structures loaded with an iron weight; Fig. 1 representing the action of a beam or girder bridge merely supported upon its abutments, and Fig. 2 representing the action of a rigid-frame bridge of one span. The same members were used in both toy structures, but in Fig. 2

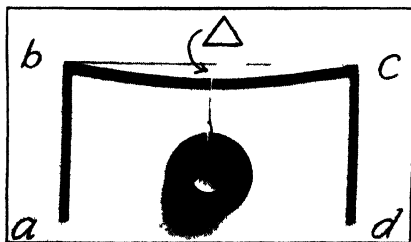


FIG. 1.

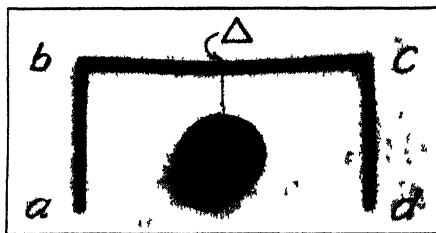


FIG. 2.

they were rigidly connected so that they were continuous from footing to footing.

The difference in action between the two structures is at once apparent. In Fig. 1 there is no flexure in the supporting members *ab* and *cd*; they serve no useful purpose other than to carry the working element *bc* and provide the necessary clearance underneath. In Fig. 2 the flexure in members *ab* and *cd* is distinctly noticeable, showing that they are performing useful work in supporting the load.

Another obvious difference is in the deflection Δ under the load in the two cases. The measured deflection in Fig. 2 is only about 0.4 that in Fig. 1.

Inherent Economy.—It is an engineering principle that the work done by a structure in supporting a load is measured by half the product of the load and the distance through which it moves after being placed upon the structure. Thus we see that in Fig. 2 all three members acting together have to perform much less work than the single member bc in Fig. 1.

In an actual rigid-frame bridge the members are not all of uniform width as in the toy structure, but the material is more efficiently disposed. Figure 28 shows the typical longitudinal section of a reinforced-concrete frame bridge requiring only about 60 per cent of the material which would be required for a constant-section frame; that is, one having members of uniform section. As a matter of fact, a constant section frame would be impractical for a bridge of much less span than this.

Incidental Economies.—The intrinsic economy of the rigid-frame construction is evident from the foregoing discussion. Figures 3 and 4 illustrate the saving in the

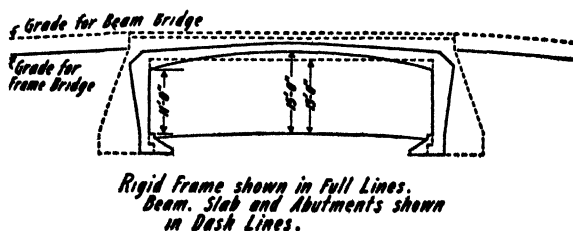


FIG. 3.

approaches permitted by reason of the slender proportions of the structure. In Fig. 3 a reinforced-concrete frame bridge and reinforced-concrete T-beam bridge are shown superimposed and the effect on the approaches of the road over, is illustrated. Figure 4 shows a like comparison for a

frame bridge and a fixed arch. The fixed arch requires a certain minimum rise in the arch rib proper in order to meet temperature stress requirements, whereas the top of the frame bridge may be flat if desired. The fixed arch also requires massive abutments to realize the condition of fixity of the arch rib as assumed in design. The frame bridge thus has the advantage of saving of material in approaches, saving of concrete for the abutments and saving of excavation for the abutments. These economies are not theoretical, but have been demonstrated by a number

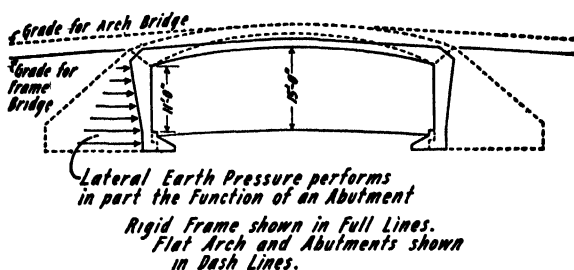


FIG. 4.

of comparative designs and estimates for actual bridges. The highway departments of several states and county commissions who have been aided by the Westchester County Park Commission in the design of this type for their bridges report the same results.

Economic Limits.—Experience with this type of construction has not been sufficient to determine definitely its economic limits. It seems that below 30-ft. span, the reinforced-concrete T-beam floor supported on plain concrete abutments has the advantage in economy. Many concrete rigid-frame bridges have been built in Westchester County, New York, from 35 to 80 ft. in span and steel-frame bridges from 80 to 120 ft. in span. Within these limits the economy of the type has been demonstrated as compared with the concrete arch or T-beam bridge and the steel girder bridge supported on concrete gravity

4 PRINCIPLE OF THE RIGID-FRAME BRIDGE

abutments. The width of bridge, established under-clearances, effect of floor depth upon approaches and other factors enter into the question of economic limits, and their relative effects cannot be determined without considerable study and a critical comparison of the results of experience.

CHAPTER II

INDETERMINACY

Degrees of Indeterminacy.—It is assumed that readers of this book have a working knowledge of the theory of structures and of the principles distinguishing structures which are statically determinate from those which are statically indeterminate. A brief exposition, by means of concrete examples, of what is meant by degrees of indetermination in regard to the external forces is, however, given here as an introduction to the demonstration of the theory of the indeterminate types treated in this book.

The curved beam in Fig. 5, simply supported and fixed in location but free to rotate at a , and resting on rollers at b , carries the inclined load $P = 5$. The load may be resolved into horizontal and vertical components say h.c. = 3 and v.c. = 4. Since end b rests on rollers, the reaction at this point can be only vertical and the h.c. of the load must therefore be taken off at a . Since $\Sigma H = 0$, the horizontal component of the left reaction $H_L = 3$. Taking moments about a , since $\Sigma M = 0$, we have $4 \times 7 - 3 \times 3 - 10V_R = 0$. From which $V_R = 1.9$. Also since $\Sigma V = 0$, we have $V_L = 4 - 1.9 = 2.1$. Observe that the structure was so supported that the two reactions could have not more than three components, H_L and V_L of the left reaction and V_R of the right reaction, due to the application of the load P . These three quantities are calculable as illustrated above, by means of the three static equations, $\Sigma H = 0$, $\Sigma M = 0$ and $\Sigma V = 0$. If the load $P = 5$ were applied vertically, that is, having no horizontal component, H_L would be equal to 0, since $\Sigma H = 0$. Also

since $\Sigma M = 0$, we have by taking moments about a , $V_R = \frac{5 \times 7}{10}$; and since $\Sigma V = 0$, we have $V_L = 5 - 3.5 = 1.5$.

Under the load P the above beam would deform and the end b being on rollers would move slightly to the right. Assume now that the above curved beam were supported as shown in Fig. 6, both ends being fixed in location but not in direction; that is free to rotate at a and b . The absence of rollers at b now permits the development of a horizontal component of the right reaction, as well as the left, due to the application of a load. Thus there will be four components of the two reactions. Since the ends are

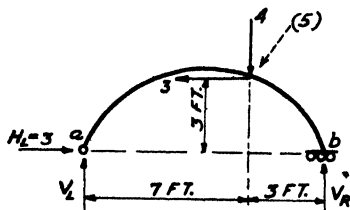


FIG. 5.

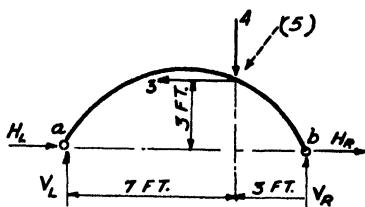


FIG. 6.

hinged, there will be no bending moments at these points and V_L and V_R may be determined by means of the two static equations $\Sigma M = 0$ and $\Sigma V = 0$ as before, because the moments of H_L and H_R about either a or b are equal to 0 and thus do not affect the values of V_L and V_R . The h.c. (3) of the load will be divided between the two components H_L and H_R of the reactions and, since $\Sigma H = 0$ the *algebraic sum* $H_L + H_R = 3$. But none of the three static equations tells us how the horizontal component of the load is divided between H_L and H_R . The vertical component also develops horizontal thrust. If the applied load is vertical, H_L and H_R must be equal and opposite since $\Sigma H = 0$; but the amount of these equal thrusts is still indeterminate. In any case we have four components of the two reactions and three static equations to solve them. One other equation must be furnished by the theory of

flexure, and the structure, as regards the external forces, is said to be statically indeterminate to the *first* degree.

If the beam is further restrained by being fixed in direction as well as in location at a , and remains fixed in location but not in direction at b (that is, free to rotate at b), there will be five components of reactions developed by the application of a load as shown in Fig. 7. That is, the left reaction is capable of developing a restraining moment M_L as well as direct components H_L and V_L . There being only three static equations, *two* other equations must be furnished by the theory of flexure in order to solve completely for the five reaction components. That is the structure is statically "indeterminate" to the *second* degree. V_L and V_R cannot now be calculated independently as

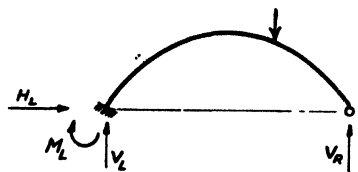


FIG. 7.

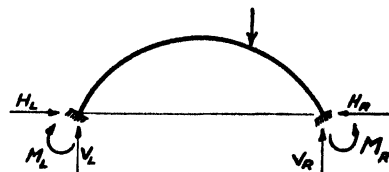


FIG. 8.

before, by taking moments about a and b (through which points the moments of H_L and $H_R = 0$) because the unknown moment M_L must be taken into account in equating moments about either a or b . The five necessary equations must be established and solved simultaneously for the unknowns.

In Fig. 8, both ends being restrained so as to be capable of developing restraining moments under load, six components of the two reactions will be developed by the application of a load—four direct components and two restraining moments as shown. *Three* equations must now be furnished by the theory of flexure, in addition to the *three* static equations, and the structure is said to be "statically indeterminate" to the *third* degree. The structure shown in Fig. 9 is indeterminate to the third degree.

The structure shown in Fig. 10 is indeterminate to the sixth degree.

Fundamentals Underlying Indeterminate Analysis.—The equations additional to the three static equations necessary for the solution of indeterminate structures of the type treated of in this book are established by certain relationships depending upon the character of internal deformation in the structure. This deformation (as in beams, arches, etc.) is caused by the bending moments, shears and direct stresses acting in the structure.

Measurements in such actual structures as well as mathematical calculation show that the bending moments contribute most largely to the deformation. Shear deforma-

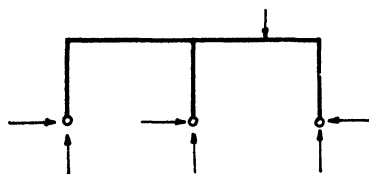


FIG. 9.

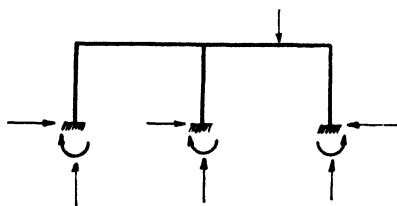


FIG. 10.

tion is small in amount and may usually be neglected entirely as is done in the following work. Deformation due to direct forces (compression or tension) are more important than shear deformation, but are usually counteractive, tending to relieve resultant stresses. In the development of equations it is simpler to consider only the deformations due to bending moments, and if desired to make a final correction, for the direct stress deformations. In arch analysis this correction is made as "rib-shortening" and is analogous to the calculation of stress due to temperature fall, as will be illustrated.

Involved in the calculations of stress deformation are quantities which are a measure of the elastic properties of the structure, all containing values for moment of inertia. In such cases the moments of inertia of the entire cross-

section are used although the unit stresses are finally calculated on the occasional "cracked section," neglecting tension in the concrete. This is for the reason that deflection measurements on structures show that the deflections are controlled more by the intact sections where tension in the concrete exists than by the sections of infinitesimal length where, in proportioning the reinforcement, tension in the concrete is assumed to be entirely destroyed up to the neutral axis.

CHAPTER III

THEORY OF INDETERMINATE ANALYSIS

The methods of design for the arch-like structures treated in this book depend upon a few fundamental laws of flexure which are illustrated in the pages immediately following by a few simple examples in beam deflection; the homogeneous steel beam being assumed in this part of the demonstration for the sake of simplicity. A value of modulus of elasticity (E) equal to 30,000,000 is used in such calculations.

In the figures illustrating deflections due to the elastic deformation of a very small interval (s) of the axis of the beam, arch rib, etc., the effects are necessarily very much exaggerated. In the actual structure, such deformations and the deflections due to them are very small relative to the dimensions of the structure. Such quantities as y will then be practically the same whether measured from the axis of the structure in its stressed or in its unstressed position. Likewise the circular functions, arc, sine and tangent, of the very small angles (θ) under consideration, are all practically the same, although there is an apparent small difference in the exaggerated figures.

Assume a very small length s of a beam originally straight as indicated in Fig. 11. After strain due to flexure alone, the change in length of a fiber distant c from the neutral axis will be (in circular measure): $s + c\Delta\theta - s = c\Delta\theta$, $\Delta\theta$ being the measure of the change in direction of the tangents at the two ends of s . The strain (change in length) of this fiber may also be expressed as $\frac{Mcs}{EI}$ in which

$\frac{Mc}{I}$ is the stress on the fiber, due to the moment M of all external forces acting on the beam, as determined by the well-known beam formula. Comparing the two equations above, $\Delta\theta = \frac{Ms}{EI}$. The change in direction of the tangent between any two points will be the sum of the small changes for all the small lengths s between the points considered, or $\sum \frac{Ms}{EI}$.

Assume next a small length s of the neutral axis of a beam originally curved and subtending an angle θ before flexure and θ' after flexure (Fig. 12). The change in length

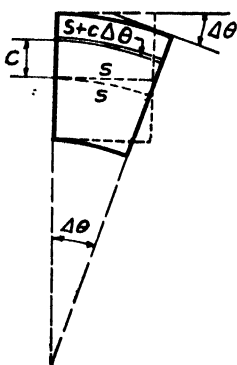


FIG. 11.

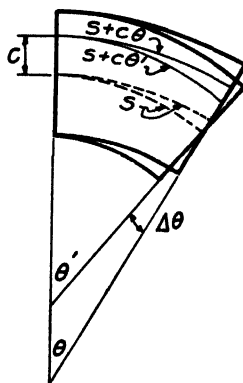


FIG. 12.

of a fiber distant c from the neutral axis (due to flexure alone) will then be $(s + c\theta') - (s + c\theta) = c\Delta\theta$. The strain (change in length) of this fiber may also be expressed as $\frac{f(s + c\theta)}{E}$ in which f is the *unit* stress on this fiber due to the external moment M on the section. We then have $c\Delta\theta = \frac{f(s + c\theta)}{E}$ from which $f = \frac{c\Delta\theta E}{s + c\theta}$. If a = the cross-sectional area of this fiber, the moment of its stress about the neutral axis $= fac = \frac{ac^2\Delta\theta E}{s + c\theta}$. Summing over the entire

cross-section

$$M = \Sigma fac = \frac{\Sigma ac^2 E \Delta \theta}{s + c \theta} = \frac{IE \Delta \theta}{s + c \theta}$$

from which

$$\Delta \theta = \frac{M(s + c \theta)}{EI}.$$

For the curvature occurring in ordinary arches, $s + c \theta$ may be assumed equal to s . Hence

$$\Delta \theta = \frac{Ms}{EI},$$

approximately. Summing over any given length of the axis the change in direction of the tangents at the ends of such length

$$\Sigma \Delta \theta = \theta = \Sigma \frac{Ms}{EI}.$$

Figure 13 represents a straight cantilever beam under flexure. Assume origin of coordinates as shown, that is,

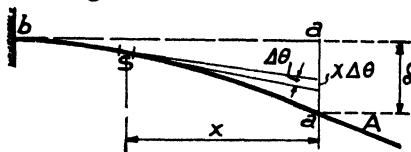


FIG. 13.

at the point a whose displacements are to be determined. The change in angle between the tangents at the ends of

any small division s of the axis due to flexure is $\Delta \theta = \frac{Ms}{EI}$,

in which M is the bending moment, on the particular division considered, due to the external loads. The total angular change between any two points is the sum of effects of all the small divisions between the points considered that

is, $\theta = \Sigma \frac{Ms}{EI}$. If the points considered are a and b , the sum-

mations will be for the divisions between these points;

that is, $\theta = \Sigma \frac{Ms}{EI}$. The vertical displacement at a con-

tributed by the flexure in s is, in circular measure, $x\Delta\theta = \frac{xMs}{EI}$. The total displacement of a from a line perpendicular to the support at $b = \sum_a^b x\Delta\theta = \sum_a^b \frac{Mxs}{EI}$, the summations being for the divisions between a and b .

Note that the quantity x is an expression for moment on any division s , due to unit load at a , that is, at the point whose displacements are desired, the unit load acting in the direction of the desired displacement. The expression for the displacement δ_a may therefore be written $\sum \frac{MM_{as}}{EI}$. If the origin of coordinates had been taken at the support b instead of at a , the expression for the vertical displacement δ_a would be $\sum_a^b \frac{M(d-x)s}{EI}$, in which d is distance between a and b . In this case, too, $(d-x)$ would be an expression for moment on s due to unit load at a , and we would have as before

$$\delta_a = \sum_a^b \frac{MM_{as}}{EI}.$$

This equation is an expression of Maxwell-Mohr's Theorem.

In the numerical example following, the total deflection of point a , from a line perpendicular to the support at b , is calculated.

The beam is assumed to be homogeneous, that is E (modulus of elasticity) is the same for all divisions, s . Consequently quantities for $\frac{Ms}{I}$ and $\frac{Mxs}{I}$ may be tabulated for the several divisions s and the summations multiplied by $\frac{1}{E}$ instead of finding the summation of the several quantities $\frac{Ms}{EI}$ and $\frac{Mxs}{EI}$; for the reason that

$$\left(\frac{a}{E} + \frac{b}{E} + \frac{c}{E} + \dots\right) = \frac{1}{E}(a + b + c + \dots).$$

That is, if E is constant,

$$\sum \frac{M_s}{EI} = \frac{1}{E} \sum \frac{M_s}{I} \quad \text{and} \quad \sum \frac{M_{xs}}{EI} = \frac{1}{E} \sum \frac{M_{xs}}{I}.$$

In this example the divisions s were also arbitrarily assumed constant, that is, all 12 in. long, and this quantity might have been treated as was the quantity E . It was retained

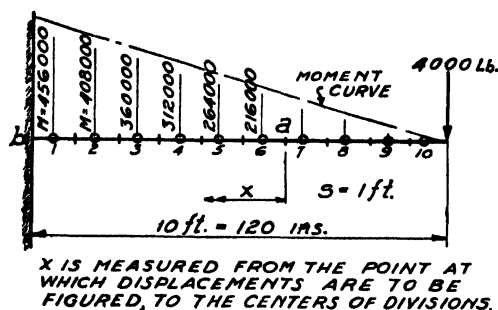


FIG. 14.

in the tabulation, however, to illustrate the process when it is convenient to vary the length of divisions.

Illustrative Example 1.—Find the deflection at a of the cantilever beam shown in Fig. 14 under the loads indicated.

Point	M Inch-Pounds	s Inches	I	x Inches	$\frac{M_s}{I}$	$\frac{M_{xs}}{I}$	$\frac{M}{EI}$
1	456,000	12	200	66	27,400	1,810,000	0.0000760
2	408,000	12	190	54	25,800	1,393,000	0.0000715
3	360,000	12	180	42	24,000	1,008,000	0.0000660
4	312,000	12	170	30	22,000	660,000	0.0000611
5	264,000	12	160	18	19,800	357,000	0.0000550
6	216,000	12	150	6	17,300	104,000	0.0000480
Σ					136,300	5,332,000	

For a steel beam E (modulus of elasticity) = 30,000,000.

Approximate angular change from support to point a

$$= \sum \frac{M_s}{EI} = \frac{1}{E} \sum \frac{M_s}{I} = \frac{136,300}{30,000,000} = 0.0045 \text{ radian.}$$

Approximate deflection at a

$$= \sum \frac{Mxs}{EI} = \frac{1}{E} \sum \frac{Mxs}{I} = \frac{5,332,000}{30,000,000} = 0.18 \text{ inch.}$$

The smaller the divisions the closer will be the approximation. In this problem the results are accurate to a small fraction of 1 per cent.

Figure 15 shows the quantities $\frac{M}{EI}$ plotted to scale. The process fol-

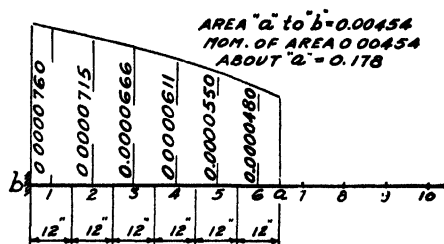


FIG. 15.

lowed in the above problem shows that the angular change between any two points will be the area of the $\frac{M}{EI}$ diagram, between such points, plotted to scale; that is $\sum \frac{Ms}{EI}$. Likewise the deflection will be the moment of the portion of the $\frac{M}{EI}$ diagram between the points considered, about the point of displacement.

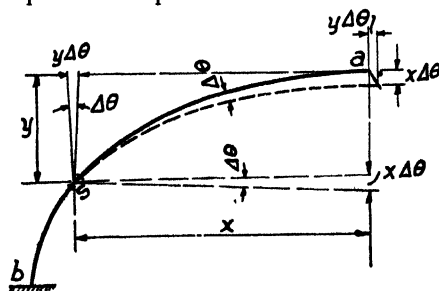


FIG. 16.

The Curved Cantilever Beam (Fig. 16).—The angular change contributed by the flexure of any division s of the axis of a member may be measured by the change in angle

between the tangents at the ends of the division or between the radii or between any lines, straight or broken, attached to the ends of the divisions. Making use of this geometric principle, the deflection of a point in any desired direction may be readily calculated as shown. Assume, as before, origin of coordinates at the point a whose calculated displacements are desired. From the figure it is seen that the vertical displacement of point a contributed by the flexure in s is $x\Delta\theta = \frac{Mxs}{EI}$ and the horizontal displacement is $y\Delta\theta = \frac{Mys}{EI}$, in which M is the bending moment on division s due to the loads acting on the beam. Summing the effects of all points on the axis (from support to a) the total vertical displacement $= \sum \frac{Mxs}{EI}$ and total horizontal displacement is $\sum \frac{Mys}{EI}$. Likewise the total angular change (from support to a) is $\sum \frac{Ms}{EI}$. Note that in the expressions $\frac{Mxs}{EI}$, above (for straight or curved cantilever beams) x is the moment on the several divisions s due to *vertical unit load placed at the point where vertical displacements are to be measured*. Whence the expression for vertical deflection may be written $\sum \frac{MM_s}{EI}$, in which M_s is the secondary moment on the several divisions s due to unit vertical load at a . Likewise for horizontal deflection at a in the curved beam, $\sum \frac{Mys}{EI}$ may be written $\sum \frac{MM_s}{EI}$, in which M_s is the secondary moment on the several divisions s due to unit horizontal load at a . In general the secondary moments are calculated in the several divisions due to a unit load acting at the point and in the direction for which the desired deflections are to be calculated.

If the coordinate system had been selected with origin at b , x and y then being measured from b , the expressions for total vertical and horizontal deflections would then be respectively $\sum \frac{M(l-x)s}{EI}$ and $\sum \frac{M(h-y)s}{EI}$. Here again $(l-x)$ and $(h-y)$ would be expressions for moments due respectively to unit vertical load and unit horizontal load acting at a ; and we have, as before, total vertical deflection at $a = \sum \frac{MM_v s}{EI}$ and total horizontal deflection $= \sum \frac{MM_h s}{EI}$, with the same definitions for M_v and M_h .

The last forms of the equations for deflection are the general forms for deflection whatever the coordinate system may be.

Simple Span Beam (Fig. 17).—For simplicity of demonstration the flexure contributed by a small length s only is

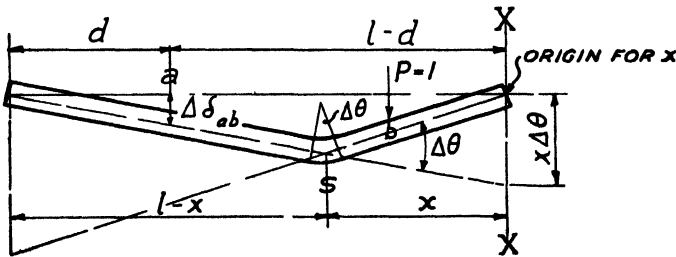


FIG. 17.

shown to exaggerated scale in the figure. It will be convenient in what follows to find the constants for a load unity (say 1 lb.). Let δ_{ab} indicate deflection at a due to unit load at b and $\Delta\delta_{ab}$ indicate the increment of deflection contributed by s . By geometry $\Delta\delta_{ab} = \frac{x\Delta\theta d}{l}$. From what

has preceded $\Delta\theta = M_b \frac{s}{EI}$ in which M_b = moment on s due to unit load at b . Then $\Delta\delta_{ab} = \frac{xd}{l} M_b \frac{s}{EI}$. Summing the

effects of flexure on all elements s , we have

$$\Sigma \Delta \delta_{ab} = \delta_{ab} = \Sigma M_b \frac{s}{EI} \cdot \frac{xd}{l}.$$

For load P greater than unity we have of course

$$P \delta_{ab} = P \Sigma M_b \frac{s}{EI} \cdot \frac{xd}{l}.$$

Note now that the expression $\frac{xd}{l}$ is the same as for moment on s due to unit load at $a = M_a$. The equation for deflection may then be expressed as

$$P \delta_{ab} = P \Sigma \frac{M_b M_a s}{EI}.$$

It is obvious from the form of this equation that

$$P \delta_{ab} = P \Sigma M_a M_b \frac{s}{EI} = P \delta_{ba}.$$

This is Maxwell's Theorem of Reciprocal Displacements.

If the origin of the coordinate system had been taken as in the other examples, through the point for which the

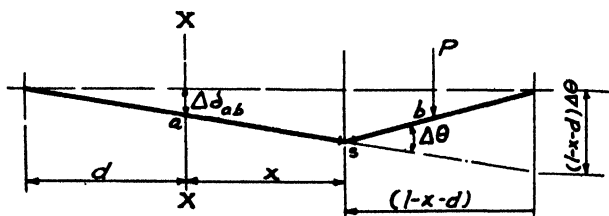


FIG. 18.

calculated deflection is desired, as shown in Fig. 18, the expression for $\Delta \delta_{ab}$ would be

$$\frac{d(l-x-d)\Delta\theta}{l} = \frac{d(l-x-d)PM_b \frac{s}{EI}}{l},$$

and total deflection

$$= P \Sigma \frac{d(l-x-d)M_b \frac{s}{EI}}{l}$$

Again note that the expression $\frac{d(l-x-d)}{l}$ is the moment on division s due to unit load at a ; whence

$$P\delta_{ab} = P \sum M_b M_a \frac{s}{EI}$$

as before. The last form of the equation is a general form of equation for deflection, whatever the coordinate system may be.

Illustrative Example 2.—Assume a simple span beam loaded as shown in Fig. 19. Find deflection at a . Moments of inertia at centers

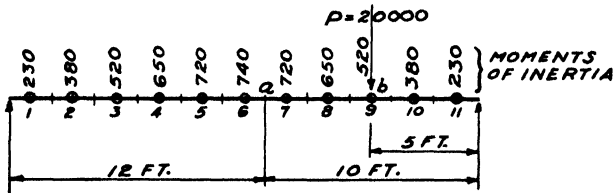


FIG. 19.

of 2-ft. divisions are indicated. In the table below, columns 1 to 5 inclusive only are involved in this calculation. Constants are first found for *unit* load at b , which are then multiplied by $P = 20,000$. $s = 24$ in.

Point	Inch Pounds		$\frac{s}{I}$	$M_a M_b \frac{s}{I}$	$M_a M_a \frac{s}{I}$
	M_a	M_b			
1	5.4	2.7	0.1042	1.5	3.0
2	16.4	8.2	0.0632	8.5	17.0
3	27.3	13.6	0.0461	17.1	34.3
4	38.2	19.1	0.0369	26.9	53.8
5	49.1	24.5	0.0333	40.1	80.4
6	60.0	30.0	0.0324	58.3	116.6
7	58.9	35.5	0.0333	69.6	115.5
8	45.8	40.9	0.0369	69.2	77.4
9	32.7	46.4	0.0461	70.0	49.3
10	19.6	27.8	0.0632	34.4	24.3
11	6.5	9.3	0.1042	6.3	4.4
Σ				401.9	576.0

$$P\delta_{ab} = \frac{P}{E} \sum M_a M_b \frac{s}{I} = \frac{20,000}{30,000,000} \times 402 = 0.27 \text{ inch}$$

Illustrative Example 3.—For the same beam, find deflection at a for upward load R at a as shown in Fig. 20.

$$R\delta_{aa} = \frac{R}{E} \Sigma M_a M_a \frac{s}{I}$$

$\Sigma M_a M_a$ is calculated in column 6 of table above. Substituting values,

$$R\delta_{aa} = \frac{R}{30,000,000} \times 576 = \frac{R}{52,000}$$

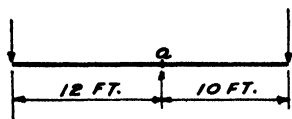


FIG. 20.

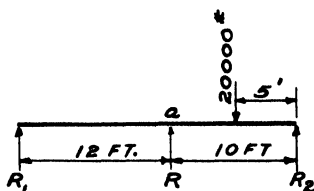


FIG. 21.

Illustrative Example 4.—Find reaction R for continuous beam over two spans of 12 ft. and 10 ft. loaded as shown in Fig. 21 and having the same moments of inertia as in preceding example. The deflection at point a of the simple span beam was calculated above separately for the 20,000-lb. load at b and for the upward load R at point a . For the continuous beam of this example the deflections at point a due to the 20,000-lb. load and that due to the reaction R must be equal and opposite. That is,

$$20,000\delta_{ab} - R\delta_{aa} = 0,$$

or

$$0.27 - \frac{R}{52,000} = 0$$

From which

$$R = + 14,000;$$

the + sign indicating that R acts as assumed in the figure.

The value of R may be found more directly, without calculating actual deflections in terms of load and reaction. Since

$$P\delta_{ab} - R\delta_{aa} = 0$$

or

$$\frac{P}{E} \Sigma M_a M_b \frac{s}{I} - \frac{R}{E} \Sigma M_a M_a \frac{s}{I} = 0$$

from which

$$R = \frac{P \Sigma M_a M_b \frac{s}{I}}{\Sigma M_a M_a \frac{s}{I}} = \frac{20,000 \times 402}{576} = 14,000 \text{ lb. } \uparrow$$

Having found the redundant reaction R , the other reactions may be found by the simple rules of statics $\Sigma M = 0$ and $\Sigma V = 0$, as follows:

By moments $20,000 \times 5 - 14,000 \times 10 - 22R_1 = 0$

from which

$$R_1 = \frac{20,000 \times 5 - 14,000 \times 10}{22} = -1800 \text{ lb. } \downarrow$$

By addition

$$R_2 = 20,000 + 1800 - 14,000 = 7800 \text{ lb. } \uparrow$$

SYMMETRICAL TWO-HINGED ARCH

Refer to Fig. 22. Assume a curved beam resting on rollers at one end a and simply supported at the other. Flexure in any small division s of the beam will cause a horizontal displacement at the free end, $y\Delta\theta = \frac{Mys}{EI}$, in which M is the bending moment on the division s due to the external loads neglecting the horizontal thrust H . The total displacement due to flexure in all the divisions s is $\sum \frac{Mys}{EI}$.

Now assume a horizontal thrust applied to the end of the beam sufficient to counteract the horizontal displacement. New moments Hy are introduced acting on the individual divisions; and we have:

Total horizontal displacement due to thrust

$$- \sum y\Delta\theta = \sum \frac{(Hy)y s}{EI} = \sum \frac{Hy^2 s}{EI}$$

The horizontal displacement due to external loads and that due to the thrust being equal and opposite, we have

$$\sum \frac{Mys}{EI} - \sum \frac{Hy^2s}{EI} = 0$$

from which

$$H = \frac{\sum \frac{Mys}{EI}}{\sum \frac{y^2s}{EI}} \quad (1)$$

If E is constant,

$$H = \frac{\sum \frac{Mys}{I}}{\sum \frac{y^2s}{I}} \quad (2)$$

In the equations above, y is also an expression for moment in the several divisions s due to horizontal load unity acting like H ; that is, at the point and in the direction for which the deflection of the unrestrained beam was calculated. Whence the expression for H may be written

$$H = \frac{\sum M M_a^s \bar{I}}{\sum M_a M_a^s \bar{I}}$$

in which M_a is the moment on the several divisions s due to such unit load.

Thrust Due to Change of Span Length.—In equation (1) for H , $\sum \frac{Mys}{EI}$ is an expression for horizontal deflection at a (change of span length) due to the *loads* on the structure before application of the replacement force H . This change of span length is $\sum y \Delta \theta$, or say Δl . The general formula for H may then be written

$$\Delta l = \frac{H}{E} \sum \frac{y^2s}{I} \quad \text{or} \quad H = \frac{E \Delta l}{\sum \frac{y^2s}{I}}$$

in which Δl is the deflection (change of span length) due to any cause whatsoever.

If the supports move *in* a distance Δl they impose upon the structure a positive thrust (that is, acting as shown in Fig. 22) which causes negative moments Hy . If they spread, the effect is opposite and H is negative, acting in

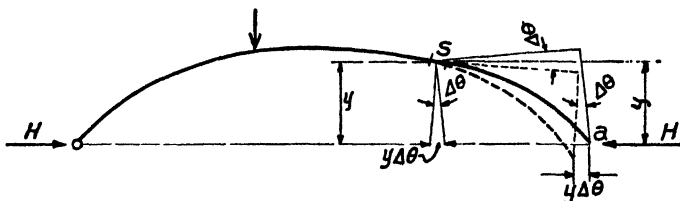


FIG. 22.

the opposite direction to that shown in Fig. 22 and causing positive moments.

Thrust Due to Temperature Change.—

Let c = coefficient of thermal expansion = 0.0000065;

t = rise or fall of temperature in degrees Fahr.;

l = span length;

$\Delta l = ct l$.

$$H = \frac{Ect l}{\sum \frac{y^2 s}{I}}$$

Temperature rise tends to increase the span length. This tendency is resisted at the footings which develops a positive H (acting in the direction assumed in Fig. 22) producing negative moments. Temperature fall produces the opposite effect.

Rib Shortening.— f_c = average direct compression in the concrete of any division, s , of the arch = normal thrust N divided by area of section ($A_c + 15A_s$). Shortening of any division s caused by direct compression = $\frac{f_c s}{E}$.

If Δx = horizontal projection of s , the change of span length

$$\Delta l = \sum \frac{f_c \Delta x}{E}.$$

Hence

$$H = - \frac{\sum f_c \Delta x}{\sum \frac{y^2 s}{I}}.$$

Rib shortening has the same effect as fall in temperature.

The axis divisions may often be assumed constant, with convenience to the calculator. The quantity s may then be placed outside the sign of summation and will cancel out of numerator and denominator of the equations for loads but not for change of span length due to temperature, etc. For constant s the convenient form of the denominators of the equations for H due to change of span length for temperature, etc., is $s \sum \frac{y^2}{I}$, in case summations have been made for $\sum \frac{y^2}{I}$ in dealing with load calculations.

SYMMETRICAL SINGLE-SPAN RIGID-FRAME BRIDGE

Fixed-End Conditions

The structure is indeterminate to the third degree as is the fixed arch shown in Fig. 8.

Refer to the demonstration for the curved cantilever beam and observe that the angular change and horizontal and vertical movements of any point on the beam are geometrical quantities resulting from the flexure in the structure. The deflections may be calculated for any point on the beam or for any point off the beam connected by a real or imaginary rigid arm. In this example, Fig. 23, a symmetrical frame is cut into two equal cantilever sec-

tions, and the unknown reactions due to a load P are assumed to be applied a certain distance z below the crown, as shown in the figure. The reason for this will be clear as we proceed. The origin of the coordinate system is at the assumed point of application of the unknown reactions. The problem is to find the values of the reactions which are alike for the two cantilever sections and which must be such that they will cause the ends of the two cantilevers to coincide as in the joined structure.

The total angular change at point O must be equal for the two cantilever halves, but opposite in direction relative to the two cantilevers; the total horizontal deflection at point O must be equal for the two cantilevers but of opposite sign because one cantilever span is lengthened and the other

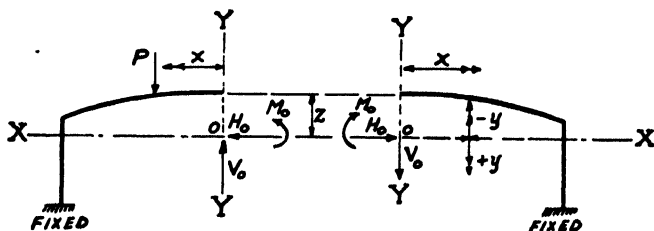


FIG. 23.

shortened by the amount of such deflection; the total vertical deflection of point O must be equal and of the same sign, because either upward or downward for the two halves. M_0 is a bending moment. Moments due to H_0 are $H_0 y$ and moments due to V_0 are $V_0 x$. In the figure an external load P is shown on the left cantilever only, but equations will be derived for loads on both spans, due to which the bending moment on any particular division s of the left half may be expressed as M_L and that on any division s of the right half may be expressed as M_R . In tabulating such moments for substitution in the formulas, the rules for algebraic signs which are explained later on must be observed, in order to arrive at correct results.

Applying the principles already deduced and noting that V_0 produces bending moments of *opposite* sign in the two cantilever halves, we have:

Equating angular changes:

$$\begin{aligned} \sum M_L \frac{s}{EI} + M_0 \sum \frac{s}{EI} + H_0 \sum \frac{ys}{EI} + V_0 \sum \frac{xs}{EI} \\ = - \left[\sum M_R \frac{s}{EI} + M_0 \sum \frac{s}{EI} + H_0 \sum \frac{ys}{EI} - V_0 \sum \frac{xs}{EI} \right] \quad (1) \end{aligned}$$

Equating horizontal deflections:

$$\begin{aligned} \sum M_L \frac{ys}{EI} + M_0 \sum \frac{ys}{EI} + H_0 \sum \frac{y^2s}{EI} + V_0 \sum \frac{xy s}{EI} \\ = - \left[\sum M_R \frac{ys}{EI} + M_0 \sum \frac{ys}{EI} + H_0 \sum \frac{y^2s}{EI} - V_0 \sum \frac{xy s}{EI} \right] \quad (2) \end{aligned}$$

Equating vertical deflections:

$$\begin{aligned} \sum M_L \frac{xs}{EI} + M_0 \sum \frac{xs}{EI} + H_0 \sum \frac{xy s}{EI} + V_0 \sum \frac{x^2s}{EI} \\ = \left[\sum M_R \frac{xs}{EI} + M_0 \sum \frac{xs}{EI} + H_0 \sum \frac{xy s}{EI} - V_0 \sum \frac{x^2s}{EI} \right] \quad (3) \end{aligned}$$

The XX axis of reference is so taken that $\sum \frac{ys}{EI} = 0$.

This will be so when $z = \frac{\sum (z+y)_I^s}{\sum_I^s}$, the process of

determining the value of z being analogous to the process of finding the distance z from the crown to the center of gravity of all the quantities $\frac{s}{I}$. This expedient, by eliminating certain terms in the final working equations, shortens the labor of calculation.

Making all cancellations in equations (1), (2) and (3), and making $\sum \frac{y^s}{EI}$ (but not $\sum M \frac{y^s}{EI}$) equal to zero, we have

$$\sum M_R \frac{s}{EI} + \sum M_L \frac{s}{EI} = -2M_0 \sum \frac{s}{EI} \quad (4)$$

$$\sum M_R \frac{y^s}{EI} + \sum M_L \frac{y^s}{EI} = -2H_0 \sum \frac{y^{2s}}{EI} \quad (5)$$

$$\sum M_R \frac{x^s}{EI} - \sum M_L \frac{x^s}{EI} = 2V_0 \sum \frac{x^{2s}}{EI} \quad (6)$$

If E is constant it may be placed outside the sign of summation and will cancel out of both sides of the above equations. In the numerical example following, s is also made constant and will cancel out. Hence (calling $M_R + M_L = M$) the final equations become:

$$\sum \frac{M}{I} = -2M_0 \sum \frac{1}{I} \quad \text{or} \quad M_0 = -\frac{\sum \frac{M}{I}}{2 \sum \frac{1}{I}} \quad (7)$$

$$\sum \frac{My}{I} = -2H_0 \sum \frac{y^2}{I} \quad \text{or} \quad H_0 = -\frac{\sum \frac{My}{I}}{2 \sum \frac{y^2}{I}} \quad (8)$$

$$\sum \frac{M_R x}{I} - \sum \frac{M_L x}{I} = 2V_0 \sum \frac{x^2}{I}$$

or

$$V_0 = \frac{\sum M_R \frac{x}{I} - \sum M_L \frac{x}{I}}{2 \sum \frac{x^2}{I}} \quad (9)$$

In the above process of derivation note that $\sum \frac{s}{EI}$, $\sum \frac{y^{2s}}{EI}$ and $\sum \frac{x^{2s}}{EI}$ (or for constant E and s , $\sum \frac{1}{I}$, $\sum \frac{y^2}{I}$ and $\sum \frac{x^2}{I}$) were summations for the *half arch*.

Reactions Due to Change of Span Length Δl .—The left-hand members of equations (1), (2) and (3) above are expressions for, respectively, angular change, horizontal deflection and vertical deflection caused by loads on the structure.

In a symmetrical structure, there will be no resultant angular change at O due to straight stretching or compressing of the arch. Hence $0 = -2M_0 \sum \frac{s}{I}$ or $M_0 = 0$.

Likewise there will be no shear at O , that is $V_0 = 0$.

In equation (5) substitute, for the left-hand member, the general expression for horizontal deflection: $+\Delta l$ for increase of span length (stretching the arch) due to any cause whatsoever, and $-\Delta l$ for decrease of span length (compressing the arch) due to any cause whatsoever.

Thus

$$\Delta l = -2H_0 \sum \frac{y^2 s}{EI} \quad \text{or} \quad H_0 = -\frac{E\Delta l}{2 \sum \frac{y^2 s}{I}} \quad \text{for stretching} \quad (10)$$

and

$$H_0 = +\frac{E\Delta l}{2 \sum \frac{y^2 s}{I}} \quad \text{for compressing} \quad (11)$$

If in the calculations for external loads with constant s , summations are made for $\sum \frac{y^2}{I}$ the convenient form for the above equations will be

$$H_0 = \mp \frac{E\Delta l}{2s \sum \frac{y^2}{I}} \quad (12)$$

If the footings spread, H_0 will be negative and act opposite to the direction shown in Fig. 23.

If the footings move in, H_0 will be positive and act as shown in Fig. 23. In the above equations $\sum \frac{y^2 s}{I}$ is the summation for the half arch.

Reactions Due to Temperature Change.—Given

c = coefficient of thermal expansion = 0.0000065;

t = temperature rise or fall in degrees Fahrenheit;

l = span length.

Then

$$\Delta l = c t l$$

The restraint of the footings resists change of span length due to temperature change; hence for a rise in temperature there will be a compressing effect and

$$H_0 = + \frac{E c t l}{2 \sum \frac{y^2 s}{I}} \quad (13)$$

or for constant s ,

$$H_0 = + \frac{E c t l}{2 s \sum \frac{y^2}{I}} \quad (14)$$

For a fall in temperature there will be a stretching effect and

$$H_0 = - \frac{E c t l}{2 \sum \frac{y^2 s}{I}} \quad (15)$$

or for constant s ,

$$H_0 = - \frac{E c t l}{2 s \sum \frac{y^2}{I}} \quad (16)$$

The summation $\sum \frac{y^2 s}{I}$ is for the half arch.

Rib Shortening.— f_c = direct compression due to normal thrust (pounds per square inch on any division s of the arch). Shortening of any division s due to direct compression = $\frac{f_c s}{E}$. If Δx = horizontal projection of s , the change of span length = $\Delta l = \sum \frac{f_c \Delta x}{E}$.

Rib shortening results in a stretching effect.

Hence

$$H_0 = - \frac{\sum f_s \Delta x}{2 \sum \frac{y^2 s}{I}} \quad (17)$$

or for constant s ,

$$H_0 = - \frac{\sum f_s \Delta x}{2s \sum \frac{y^2}{I}} \quad (18)$$

The summation $\sum \frac{y^2 s}{I}$ is for the half arch.

(Rib shortening is neglected in the numerical example.)

In all the formulas for H_0 and V_0 note that for the system of coordinates used (origin at point where deflections are measured for the two cantilever halves) x is an expression for moment M_s on any division s due to unit load acting like V_0 , and y is an expression for moment M_h due to unit load acting like H_0 . The various equations derived above might therefore be expressed as follows:

For external loads

$$M_0 = \frac{\sum \frac{M}{I}}{2 \sum \frac{1}{I}} \quad (19)$$

$$H_0 = \frac{\sum \frac{MM_h}{I}}{2 \sum \frac{M_h^2}{I}} \quad (20)$$

$$V_0 = \frac{\sum \frac{M_R M_s}{I} - \sum \frac{M_L M_s}{I}}{2 \sum \frac{M_s^2}{I}} \quad (21)$$

In the equations for H_0 due to change of span length, temperature change and rib shortening, the denominators may be expressed as $2 \sum \frac{M_v^2}{I}$.

Likewise the fundamental equations for deflection (1), (2) and (3) may be expressed as follows:

$$\begin{aligned} \sum \frac{M_{Ls}}{EI} + M_0 \sum \frac{s}{EI} + H_0 \sum \frac{M_{hs}}{EI} + V_0 \sum \frac{M_{vs}}{EI} \\ = - \sum M_R \frac{s}{EI} - M_0 \sum \frac{s}{EI} - H_0 \sum \frac{M_{hs}}{EI} + V_0 \sum \frac{M_{vs}}{EI} \end{aligned} \quad (22)$$

$$\begin{aligned} \sum \frac{M_L M_{hs}}{EI} + M_0 \sum \frac{M_{hs}}{EI} + H_0 \sum \frac{M_{hs}^2}{EI} + V_0 \sum \frac{M_v M_{hs}}{EI} \\ = - \sum \frac{M_R M_{hs}}{EI} - M_0 \sum \frac{M_{hs}}{EI} - H_0 \sum \frac{M_{hs}^2}{EI} - V_0 \sum \frac{M_h M_{vs}}{EI} \end{aligned} \quad (23)$$

$$\begin{aligned} \sum \frac{M_L M_{vs}}{EI} + M_0 \sum \frac{M_{vs}}{EI} + H_0 \sum \frac{M_v M_{hs}}{EI} + V_0 \sum \frac{M_v^2}{EI} \\ = \sum \frac{M_R M_{vs}}{EI} + M_0 \sum \frac{M_{vs}}{EI} + H_0 \sum \frac{M_v M_{hs}}{EI} - V_0 \sum \frac{M_v^2}{EI} \end{aligned} \quad (24)$$

If a different coordinate system had been selected, the form of all equations would change, including the fundamental equations as expressed in (1), (2) and (3), but excepting the fundamental equations as expressed in (22), (23) and (24). In (1), (2) and (3) x and y would be replaced by other terms containing x and y but these would still be expressions for moments due to unit loads acting like the reaction components whose value it is desired to find, thus resulting in equations expressed as in (22), (23) and (24).

UNSYMMETRICAL SINGLE-SPAN 'RIGID FRAME

Designed for Hinged Conditions at the Base

If the frame is unsymmetrical, as shown in Fig. 24, calculate the simple span moments $\sum \frac{Px(l-x)}{l}$ on the

several divisions s as for the symmetrical structure.

Moments due to the thrust $H \left(= \frac{\sum \frac{My_s}{I}}{\sum \frac{y^2 s}{I}} \right)$ will be Hy ;

y being measured from the centers of divisions, perpendicular to the axis XX . In this case, however, all summations must extend over the full span.

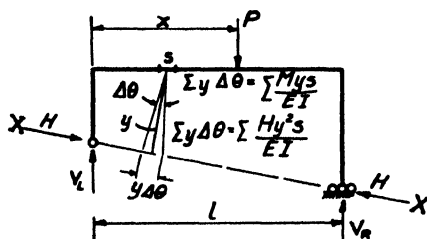


FIG. 24.

An alternative system of calculation is as follows (Fig. 25): Measure y vertically to the XX axis.

$$H = \frac{\sum \frac{My_s}{I}}{\sum \frac{y^2 s}{I}}$$

will act horizontally and the moment on any division s due

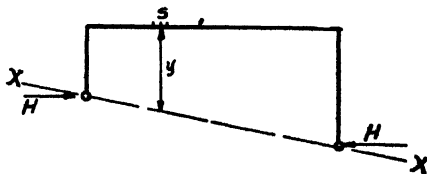


FIG. 25.

to it will be Hy . In the numerical example in Chapter VII, the first system is followed.

CHAPTER IV

CALCULATIONS

Convention of Algebraic Signs.—In order to obtain correct results in calculation, it is necessary to adopt a convention of algebraic signs. Bending moments on any division of the arch or frame which cause tension on the inside or soffit face and compression on the outside face are considered positive, and contrary moments are considered negative. The character of the bending moment determines, of course, the direction of the contribution of the division to the potential deflection at the reaction point. The resultant of all increments of deflection determines the reaction which opposes it.

In illustrative example 4, Chapter III, the direction of the redundant reaction R of the continuous beam, under the downward vertical load, is obvious at the outstart; and the terms for load and reaction can be equated numerically without consideration of the algebraic sign of the summation quantities into which bending moments are entered. Likewise the horizontal thrust reactions of the single-span two-hinged arch will obviously act inward for downward vertical loads and outward for upward vertical loads; while for earth pressure on one side the redundant horizontal reactions will evidently act in the direction shown in the numerical example for the symmetrical single-span frame with hinged-end conditions. Calculations for earth pressure on the steel frame bridge, Chapter VIII, and for the unsymmetrical concrete frame bridge, Chapter VII, are made for horizontal pressures acting inward, at both ends simultaneously, and the horizontal thrust reactions will obviously act outward.

In all these cases, equations for the redundant reaction, H , the direction of action of which is known, may be formed

numerically without attention to the algebraic sign of the summation quantity. The value of H having been determined, however, the bending moments due to it must be given their correct algebraic signs, as determined by inspection, so that they may be combined properly with the other bending moments having their correct algebraic signs.

For multiple-span arches or frames, however, it may not always be obvious in which direction the redundant reactions will act; but the observance of an additional convention of algebraic signs will make it unnecessary to predetermine the right direction. Any redundant reaction may be assumed in the beginning to act in either direction along its line of action. Instead of equating, numerically, the deflections at the reaction point due to load and the opposite deflection due to the reaction itself, all deflections at the same point are equated algebraically to zero; and the ordinates x or y are given algebraic signs in agreement with the character of the bending moments produced by the redundant reactions as assumed in direction. If the solution of the equations results in a positive value for a reaction, the assumed direction is correct; if negative, the opposite direction is correct. Applying this system to the two-hinged arch, the form of the equation for H due to loads would be $\sum \frac{Mys}{EI} + H \sum \frac{y^2s}{EI} = 0$, or as explained in Chapter III, $\sum \frac{MM_{as}}{EI} + H \sum \frac{M_a M_{as}}{EI} = 0$, in which M_a is a substitute expression for y and is the moment on any division due to unit load acting like H which may tentatively be assumed to act in one direction or the other. Values of y or M_a are now to be substituted into the tabulations with an algebraic sign: positive if the redundant reaction as assumed in direction would produce positive moment and negative if it would produce negative moment. Thus in the tabulations in Chapter V, y would be entered as negative, in agreement with the assumed direction of H , instead of positive.

$\sum \frac{Mys}{EI}$ would be negative and $\sum \frac{y^2s}{EI}$, of course, positive.

Substituting the numerical values of these quantities with their proper algebraic signs into the equation of H as written above, a positive value for H would result, indicating that the direction as assumed in Fig. 28 is correct, that is, acting inward for downward vertical loads. If H had been assumed in the beginning as acting outward, values for y (or M_a) would be entered into the tabulations as positive, since the assumed direction of H would cause positive moments on the several divisions, and a negative value for H in the resulting solution would show that the correct direction for H is opposite to that assumed.

If some vertical reactions act upward and some downward, moments due to them will, of course, be entered into the calculations with their proper algebraic signs. Nevertheless, the correct direction of the redundant reaction for the combined loading may not be obvious at the outstart, if direct calculation is made instead of following the influence-line method. Under such circumstances it may be advisable to follow the full convention of algebraic signs to be explained later on.

Calculation for the double-span frame, Chapter IX, and for the skew frame bridge, Chapter X, are carried out in accordance with the complete convention of signs.

In the analysis of the fixed-end frame (Fig. 34) it is impossible to equate the algebraic sum of the calculated deflections at the crown to zero, since actual movement does occur. The deflections at the crown of the left half are therefore equated to the deflections of the right half, the algebraic signs being governed by the effects of the deflection on each half. This is explained in Chapter III. Influence tables are derived for downward vertical load on the left half. Values for y (moment due to unit value of H_0) are negative for points 7L to 11L (also 7R to 11R) because H_0 applied as shown would cause negative moments at these

points. Values for y are positive for the remaining points because H_0 would cause positive moments at such points. Values for x (moments due to unit values of V_0) are positive for points on the left half with load on the left half because V_0 acting as shown would produce positive moments. Values of x are negative for the right half because V_0 as assumed would produce negative moments to the right. Substitution of negative $\sum \frac{M}{I}$, negative $\sum \frac{My}{I}$, and negative $\sum \frac{M_L x}{I}$ in formulas (7), (8) and (9) results in positive values for M_0 , H_0 , and V_0 respectively, on account of the double negative, indicating that, for load on the left half, the assumed directions of these reactions are correct, as is almost obvious. If the wrong direction had been assumed for any of them, but algebraic signs for x , y , and unit value of M_0 had been entered into the tabulations consistent with the assumed directions, a negative value would have indicated the error. All this will become clearer as the calculations are developed.

Denomination of Units of Calculation.—In all deflection calculations particular care must be taken to use units of single denomination—either all inch units or all foot units. In the preceding numerical examples all units were in inches (bending moments in inch-pounds, moments of inertia and modulus of elasticity in inch units, axis divisions s in inches, etc.), and the resulting calculated deflections were in inches. In the calculations for rigid-frame structures which follow later on, foot units are used. Bending moments, moments of inertia, all coordinates, etc., are expressed in foot units. In the final equations for reactions, E (modulus of elasticity) cancels out, but it appears in the final equation for horizontal thrust due to thermal expansion, as seen above. The familiar value of 2,000,000 for modulus of elasticity of concrete (E) which is in inch units must therefore be converted into foot units. That is, in this equation $E = 144 \times 2,000,000 = 288,000,000$. Likewise, in the equa-

tion for rib shortening (if used), f_c = pounds per square foot and l is in feet.

Free End Conditions.—Before proceeding with the design calculations of typical rigid-frame bridges an explanation will be given of the assumptions and short cuts used.

Referring to Fig. 33, p. 59, it will be observed that the structure rests on a rather wide base, the width being determined by the supporting value of the soil upon which the base rests. This figure shows the type used for a bridge resting "free" upon the soil. In Fig. 33*a* is shown the type used when the structure rests "free" upon rock foundation—that is, not anchored down to the rock so as to be capable of developing tension over part of the area, and therefore a moment couple. In either case it is obvious that the reaction cannot go beyond the edge of the base if the base is not anchored down. In Fig. 33 the reaction point cannot come *very* near the edge because this would presume impossible conditions of soil pressure at the edge. If it could suddenly come very close to the edge, causing extremely high local pressure, slight yielding of the soil would automatically throw it in again. There is therefore a reasonable range on the base within which the reaction must come. That is, an imaginary hinge may be assumed traveling within a limited range, and calculations made accordingly. In the first rigid-frame bridges designed by the author, calculations were made for imaginary hinges in extreme positions and critical stresses determined for all sections. This proved to be an unnecessary refinement, and calculations are now made as for hinges in one position only—near the center of the base. The detail shown for a footing on rock has proved adequate. The vertical reinforcement near the bottom of the vertical legs is hooped as for a column, and no spalling of the concrete due to undue concentration of the reaction at the edge has been observed.

The assuming of hinged condition at the base permits the design of the single-span rigid-frame structure to be

made as for the two-hinged arch for which the equations for horizontal thrust have been derived in the preceding text. The designer should be able to follow the numerical example through without further discussion.

Derivation of the equations for a fixed-end single-span rigid-frame bridge structure is given, and influence lines are calculated in an illustrative example.

Restraint at Footings.—If pile foundations are needed, some restraint due to the grip of the concrete on the piles is introduced. This is unknown in amount, but if the structure is analyzed for *both* fixed and hinged conditions, the stresses will lie somewhere between those calculated and the structure will be conservatively designed. Figure 38, p. 74, shows the moment curves as calculated for both conditions in a single-span frame bridge. It has been found that but little extra steel is required to meet both conditions. Whether the positive moment at the crown will be slightly increased or slightly decreased by restraint at the footing depends upon the ratio of span length to height.

Effects of Earth Pressure.—In addition to active earth pressure from the approach fill acting at the ends of the frame, passive earth pressure may be developed due to flexure under live loads, or due to dead load if the earth fill is placed before striking the falsework. In one of the frame bridges built by the Bronx Parkway Commission an attempt was made to measure this by means of pressure gages installed before the earth fill was placed and false-work struck. The tests indicated that but little passive earth pressure was developed. This is due to the very small deflection in the vertical legs against the earth. An examination of the summaries of stresses in the design calculations following shows that earth pressures (acting on both ends) usually assist, and that heavy passive pressure might be developed without harm. In multiple-span frames where earth pressure may be a determining factor for some points of the frame, the calculated active earth pressure may, if

desired, be multiplied by a factor up to say 2 to allow for uncertainties.

The frame may be called upon to carry its dead load without the assistance of earth pressure, as when the false-work is struck before the approach fill is placed. Under some particular circumstances it may also be expedient to permit the contractor to fill in the approaches beginning at one end of the bridge so that trucks may go over the span and fill the other approach from above. This has been true for some of the Westchester bridges. Such conditions should be investigated by supplementary calculation to be sure that safe stresses are not exceeded, although stresses higher than the usual working stresses may be permitted. In most of the calculations shown in this book, stresses due to earth pressure acting on each end are tabulated separately, to permit such supplementary calculation of unit stresses. The calculation of unit stresses for these examples has not, however, been carried through.

Special Notes

Selection of Coordinate Systems.—It will be noted that a different coordinate system is used for the symmetrical

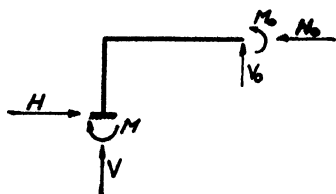


FIG. 26.

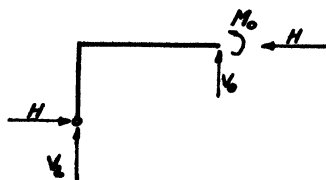


FIG. 27.

single-span frame when fixed-end conditions are assumed from that when hinged-end conditions are assumed. In the fixed frame three components of reactions exist at each footing as well as at the crown of the half frame (Fig. 26). Advantage is therefore taken of symmetry, and the YY axis

is taken through the crown. In the hinged frame, one indeterminate component (H) of the reactions exists at the hinge point and two (H and M) at the crown (Fig. 27). Calculations are therefore shortened by making one of the assumed hinge points the origin of the coordinate system.

Moments of Inertia.—Moments of inertia of a section with unbalanced reinforcement (that is, more reinforcement in one face of the section than in the other) are calculated as though the neutral axis were at the center of the section and the total reinforcement were equally divided, top and bottom. Error negligible.

Division of Axis.—In the following numerical examples the axis is divided into equal divisions s , and in such manner that a center-of-division point occurs at the point of maximum negative moment at the bend of the knee. This usually results in divisions of odd length at the bottoms of the vertical legs. Examination of the tabulations will show that, in the hinged structure, the quantities for these odd divisions have very little effect on the final summations. Correction for the odd lengths is therefore neglected. In the fixed structure, the quantities in the tabulations are largest for the divisions near the footings, and correction for the variation of s of these end divisions is made (as noted in the calculations) by multiplying the quantities pertaining thereto by the ratio of length of end division to length of regular divisions.

In the single- and double-span concrete frames selected for analysis, the inclination of the axis of the vertical legs is slight, and the imaginary hinged points at the bottoms of the bases of the hinged structure are assumed at such points *near* the centers of the bases that the vertical load moments for points in the vertical legs are negligible and about counterbalance, positive and negative. As a consequence, the quantities M and $\frac{My}{I}$ for such points (which would be very small anyway) are entered as zero in the tabulations, and the

calculations are to that extent shortened. Where the inclination of the axis of the vertical legs is considerable, the negative moments of such points may have to be dealt with. For the fixed-end frame the exact coordinates of points on the vertical-leg axis are used in calculating the cantilever moments in the half-frame.

The slight curvature of the axis in the top of the single-span and double-span concrete frames selected for analysis permits the assumption that the horizontal projections of the equal axis divisions are equal to the lengths of the divisions (4 ft. in the single-span structure and 5 ft. in the double-span structure). As a consequence of this slight approximation, observe that in Chapters V and VII the quantities in the several columns of the tabulation headed "Moment" are in exact arithmetical progression (reading vertically) both above and below the heavy zigzag line. The progressions above, however, are different from those below. Likewise reading horizontally from column to column headed "Moment," the quantities are in exact arithmetical progression up to the heavy zigzag line, but are in different progression to the right from what they are to the left. Also reading horizontally from column to column headed $\frac{My}{I}$ the quantities are in exact arithmetical progression up to the zigzag line, but in different progression to the right and to the left. These observations assist in rapid calculation. Like results obtain in the calculations for the double-span frame. Where the curvature of the axis in the top of the frame is considerable, one of two procedures may be followed. All the axis divisions may be made equal, and exact horizontal distances between the centers-of-division points (used also as influence-load points) may be used in the calculations. Or the arithmetical progression of vertical load moments may be retained by making the unequal axis divisions correspond to their equal horizontal projections. Then s will be variable and must be carried through the

calculations; that is, $\frac{My_s}{I}$, etc., instead of $\frac{My}{I}$ etc., must be calculated and tabulated for each point.

Influence Load.—In deriving the quantities for influence lines, an influence load different from unity is used in the calculations, that is, one of such magnitude that fractions will be avoided in the influence-load moments. In the analysis of the single-span frame, for example, note that the span is divided into 13 equal parts of 4 ft. each. If an influence load of $\frac{13}{4}$ is used, the smallest moment dealt with (that at point 6L with influence load at 6R) will be

$$\frac{1}{13} \times \frac{13}{4} \times 4 = 1.$$

Beginning with this, the arithmetical progressions referred to above are very simple, as shown in the example. In plotting the influence line diagrams for load unity, the ordinates are plotted to scale $\frac{4}{13}$ of those calculated for the influence load of $\frac{13}{4}$. The same expedient is used in the calculations for the double-span frame, as will be observed.

The influence-line diagram shows influence lines for all points of the half span as the influence load travels over the full span, whereas the tables, for convenience in calculation, have been derived for all points of the full span as the load travels over the half span. Referring to Fig. 29, observe, however, that the moment for point 8R, for example, when the load is at 10L, is the same as the moment for point 8L when the load is at point 10R. Thus the tables give all the necessary information.

For an unsymmetrical frame, moments at all points of the *full* span must be calculated for all positions of the load.

Proportioning Steel Reinforcement.—In proportioning the steel reinforcement of the various sections for final stresses, the required amount of tensile steel is calculated, neglecting the effect of any small amount of compressive steel that may be added as a result of carrying the tensile of steel adjacent sections past the points of contraflexure, or by reason

of providing shrinkage reinforcement, etc. This approximation is on the safe side.

Sometimes it will be advantageous to reinforce the crown section for compression rather than to increase the depth of section or to over-reinforce the tension side to reduce compressive stress in the concrete. In the calculation of steel reinforcement for the unsymmetrical single-span concrete frame bridge, for example, compression steel is used at points 12 and 13 near the crown. Calculations are shown below the table. The reader is referred to Hool and Kinne's "Concrete Engineer's Handbook," or other standard treatises, for explanation of the theory of proportioning sections reinforced for tension and compression and subjected to combined bending and direct stress. Another method of proportioning sections for such conditions is given in Section 11 of the Fifth Revised Edition of the "American Civil Engineers' Handbook," Merriman-Wiggin.

Adjustment of Calculations.—The depths of sections, reinforcing steel ratio, and consequently the moments of inertia assumed for analysis need agree only fairly well with the final results.

It is evident from the form of the equations for *load* reactions that, if *all* the assumed moments of inertia for the various sections involve the *same* percentage error, the calculated reactions will be exactly correct, and no adjustment of the detail calculations will be necessary. The formulas for temperature, etc., however, contain quantities for the reciprocal of moments of inertia in the denominator only. Therefore a correction for temperature reactions will be required, and it will be in direct ratio of actual to assumed moments of inertia.

If the errors in the assumed moments of inertia are irregular and serious in amount, correction of the detailed calculations may be necessary. Even then it has sometimes been found that as much as 10 to 20 per cent error for a few sections will affect the final results but little. A study of the

tabulations for a particular structure, and supplementary calculation of the effect of particular sections upon the summation quantities, will often avoid a complete recalculation. In some of the designs contained in this book a few sections were slightly increased in depth to meet stress conditions, but the tabulated moments of inertia assumed for analysis were not corrected.

The structures selected for analysis are of comparatively short span so that the methods may be illustrated the more briefly. Single-span concrete frame bridges have been built by the Westchester County Park Commission up to about 80-ft. span, and steel frame bridges up to about 120-ft. span.

CHAPTER V

CALCULATIONS FOR SYMMETRICAL SINGLE-SPAN CONCRETE FRAME BRIDGE; FREE-END CONDITIONS

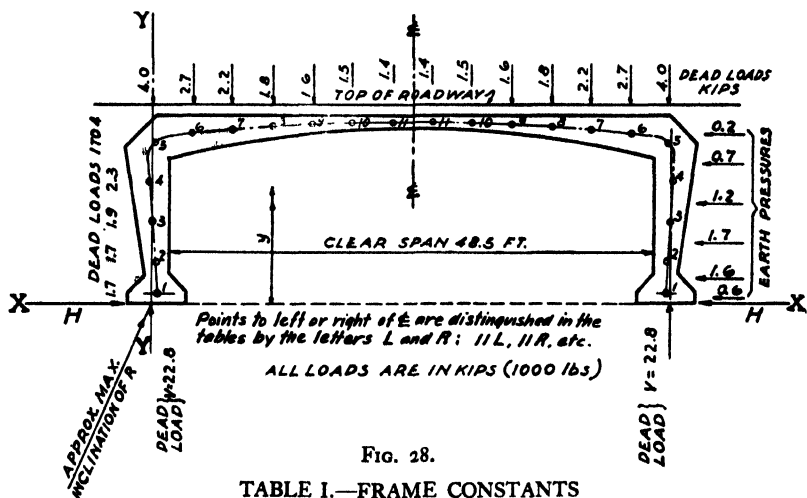


FIG. 28.

TABLE I.—FRAME CONSTANTS

Point	t Feet	I_c $\frac{1}{12} b t^3$	A_s Sq. Ft.	$\frac{t}{2} D$ -0.17	I_s $15 A_s D^3$	I $I_c + I_s$	y	$\frac{y^2}{I}$
1	6.00	18.00	18.00	1.0	0
2	2.65	1.55	0.0083	1.16	0.17	1.72	4.0	9
3	3.21	2.76	0.0140	1.45	0.43	3.19	8.0	20
4	3.85	4.75	0.0140	1.76	0.65	5.40	12.0	27
5	4.00	5.33	0.0140	1.84	0.70	6.03	15.9	42
6	3.55	3.73	0.0113	1.61	0.44	4.17	16.9	69
7	2.75	1.73	0.0076	1.21	0.17	1.90	17.3	158
8	2.15	0.83	0.0076	0.91	0.09	0.92	17.7	340
9	1.70	0.41	0.0134	0.69	0.09	0.50	17.9	641
10	1.40	0.23	0.0172	0.54	0.07	0.30	18.1	1092
11	1.25	0.16	0.0172	0.465	0.05	0.21	18.2	1577
Σ								3975

$$\sum \frac{y^2}{I} \text{ for full arch} = 2 \times 3975 = 7950$$

$$\text{Influence Load} = \frac{13}{4}; s = 4 \text{ ft.}$$

Point	I	y	Influence Load at 6R				Influence Load at 7R				Influence Load at 8R				Point
			Mom.	$\frac{My}{I}$	H _y	Total M	Mom.	$\frac{My}{I}$	H _y	Total M	Mom.	$\frac{My}{I}$	H _y	Total M	
1L	18.0	1.0	0	0	-0.4	-0.4	0	0	-0.7	-0.7	0	0	-1.0	-1.0	1L
2L	1.72	4.0	0	0	-1.4	-1.4	0	0	-2.8	-2.8	0	0	-4.1	-4.1	2L
3L	3.19	8.0	0	0	-2.8	-2.8	0	0	-5.6	-5.6	0	0	-8.2	-8.2	3L
4L	5.40	12.0	0	0	-4.2	-4.2	0	0	-8.4	-8.4	0	0	-12.4	-12.4	4L
5L	6.03	15.9	0	0	-5.6	-5.6	0	0	-11.1	-11.1	0	0	-16.4	-16.4	5L
6L	4.17	16.9	1	4	-5.9	-4.9	2	8	-11.8	-9.8	3	12	-17.4	-14.4	6L
7L	1.90	17.3	2	18	-6.1	-4.1	4	36	-12.1	-6.1	6	54	-17.8	-11.8	7L
8L	0.92	17.7	3	58	-6.2	-3.2	6	116	-12.4	-6.4	9	174	-18.2	-9.2	8L
9L	0.50	17.9	4	143	-6.3	-2.3	8	286	-12.5	-4.5	12	429	-18.5	-6.5	9L
10L	0.30	18.1	5	302	-6.3	-1.3	10	604	-12.7	-2.7	15	906	-18.6	-3.6	10L
11L	0.21	18.2	6	520	-6.4	-0.4	12	1040	-12.7	-0.7	18	1560	-18.7	-0.7	11L
11R	0.21	18.2	7	606	-6.4	+0.6	14	1212	-12.7	+1.3	21	1818	-18.7	+2.3	11R
10R	0.30	18.1	8	483	-6.3	+1.7	16	966	-12.7	+3.3	24	1449	-18.6	+5.4	10R
9R	0.50	17.9	9	322	-6.3	+2.7	18	644	-12.5	+5.5	27	966	-18.5	+8.5	9R
8R	0.92	17.7	10	192	-6.2	+3.8	20	384	-12.4	+7.6	30	576	-18.2	+11.8	8R
7R	1.90	17.3	11	100	-6.1	+4.9	22	200	-12.1	+9.9	20	182	-17.8	+2.2	7R
6R	4.17	16.9	12	49	-5.9	+6.1	11	44	-11.8	-0.8	10	40	-17.4	-7.4	6R
5R	6.03	15.9	0	0	-5.6	-5.6	0	0	-11.1	-11.1	0	0	-16.4	-16.4	5R
4R	5.40	12.0	0	0	-4.2	-4.2	0	0	-8.4	-8.4	0	0	-12.4	-12.4	4R
3R	3.19	8.0	0	0	-2.8	-2.8	0	0	-5.6	-5.6	0	0	-8.2	-8.2	3R
2R	1.72	4.0	0	0	-1.4	-1.4	0	0	-2.8	-2.8	0	0	-4.1	-4.1	2R
1R	18.0	1.0	0	0	-0.4	-0.4	0	0	-0.7	-0.7	0	0	-1.0	-1.0	1R
Σ				2797				5540				8166			
				$H = \sum \frac{My}{I} = \frac{2797}{7950}$				$H = \frac{5540}{7950}$				$H = \frac{8166}{7950}$			

FREE-END CONDITIONS

47

Point	I	y	Influence Load at 9R				Influence Load at 10R				Influence Load at 11R				Point
			Mom.	$\frac{My}{I}$	H_y	Total M	Mom.	$\frac{My}{I}$	H_y	Total M	Mom.	$\frac{My}{I}$	H_y	Total M	
1L	18.0	1.0	0	0	-1.3	-1.3	0	0	-1.6	-1.6	0	0	-1.7	-1.7	1L
2L	1.72	4.0	0	0	-5.3	-5.3	0	0	-6.3	-6.3	0	0	-6.8	-6.8	2L
3L	3.19	8.0	0	0	-10.6	-10.6	0	0	-12.6	-12.6	0	0	-13.7	-13.7	3L
4L	5.40	12.0	0	0	-16.0	-16.0	0	0	-18.9	-18.9	0	0	-20.5	-20.5	4L
5L	6.03	15.9	0	0	-21.2	-21.2	0	0	-25.0	-25.0	0	0	-27.2	-27.2	5L
6L	4.17	16.9	4	16	-22.5	-18.5	5	20	-26.5	-21.5	6	24	-28.9	-22.9	6L
7L	1.90	17.3	8	72	-23.0	-15.0	10	90	-27.2	-17.2	12	108	-29.6	-17.6	7L
8L	0.92	17.7	12	232	-23.5	-11.5	15	290	-27.8	-12.8	18	348	-30.3	-12.3	8L
9L	0.50	17.9	16	572	-23.8	-7.8	20	715	-28.1	-8.1	24	858	-30.6	-6.6	9L
10L	0.30	18.1	20	1,208	-24.0	-4.0	25	1,510	-28.4	-3.4	30	1,812	-31.0	-1.0	10L
11L	0.21	18.2	24	2,080	-24.2	-0.2	30	2,600	-28.6	+1.4	36	3,120	-31.1	+4.9	11L
11R	0.21	18.2	28	2,424	-24.2	+3.8	35	3,030	-28.6	+6.4	42	3,636	-31.1	+10.9	11R
10R	0.30	18.1	32	1,932	-24.0	+8.0	40	2,415	-28.4	+11.6	35	2,110	-31.0	+4.0	10R
9R	0.50	17.9	36	1,288	-23.8	+12.2	32	1,145	-28.1	+3.9	28	1,001	-30.6	-2.6	9R
8R	0.92	17.7	27	519	-23.5	+3.5	24	461	-27.8	-3.8	21	404	-30.3	-9.3	8R
7R	1.90	17.3	18	164	-23.0	-5.0	16	146	-27.2	-11.2	14	127	-29.6	-15.6	7R
6R	4.17	16.9	9	36	-22.5	-13.5	8	32	-26.5	-18.2	7	28	-28.9	-21.9	6R
5R	6.03	15.9	0	0	-21.2	-21.2	0	0	-25.0	-25.0	0	0	-27.2	-27.2	5R
4R	5.40	12.0	0	0	-16.0	-16.0	0	0	-18.9	-18.9	0	0	-20.5	-20.5	4R
3R	3.19	8.0	0	0	-10.6	-10.6	0	0	-12.6	-12.6	0	0	-13.7	-13.7	3R
2R	1.72	4.0	0	0	-5.3	-5.3	0	0	-6.3	-6.3	0	0	-6.8	-6.8	2R
1R	18.0	1.0	0	0	-1.3	-1.3	0	0	-1.6	-1.6	0	0	-1.7	-1.7	1R
Σ				10,543				12,454				13,576			
				$H = \frac{10,543}{7950} = 1.33$				$H = \frac{12,454}{7950} = 1.57$				$H = \frac{13,576}{7950} = 1.71$			

NOTE.—Simple-span moments M due to vertical loads cause tension on the inside fibers and are +. Moments caused by the horizontal thrust H cause compression on the inside and are -.

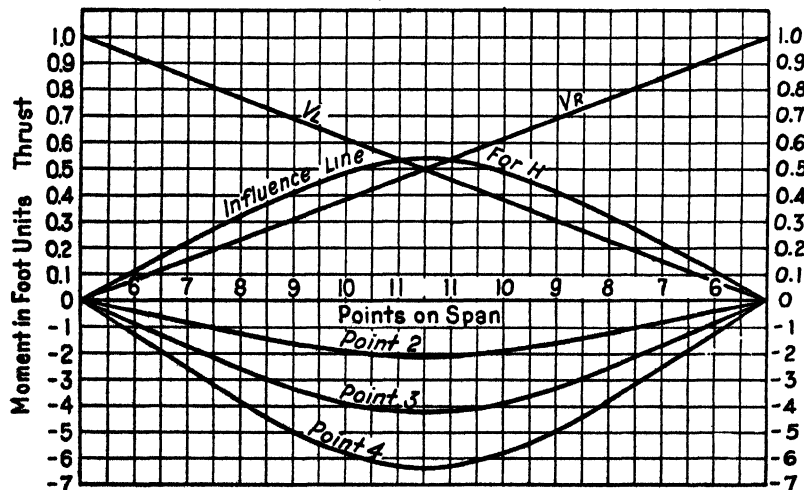
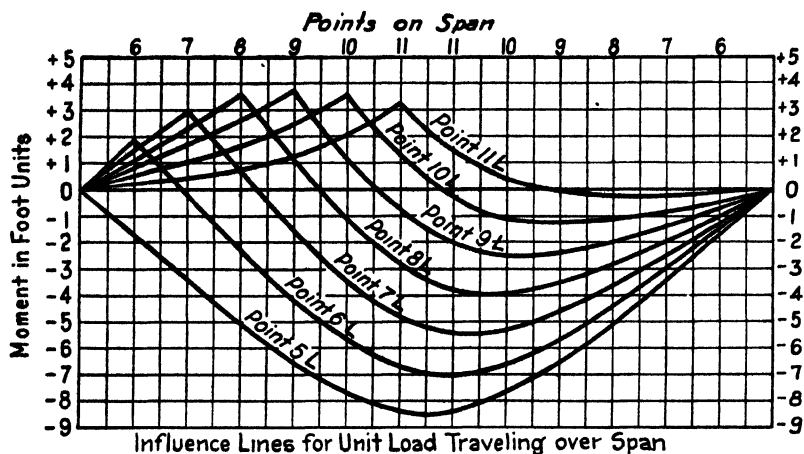


FIG. 29.

Moments for unit load = $\frac{4}{13}$ of moments calculated in tables.

DEAD LOAD MOMENTS

Moment factors (MF) are scaled from the influence line diagram. The product of load and moment factor will give the actual dead load moment M .

Load Point	Load	Point 2		Point 3		Point 4		Point 5		Point 6	
		MF	M	MF	M	MF	M	MF	M	MF	M
6L	2.7	-0.4	-1.1	-0.8	-2.2	-1.3	-3.5	-1.7	-4.6	+1.9	+5.1
7L	2.2	-0.8	-1.7	-1.7	-3.7	-2.6	-5.7	-3.4	-7.5	-0.2	-0.4
8L	1.8	-1.2	-2.2	-2.6	-4.7	-3.8	-6.8	-5.1	-9.2	-2.3	-4.2
9L	1.6	-1.6	-2.6	-3.3	-5.3	-5.0	-8.0	-6.5	-10.4	-4.2	-6.7
10L	1.5	-1.9	-2.8	-3.9	-5.9	-5.8	-8.7	-7.7	-11.6	-5.6	-8.4
11L	1.4	-2.1	-2.9	-4.2	-5.9	-6.3	-8.8	-8.4	-11.8	-6.7	-9.4
11R	1.4	-2.1	-2.9	-4.2	-5.9	-6.3	-8.8	-8.4	-11.8	-7.0	-9.8
10R	1.5	-1.9	-2.8	-3.9	-5.9	-5.8	-8.7	-7.7	-11.6	-6.6	-9.9
9R	1.6	-1.6	-2.6	-3.3	-5.3	-5.0	-8.0	-6.5	-10.4	-5.7	-9.1
8R	1.8	-1.2	-2.2	-2.6	-4.7	-3.8	-6.8	-5.1	-9.2	-4.4	-7.9
7R	2.2	-0.8	-1.7	-1.7	-3.7	-2.6	-5.7	-3.4	-7.5	-3.0	-6.6
6R	2.7	-0.4	-1.1	-0.8	-2.2	-1.3	-3.5	-1.7	-4.6	-1.5	-4.1
Totals	-26.6	-55.4	-83.0	-110.2	-71.4

Load Point	Load	Point 7		Point 8		Point 9		Point 10		Point 11	
		MF	M	MF	M	MF	M	MF	M	MF	M
6L	2.7	+1.5	+4.3	+1.1	+3.0	+0.8	+2.2	+0.5	+1.4	+0.2	+0.5
7L	2.2	+3.0	+6.6	+2.3	+5.1	+1.7	+3.8	+1.0	+2.2	+0.4	+0.9
8L	1.8	+0.7	+1.3	+3.6	+6.5	+2.6	+4.7	+1.6	+2.9	+0.7	+1.3
9L	1.6	-1.5	-2.4	+1.1	+1.8	+3.8	+6.1	+2.4	+3.8	+1.2	+1.9
10L	1.5	-3.4	-5.1	-1.2	-1.8	+1.2	+1.8	+3.6	+5.4	+2.1	+3.2
11L	1.4	-4.8	-6.7	-2.8	-3.9	-0.8	-1.1	+1.2	+1.7	+3.3	+4.6
11R	1.4	-5.4	-7.6	-3.8	-5.3	-2.0	-2.8	-0.3	-0.4	+1.5	+2.1
10R	1.5	-5.3	-8.0	-3.9	-5.9	-2.5	-3.8	-1.0	-1.5	+0.4	+0.6
9R	1.6	-4.6	-7.4	-3.5	-5.6	-2.4	-3.9	-1.2	-1.9	-0.0	-0.0
8R	1.8	-3.6	-6.5	-2.8	-5.0	-2.0	-3.6	-1.1	-2.0	-0.2	-0.4
7R	2.2	-2.5	-5.5	-2.0	-4.4	-1.4	-3.2	-0.8	-1.8	-0.2	-0.4
6R	2.7	-1.3	-3.5	-1.0	-2.7	-0.7	-1.9	-0.4	-1.1	-0.1	-0.3
Totals	-40.5	-18.2	-1.7	+8.7	+14.

NOTE.—Loads at points 1 to 5 inclusive produce very small moments in the structure which are neglected. They cause direct stresses, however, which are calculated as normal thrusts.

Dead Load Thrusts: see Fig. 28 for Dead Loads on Structure.

Point 1. $N = V = 22.8$.

Point 2. $N = 22.8 - 1.7 = 21.1$.

Point 3. $N = 21.1 - 1.7 = 19.4$.

Point 4. $N = 19.4 - 1.9 = 17.5$.

Point 5. $N =$ components at 45° of V and H . $(17.5 - 2.3) \times 0.71 + 7.0 \times 0.71 = 15.8$.

Points 6 to 11. $N = H$ as calculated from individual dead loads and H factors obtained from influence line for H as follows:

$$(2.7 \times 0.11 + 2.2 \times 0.22 + 1.8 \times 0.32 + 1.6 \times 0.41 + 1.5 \times 0.48 + 1.4 \times 0.53) \times 2 = 7.0.$$

Live Load Moments and Normal Thrusts

This bridge carries a 40-ft. roadway and is designed for H20 loading. (Refer to Appendix.) Allowing for reduction of traffic intensity for the 22-ft. width in excess of 18, we have from the rear axle of a 20-ton truck:

$$\frac{32000}{8} (1.00 - 0.22) = 2800 \text{ lb. per foot width of bridge;}$$

and from the front axle:

$$\frac{8000}{8} (1.00 - 0.22) = 700 \text{ lb. per foot width of bridge.}$$

Adding impact allowance, $\frac{50}{L + 150} = \frac{50}{50 + 150} = 25$ per cent, we have concentrations of 3500 and 900 at 14-ft. centers, from the one 20-ton truck. Loads from the preceding and following 15-ton trucks of the train spaced according to the specification will not affect this structure.

Normal Thrusts.—Normal thrusts N for points 1 to 4 are reactions V ; loads are in the same position as when calculating the corresponding moments.

Normal thrusts for points 6 to 11 are horizontal thrust H ; loads are in the same position as when calculating the corresponding moments.

Normal thrust for point 5 is the resultant at 45° of V and H , with loads in same position as when calculating the corresponding moments.

$$\text{For 3.5 load } V \text{ factor} = 0.71 \times 0.54 = 0.38$$

$$H \text{ factor} = 0.71 \times 0.53 = 0.38$$

$$N \text{ factor} = \underline{0.76}$$

$$\text{For 0.9 load } V \text{ factor} = 0.71 \times 0.27 = 0.19$$

$$H \text{ factor} = 0.71 \times 0.37 = 0.26$$

$$N \text{ factor} = \underline{0.45}$$

CONCENTRATED LIVE LOAD MOMENTS M AND NORMAL THRUSTS N

Moment Factors (MF) and Thrust Factors (NF) are read directly from Influence Line Diagrams. The product of load and moment factor gives actual moments M and product of load and thrust factor gives actual thrusts N .

Load (Kips)	Point 2			Point 3			Point 4			Point 5			Point 6		
	MF	M	NF	N	MF	M	MF	M	NF	N	MF	M	MF	M	NF
3.5	-2.1	-7.3	0.54	1.9	-4.2	-14.7	-6.3	-22.0	0.54	1.9	-8.4	-29.4	-8.4	-24.5	0.53
0.9	-1.5	-1.3	0.27	0.2	-2.9	-2.6	-4.4	-4.0	0.27	0.2	-5.9	-5.3	-4.4	-3.3	0.32
Total	-8.6	2.1	-17.3	-26.0	2.1	-34.7	-27.8

Load (Kips)	Point 7			Point 8			Point 8			Point 9			Point 9		
	MF	M	NF	N	MF	M	MF	M	NF	N	MF	M	MF	M	NF
3.5	-5.4	-18.9	0.53	1.9	-3.9	-13.6	+3.6	+12.6	0.32	1.1	-2.5	-8.8	-2.5	+13.3	0.41
0.9	-3.1	-2.8	0.27	0.2	-2.0	-1.8	0.0	-1.1	-1.0	+0.4	+0.4	0.06
Total	-21.7	2.1	-15.4	+12.6	1.1	-9.8	+13.7

Load (Kips)	Point 10			Point 10			Point 11			Point		
	MF	M	NF	N	MF	M	MF	M	NF	N	MF	M
3.5	-1.2	-4.2	0.41	1.4	+3.6	+12.6	+3.3	+11.6	0.53	1.9
0.9	-0.2	-0.2	0.06	0.1	+0.7	+0.6	+0.5	+0.5	0.28	0.3
Total	-4.4	1.5	+13.2	+12.1	2.2

Uniform Live Load Stresses

100 lb. per sq. ft.

Area of moment curve for point 5 = 263 units.

Moment = $263 \times 100 = 26,300$ ft.-lb. = 26.3 kip.-ft.

Concentrated live load moment is greater, 34.7 kip.-ft.

It is obvious that concentrations will therefore give greater moments than uniform live load for all points.

The structure will carry a uniform live load of

$$\frac{34.7}{26.3} \times 100 = 132 \text{ lb. per sq. ft.}$$

without over-stressing the critical section at Point 5.

Temperature Stresses

c = coefficient of thermal expansion = 0.0000065;

t = temperature change in degrees Fahrenheit

= + 35° or - 45°;

l = span length in feet = 52;

E = modulus of elasticity of concrete

= $144 \times 2,000,000 = 288,000,000$ lb. per sq. ft.

s = length of axis divisions = 4 ft.;

$$H = \frac{Ectl}{s \sum \frac{y^2}{I}}$$

NOTE.— s is placed outside summation sign because assumed constant in calculations.

$$H = + \frac{288,000,000 \times 0.0000065 \times 35 \times 52}{4 \times 7950}$$

= + 107 lb. = 0.107 kip;

$$H = - \frac{45}{35} \times 107 = - 138 \text{ lb.} = - 0.138 \text{ kip.}$$

Point	y	H_y	H_y	Point	y	H_y	H_y
2	4 0	-0 4	+0 6	7	17 3	-1 9	+2 4
3	8 0	-0 9	+1 1	8	17 7	-1 9	+2 4
4	12 0	-1 3	+1 7	9	17 9	-1 9	+2 5
5	15 9	-1 7	+2 2	10	18 1	-1 9	+2 5
6	16 9	-1 8	+2 3	11	18 2	-1 9	+2 5

Positive H causes negative moments; negative H causes positive moments. See p. 33.

Earth Pressure

Figure 30 shows the reactions for the free structure, with the horizontal reaction for earth pressure right at the right footing. Bending moments in the frame for the earth-pressure loads shown in Fig. 28 and for the reactions shown in Fig. 30 are calculated in the first ten columns of the following table by moment increments—a method that is partly self-checking. From the succeeding calculations in the table a value of 1.1 kips for the redundant horizontal thrust is derived. The final horizontal reactions will then be 1.1 kips at the left footing and $6.0 - 1.1 = 4.9$ kips at the right footing.

SUMMARY OF MAXIMUM MOMENTS (KIP-FT.) AND NORMAL THRUSTS (KIPS)

Loading	Point 2		Point 3		Point 4		Point 5	
	M	N	M	N	M	N	M	N
Dead.....	-26.6	21.1	-55.4	19.4	-83.0	17.5	-110.2	15.8
Earth P. Right.....	-4.4	0.8	-8.9	0.8	-13.3	0.3	-17.6	1.4
Earth P. Left.....	+15.1	-0.8	+22.4	-0.8	+24.0	-0.8	+21.9	0.2
Sub Total.....	-15.9	21.1	-41.9	19.4	-72.3	17.5	-105.9	17.4
Live -.....	-8.6	2.1	-17.3	2.1	-26.0	2.1	-34.7	3.1
Temperature.....	+0.6	0	+1.1	0	+1.7	0	+2.2	-0.1
Temperature.....	-0.4	0	-0.9	0	-1.3	0	-1.7	+0.1
Maximum Total....	-24.9	23.2	-60.1	21.5	-99.6	19.6	-142.3	20.6

Loading	Point 6		Point 7		Point 8		Point 9	
	M	N	M	N	M	N	M	N
Dead.....	-71.4	7.0	-40.5	7.0	-18.2	7.0	-1.7	7.0
Earth P. Right.....	-15.7	1.1	-13.1	1.1	-10.5	1.1	-7.7	1.1
Earth P. Left.....	+17.9	1.1	+14.4	1.1	+10.9	1.1	+7.6	1.1
Sub Total.....	-69.2	9.2	-39.2	9.2	-17.8	9.2	-1.8	9.2
Live +.....					+12.6	1.1	+13.7	1.5
Live -.....	-27.8	2.2	-21.7	2.1	-15.4	2.0	-9.8	1.8
Temperature.....	+2.3	-0.1	+2.4	-0.1	+2.4	-0.1	+2.5	-0.1
Temperature.....	-1.8	+0.1	-1.9	+0.1	-1.9	+0.1	-1.9	+0.1
Maximum Total....	-98.8	11.5	-62.8	11.4	-35.1	11.3	-13.5	11.1
Maximum Total....							+14.4	10.6

Loading	Point 10		Point 11		Point		Point	
	M	N	M	N	M	N	M	N
Dead.....	+8.7	7.0	+14.0	7.0				
Earth P. Right.....	-4.8	1.1	-1.9	1.1				
Earth P. Left.....	+4.3	1.1	+1.2	1.1				
Sub Total.....	+8.2	9.2	+13.3	9.2				
Live +.....	+13.2	1.8	+12.1	2.2				
Live -.....	-4.4	1.5						
Temperature.....	+2.5	-0.1	+2.5	-0.1				
Temperature.....	-1.9	+0.1	-1.9	+0.1				
Maximum Total....	+23.9	10.9	+27.9	11.3				

Design of Sections

The following table gives the calculation of required tensile reinforcement neglecting effect of steel in compression face, excepting at a few critical points as will be noted. The required amount of tensile steel per foot width of structure is obtained from a diagram in Hool and Johnson's "Concrete Engineer's Handbook," reproduced in the Appendix, by permission of the authors and the

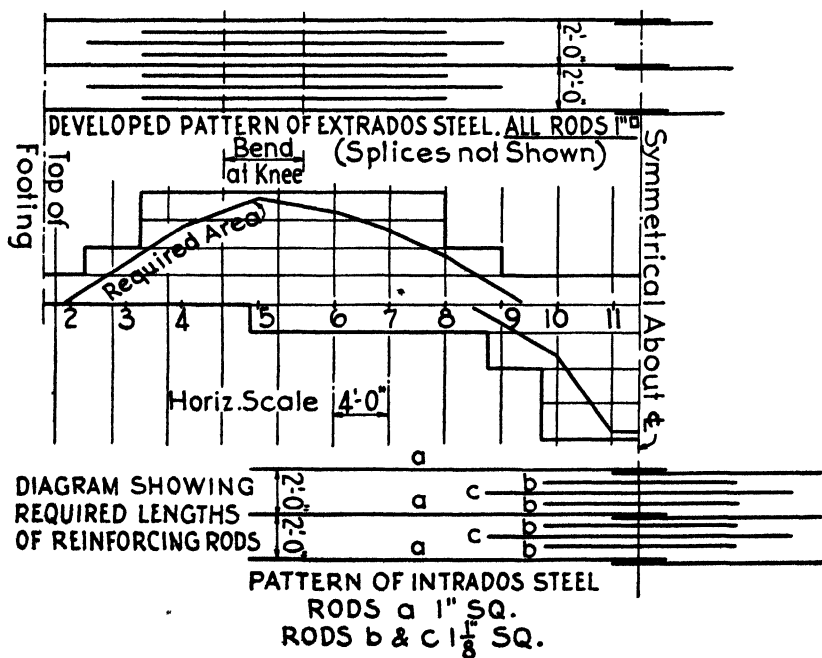


FIG. 31.

publisher, McGraw-Hill Book Company. Having calculated $K = \frac{Ne'}{bd^2}$, enter the diagram at the left and at the bottom. Follow vertically upward to the intersection of the line for $f_c = 800$ or $f_c = 18,000$, whichever governs. From this intersection follow horizontally to the right to the proper line for $\frac{e'}{d}$, thence vertically downward to the

bottom of the diagram, and read off the required percentage of tensile steel reinforcement. The required cross-sectional area of steel (A_s) = pbd , which is tabulated for each point in the last column of the table to the right.

Note that the thicknesses t finally used in the table for proportioning the steel reinforcement are less than the thicknesses assumed for analysis. The early bridges on the Bronx River Parkway and Westchester County Parkways were "over-designed." Later experience showed that more slender proportions could be used. The tables in Chapters V and VI for proportioning the sections and steel reinforcement have therefore been revised in this new edition to indicate the proper proportions for a bridge of about 49-ft. span carrying a separate roadway surface and designed for H20 loading, despite the fact that the analysis is based upon thicker sections.

CALCULATION FOR STEEL REINFORCEMENT

Note that the thicknesses (t) of sections finally used are less than originally assumed for analysis. The error involved will be negligible. The reduction in section was made to develop fully the area of steel reinforcement shown in Fig. 31.

Point	Moment		N Lb.	$e = \frac{M}{N}$ In.	t In.	$d = t - 2$	$e' = \frac{t}{2} - 2$	$\frac{e'}{d}$	$k = \frac{Ne'}{bd^2}$	f_c	f_s	Required p	Required A_s Sq. In. Per Ft Width	A'_s
	Ft.-Lb.	Inch.-Lb.												
2	- 24,900	- 299,000	23,200	12.9	32	30	26.9	0.9	58	470	18,000	.0017	0.72
3	- 60,100	- 721,000	21,500	33.5	37	35	50.0	1.4	74	550	18,000	.0028	1.35
4	- 99,600	- 1,195,000	19,600	61.0	42	40	80.0	2.0	82	580	18,000	.0037	1.90
5	- 142,300	- 1,708,000	20,600	82.9	45	43	103.4	2.4	97	640	18,000	.0036	1.64
6	- 98,800	- 1,186,000	11,500	103.0	40	38	121.5	3.2	80	560	18,000	.0038	0.34
7	- 62,800	- 754,000	11,400	61.1	31.5	29.5	79.9	2.7	88	600	18,000	.0031	0.86
8	- 35,100	- 421,000	11,300	37.2	25	23	47.7	2.1	86	600	18,000	.0012	0.26
9	- 13,500	- 161,000	11,100	14.5	20	18	22.5	1.3	65	500	18,000	.0014	0.30
9	+ 14,400	+ 174,000	10,600	16.4	20	18	24.4	1.4	67	500	18,000	.0050	0.90
10	+ 23,900	+ 287,000	10,900	26.3	17	15	32.8	2.2	133	800	18,000	2.33
11	+ 27,900	+ 335,000	11,300	29.7	15	13	35.2	2.7	197	800	11,000	0.5

Reinforcement for point 11. Assume $k = 0.52$, $kd = 6.8$ in., $jd = 13 - \frac{6.8}{3} = 10.73$,

$$f_s = 15 \times 800 \times \frac{6.2}{6.8} = 11,000, f'_s = 15 \times 800 \times \frac{4.8}{6.8} = 8,500.$$

Moment to be carried = $Ne' = 11,300 \times 35.2 = 398,000$

Normal moment of resistance $12 \times 6.8 \times 400 \times 10.73 = \frac{359,000}{48,000}$

To be carried by additional steel

$$\text{Required area compression steel} = \frac{48,000}{8,500 \times 11} = 0.5 \text{ sq. in.}$$

$$\text{Net area tension steel} = \frac{350,000}{11,000 \times 10.7} + \frac{48,000}{11,000 \times 11} - \frac{11,300}{11,000} = 2.33 \text{ sq. in.}$$

NOTE.—Smaller value for k would give larger A'_s , and smaller A_s .

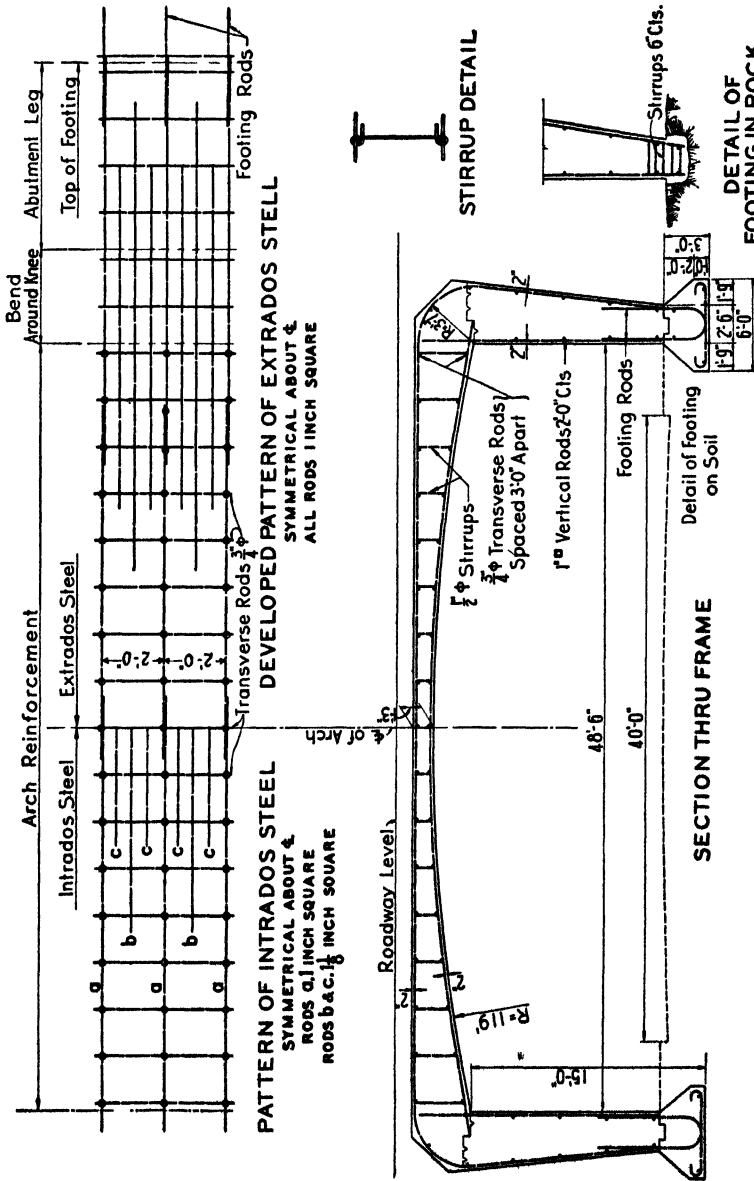


FIG. 33.

FIG. 33a.

DETAIL OF
FOOTING IN ROCK

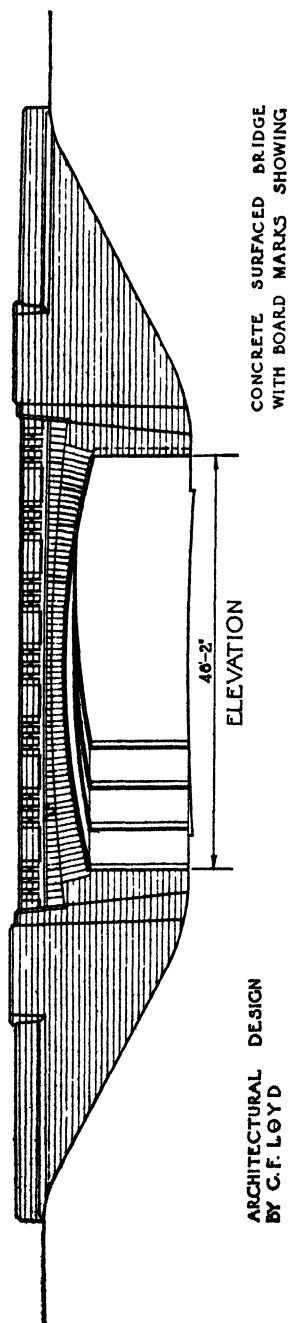


FIG. 32.

CHAPTER VI

CALCULATIONS FOR SYMMETRICAL SINGLE-SPAN CONCRETE FRAME BRIDGE; FIXED-END CONDITIONS

In the tabulations, the following rules as to algebraic signs are observed. Moments causing tension on the inside fibers of the frame are considered positive and moments causing compression on the inside fibers are considered negative. Thus, referring to Fig. 34, p. 62, and assuming the reactions in the directions indicated, moments on the *left* cantilever due to P are all negative; those due to M_0 and V_0 are all positive; and those due to H_0 are negative for all points above the XX axis and positive for all points below the XX axis. Moments on the right cantilever due to M_0 are all positive; those due to H_0 are negative for all points above the XX axis and positive for all points below the XX axis; those due to V_0 are all negative.

In calculating the table for Influence Load Moments, the summations of $\frac{M}{I}$, $\frac{M_y}{I}$, and $\frac{M_x}{I}$ are found first. These values are then used in the calculation of Reactions M_0 , H_0 and V_0 , following the Influence Load Calculations, after which M_0 , H_0y and V_0x may be entered in the Influence Load tables. Total Moments for influence load at the various points = $M + M_0 + H_0y + V_0x$.

Observe that calculated reinforcement (vertical rods 1 sq. in. area per foot width of structure), is required at the inside face of the vertical legs of the frame, due to positive moment at points 1, 2 and 3.

For free-end conditions, nominal reinforcement only is used (Fig. 33); vertical rods being placed at the inside face of the vertical legs at wider intervals, overlapping the dowels projecting from the footings.

62 SYMMETRICAL CONCRETE FRAME BRIDGE

Compare steel areas required for free-end conditions and for fixed-end conditions.

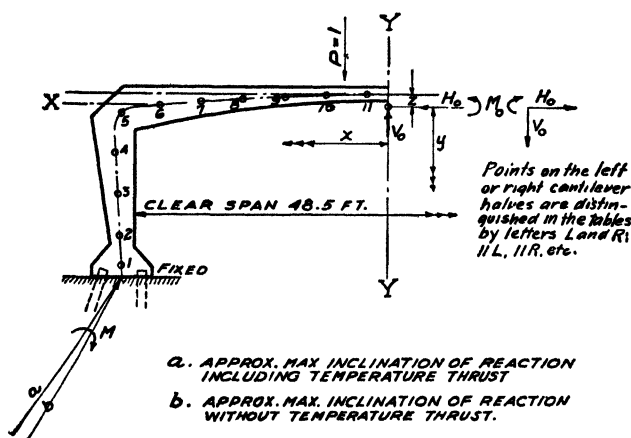


Fig. 34.

TABLE 1. FRAME CONSTANTS

NOTE FOR THICKNESSES OF SECTIONS AND CALCULATION OF MOMENTS OF INERTIA SEE CALCULATIONS FOR FRAME WITH FREE ENDS.

POINT	x	z+y	I	$\frac{I}{I}$	$\frac{z+y}{I}$	z	y	$\frac{y}{I}$	$\frac{x}{I}$	$\frac{y^2}{I}$	$\frac{x^2}{I}$
11	2	0.0	0.21	4.76	0.0	1.2	-1.2	-5.70	9.5	6.9	19
10	6	0.1	0.30	3.33	0.33	"	-1.1	-3.66	20.0	4.0	120
9	10	0.3	0.50	2.00	0.60	"	-0.9	-1.80	20.0	1.6	200
8	14	0.5	0.92	1.09	0.54	"	-0.7	-0.76	15.2	0.5	212
7	18	0.9	1.90	.53	0.47	"	-0.3	-0.16	9.5	0.1	170
6	22	1.3	4.17	.24	0.31	"	+0.1	+0.02	5.3	0.0	116
5	25.8	2.3	6.03	.17	0.38	"	+1.1	+0.18	4.3	0.2	110
4	26.2	6.2	5.40	.19	1.15	"	+5.0	+0.93	4.6	4.6	127
3	25.9	10.2	3.19	.31	3.20	"	+9.0	+2.82	6.1	25.4	210
2	25.6	14.2	1.72	.58	8.25	"	+13.0	+7.55	14.9	98.2	381
1	25.5	17.8	36.80	.03	0.48	"	+16.0	+0.44	0.7	7.1	76
Σ FOR HALF ARCH			13.23	15.71				-0.14	112.3	148.6	1683

NOTE: LENGTH OF DIVISION WHOSE CENTER POINT IS 1 IS 8 FT. OR ONE-HALF LENGTH OF REGULAR DIVISIONS. QUANTITIES PERTAINING TO THIS DIVISION ARE THEREFORE GIVEN HALF WEIGHT IN THE TABULATIONS, BY DOUBLING THE VALUE OF I IN THE DENOMINATOR OF ALL QUANTITIES, AND 3 IS ELIMINATED IN THE SUMMATION PROCESS

$$z = \frac{\sum \frac{z+y}{I}}{\sum \frac{1}{I}} = \frac{15.71}{13.23} = 1.2 \text{ FT.}$$

Point	I	y	x	Influence Load I at Crown					Influence Load I at Point $10\frac{1}{2}L$										
				M	$\frac{M}{I}$	$\frac{My}{I}$	$\frac{Mx}{I}$	M ₀	H ₀ y	V ₀ x	Total Mom.	M	$\frac{M}{I}$	$\frac{My}{I}$	$\frac{Mx}{I}$	M ₀	H ₀ y	V ₀ x	Total Mom.
11L	0.21	-1.2	2.0	-2.0	-9.5	+11.4	-19	4.25	-0.98	1.0	+2.3	0			2.61	-0.93	0.74	+2.4	
10L	0.30	-1.1	6.0	-6.0	-20.0	+22.0	-120	"	-0.90	3.0	+0.35	-2.0	-6.7	+7.3	-40	"	-0.86	2.23	+2.0
9L	0.50	-0.9	10.0	-10.0	-20.0	+18.0	-200	"	-0.73	5.0	-7.5	-6.0	-12.0	+10.8	-120	"	-0.70	3.72	-0.4
8L	0.92	-0.7	14.0	-14.0	-15.2	+10.6	-213	"	-0.57	7.0	-3.3	-10.0	-10.9	+7.6	-152	"	-0.54	5.20	-2.7
7L	1.90	-0.3	18.0	-18.0	-9.5	+2.8	-171	"	-0.24	9.0	-5.0	-14.0	-7.4	+2.2	-133	"	-0.23	6.70	-4.9
6L	4.17	+0.1	22.0	-22.0	-5.3	-0.5	-116	"	+0.08	11.0	-6.7	-18.0	-4.3	-0.4	-95	"	+0.08	8.20	-7.1
5L	6.03	+1.1	25.8	-25.8	-4.3	-4.7	-110	"	+0.90	12.9	-7.75	-21.8	-3.6	-4.0	-93	"	+0.85	9.60	-8.7
4L	5.40	+5.0	26.2	-26.2	-4.8	-24.2	-127	"	+4.07	13.1	-4.8	-22.2	-4.1	-20.6	-107	"	+3.89	9.75	-5.95
3L	3.19	+9.0	25.9	-25.9	-8.1	-73.0	-210	"	+7.32	12.95	-1.4	-21.9	-6.9	-61.7	-178	"	+7.00	9.65	-2.65
2L	1.72	+13.0	25.6	-25.6	-14.9	-193.3	-361	"	+10.60	12.8	+2.05	-21.6	-12.5	-163.1	-322	"	+10.10	9.52	+0.6
1L	36.0	+16.0	25.5	-25.5	-0.7	-11.0	-18	"	+13.03	12.75	+4.53	-21.5	-0.6	-9.6	-15	"	+12.43	9.50	+3.05
1R				0				"	+13.03	-12.75	+4.53	0				"	+12.43	-9.50	+5.55
2R				0				"	+10.60	-12.8	+2.05	0				"	+10.10	-9.52	+3.2
3R				0				"	+7.32	-12.95	-1.4	0				"	+7.00	-9.65	-0.05
4R				0				"	+4.07	-13.1	-4.8	0				"	+3.89	-9.75	-3.25
5R				0				"	+0.90	-12.9	-7.75	0				"	+0.85	-9.60	-6.15
6R				0				"	+0.08	-11.0	-6.7	0				"	+0.08	-8.20	-5.5
7R				0				"	-0.24	-9.0	-5.0	0				"	-0.23	-6.70	-4.3
8R				0				"	-0.57	-7.0	-3.3	0				"	-0.54	-5.20	-3.1
9R				0				"	-0.73	-5.0	-1.5	0				"	-0.70	-3.72	-1.8
10R				0				"	-0.90	-3.0	+0.35	0				"	-0.85	-2.23	-0.5
11R				0				"	-0.98	-1.0	+2.3	0				"	-0.93	-0.74	+0.95
Σ					-112.3	-241.3	-168.5						-69.0	-231.5	-125.5				

Moments producing tension on the soffit (inside face) of the frame are considered +.
 Moments producing compression on the soffit (inside face) of the frame are considered -.

Point	I	y	x	Influence Load 1 at Point 9½ L							Influence Load 1 at Point 8½ L								
				M	$\frac{M}{I}$	$\frac{My}{I}$	$\frac{Mx}{I}$	M ₀	H ₀ y	V ₀ x	Total Mom.	M	$\frac{M}{I}$	$\frac{My}{I}$	$\frac{Mx}{I}$	M ₀	H ₀ y	V ₀ x	Total Mom.
11L	0.21	-1.2	2.0	0	0	0		1.58	-0.82	0.52	+1.3	0				0.96	-0.65	0.35	+0.66
10L	0.30	-1.1	6.0	0	0	0		"	-0.75	1.57	+2.4	0				"	-0.60	1.06	+1.42
9L	0.50	-0.9	10.0	-2.0	-4.0	+3.6	-4.0	"	-0.61	2.62	+1.6	0				"	-0.49	1.76	+2.23
8L	0.92	-0.7	14.0	-6.0	-6.5	+4.6	-9.1	"	-0.47	3.67	-1.2	-2.0	-2.2	+1.5	-3.0	"	-0.38	2.46	+1.04
7L	1.90	-0.3	18.0	-10.0	-5.2	+1.6	-9.5	"	-0.20	4.71	-3.9	-6.0	-3.2	+0.9	-5.7	"	-0.16	3.17	+2.03
6L	4.17	+0.1	22.0	-14.0	-3.4	-0.3	-7.4	"	+0.07	5.76	-6.6	-10.0	-2.4	-0.2	-5.3	"	+0.05	3.87	-5.12
5L	6.03	+1.1	25.8	-17.8	-3.0	-3.3	-7.6	"	+0.75	6.76	-8.7	-13.8	-2.3	-2.5	-5.9	"	+0.60	4.54	-7.7
4L	5.40	+5.0	26.2	-18.2	-3.4	-16.9	-8.8	"	+3.40	6.86	-6.35	-14.2	-2.6	-13.0	-6.9	"	+2.72	4.61	-5.9
3L	3.19	+9.0	25.9	-17.9	-5.6	-50.5	-14.5	"	+6.11	6.80	-3.4	-13.9	-4.4	-3.92	-11.3	"	+4.89	4.56	-3.5
2L	1.72	+13.0	25.6	-17.6	-10.2	-133.0	-26.2	"	+8.82	6.71	-0.5	-13.6	-7.9	-102.9	-20.3	"	+7.06	4.50	-1.1
1L	36.0	+16.0	25.5	-17.5	-0.5	-7.8	-12	"	+10.87	6.69	+1.65	-13.5	-0.4	-6.0	-9	"	+8.70	4.49	+0.65
1R				0				"	+10.87	-6.69	+5.75	0				"	+8.70	-4.49	+5.17
2R				0				"	+8.82	-6.71	+3.7	0				"	+7.06	-4.50	+3.52
3R				0				"	+6.11	-6.80	+0.9	0				"	+4.89	-4.56	+1.29
4R				0				"	+3.40	-6.86	-1.9	0				"	+2.72	-4.61	-0.93
5R				0				"	+0.75	-6.76	-4.43	0				"	+0.60	-4.54	-2.98
6R				0				"	+0.07	-5.76	-4.10	0				"	+0.05	-3.87	-2.86
7R				0				"	-0.20	-4.71	-3.33	0				"	-0.16	-3.17	-2.37
8R				0				"	-0.47	-3.67	-2.56	0				"	-0.38	-2.46	-1.88
9R				0				"	-0.61	-2.62	-1.65	0				"	-0.49	-1.76	-1.29
10R				0				"	-0.75	-1.57	-0.74	0				"	-0.60	-1.06	-0.70
11R				0				"	-0.82	-0.52	+0.24	0				"	-0.65	-0.35	-0.04
Σ					-41.8	-2020	-88.3						-25.4	-161.4	-593				

Point	I	y	x	Influence Load 1 at Point 7½ L							Influence Load 1 at Point 6½ L								
				M	$\frac{M}{I}$	$\frac{My}{I}$	$\frac{Mx}{I}$	M _o	H _o y	V _o x	Total Mom.	M	$\frac{M}{I}$	$\frac{My}{I}$	$\frac{Mx}{I}$	M _o	H _o y	V _o x	Total Mom.
11L	0.21	-1.2	2.0	0				0.56	-0.47	0.22	+0.31	0				0.30	-0.28	0.12	+0.14
10L	0.30	-1.1	6.0	0				"	-0.43	0.66	+0.79	0				"	-0.25	0.36	+0.41
9L	0.50	-0.9	10.0	0				"	-0.35	1.11	+1.32	0				"	-0.21	0.60	+0.69
8L	0.92	-0.7	14.0	0				"	-0.27	1.55	+1.84	0				"	-0.16	0.84	+0.98
7L	1.90	-0.3	18.0	-2.0	-1.0	+0.3	-19	"	-0.12	2.00	+0.44	0				"	-0.07	1.07	+1.30
6L	4.17	+0.1	22.0	-6.0	-1.4	-0.1	-32	"	+0.04	2.44	-2.96	-2.0	-0.5	0	-11	"	+0.02	1.32	-0.36
5L	6.03	+1.1	25.8	-9.8	-1.6	-1.8	-42	"	+0.43	2.86	-5.95	-5.8	-1.0	-1.1	-25	"	+0.25	1.54	-3.71
4L	5.40	+5.0	26.2	-10.2	-1.9	-9.4	-50	"	+1.95	2.91	-4.78	-6.2	-1.2	-5.7	-30	"	+1.15	1.57	-3.18
3L	3.19	+9.0	25.9	-9.9	-3.1	-2.79	-80	"	+3.50	2.88	-2.96	-5.9	-1.9	-16.6	-48	"	+2.07	1.55	-1.98
2L	1.72	+13.0	25.6	-9.6	-5.6	-72.5	-144	"	+5.05	2.84	-1.15	-5.6	-3.2	-42.3	-83	"	+2.99	1.53	-0.78
1L	36.0	+16.0	25.5	-9.5	-0.3	-4.2	-7	"	+6.22	2.83	+0.10	-5.5	-0.2	-2.5	-4	"	+3.68	1.52	0
1R				0				"	+6.22	-2.83	+3.95	0				"	+3.68	-1.52	+2.46
2R				0				"	+5.05	-2.84	+2.77	0				"	+2.99	-1.53	+1.76
3R				0				"	+3.50	-2.88	+1.18	0				"	+2.07	-1.55	+0.82
4R				0				"	+1.95	-2.91	-0.40	0				"	+1.15	-1.57	-0.12
5R				0				"	+0.43	-2.86	-1.87	0				"	+0.25	-1.54	-1.00
6R				0				"	+0.04	-2.44	-1.84	0				"	+0.02	-1.32	-1.00
7R				0				"	-0.12	-2.00	-1.56	0				"	-0.07	-1.07	-0.84
8R				0				"	-0.27	-1.55	-1.26	0				"	-0.16	-0.84	-0.70
9R				0				"	-0.35	-1.11	-0.90	0				"	-0.21	-0.60	-0.52
10R				0				"	-0.43	-0.66	-0.53	0				"	-0.25	-0.36	-0.31
11R				0				"	-0.47	-0.22	-0.13	0				"	-0.28	-0.12	-0.10
Σ					-14.9	-115.6	-374						-8.0	-68.2	-201				

Calculation of Reactions M_o H_o and V_o

Note that summations for "Frame Constants" are for the half arch.
For full arch, multiply by 2.

$M_o = \frac{-\sum \frac{M}{I}}{\sum \frac{1}{I}}$	$H_o = \frac{-\sum \frac{My}{I}}{\sum \frac{y^2}{I}}$	$V_o = \frac{\sum \frac{M_o x}{I} - \sum \frac{M_L x}{I}}{\sum \frac{x^2}{I}}$	$\sum \frac{M_o x}{I} = 0$
	M_o	H_o	V_o
Load at Crown	$\frac{112.3}{2 \times 13.23} = 4.25$	$\frac{241.9}{2 \times 148.6} = 0.82$	$\frac{1685}{2 \times 1683} = 0.50$
Load at $10\frac{1}{2}L$	$\frac{69.0}{2 \times 13.23} = 2.61$	$\frac{231.5}{2 \times 148.6} = 0.78$	$\frac{1255}{2 \times 1683} = 0.37$
Load at $9\frac{1}{2}L$	$\frac{41.8}{2 \times 13.23} = 1.58$	$\frac{202}{2 \times 148.6} = 0.68$	$\frac{883}{2 \times 1683} = 0.26$
Load at $8\frac{1}{2}L$	$\frac{25.4}{2 \times 13.23} = 0.96$	$\frac{161.4}{2 \times 148.6} = 0.54$	$\frac{593}{2 \times 1683} = 0.18$
Load at $7\frac{1}{2}L$	$\frac{14.9}{2 \times 13.23} = 0.56$	$\frac{115.6}{2 \times 148.6} = 0.39$	$\frac{374}{2 \times 1683} = 0.11$
Load at $6\frac{1}{2}L$	$\frac{8.0}{2 \times 13.23} = 0.30$	$\frac{68.2}{2 \times 148.6} = 0.23$	$\frac{201}{2 \times 1683} = 0.06$

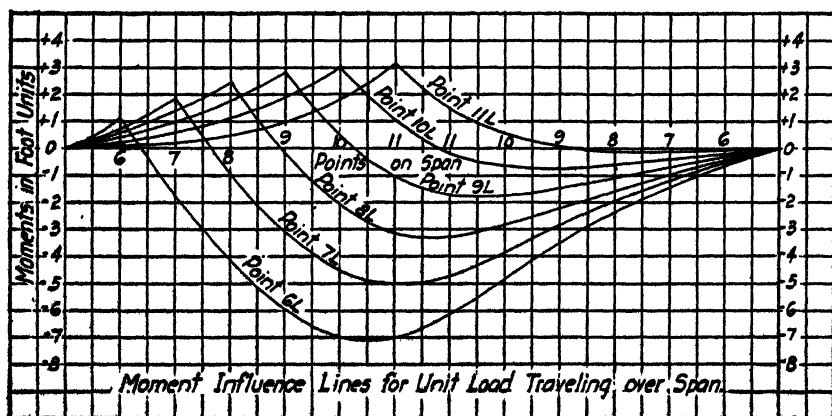


FIG. 35.

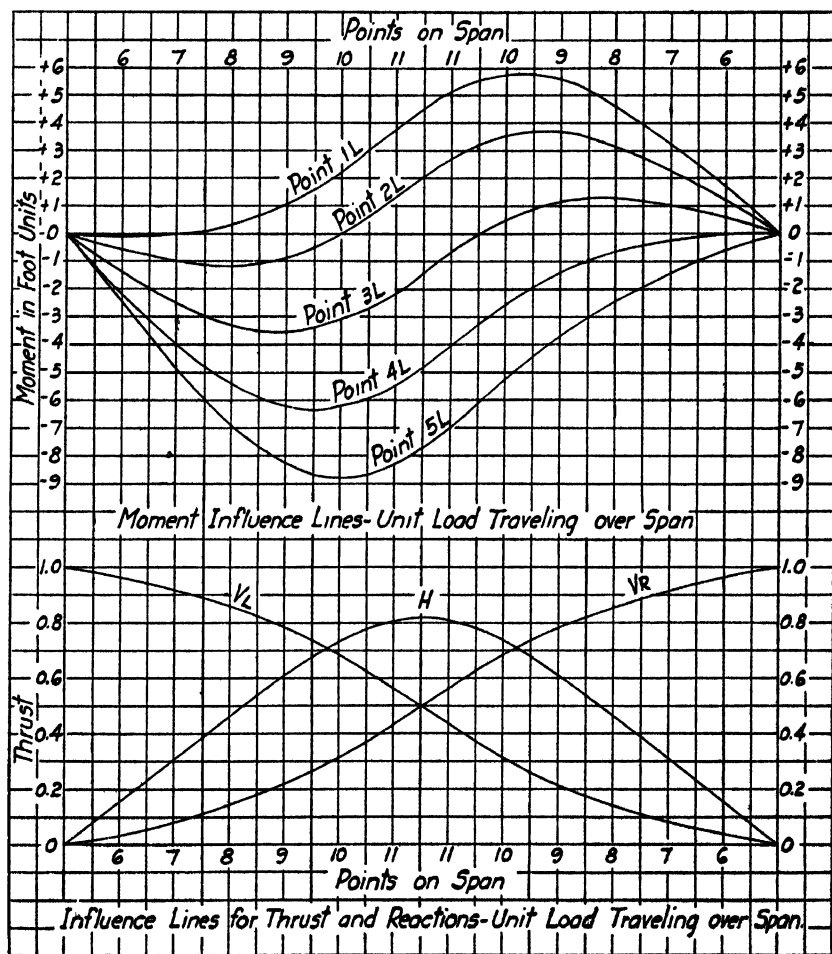


FIG. 36.

DEAD LOAD MOMENTS

Moment factors (MF) are scaled from the influence line diagram. The product of load and moment factor will give the actual dead load moment M.

POINT LOAD	POINT 1		POINT 2		POINT 3		POINT 4		POINT 5		POINT 6		POINT 7		POINT 8		POINT 9		POINT 10		POINT 11	
	NF	M	NF	M	NF	M	NF	M	NF	M	NF	M	NF	M	NF	M	NF	M	NF	M	NF	M
6L 2.7	0	0	-0.5	-1.4	-1.4	-3.8	-2.1	-5.7	-2.5	-6.9	-0.6	-1.6	-0.8	-2.2	-0.6	-1.6	-0.4	-1.1	-0.2	-0.5	-0.1	-0.3
7L 2.2	0	0	-1.0	-2.2	-2.5	-5.5	-4.0	-8.8	-4.8	-10.5	-1.7	-3.7	-1.4	-3.1	-1.4	-3.1	-1.0	-2.2	-0.6	-1.3	-0.2	-0.4
8L 1.8	+0.3	+0.5	-1.2	-2.2	-3.3	-5.9	-5.4	-9.7	-6.9	-12.4	-4.1	-7.4	-1.0	-1.8	-2.0	-3.6	-1.7	-3.1	-1.1	-2.0	-0.5	-0.9
9L 1.6	+1.0	+1.6	-0.9	-1.4	-3.6	-5.8	-6.2	-9.5	-8.3	-13.3	-5.9	-9.5	-3.1	-5.0	-0.2	-0.3	-2.5	-4.0	-1.8	-2.9	-0.9	-1.4
10L 1.5	+2.2	+3.3	0	0	-3.2	-4.8	-6.3	-9.4	-8.8	-13.2	-7.0	-10.5	-4.5	-6.8	-2.0	-3.0	-0.5	-0.7	-2.6	-3.9	-1.8	-2.7
11L 1.4	+3.8	+5.9	+1.4	+2.0	-2.2	-3.1	-5.5	-7.7	-8.3	-11.6	-7.0	-9.8	-5.0	-7.0	-3.2	-4.5	-1.0	-1.4	-1.0	-1.4	-2.7	-3.8
12L 1.4	+5.1	+7.1	+2.7	+3.8	-0.7	-1.0	-4.0	-5.6	-7.0	-9.8	-6.2	-8.7	-4.7	-6.6	-3.3	-4.6	-1.7	-2.4	-0.2	-0.3	-1.5	-2.1
13L 1.5	+5.8	+8.7	+3.5	+5.3	+0.8	+0.8	-2.6	-3.9	-5.2	-7.8	-4.8	-7.2	-3.9	-5.8	-2.8	-4.2	-1.8	-2.7	-0.6	-0.9	-0.5	-0.8
14L 1.6	+5.6	+9.0	+3.7	+5.9	+1.2	+1.9	-1.4	-2.2	-3.7	-5.9	-3.5	-5.6	-2.8	-4.5	-2.2	-3.5	-1.5	-2.4	-0.8	-1.3	-0.1	-0.2
15L 1.8	+4.6	+8.3	+3.2	+5.8	+1.3	+2.3	-0.6	-1.1	-2.4	-4.3	-2.4	-4.3	-2.4	-4.3	-1.6	-2.9	-1.1	-2.0	-0.6	-1.1	-0.1	-0.2
16L 2.2	+3.2	+7.0	+2.2	+4.8	+1.0	+2.2	-0.2	-0.4	-1.4	-3.1	-1.4	-3.1	-1.2	-2.6	-1.0	-2.2	-0.7	-1.5	-0.4	-0.9	-0.1	-0.2
17L 2.7	+1.7	+4.6	+1.2	+3.2	+0.6	+1.6	0	0	-0.6	-1.6	-0.7	-1.9	-0.6	-1.6	-0.5	-1.4	-0.4	-1.1	-0.2	-0.5	-0.1	-0.3
Σ			+23.0		-21.1		-64.4		-100.5		-70.1		-40.0		-18.3		-2.4		+7.0		+11.9	

Note: M.F. for divisions under the cusps of influence lines are, to scale, average ordinates.

DEAD LOAD THRUSTS

- Point (1) 228 - 0.8 = 22.0
 (2) 22.0 - 1.7 = 20.3
 (3) 20.3 - 1.8 = 18.5
 (4) 18.5 - 2.1 = 16.4

Point (5) N = Components at 45° of N and H

$$(16.4 - 3.2) \times 0.71 + 10.3 \times 0.71 = 16.7$$

Points 6 to 11: N = H as calculated from individual dead loads and

H-factors obtained from influence line, as follows:

$$[2.7 \times 0.15 + 2.2 \times 0.31 + 1.8 \times 0.46 + 1.6 \times 0.61 + 1.5 \times 0.74 + 1.4 \times 0.8] \times 2 = 10.3$$

Live Load Normal Thrusts

The tabulated normal thrusts for points (1) to (4) are the reactions V with the concentrations in the same position as for calculating maximum moments. N -factors ($N.F.$) for these points are obtained from influence line for V . At point (5) the normal thrust N is the resultant at 45° of V and H with 3.5 kip load at point $9\frac{3}{4}L$ and 0.9 kip load at $9\frac{3}{4}R$. Calculation as follows:

$$\begin{aligned}\text{For 3.5 load. } V \text{ factor} &= 0.71 \times 0.71 = 0.50 \\ H \text{ factor} &= 0.71 \times 0.71 = 0.50 \\ N \text{ factor} &= \underline{1.00}\end{aligned}$$

$$\begin{aligned}\text{For 0.9 load. } V \text{ factor} &= 0.71 \times 0.29 = 0.20 \\ H \text{ factor} &= 0.71 \times 0.71 = 0.50 \\ N \text{ factor} &= \underline{0.70}\end{aligned}$$

Temperature Stresses

c = coefficient of thermal expansion = 0.0000065.

t = 35° rise or 45° fall.

l = 51 feet.

E = $144 \times 2000000 = 288000000$ lbs. per sq. ft.

$$H = \pm \frac{Ectl}{5 \sum \frac{y^2}{I}} = \frac{288000000 \times 0.0000065 \times 35 \times 51}{4 \times 2 \times 148.6} = +2.8k$$

$$\text{or } H = -3.6k$$

Point	y	H_y	
11	-1.2	-3.4	+4.3
10	-1.1	-3.1	+3.9
9	-0.9	-2.5	+3.2
8	-0.7	-2.0	+2.5
7	-0.3	-0.8	+1.1
6	+0.1	+0.3	-0.4
5	+1.1	+3.1	-3.9
4	+5.0	+14.0	-18.0
3	+9.0	+25.2	-32.3
2	+13.0	+36.5	-46.7
1	+16.0	+44.9	-57.5

Temperature rise causes positive thrusts acting as shown in Fig. 34.

Temperature fall causes negative thrusts acting in the opposite direction.

Point	Wgt. Dist. between	Earth Press. Right-hand Loads (lateral)	Sum of Inc. of Partial Mom. M.	I	y	x	M	M _y	M _x	M ₀	H ₀ y	V ₀ x	Total Mom.	Sum
11R				0.21	-1.2	2.0				0.6	-0.8	0.2	0.0 11R	
10R				0.30	-1.1	6.0				0.6	-0.7	0.7	+0.6 10R	
9R				0.50	-0.9	10.0				0.6	-0.6	1.2	+1.2 9R	
8R				0.92	-0.7	14.0				0.6	-0.5	1.6	+1.7 8R	
7R				1.90	-0.3	18.0				0.6	-0.2	2.1	+2.5 7R	
6R				4.17	+0.1	22.0				0.6	0.0	2.6	+3.4 6R	
E6	1.1	0.2	0.22	6.03	+1.1	25.8	0.0	0.0	-0.9	0.6	+0.7	3.0	+4.1 5R	
5R	1.9	0.7	0.38	5.40	+5.0	26.2	-0.4	-2.2	-11.7	0.6	+3.2	3.1	+4.5 4R	
4R	2.0	1.2	0.9	3.19	+4.0	25.9	-2.6	-23.8	-60.2	0.6	+5.8	3.0	+1.0 3R	
3R	2.0	1.7	2.1	1.72	+13.0	25.6	-11.8	-152.5	-300.5	0.6	+8.4	3.0	-8.2 2R	
E2	1.5	1.6	3.8	36.0	+16.0	25.5	-0.9	-15.1	-24.1	0.6	+10.8	3.0	-20.0 1R	
1R	0.5	0.6	5.4											
E1			6.0											
0														

$\Sigma M = -\frac{\Sigma M}{\Sigma I} = -\frac{15.7}{2 \times 13.23} = +0.6$	$M_1, M_2, M_3 \text{ and } M_4 \text{ are 0 for points on the left cantilever half.}$	$\text{Total Mom.} = M + M_0 + H_0 y + V_0 x$
$H_0 = \frac{\Sigma M y}{\Sigma I} = -\frac{193.6}{2 \times 140.6} = +0.65$		
$V_0 = \frac{\Sigma M y - \Sigma M x}{\Sigma I} = \frac{-(-405.4)}{2 \times 1603} = +0.12$		

Fig. 37

Normal Thrust N at (S) inclined 45°
 Right: $-0.71 \times 0.12 + 0.71 \times 0.65 = 0.4$
 Left: $+0.71 \times 0.12 + 0.71 \times 0.65 = 0.5$

For individual earth pressure loads at the several points, see Fig. 2B

SUMMARY OF MAXIMUM MOMENTS (KIP FT.) AND NORMAL THRUSTS (KIPS)

LOADING	POINT 1		POINT 2		POINT 3		POINT 4		POINT 5		POINT 6		POINT 7		POINT 8	
	M	N	M	N	M	N	M	N	M	N	M	N	M	N	M	N
BREAD	+ 55.4	22.0	+ 23.6	20.3	- 21.1	18.5	- 64.4	16.4	- 100.3	16.7	- 70.2	10.3	- 40.0	10.3	- 18.3	10.3
EARTH S. LEFT	- 20.0	- 0.1	- 8.2	- 0.1	+ 1.0	- 0.1	+ 4.5	- 0.1	+ 4.1	0.4	+ 3.4	0.7	+ 2.5	0.7	+ 1.7	0.7
EARTH P. RIGHT	+ 8.0	+ 0.1	+ 6.0	+ 0.1	+ 3.4	+ 0.1	+ 0.7	+ 0.1	- 1.7	0.5	- 2.0	0.7	- 1.7	0.7	- 1.5	0.7
SUN TOTAL	+ 43.4	22.0	+ 21.4	20.3	- 16.7	18.5	- 59.2	16.4	- 97.9	16.6	- 68.8	11.7	- 39.2	11.7	- 18.1	11.7
LIVE +	+ 22.1	1.0	+ 14.0	0.9											+ 8.4	1.6
LIVE -			- 4.2	3.0	- 13.0	3.2	- 24.8	3.1	- 35.2	4.1	- 28.2	3.3	- 19.8	3.3	- 12.9	3.3
Temperature	+ 44.9	0	+ 36.5	0	+ 25.2	0	+ 14.0	0	+ 3.1	2.0	+ 0.3	2.8	- 0.8	2.8	- 2.0	2.8
TEMPERATURE	- 57.5	0	- 46.7	0	- 32.3	0	- 18.0	0	- 3.9	- 2.6	- 0.4	- 3.6	+ 1.1	- 3.6	+ 2.5	- 3.6
MAX. TOTAL +	+ 110.4	23.0	+ 71.9	21.2	+ 8.5	18.5	- 102.0	19.5	- 137.0	18.1	- 97.4	11.4	- 59.8	17.8	- 33.0	17.8
MAX. TOTAL -	- 14.1	22.0	- 29.5	23.3	- 62.0	21.7	- 102.0	19.5	- 137.0	18.1	- 97.4	11.4	- 59.8	17.8	- 33.0	17.8

[illegible]

Calculation for Reinforcement for $n=15$. Note that the thicknesses t of sections finally used are less than originally assumed for analysis. The error involved will be negligible. The reduction in section was made to develop the area of steel reinforcement selected.

Point	MOMENTS		N Lbs.	$e = \frac{M}{N}$ Inches	t Inches	$d = t - 2$ $e + \frac{t}{2} - 2$	\bar{y}' $\frac{N}{b d^2}$	$K = \frac{N}{b d^2}$	f_c	f_s	Reqd $\frac{P}{D}$	Reqd A_s sq. ins. per ft. width	A_s'
	Ft. lbs.	Inch Lbs.											
1	+10400	+1325000	23000	57.5	58	55	1.47	49	430	18000	0.0012	0.84	1
1	-14100	-159000	22000	7.7	60	58	35.7	20					1
2	+71900	+862000	21200	40.6	32	30	54.5	107	680	18000	0.0034	1.22	2
2	-29500	-354000	23300	15.2	32	30	29.2	63	500	18000	0.0003	0.11	2
3	+8500	+102000	18500	5.5	37	35	22.0	28					3
3	-62000	-744000	21700	34.2	37	35	50.7	76	550	18000	0.0018	0.76	3
4	-102000	-1223000	19500	62.9	42	40	81.9	83	580	18000	0.0030	1.44	4
5	-137000	-1644000	18100	90.7	45	43	111.2	91	610	18000	0.0037	1.91	5
6	-97400	-1170000	11400	102.6	50	48	125.6	52	450	18000	0.0020	1.15	6
7	-59800	-718000	17800	40.3	31.5	29.5	54.1	93	630	18000	0.0030	1.06	7
8	-33000	-396000	17800	22.2	25	23	32.7	92	620	18000	0.0022	0.61	8
9	-11800	-142000	17500	8.1	20	18	16.1	72	530	18000			9
9	+10800	+129600	10400	12.5	20	18	20.5	55	450	18000	0.0007	0.15	9
10	+21600	+259000	10900	23.8	17	15	30.3	122	750	18000	0.0043	0.78	10
11	+27300	+328000	11200	29.2	15	13	34.7	192	800	11000		2.26	0.42 11

Reinforcement for Point 11. Assume $k = 0.52$ $kd = 6.8$ $jd = 13 - \frac{6.8}{3} = 10.7$

$$f_s = 15 \times 800 \times \frac{6.8}{6.3} = 11000 \quad f_s' = 15 \times 800 \times \frac{4.8}{6.8} = 8500$$

$$\text{Moment to be carried} = N e' = 11200 \times 34.7 = 389000 \text{ inch lbs.}$$

$$\text{Normal Moment of Resistance} = 12 \times 6.8 \times 400 \times 10.7 = 350000$$

$$\text{To be carried by additional steel} = \frac{39000}{350000} = 0.111$$

$$\text{Reqd area compressive steel} = \frac{39000}{8500 \times 11} = 0.42 \text{ sq. ins.}$$

$$\text{Net area tension steel} = \frac{350000}{11000 \times 10.7} + \frac{39000}{11000 \times 11} = 2.26 \text{ sq. ins.}$$

Steel is required at the inside face (soffit) for positive moments and at the outside face for negative moments.

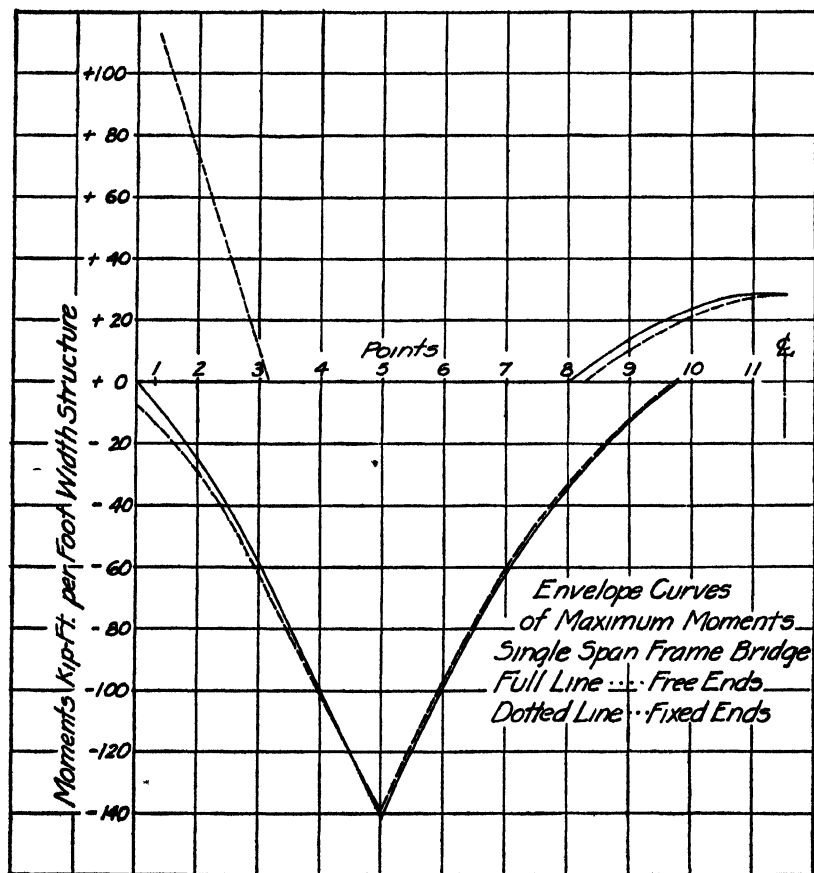


FIG. 38.

Several comparisons like that shown above have been made for single- and double-span rigid-frame bridges from which certain conclusions may be drawn as explained in Chapter XI.

CHAPTER VII

CALCULATIONS FOR UNSYMMETRICAL SINGLE-SPAN CONCRETE FRAME BRIDGE; FREE-END CONDITIONS

The calculation for earth pressure acting on the ends of the frame, it will be noticed, is made for a single load 2.5 kips (2500 lb.). This structure was designed to span a stream in which the water level is constant and can be relied upon to counteract or partly counteract the earth pressure below a certain elevation. The single earth pressure load indicated in Fig. 39 was therefore assumed as an approximation of the actual conditions and water pressure was neglected in the calculation.

The footings of this structure were in rock and a detail like that shown in Fig. 33*a* was designed.

In the Table of Frame Constants the steel areas A_s at the various points are not entered. This is for the reason that the approximate effect of the reinforcing steel upon the moments of inertia of the concrete sections had been determined in another like structure.

Influence load moments are calculated in Table 2 for the influence load at alternate points (17, 15, 13, etc.). The uncalculated peaks of the influence lines in Fig. 40, at 16, 14, 12, etc., may be accurately located by observing that all peaks are located on a smooth curve.

In Fig. 42 are plotted required steel areas, and actual steel areas determined from bar areas and spacings. From this plot, the cut-off points of bars may be found and the steel patterns of extrados rods and intrados rods may be arranged.

76 UNSYMMETRICAL CONCRETE FRAME BRIDGE

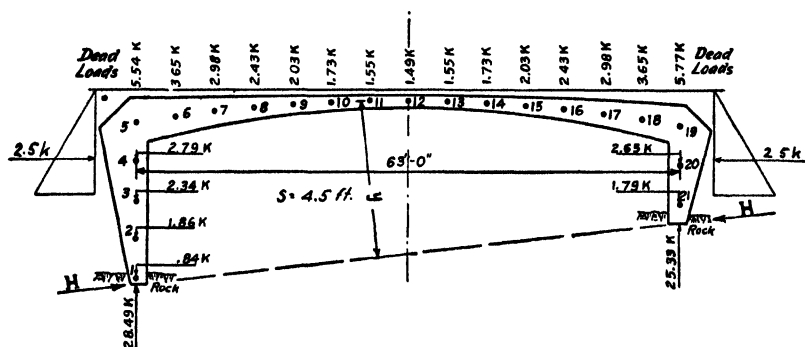


FIG. 39.

PROPERTIES OF SECTIONS 1 FT. WIDE IN FOOT UNITS

Point	Depth t	I_c	A_s	$D = \frac{t}{2} - 0.16$	$I_s = nA_sD^2$	$I = I_c + I_s$	y	$\frac{y^2}{I}$	x
				Per Cent					
1	2 04	0.71			11	0 79	0 3	0	
2	2 74	1.71			11	1 90	4.8	12	
3	3 44	3.49			16	4 05	9 2	21	
4	4 12	5.82			14	6 64	13 7	28	
5	4 50	7.60			13	8.58	18.2	39	
6	3 84	4.72			12	5 29	18.6	65	
7	3 13	2.56			10	2.82	18.8	125	
8	2 54	1.37			11	1.52	18.8	232	
9	2.08	0.75			16	0.87	18.6	397	
10	1.76	0.45			25	0 56	18.4	604	
11	1.57	0 32			30	0.42	18.1	780	
12	1.50	0.28			31	0.37	17.6	837	
13	1.57	0 32			30	0 42	17.1	697	
14	1.76	0.45			25	0 56	16.4	481	
15	2 08	0.75			16	0.87	15.7	284	
16	2.54	1.37			11	1.52	14.8	144	
17	3 13	2.56			10	2.82	13.8	68	
18	3.84	4.72			12	5.29	12.7	31	
19	4.50	7.60			13	8.58	11.2	15	
20	3.86	4.80			16	4.48	6.8	10	
21	2.62	1.50			11	1.66	2.3	3	
								$\Sigma = 4870$	

NOTE. The approximate ratios I_s/I_c shown in the next column were determined from another like structure and $I = I_c + I_s$ was calculated directly from I_c .

$$s = 4.5 \text{ ft.}$$

FREE-END CONDITIONS

77

Point	I	y	Influence Load at 17				Influence Load at 15				Influence Load at 13				Point
			Mom.	$\frac{My}{I}$	H_y	Total M	Mom.	$\frac{My}{I}$	H_y	Total M	Mom.	$\frac{My}{I}$	H_y	Total M	
1	0.79	0.3	0	-0.1	-0.1	0	-0.2	-0.2	0	-0.3	-0.3	1
2	1.90	4.8	0	-1.8	-1.8	0	-3.5	-3.5	0	-4.7	-4.7	2
3	4.05	9.2	0	-3.5	-3.5	0	-6.7	-6.7	0	-8.9	-8.9	3
4	6.64	13.7	0	-5.2	-5.2	0	-10.0	-10.0	0	-13.3	-13.3	4
5	8.58	18.2	0	-6.9	-6.9	0	-13.3	-13.3	0	-17.7	-17.7	5
6	5.29	18.6	1	4	-7.1	-6.1	2	7	-13.6	-11.6	3	11	-18.0	-15.0	6
7	2.82	18.8	3	13	-7.1	-5.1	4	27	-13.7	-9.7	6	40	-18.2	-12.2	7
8	1.52	18.8	3	37	-7.1	-4.1	6	74	-13.7	-7.7	9	111	-18.2	-9.2	8
9	0.87	18.6	4	86	-7.1	-3.1	8	171	-13.6	-5.6	12	257	-18.0	-6.0	9
10	0.56	18.4	5	164	-7.0	-2.1	10	328	-13.4	-3.4	15	493	-17.8	-2.8	10
11	0.42	18.1	6	259	-6.9	-0.9	12	517	-13.2	-1.2	18	775	-17.5	+0.5	11
12	0.37	17.6	7	333	-6.7	0.3	14	666	-12.8	+1.2	21	998	-17.1	+3.9	12
13	0.42	17.1	8	326	-6.5	1.5	16	651	-12.5	+3.5	24	977	-16.6	+7.4	13
14	0.56	16.4	9	264	-6.2	2.8	18	528	-12.0	+6.0	20	587	-15.9	+4.1	14
15	0.87	15.7	10	181	-6.0	4.0	20	361	-11.5	+8.5	16	289	-15.2	+0.8	15
16	1.52	14.8	11	107	-5.6	5.4	15	146	-10.8	+4.2	12	117	-14.3	-2.3	16
17	2.82	13.8	12	59	-5.2	6.8	10	49	-10.1	-0.1	8	39	-13.4	-5.4	17
18	5.29	12.7	6	14	-4.8	1.2	5	12	-9.3	-4.3	4	10	-12.3	-8.3	18
19	8.58	11.2	0	-4.3	-4.3	0	-8.2	-8.2	0	-10.9	-10.9	19
20	4.48	6.8	0	-2.6	-2.6	0	-5.0	-5.0	0	-6.6	-6.6	20
21	1.66	2.3	0	-0.9	-0.9	—	0	-1.7	-1.7	0	-2.2	-2.2	21
Σ	1847	3537	4704	
			$H = \frac{\sum My}{\sum y^2} = \frac{1847}{4870} = 0.38$				$H = \frac{3537}{4870} = 0.73$				$H = \frac{4704}{4870} = 0.97$				

Influence Load used in calculating these tables = $\frac{14}{4.5 \times 2} = \frac{14}{9}$. Therefore "Total M" calculated above are multiplied by $\frac{9}{14}$ to obtain ordinates in Influence Line Diagram for unit load.

Point	I	y	Influence Load at II				Influence Load at 9				Influence Load at 7				Point
			Mom.	$\frac{My}{I}$	H_y	Total M	Mom.	$\frac{My}{I}$	H_y	Total M	Mom.	$\frac{My}{I}$	H_y	Total M	
1	0.79	0.3	0	-0.3	-0.3	90	-0.2	-0.2	0	-0.1	-0.1	1
2	1.90	4.8	0	-4.7	-4.7	0	-3.6	-3.6	0	-1.9	-1.9	2
3	4.05	9.2	0	-9.0	-9.0	0	-6.9	-6.9	0	-3.7	-3.7	3
4	6.64	13.7	0	-13.4	-13.4	0	-10.3	-10.3	0	-5.5	-5.5	4
5	8.58	18.2	0	-17.8	-17.8	0	-13.7	-13.7	0	-7.3	-7.3	5
6	5.29	18.6	4	14	-18.2	-14.2	5	18	-14.0	-9.0	6	21	-7.4	-1.4	6
7	2.82	18.8	8	53	-18.4	-10.4	10	67	-14.1	-4.1	12	80	-7.5	+4.5	7
8	1.52	18.8	12	149	-18.4	-6.4	15	186	-14.1	+0.9	11	136	-7.5	+3.5	8
9	0.87	18.6	16	342	-18.2	-2.2	20	428	-14.0	+6.0	10	214	-7.4	+2.6	9
10	0.56	18.4	20	657	-18.0	+2.0	18	591	-13.8	+4.2	9	296	-7.4	+1.6	10
11	0.42	18.1	24	1033	-17.7	+6.3	16	689	-13.6	+2.4	8	345	-7.2	0.8	11
12	0.37	17.6	21	998	-17.3	+3.7	14	666	-13.2	+0.8	7	333	-7.0	+0	12
13	0.42	17.1	18	733	-16.8	+1.2	12	488	-12.8	-0.8	6	244	-6.8	-0.8	13
14	0.56	16.4	15	440	-16.1	-1.1	10	293	-12.3	-2.3	5	147	-6.6	-1.6	14
15	0.87	15.7	12	217	-15.4	-3.4	8	144	-11.8	-3.8	4	72	-6.3	-2.3	15
16	1.52	14.8	9	88	-14.5	-5.5	6	58	-11.1	-5.1	3	29	-5.9	-2.9	16
17	2.82	13.8	6	29	-13.5	-7.5	4	20	-10.3	-6.3	2	10	-5.5	-3.5	17
18	5.29	12.7	3	7	-12.4	-9.4	2	5	-9.5	-7.5	1	2	-5.1	-4.1	18
19	8.58	11.2	0	-11.0	-11.0	0	-8.4	-8.4	0	-4.5	-4.5	19
20	4.48	6.8	0	-6.7	-6.7	0	-5.1	-5.1	0	-2.7	-2.7	20
21	1.66	2.3	0	-2.3	-2.3	0	-1.7	-1.7	0	-0.9	-0.9	21
Σ				4760				3653				1929			
			$H = \frac{4760}{4870} = 0.98$				$H = \frac{3653}{4870} = 0.75$				$H = \frac{1929}{4870} = 0.40$				

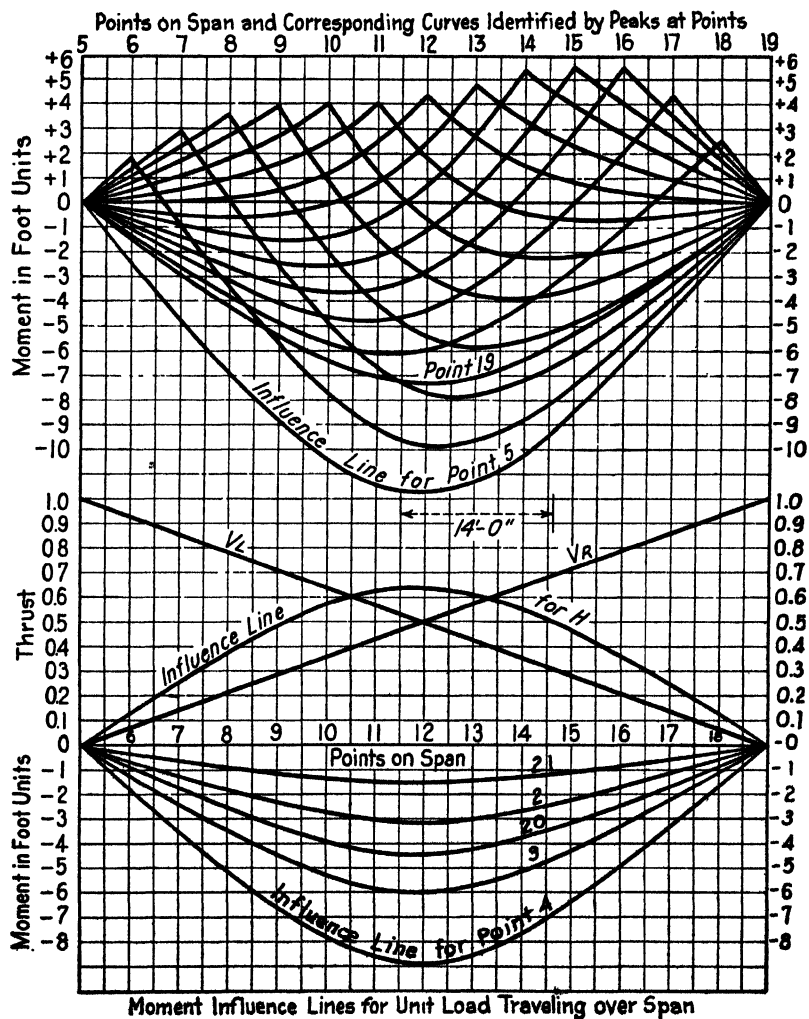


FIG. 40.

80 UNSYMMETRICAL CONCRETE FRAME BRIDGE

DEAD LOAD MOMENTS

Moment factors (*MF*) are scaled from the influence line diagram. The product of load and moment factor will give the actual dead load moment *M*.

Point	Load	Point 3		Point 5		Point 7		Point 9		Point 11		Point 12	
		<i>MF</i>	<i>M</i>	<i>MF</i>	<i>M</i>	<i>MF</i>	<i>M</i>	<i>MF</i>	<i>M</i>	<i>MF</i>	<i>M</i>	<i>MF</i>	<i>M</i>
6	3.65	-1.2	-4.4	-2.4	-8.8	+1.4	+5.1	+0.8	+2.9	+0.2	+0.7	0	0
7	2.98	-2.4	-7.2	-4.7	-14.0	+2.9	+8.6	+1.7	+5.1	+0.5	+1.5	+0.1	+0.3
8	2.43	-3.4	-8.3	-6.9	-16.8	+0.1	+0.2	+2.7	+6.6	+1.0	+2.4	+0.2	+0.5
9	2.03	-4.4	-8.9	-8.8	-17.9	-2.5	-5.1	+3.9	+7.9	+1.6	+3.2	+0.5	+1.0
10	1.73	-5.2	-9.0	-10.4	-18.0	-4.9	-8.5	+0.9	+1.6	+2.5	+4.3	+1.2	+2.1
11	1.55	-5.8	-9.0	-11.4	-17.7	-6.7	-10.4	-1.4	-2.2	+4.0	+4.6	+2.5	+3.9
12	1.49	-6.0	-8.9	-11.7	-17.4	-7.7	-11.5	-3.0	-4.5	+1.8	+2.7	+4.4	+6.6
13	1.55	-5.7	-8.8	-11.3	-17.5	-7.8	-12.1	-3.7	-5.7	+0.3	+0.5	+2.6	+4.0
14	1.73	-5.2	-9.0	-10.3	-17.8	-7.2	-12.4	-3.9	-6.7	-0.4	-0.7	+1.5	+2.6
15	2.03	-4.3	-8.7	-8.6	-17.5	-6.2	-12.6	-3.5	-7.1	-0.7	-1.4	+0.9	+1.8
16	2.43	-3.3	-8.0	-6.5	-15.8	-4.9	-11.9	-2.8	-6.8	-0.7	-1.7	+0.4	+1.0
17	2.98	-2.3	-6.9	-4.4	-13.1	-3.3	-9.8	-2.0	-6.0	-0.6	-1.8	+0.2	+0.6
18	3.65	-1.1	-4.0	-2.2	-8.0	-1.7	-6.2	-1.0	-3.6	-0.3	-1.1	0	0
$\frac{1}{2} =$	15.12												
Totals	-101.1	-200.3	-86.6	-18.5	+13.2	+24.4

Point	Load	Point 13		Point 15		Point 17		Point 19		Point 21	
		<i>MF</i>	<i>M</i>	<i>MF</i>	<i>M</i>	<i>MF</i>	<i>M</i>	<i>MF</i>	<i>M</i>	<i>MF</i>	<i>M</i>
6	3.65	-0.3	-1.1	-0.7	-2.6	-1.1	-4.0	-1.5	-5.5	-0.3	-1.1
7	2.98	-0.5	-1.5	-1.4	-4.2	-2.2	-6.6	-2.9	-8.6	-0.6	-1.8
8	2.43	-0.6	-1.5	-2.0	-4.9	-3.1	-7.5	-4.2	-10.2	-0.9	-2.2
9	2.03	-0.5	-1.0	-2.4	-4.9	-4.1	-8.3	-5.4	-11.0	-1.1	-2.2
10	1.73	-0.1	-0.2	-2.5	-4.3	-4.6	-8.0	-6.4	-11.1	-1.3	-2.2
11	1.55	+0.8	+1.2	-2.2	-3.4	-4.8	-7.4	-7.1	-11.0	-1.5	-2.3
12	1.49	+2.4	+3.6	-1.1	-1.6	-4.3	-6.4	-7.3	-10.9	-1.5	-2.2
13	1.55	+4.8	+7.4	+0.6	+0.9	-3.4	-5.3	-7.0	-10.8	-1.4	-2.2
14	1.73	+3.3	+5.7	+2.8	+4.8	-1.9	-3.3	-6.4	-11.1	-1.3	-2.2
15	2.03	+2.3	+4.7	+5.5	+11.2	0	0	-5.4	-11.0	-1.1	-2.2
16	2.43	+1.5	+3.6	+4.0	+9.7	+2.1	+5.1	-4.2	-10.2	-0.9	-2.2
17	2.98	+0.9	+2.7	+2.6	+7.7	+4.3	+12.8	-2.9	-8.6	-0.6	-1.8
18	3.65	+0.4	+1.5	+1.3	+4.7	+2.1	+7.7	-1.4	-5.1	-0.4	-1.5
$\frac{1}{2} =$	15.12										
Totals	+25.1	+13.1	-31.2	-125.1	-26.1

Dead Load Thrusts:

V_L (loads) 28.49	V_R (loads) 25.33
V.C. of H 1.24	V.C. of H 1.24
Point 1: 29.73	Point 21: 24.09
0.84	1.79
Point 2: 28.89	Point 20: 22.30
1.86	2.65
Point 3: 27.03	19.65
2.34	
Point 4: 24.69	
2.79	
21.90	

Points 5 and 19: N = components @ 45° of V and H .

Point 5: $N = 21.9 \times 0.71 + 11.19 \times 0.71 = 23.5$

Point 19: $N = 19.65 \times 0.71 + 11.19 \times 0.71 = 21.9$

Points 6 to 18: N = approximately H , as calculated from individual dead loads and H factors, obtained from influence line for H .

$$3.65 \times 0.13 + 2.98 \times 0.26 + 2.43 \times 0.38 + 2.03 \times 0.48 + 1.73 \times 0.57 + 1.55 \times 0.63 + 1.49 \times 0.64 + 1.55 \times 0.60 + 1.73 \times 0.55 + 2.03 \times 0.47 + 2.43 \times 0.36 + 2.98 \times 0.25 + 3.65 \times 0.13 = 11.19.$$

LIVE LOAD 20-TON TRUCKS

Axle loads 32,000 and 8000 lb. on 9-ft. lane. Reduction (up to 25 per cent) 1 per cent per foot width of roadway in excess of 18 ft. Roadway on this bridge 30 ft. Reduction 12 per cent. Impact allowance 25 per cent. Concentrations, on 14-ft. wheel base, per foot width of bridge

$$\frac{32000}{9} \times 0.88 \times 1.25 = 3.9 \text{ kips;}$$

$$\frac{8000}{9} \times 0.88 \times 1.25 = 1.0 \text{ kip.}$$

Normal thrusts N for points 1, 2, 3, 4, 20, 21 are vertical reactions V , calculated from influence lines for V , with loads in same position as when calculating corresponding moments, corrected for the vertical component of H .

Normal thrusts for points 5 and 19 are resultants at 45° of V and H with loads in same position as when calculating corresponding moments.

Points 3 and 5. Rear axle at point $11\frac{1}{2}$; front axle at $14\frac{1}{2}$.

Point 3

$$V_L = 0.53 \times 3.9 + 0.31 = 2.38.$$

$$H = 0.64 \times 3.9 + 0.50 = 3.00.$$

$$N = 2.38 + \frac{1}{9} \times 3.00 = 2.71.$$

Point 5

$$N = 0.71 (2.71 + 3.00) = 4.05$$

Points 19 and 21. Rear axle at point $12\frac{1}{2}$; front axle at $9\frac{1}{2}$. Factors same as for points 3 and 5.

$$\text{Point 21. } N = 2.38 - \frac{1}{9} \times 3 = 2.05.$$

$$\text{Point 19. } N = 0.71(2.05 + 3.0) = 3.58.$$

CONCENTRATED LIVE LOAD MOMENTS M AND NORMAL THRUSTS N

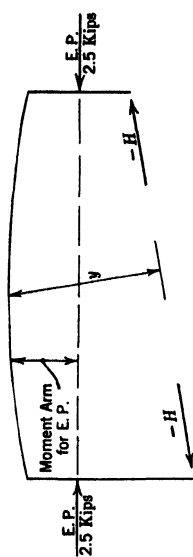
Moment Factors (MF) and Thrust Factors (NF) are read directly from Influence Line Diagrams. The product of load and moment factor gives actual moments M and product of load and thrust factor gives actual thrusts N . Note that the position of the load system is not necessarily the same for maximum positive M and N as for maximum negative M and N .

Load (Kips)	Point 3			Point 5			Point 7			Point 9			Point 9		
	MF	M	NF	MF	M	NF	MF	M	NF	MF	M	NF	MF	M	NF
3.9	-6.0	-23.4	-11.7	-45.6	-7.8	-30.4	-0.63	-3.9	-15.2	0.58	-2.3	+3.8	0.48
1.0	-4.7	-4.7	-9.3	-9.3	-5.8	-5.8	-0.43	-2.3	-2.3	0.29	0.3
Total	-28.1	2.7	-54.9	4.1	-36.2	-17.5	+14.8	1.9

Load (Kips)	Point 11			Point 12			Point 13			Point 15			Point 15		
	MF	M	NF	MF	M	NF	MF	M	NF	MF	M	NF	MF	M	NF
3.9	+4.1	+16.0	0.63	+4.4	+17.2	0.64	+4.8	+18.7	0.60	+5.5	+21.4	0.47	+5.5	-2.5	0.59
1.0	+0.9	+0.9	0.37	+0.8	+0.8	0.45	+1.5	+1.5	0.35	+1.2	+1.2	0.12	+1.2	-1.4	0.27
Total	+16.9	2.9	+18.0	3.0	+20.2	+22.6	-11.2	2.6

Load (Kips)	Point 17			Point 19			Point 21		
	MF	M	NF	MF	M	NF	MF	M	NF
3.9	-4.8	-18.7	0.63	-7.4	-28.9	-1.5	-5.8
1.0	-3.0	-3.0	0.37	-5.3	-5.3	-1.3	-1.3
Total	-21.7	2.9	-34.2	3.6	-7.1	2.1

Point	Moment Arm for E.P.	Load, Kips	Moment, Kip-ft.	y	I	$\frac{My}{I}$	H_y	Total Moment Kip-ft.	Point
1	0.3	0.79	+ 0.3	+ 0.3	1
2	4.8	1.90	+ 4.4	+ 4.4	2
3	9.2	4.05	+ 8.5	+ 8.5	3
EP	2.5	13.7	6.64	+ 12.6	+ 12.6	4
5	4.1	2.5	-10.2	18.2	8.58	- 22	+ 16.7	+ 6.5	5
6	4.8	2.5	-12.0	18.6	5.29	- 42	+ 17.1	+ 5.1	6
7	5.4	2.5	-13.5	18.8	2.82	- 90	+ 17.3	+ 3.8	7
8	5.9	2.5	-14.8	18.8	1.52	- 183	+ 17.3	+ 2.7	8
9	6.3	2.5	-15.7	18.6	0.87	- 336	+ 17.1	+ 1.4	9
10	6.7	2.5	-16.8	18.4	0.56	- 552	+ 16.9	+ 0.1	10
11	6.8	2.5	-17.0	18.1	0.42	- 732	+ 16.7	- 0.3	11
12	6.8	2.5	-17.0	17.6	0.37	- 810	+ 16.2	- 0.8	12
13	6.8	2.5	-17.0	17.1	0.42	- 692	+ 15.7	- 1.3	13
14	6.7	2.5	-16.8	16.4	0.56	- 492	+ 15.1	- 1.7	14
15	6.3	2.5	-15.7	15.7	0.87	- 283	+ 14.4	- 1.3	15
16	5.9	2.5	-14.8	14.8	1.52	- 144	+ 13.6	- 1.2	16
17	5.4	2.5	-13.5	13.8	2.82	- 66	+ 12.7	- 0.8	17
18	4.8	2.5	-12.0	12.7	5.29	- 29	+ 11.7	- 0.3	18
19	4.1	2.5	-10.2	11.2	8.58	- 13	+ 10.3	+ 0.1	19
EP	2.5	6.8	4.48	+ 6.3	+ 6.3	20
21	2.3	1.66	+ 2.1	+ 2.1	21
Σ	- 4486



$$\Sigma \frac{My}{I} = \frac{4486}{4870} = 0.9 \text{ kip.}$$

$$-H = \frac{4486}{4870} = 0.9 \text{ kip.}$$

Normal Thrusts N :

- Sections 6 to 18. $N = 2.5 - 0.9 = 1.6$.
- Sections 1 to 4. $N = -\frac{1}{3} \times 0.9 = -0.1$.
- Sections 20 and 21. $N = +0.1$.
- Section 5. $N = 0.71(1.6 - 0.1) = 1.1$
- Section 19. $N = 0.71(1.6 + 0.1) = 1.2$.

Calculations: Earth pressure at both ends.

Earth pressure loads below that shown are practically balanced by water pressure.

TEMPERATURE STRESSES

$$H = \frac{EctI}{\sum y^2} \quad t = + 35^\circ \text{ or } -45^\circ.$$

For $+ 35^\circ$, $H =$

$$\frac{144 \times 2,000,000 \times 0.0000065 \times 35 \times 63}{4.5 \times 4870} = + 0.19 \text{ kip.}$$

For -45° , $H = - 0.24 \text{ kip.}$ Moment = Hy for each point.
Positive thrusts cause negative moments, and vice versa.

Point 5. $N = 0.71 (0.19 + \frac{1}{8} \times 0.19) = 1.5$ for 35° rise.
 $- 0.71 (0.24 + \frac{1}{8} \times 0.24) = - 1.9$ for 45° fall.

Point 19. $N = 0.71 (0.19 - \frac{1}{8} \times 0.19) = 1.2$ for 35° rise.
 $- 0.71 (0.24 - \frac{1}{8} \times 0.24) = - 1.5$ for 45° fall.

DIAGRAM SHOWING REQUIRED AND ACTUAL AREAS
OF STEEL REINFORCEMENT

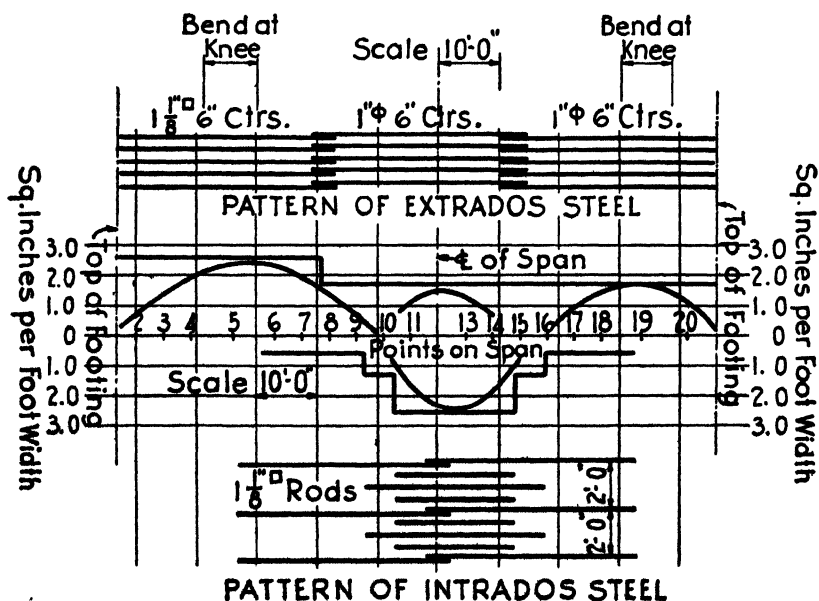


FIG. 42.

SUMMARY OF MAXIMUM MOMENTS (KIP-FT.) AND NORMAL THRUSTS (KIPS)

Loading	Point 3		Point 5		Point 7		Point 9	
	M	N	M	N	M	N	M	N
Dead.....	-101.1	27.0	-200.3	23.5	-86.6	11.2	-18.5	11.2
Earth Pressure.....	+ 8.5	- 0.1	+ 6.5	1.1	+ 3.8	1.6	+ 1.4	1.6
Subtotal.....	- 92.6	26.9	-193.8	24.6	-82.8	12.8	-17.1	12.8
Live +.....							+14.8	1.9
Live -.....	- 28.1	2.7	- 54.9	4.1	- 36.2	2.9	-17.5	2.6
Temperature.....	+ 2.2	- 0.3	+ 4.4	- 1.9	+ 4.5	- 0.2	+ 4.5	- 0.2
Temperature.....	- 1.8	+ 0.2	- 3.5	+ 1.5	- 3.6	+ 0.2	- 3.5	+ 0.2
Maximum total.....							+ 2.2	14.5
Maximum total.....	-122.5	29.8	-251.2	30.2	-122.6	15.9	-38.1	15.6

Loading	Point 11		Point 12		Point 13		Point 15	
	M	N	M	N	M	N	M	N
Dead.....	+ 13.2	11.2	+ 24.4	11.2	+ 25.1	11.2	+13.1	11.2
Earth pressure.....	- 0.3	1.6	- 0.8	1.6	- 1.3	1.6	- 1.3	1.6
Subtotal.....	+ 12.9	12.8	+ 23.6	12.8	+ 23.8	12.8	+11.8	12.8
Live +.....	+ 16.9	2.9	+ 18.0	3.0	+ 20.2	2.8	+22.6	1.9
Live -.....							-11.2	2.6
Temperature.....	+ 4.4	- 0.2	+ 4.2	- 0.2	+ 4.1	- 0.2	+ 3.8	- 0.2
Temperature.....	- 3.4	+ 0.2	- 3.3	+ 0.2	- 3.2	+ 0.2	- 3.0	+ 0.2
Maximum total.....	+ 34.2	+15.5	+ 45.8	15.6	+ 48.1	+15.4	+38.2	14.5

Loading	Point 17		Point 19		Point 21			
	M	N	M	N	M	N		
Dead.....	- 31.2	11.2	-125.1	21.9	- 26.1	24.1		
Earth Pressure.....	- 0.8	1.6	+ 0.1	1.2	+ 2.1	0.1		
Subtotal.....	- 32.0	12.8	-125.0	23.1	- 24.0	24.1		
Live.....	- 21.7	2.9	- 34.2	3.6	- 7.1	2.1		
Temperature.....	+ 3.3	- 0.2	+ 2.7	- 1.5	+ 0.6	- 0.2		
Temperature.....	- 2.6	+ 0.2	- 2.1	+ 1.2	- 0.4	+ 0.3		
Maximum total.....	- 56.3	15.9	-161.3	27.9	- 31.5	26.5		

CALCULATION OF STEEL REINFORCEMENT

Point	Moment Ft. Lbs.	Inch-Lbs.	N = M/N	Arm e Inches	t Inches	d = t-2	e' = e + $\frac{t}{2}$	$\frac{e'}{d}$	K = $\frac{N e'}{b d^2}$	f_c Lbs. per Sq. In.	f_s Lbs. per Sq. In.	Reqd P	Reqd As = Pbd	Reqd As = Comp Steel	Point
3	-172300	-1470000	29800	49.4	46.5	44.2	70.7	1.6	89	600	18000	.0026	1.34	—	3
5	-251200	-3015000	30200	59.9	43.0	61.0	119.5	2.1	88	600	18000	.0032	2.34	—	5
7	-122600	-1470000	15700	92.5	41.9	99.9	111.5	2.8	93	600	18000	.0040	1.92	—	7
9	-38100	-457000	5600	29.4	26.2	24.2	40.5	1.7	90	600	18000	.0021	0.78	—	9
11	341000	4100000	15500	26.4	18.8	16.8	13.8	8	2.1	154	800	14200	.0074	1.49	11
12	45800	1550000	15600	35.2	18.0	16.0	14.2	2	2.1	84	800	14000	.0074	1.49	12
13	48100	577000	5700	31.5	18.8	16.8	44.9	2.7	204	800	14000	—	2.35	1.23	13
15	31700	453000	4500	31.6	25.0	23.0	42.1	1.8	96	620	18000	.0030	0.83	—	15
17	56300	675000	5900	42.4	37.6	35.6	59.2	1.7	62	410	18000	.0018	0.77	—	17
19	-161300	-1940000	27900	69.5	54.0	52.0	94.5	1.8	81	575	18000	.0026	1.62	—	19
21	-31500	-378000	26500	14.3	31.4	29.4	28.0	0.9	72	525	18000	.0003	—	—	21

Note: Final depths of sections 1 to 9 were increased to make $1\frac{1}{8}$ inch square rods at 6 inch centers effective around the knee. The increase over tentative sections will make no appreciable error in calculation of H. Tensile steel reinforcement is required near the soffit (inside face) of the frame, for positive moment near the back (outside face) for negative moment.

CALCULATION OF REINFORCEMENT FOR POINT 13

Assume $k = 0.46$ $kd = 7.4$ $j = 16 - \frac{7.4}{3} = 13.6$

$f_s = 800 \times 15 \times \frac{8.6}{7.4} = 14000$ $f_s = 800 \times 15 \times \frac{5.1}{7.4} = 8700$

Moment to be carried = $N e = 15600 \times 42.2 = 658000$

Moment of Resistance $12 \times 7.4 \times 400 \times 13.6 = 480000$

To be carried by additional steel = 178000

$A_s = \frac{178000}{8700 \times 14} = 1.46 \text{ in}^2$

$A_s = \frac{480000}{14000 \times 13.6} + \frac{178000}{14000 \times 14} - \frac{15600}{14000} = 2.33 \text{ in}^2$

To be carried by additional steel = 162000

$A_s = \frac{162000}{8900 \times 14.8} = 1.23 \text{ in}^2$

$A_s = \frac{530000}{14000 \times 14.2} + \frac{162000}{14000 \times 14.8} - \frac{15400}{14000} = 2.35 \text{ in}^2$

CHAPTER VIII

CALCULATIONS FOR SYMMETRICAL SINGLE-SPAN STEEL GIRDER FRAME BRIDGE

In the following pages only those portions of the design which are peculiar to the rigid-frame type of construction are given. Design calculations are not given for the floor slab; the girder bases; the footings; the cross-frames which provide lateral support to the girder flanges and also act as floor-beams; the end walls retaining the approach fill and reinforced as vertical slabs spanning between the vertical legs of the frame girders; the connection between the component parts of the structure. This part of the design involves nothing new. When the maximum moments, thrusts and shears have been calculated for various points along the girders, the design of stiffeners, splices and determination of rivet spacing may be carried forward as for ordinary girders subjected to combined bending and direct stress.

In these calculations the effect of the concrete protective encasement of the vertical legs of the girders has been neglected both in calculating the moments of inertia and in proportioning the sections. Also the effect of non-parallelism of the girder flanges, which tends to increase slightly the flange stresses and decrease slightly the shears, has been neglected.

The curved portion of the girder at the knee or bend demands special consideration. In this region there is a strong tendency for web buckling and also tendency of the outstanding portions of both flanges to curl inward on account of the change in direction of flange stress. Closely spaced radial stiffeners faced to bear on the outstanding legs of both flanges are therefore used as shown in the details.

In addition, the curvature of the girder in this region affects the position of the neutral axis, throwing it inward from the center of gravity of the section toward the concave flange—in this case the compression flange. This tends to increase the stress in the compression flange and decrease that in the tension flange as calculated for the neutral axis at the center of gravity of the section. The formulas for the position of the neutral axis of a curved beam in which the curves of the outer and inner flanges or faces are concentric are given in Fuller and Johnston's *Applied Mechanics*, Volume II, and other standard textbooks on Mechanics. These formulas do not apply in this case, however, as the flange curves are not concentric. The derivation of formulas for such a case would be a complicated process if not impossible and a summation process of calculation remains to be developed. Until this is done, only approximations can be made based on the formulas for concentric curvature of both flanges and making allowance for the factors that tend to increase or decrease the calculated flange stresses. Such a calculation is not given here as the process of approximation will vary with each particular case. As a result of the approximation used in the design of this bridge, one cover plate was added to the section assumed for calculation of reactions as shown in Fig. 46.

The design of only a few girder sections is given in the following calculations. The procedure is the same for points 2, 4, 6 and 8 as for points 1, 3, 5, 7 and 9. The allowable unit stress in the compression flange at points 4, 5, 6 and 7 is calculated for an unsupported length of 11.5 ft. between cross-frames or floor-beams. The compression flange at points 1, 2 and 3 is embedded in the reinforced-concrete back-wall retaining the approach fill, and higher unit stresses are permissible. The compression flange at point 9 is supported laterally by the floor slab, and higher unit stresses are permissible.

A calculation for stresses at point 3 is given based on

the assumption that the neutral axis is at the center of gravity of the section.

It will be observed that axis divisions of considerable length (7.67 ft.) are used in this calculation. This was done for the purpose of illustrating the method of design without an undue quantity of figures. In the original calculation for this bridge, the axis was divided into 30 divisions whereas in this calculation 17 divisions are shown. An interesting result of this recalculation was the comparison of results which showed almost precise agreement. In other words, the use of the longer divisions resulted in no appreciable error.

The girder depths shown in Fig. 46 do not agree with those assumed at the beginning of calculation. After the bridge had been designed advantage was taken of a slight increase in headroom available and the depths of the girders were increased throughout. This increase amounted to 2 in. at the crown and 12 in. at point 3. Experience has shown that the calculated reactions will be disturbed a negligible amount and if anything, on the safe side.

Effects of Skew.—In a skewed bridge of this type certain effects of skew exist, though they may usually be neglected in proportioning. These effects are indicated in Fig. 43. The earth pressure E against the back-walls may be considered as being resisted by the reactions G , from the girders or the floor slab or both, and the components W acting along the back-walls. The components W are finally taken off at the footing, being counteracted by resistance of the back-wall against sliding. The overturning effect of the couple We is counteracted by the variation of pressure longitudinally along the footings. Torsional effects in the girders are negligible.

Expansion Joints.—A complete separation of the structure proper from the wing-walls retaining the sides of the approach fill should be made by means of expansion joints near the main structure.

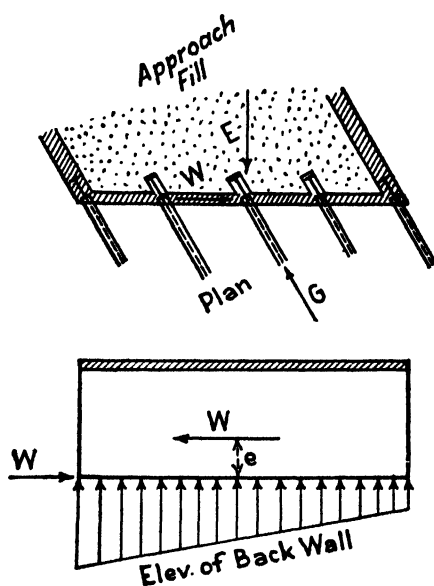


FIG. 43.

PROPERTIES OF SECTIONS

Point	Make up of Section ½-inch Web 4½ 6×6×½ Cov. Pls. 14×½	Depth bb in., Inches	Total Area of Sections, Sq. In.	Moment Inertia of Section (In.) ⁴	Moment Inertia of Section (Ft.) ⁴	y Ft.	$\frac{y^2}{I}$ Foot Units
1	Web/½ / 1 cov.	30	63.4	10,600	0.51	5.1	51
2	Web/½ / 2 cov.	50.5	91.1	45,700	2.20	12.8	74
3	Web/½ / 2 cov.	64.5	98.1	77,600	3.74	20.5	112
4	Web/½ / 2 cov.	52	91.1	48,700	2.35	21.7	200
5	Web/½ / 2 cov.	39	85.4	26,300	1.27	22.3	390
6	Web/½ / 1 cov.	29.5	63.1	10,200	0.491	22.8	1060
7	Web/½ / 1 cov.	22	59.4	5,280	0.254	23.2	2120
8	Web/½ / 1 cov.	18.5	57.6	3,560	0.172	23.4	3190
9	Web/½ / 1 cov.	18.0	57.4	3,340	0.161	23.5	*1710

 Σ (for half arch) 8,907 Σ (for full arch) 17,814

* NOTE. $\frac{y^2}{I}$ for Point 9 is for half an axis division on the half-arch, since the division of which 9 is the center-point is divided between the two half-spans.

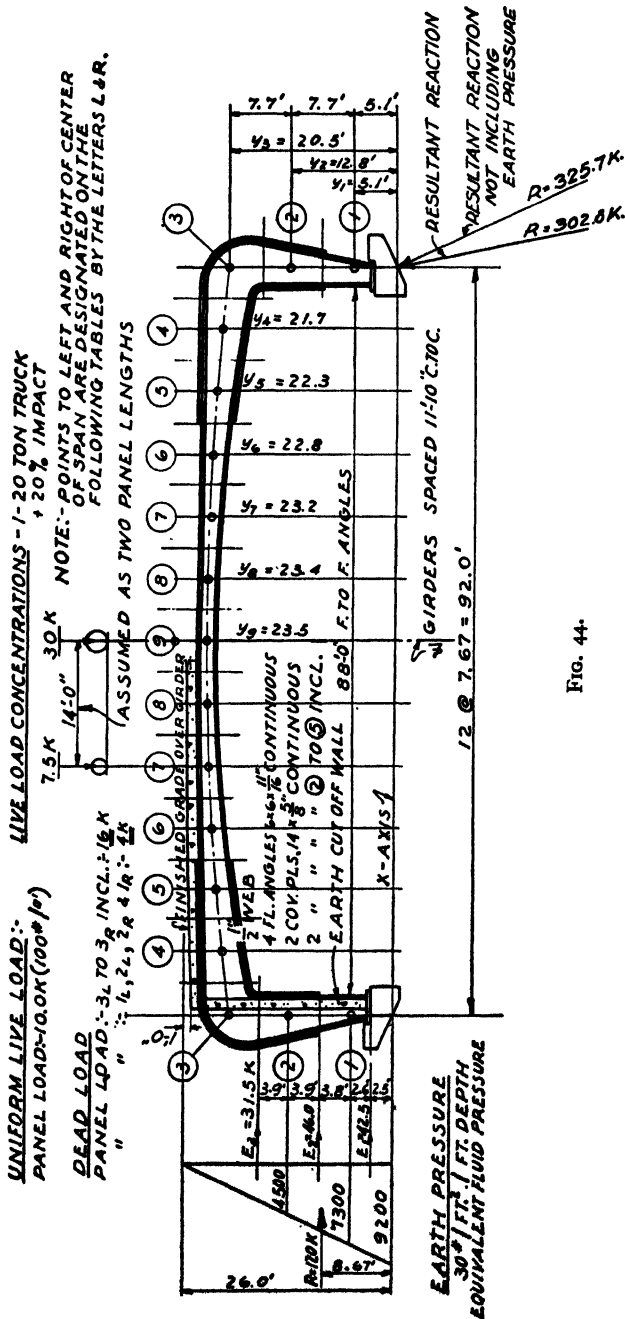


FIG. 44.

MOMENTS DUE TO INFLUENCE LOAD = 1.57

Point	<i>I</i>	<i>y</i>	Influence Load at 4R				Influence Load at 5R				Influence Load at 6R				Point
			Mom.	$\frac{M_y}{I}$	<i>H_y</i>	Total <i>M</i>	Mom.	$\frac{M_y}{I}$	<i>H_y</i>	Total <i>M</i>	Mom.	$\frac{M_y}{I}$	<i>H_y</i>	Total <i>M</i>	
1L	0.51	5.1	0	0	-1.3	-1.3	0	0	-2.6	0	0	-3.7	-3.7	1L	
2L	2.20	12.8	0	0	-3.2	-3.2	0	0	-6.4	0	0	-9.3	-9.3	2L	
3L	3.74	20.5	0	0	-5.1	-5.1	0	0	-10.2	0	0	-15.0	-15.0	3L	
4L	2.35	21.7	1	9	-5.4	-4.4	2	18	-10.8	3	27	-15.8	-15.8	4L	
5L	1.27	22.3	2	35	-5.6	-3.6	4	70	-11.2	6	105	-16.3	-16.3	5L	
6L	0.491	22.8	3	139	-5.7	-2.7	6	278	-11.4	9	417	-16.6	-16.6	6L	
7L	0.254	23.2	4	365	-5.8	-1.8	8	730	-11.6	12	1,095	-16.9	-16.9	7L	
8L	0.172	23.4	5	680	-5.8	-0.8	10	1360	-11.6	15	2,040	-17.1	-17.1	8L	
9	0.161	23.5	6	876	-5.9	+0.1	12	1752	-11.8	18	2,628	-17.2	-17.2	9	
8R	0.172	23.2	7	953	-5.8	+1.2	14	1906	-11.6	21	2,859	-17.1	-17.1	8R	
7R	0.254	23.4	8	731	-5.8	+2.2	16	1462	-11.6	24	2,193	-16.9	-16.9	7R	
6R	0.491	22.8	9	418	-5.7	+3.3	18	836	-11.4	27	1,254	-16.6	-16.6	6R	
5R	1.27	22.3	10	175	-5.6	+4.4	20	350	-11.2	18	316	-16.3	-16.3	5R	
4R	2.35	21.7	11	101	-5.4	+5.6	10	92	-10.8	9	83	-15.8	-15.8	4R	
3R	3.74	20.5	0	0	-5.1	-5.1	0	0	-10.2	0	0	-15.0	-15.0	3R	
2R	2.20	12.8	0	0	-3.2	-3.2	0	0	-6.4	0	0	-9.3	-9.3	2R	
1R	0.51	5.1	0	0	-1.3	-1.3	0	0	-2.6	0	0	-3.7	-3.7	1R	
Σ				4482				8854			13,017				
					$H = \frac{4482}{17,814} = 0.25$				$H = \frac{8854}{17,814} = 0.50$				$H = \frac{13,017}{17,814} = 0.73$		

Influence Load = $\frac{\text{Number divisions in span length}}{\text{Length of division}} = \frac{12}{7.67} = 1.57$

MOMENTS DUE TO INFLUENCE LOAD = 1.57

Point	I	y	Influence Load at 7R				Influence Load at 8R				Influence Load at 9				Point
			Mom.	$\frac{My}{I}$	H_y	Total M	Mom.	$\frac{My}{I}$	H_y	Total M	Mom.	$\frac{My}{I}$	H_y	Total M	
1L	0.51	5.1	0	0	-4.7	-4.7	0	0	-5.4	-5.4	0	0	-5.7	-5.7	1L
2L	2.20	12.8	0	0	-11.9	-11.9	0	0	-13.7	-13.7	0	0	-14.3	-14.3	2L
3L	3.74	20.5	0	0	-19.1	-19.1	0	0	-21.9	-21.9	0	0	-23.0	-23.0	3L
4L	1.27	21.7	4	36	-20.2	-16.2	5	46	-23.2	-18.2	6	54	-24.3	-18.3	4L
5L	1.37	22.3	8	140	-20.7	-12.7	10	176	-23.8	-13.8	12	210	-25.0	-13.0	5L
6L	0.491	22.8	12	556	-21.2	-9.2	15	695	-24.4	-9.4	18	834	-25.5	-7.5	6L
7L	0.254	23.2	16	1,460	-21.6	-5.6	20	1,825	-24.8	-4.8	24	2,190	-26.0	-2.0	7L
8L	0.172	23.4	20	2,750	-21.8	-1.8	25	3,400	-25.0	0.0	30	4,080	-26.2	+3.8	8L
9	0.161	23.5	24	3,504	-21.9	+2.1	30	4,380	-25.1	+4.9	36	5,256	-26.3	+9.7	9
8R	0.172	23.4	28	3,812	-21.8	+6.2	35	4,765	-25.0	+10.0	30	4,080	-26.2	+3.8	8R
7R	0.254	23.2	32	2,924	-21.6	+10.4	28	2,560	-24.8	+3.2	24	2,190	-26.0	-2.0	7R
6R	0.491	22.8	24	1,113	-21.2	+2.8	21	975	-24.4	-3.4	18	836	-25.5	-7.5	6R
5R	1.27	22.3	16	281	-20.7	-4.7	14	246	-23.8	-9.8	12	211	-25.0	-13.0	5R
4R	2.35	21.7	8	74	-20.2	-12.2	7	64	-23.2	-16.2	6	55	-24.3	-18.3	4R
3R	3.74	20.5	0	0	-19.1	-19.1	0	0	-21.9	-21.9	0	0	-23.0	-23.0	3R
2R	2.20	12.8	0	0	-11.9	-11.9	0	0	-13.7	-13.7	0	0	-14.3	-14.3	2R
1R	0.51	5.1	0	0	-4.7	-4.7	0	0	-5.4	-5.4	0	0	-5.7	-5.7	1R
Σ	16,620	19,132	19,996	
				$H = \frac{16,620}{17,814} = 0.93$				$H = \frac{19,132}{17,814} = 1.07$				$H = \frac{19,996}{17,814} = 1.12$			

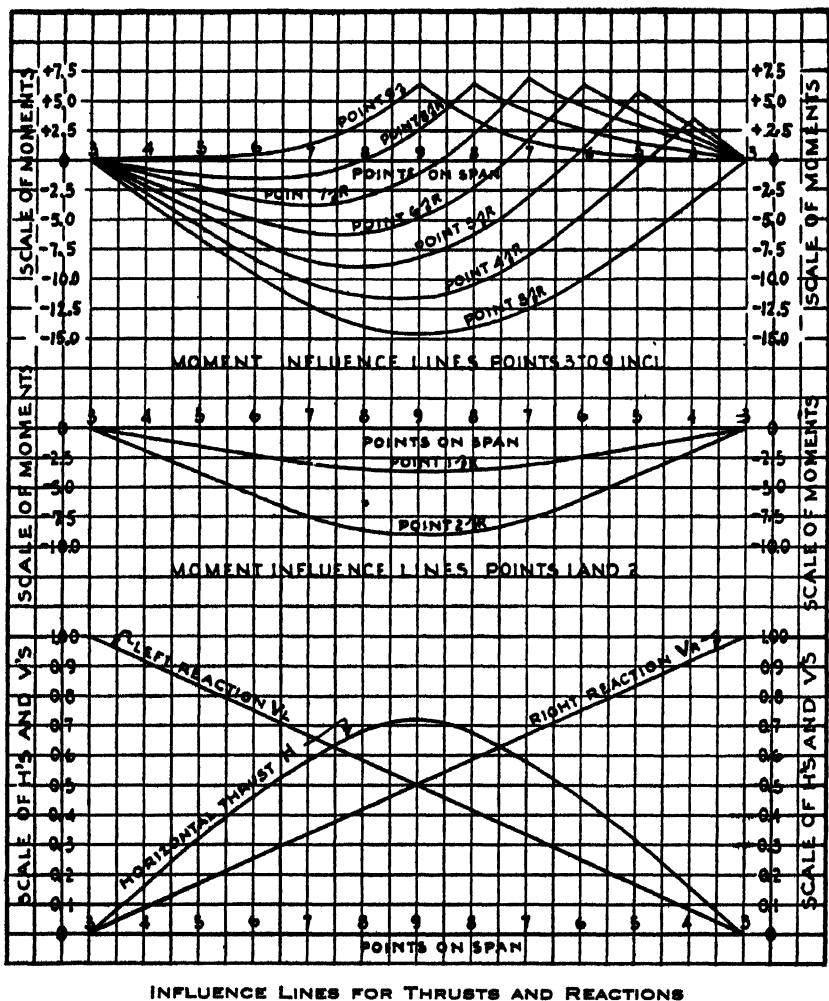


FIG. 45.—Structural Steel Rigid Frame. Influence Lines for Vertical Unit Loads.

95

DEAD LOAD MOMENTS, THRUSTS AND SHEARS

[illegible]

NOTE.—Thrust at Point x = Vertical Shear V and Shear = Horizontal Thrust H .

Thrust at Point 3 = $H \cos \theta + V \sin \theta$ and Shear = $H \sin \theta + V \cos \theta$ in which θ = slope of neutral axis = 45° .
Thrust at Points 5-9 inclusive = H and Shear = V neglecting slope of neutral axis, which is small.

FREE-END CONDITIONS

97

UNIFORM LIVE LOAD MOMENTS, SHEARS, AND THRUSTS

100 LB. PER SQ. FT. FLOOR AREA = 10 KIPS PER PANEL PER GIRDER

Load, Kips	At Point	Point 7R (Positive)				Point 7R (Negative)				Point 9			
		Moment		Vert. Shear		Horiz. Thrust		Moment		Vert. Shear		Moment	
		MF	M	VF	V	HF	H	MF	M	VF	V	MF	M
0	1L												
0	2L												
10	3L												
10	4L												
10	5L												
10	6L												
10	7L												
10	8L												
10	9												
10	8R	+2 20	180.0 X 10 = 180.0 kip-ft.	+0 42	1.25 X 10 = 12.5 kips	0 68	2.21 X 10 = 22.1 kips	-1 20	14.60 X 10 = 146.0 kip-ft.	-0 08	1.25 X 10 = 12.5 kips	0 16	2.92 X 10 = 29.2 kips
10	7R	+6 80		+0 33		0 59		-2 30		-0 17		0 32	
10	6R	+4 50		+0 25		0 46		-3 20		-0 25		0 46	
10	5R	+3 00		+0 17		0 32		-3 70		+0 67		0 59	
10	4R	+1 50		+0 08		0 16		-3 10		+0 58		0 68	
10	3R	18 00		1 25		2 21		-1 10		+0 50		0 71	
10	2R							14 60		1 25		2 92	
0	1R												
		Point 7R (Maximum Positive Moment) Moment = +180.0 kip-ft. Thrust = 22.1 kips Shear = 12.5 kips					Point 7R (Maximum Negative Moment) Moment = -146.0 kip-ft. Thrust = 29.2 kips Shear = 5.0 kips					Point 9 Moment = +180.0 kip-ft. Thrust = 51.5 kips Shear = 5.0 kips	
		Maximum shear, regardless of moment = 5.15 kips Maximum thrust, regardless of moment = 5.15 kips					Maximum shear, regardless of moment = 5.15 kips Maximum thrust, regardless of moment = 5.15 kips					Maximum shear, regardless of moment = 5.15 kips Maximum thrust, regardless of moment = 5.15 kips	

Since maximum positive moments, shears and thrusts are obtained by loading entire span, the values for Point 9 are obtained directly by proportion from corresponding dead load values.

$$M = \frac{(288)}{8} = 180$$

$$V = \frac{(8)}{8} = 5$$

$$H = \frac{(82 \ 24)}{8} = 51.5$$

98 SYMMETRICAL STEEL GIRDER FRAME BRIDGE

CONCENTRATED LIVE LOAD MOMENTS AND CORRESPONDING THRUSTS AND SHEARS

POINT 9 (CROWN)

Load, Kips	<i>MF</i>	<i>M</i>	<i>HF</i>	<i>H</i>	<i>VF</i>	<i>V</i>
30 at Point 9.....	+6.40	+192.0	0.71	21.3	0.50	15.0
7.5 at Point 7.....	+1.40	+ 10.5	0.59	4.4	0.33	2.5
Total.....	+202.5	25.7	17.5

POINT 7R (POSITIVE MOMENT)

Load, Kips	<i>MF</i>	<i>M</i>	<i>HF</i>	<i>H</i>	<i>VF</i>	<i>V</i>
30 at Point 7R.....	+6.80	+204.0	0.59	17.7	0.33	10.0
7.5 at Point 5R.....	+3.00	+ 22.5	0.32	2.4	0.17	1.3
Total.....	226.5	20.1	11.3

POINT 7R (NEGATIVE MOMENT)

Load, Kips	<i>MF</i>	<i>M</i>	<i>HF</i>	<i>H</i>	<i>VF</i>	<i>V</i>
30 at Point 7L.....	-3.70	-111.0	0.59	17.7	+0.67	+20.1
7.5 at Point 5L.....	-2.30	- 17.2	0.32	2.4	-0.17	- 1.3
Total.....	-128.2	20.1	18.8

NOTE.—Since it is evident that the greater the distance from crown the less likelihood there is of concentrated live load moments exceeding those for uniform live load, the remaining points are not investigated for concentrated loading.

100 SINGLE-SPAN STEEL GIRDER FRAME BRIDGE

SUMMARY OF MAXIMUM MOMENTS (KIP-FT.) AND CORRESPONDING NORMAL THRUSTS (KIPS)

Loading	Point 1		Point 3		Point 5		Point 7		Point 9	
	M	N	M	N	M	N	M	N	M	N
Dead.....	-411.2	111.0	-1704.0	131.0	- 617.6	82.2	+ 54.4	82.2	+288.0	82.2
Earth P.....	+260.0	0	+ 105.0	32.2	+ 24.0	45.6	- 14.0	45.6	- 30.0	45.6
Sub Total.....	-151.2	111.0	-1599.0	163.3	- 593.6	127.8	+ 40.4	127.8	+258.0	127.8
Unif. Live +...	+ 99.0	9.4	+180.0	22.1	+180.0	51.4
Unif. Live -...	-257.0	64.4	-1065.0	82.0	- 485.0	41.9	-146.0	29.2
Concentrated +	+226.5	20.1	+202.5	25.7
Concentrated -	-128.2	20.1
Temperature...	Negligible— see sheet No.		
Max. Total +...	+266.9	147.9	+460.5	153.5
Max. Total -...	-408.2	175.5	-2664.0	245.3	-1078.6	169.7	-105.6	157.0

SUMMARY OF MAXIMUM SHEARS

Loading	Point 1		Point 3		Point 5		Point 7		Point 9	
		Shear		Shear		Shear		Shear		Shear
Dead.....	82.2	131.0	71.0	40.0	8.0
Earth P.....	-31.9	32.2	0	0	0
Sub Total.....	50.3	163.3	71.0	40.0	8.0
Unif. Live +...	51.4	82.0	45.0	30.0	17.5
Unif. Live -...
Concentrated +	11.3	17.5
Concentrated -	18.8
Temperature...	Negligible		
Max. Total +...	70.0	25.5
Max. Total -...	101.7	245.2	116.0	58.8

Stresses Due to Temperature Change

For a change of 50° F. above or below normal,

$$H = \frac{Ect\ell}{\sum y^2} = \frac{144 \times 30,000,000 \times 0.000065 \times 50 \times 92}{7.67 \times 17,814}$$

$$= \pm 1.0 \text{ kip.}$$

Max. Mom. at Crown = 23.5 × 1.0 = 23.5 kip-ft.

Rib-shortening effects (calculations not shown here) will be equivalent to about 25 per cent of the effects due to a drop of temperature of 50° F.

According to usual specifications, temperature and rib-shortening effects may be neglected if they do not exceed 25 per cent of other stresses combined.

Design of Sections

See Table of Properties of Sections for Areas and Moments of Inertia of Sections in Inch Units.

$$\text{Unit Stress} = \frac{N}{A} \pm \frac{Mc}{I}$$

$$\text{Point 1. } f_s = - \frac{175.5}{63.4} \mp \frac{408.2 \times 12 \times 15.6}{10,600}$$

$$= - 2.8 \mp 7.2 = - 10.0 \text{ kips}$$

$$10,000 \text{ lb. per sq. in. Comp.}$$

Point 3. Calculation based on neutral axis at C. G. of section.

$$f_s = - \frac{245.3}{98.1} \mp \frac{2664 \times 12 \times 33.5}{77,600}$$

$$= - 2.5 \mp 13.8 = - 16.3 \text{ kips}$$

$$16,300 \text{ lb. per sq. in. Comp.}$$

$$\begin{aligned}\text{Point 5. } f_s &= - \frac{169.7}{85.4} \mp \frac{1078.6 \times 12 \times 20.8}{26,300} \\ &= - 2.0 \mp 11.2 = - 13.2 \text{ kips} \\ &\quad 13,200 \text{ lb. per sq. in. Comp.}\end{aligned}$$

$$\begin{aligned}\text{Point 7. } f_s &= - \frac{147.9}{59.4} \mp \frac{267.9 \times 12 \times 11.6}{5280} \\ &= - 2.5 \mp 7.1 = - 9.6 \text{ kips} \\ &\quad 9,600 \text{ lb. per sq. in. Comp.}\end{aligned}$$

$$\begin{aligned}\text{Point 9. } f_s &= - \frac{153.5}{57.4} \mp \frac{460.5 \times 12 \times 9.6}{3340} \\ &= - 2.7 \mp 15.9 = - 18.6 \text{ kips}\end{aligned}$$

Depth at crown, finally increased from 18 in. to 20 in. as previously mentioned.

Allowable unit stress for compression flange *not* supported laterally by the floor slab or by the vertical cut-off walls supporting the approach fill is calculated as follows:

$$\frac{l}{b} = \frac{11.5 \times 12}{14} = 10$$

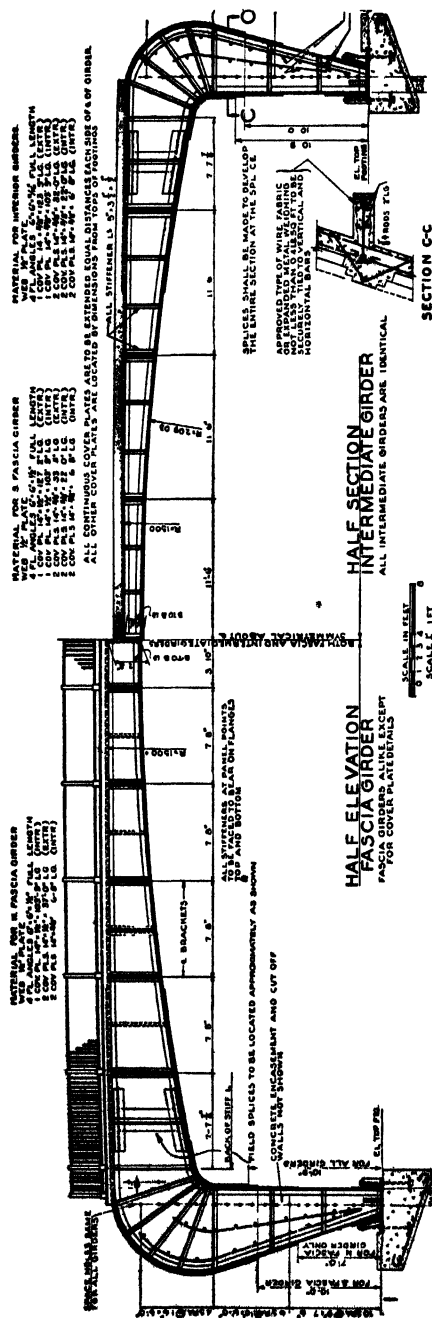
Allowable compression

$$= \frac{18,000}{1 + \frac{l^2}{2000b^2}} = \frac{18,000}{1 + \frac{100}{2000}} = 17,000 \text{ lb. per sq. in.}$$

Recent Developments in Design

The first steel rigid-frame bridge built by the Westchester County Park Commission was originally detailed with a rectangular knee section instead of with curved flanges around the bend at Section 3 as shown in Figs. 44 and 46. It was realized that there was no satisfactory basis for predicting the paths of stress in the rectangular section, and, to satisfy other parties interested in the construction of the bridge, the detail was changed and curved flanges were used. Although some approximation is involved in the design of the curved flanges at the knee, the stresses can be calculated with some degree of accuracy. This type of construction does, however, involve expensive fabrication, which militated against steel construction of rigid-frame bridges.

Recent research shows that the simpler knee detail is safe. Several important bridges with straight flanges have been built and are giving satisfactory service. The cost of fabrication was materially reduced. The reader is referred to Chapter XIV for further information.



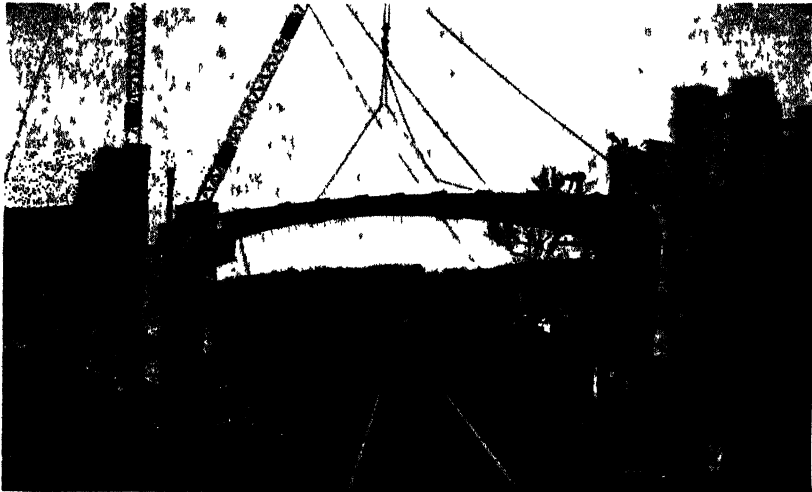
Rigid-Frame Steel Girders for Central Boulevard Bridge. Bridge consists of three intermediate girders and two outside (fascia) girders all spaced 11 ft. 10 in. on centers. Cross frames, 11 ft. 6 in. on centers, span between the girders. Girders and cross-frames support the two-way reinforced-concrete floor deck. Vertical reinforced-concrete cut-off walls, spanning between the vertical legs of the girders, retain the approach fill. The vertical legs of the girders buried in the approach fill are encased in protective concrete.

In later designs of steel rigid-frame girders of this span length, 8 in. by 8 in. flange angles were used to avoid congestion at the splices and to reduce the number of cover plates.



Construction View of a Steel Rigid-Frame Bridge.

106 SINGLE-SPAN STEEL GIRDER FRAME BRIDGE



Erection of a Steel Frame Girder Bridge.



Steel Rigid-Frame Bridge carrying Palmer Avenue over Central Park Avenue, Yonkers, N. Y. Built by Westchester County Engineer. Span 115 ft. between vertical legs of girders.

CHAPTER IX

THEORY AND DESIGN OF DOUBLE-SPAN FRAME BRIDGE. HINGED CONDITIONS AT FOOTINGS

Assume a structure as indicated in Fig. 47 hinged at (2), resting upon rollers at (1), and without support at (3). This structure is statically determinate, and its reactions and the deflections at any point may be easily calculated. A system of loads, P , C , D , and F , is indicated on the structure, the reactions being V_L , V_R , and H . Displacements at the reaction points are designated as follows; the total horizontal

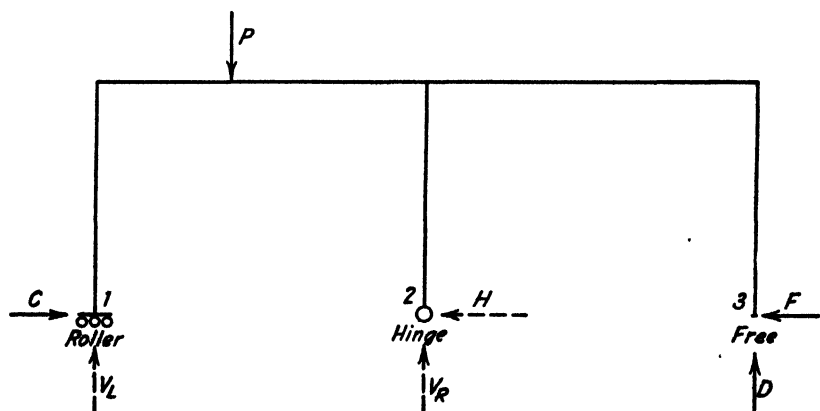


FIG. 47.

displacement at (1) is δ_c , being that occurring along the line of action of C . The portion of this displacement due to load P is designated as $P\delta_{cp}$, δ_{cp} being the deflection along the line of C due to unit load acting like P and being used as a coefficient of P . The portion due to load C is designated as $C\delta_{cc}$, that due to D as $D\delta_{cd}$, and that due to F as $F\delta_{cf}$. The total horizontal displacement at (3) is δ_f , being that along the line of action of F , and the several partial displacements

are $P\delta_{fp}$, $C\delta_{fc}$, $D\delta_{fd}$, and $F\delta_{ff}$. Likewise the several vertical displacements at (3) are: total δ_d ; partial, $P\delta_{dp}$, $C\delta_{dc}$, $D\delta_{dd}$, $F\delta_{df}$. This way of expressing displacements makes use of the calculated displacements due to *unit* load as coefficients of the known or unknown loads. The increments of the total, or any one of the partial displacements contributed by flexure in a single small division s of the structure, is designated by the symbol Δ , for example, $\Delta\delta_{df}$, $\Delta\delta_{fp}$, etc.

Let us now assume that, for a known load P , a set of values may be selected for C , D , and F such that the algebraic sum of all the partial deflections is equal to zero; that is,

$$\delta_c = P\delta_{cp} + C\delta_{cc} + D\delta_{cd} + F\delta_{cf} = 0. \quad (1)$$

$$\delta_d = P\delta_{dp} + C\delta_{dc} + D\delta_{dd} + F\delta_{df} = 0. \quad (2)$$

$$\delta_f = P\delta_{fp} + C\delta_{fc} + D\delta_{fd} + F\delta_{ff} = 0. \quad (3)$$

Then C , D , and F , whose values are unknown at first, will be the true reactions in a double-span frame supported on hinges at (1), (2), and (3) which are fixed in location. The problem then is to find numerical values for the coefficients of C , D , and F ; substitute these values in equations (1), (2), and (3); and solve the three simultaneous equations for C , D , and F .

The directions of C , D , and F along their lines of action need not be known at the outstart. They may be assumed to act in either direction, and, if algebraic signs, consistent with the assumed directions, are given to their coefficients, the correctness or incorrectness of the assumed directions will be indicated by the algebraic signs of the numerical results. If positive, the assumed direction was correct; if negative, the correct direction is opposite to that assumed. See Chapter IV.

The increments $\Delta\delta_c$, $\Delta\delta_d$, and $\Delta\delta_f$ of the displacements δ_c , δ_d , and δ_f contributed by flexure in typical divisions s of the structure are indicated in Fig. 48. These increments are grossly exaggerated, but in reality they are so small compared with the dimensions of the structure that the evident approximations made in the geometric demonstrations

are negligible. (See discussion in Chapter III.) In Fig. 48a we have, by geometry, the external angle $\Delta\theta$ equal to the sum of the internal angles $\Delta\alpha$ and $\Delta\beta$. Hence $\Delta\delta_c = y\Delta\alpha + y\Delta\beta = y\Delta\theta = My \frac{s}{EI}$, in which M is the bending moment on division s . If the calculated moment is due to *unit*

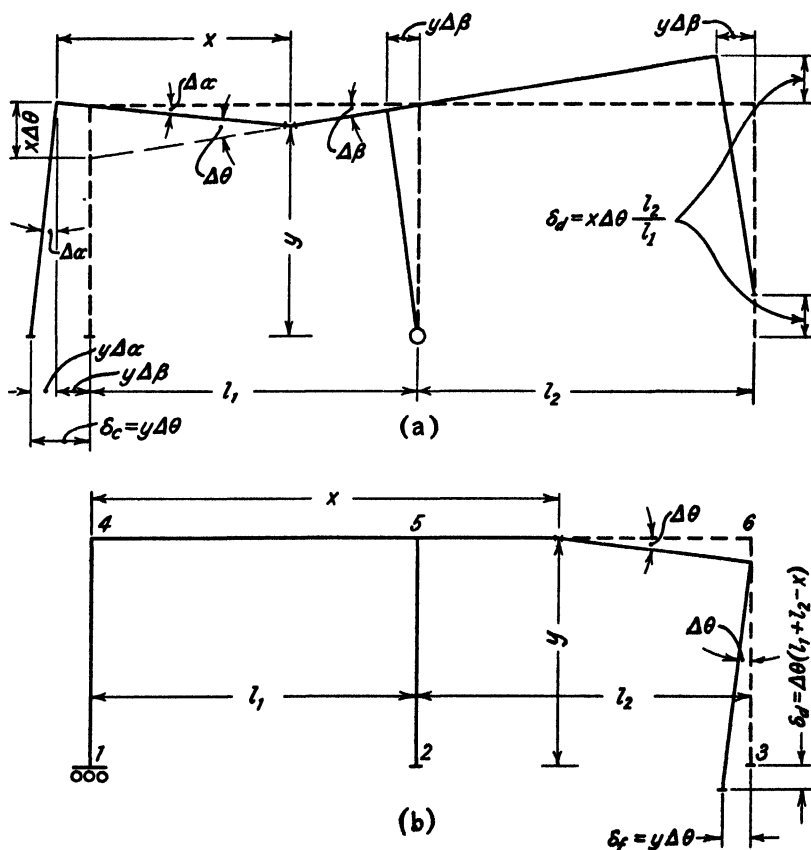


FIG. 48. (a and b).

load acting like P or C , or D or F , we have respectively $\Delta\delta_{cp} = M_p \frac{ys}{EI}$; $\Delta\delta_{cc} = M_c \frac{ys}{EI}$; $\Delta\delta_{cd} = M_d \frac{ys}{EI}$ and $\Delta\delta_{cf} = M_f \frac{ys}{EI}$. Note now that y is an expression for moment due to unit load acting like C , that is, M_c . Substituting M_c for y in

these equations and summing the effect of flexure in all divisions s contributing to the deflection δ_c , we have for these unit loads:

$$\left. \begin{aligned} \delta_{cp} &= \sum M_p M_c \frac{s}{EI} \\ \delta_{cc} &= \sum M_c M_c \frac{s}{EI} \\ \delta_{cd} &= \sum M_d M_c \frac{s}{EI} \\ \delta_{cf} &= \sum M_f M_c \frac{s}{EI} \end{aligned} \right\} \text{Equations A.}$$

By the same reasoning we have

$$\left. \begin{aligned} \delta_{fp} &= \sum M_p M_f \frac{s}{EI} \\ \delta_{fc} &= \sum M_c M_f \frac{s}{EI} \\ \delta_{fd} &= \sum M_d M_f \frac{s}{EI} \\ \delta_{ff} &= \sum M_f M_f \frac{s}{EI} \end{aligned} \right\} \text{Equations B.}$$

In Fig. 48a we have by geometry

$$\Delta\delta_d = x\Delta\theta \frac{l_2}{l_1} = M \frac{s}{EI} x \frac{l_2}{l_1}$$

In Fig. 48b,

$$\begin{aligned} \Delta\delta_d &= \Delta\theta(l_1 + l_2 - x) \\ &= M \frac{s}{EI} (l_1 + l_2 - x) \end{aligned}$$

Note that in each case the quantities $\frac{l_2}{l_1}x$ and $(l_1 + l_2 - x)$ are expressions for bending moment in the division s under consideration, due to unit load along the line of action of $D = M_d$. Hence $\Delta\delta_d = M_d M \frac{s}{EI}$.

The partial moments due to unit loads acting like P or C or D or F are M_p , M_c , M_d , and M_f , and the corresponding partial deflections are $\Delta\delta_{dp}$, $\Delta\delta_{dc}$, $\Delta\delta_{dd}$, and $\Delta\delta_{df}$. Hence,

summing the effects of flexure in all divisions s contributing to the several partial deflections, we have

$$\left. \begin{aligned} \delta_{dp} &= \sum M_p M_d \frac{s}{EI} \\ \delta_{dc} &= \sum M_c M_d \frac{s}{EI} \\ \delta_{dd} &= \sum M_d M_d \frac{s}{EI} \\ \delta_{df} &= \sum M_f M_d \frac{s}{EI} \end{aligned} \right\} \text{Equations C.}$$

The substitution of Equations A, B, and C in equations (1), (2), and (3) will give the final equations. For a homogeneous structure, E is constant; and if the arch axis is divided into equal divisions s , both these quantities may be placed outside the sign of summation and will cancel from both sides of the equations. Then the final forms of the working equations are:

$$\begin{aligned} \delta_c &= P \sum \frac{M_c M_p}{I} + C \sum \frac{M_c M_c}{I} + D \sum \frac{M_c M_d}{I} + F \sum \frac{M_c M_f}{I} = 0. \\ \delta_d &= P \sum \frac{M_d M_p}{I} + C \sum \frac{M_d M_c}{I} + D \sum \frac{M_d M_d}{I} + F \sum \frac{M_d M_f}{I} = 0. \\ \delta_f &= P \sum \frac{M_f M_p}{I} + C \sum \frac{M_f M_c}{I} + D \sum \frac{M_f M_d}{I} + F \sum \frac{M_f M_f}{I} = 0. \end{aligned}$$

Figures 48*a*, 48*b*, 48*c*, and 48*d* show that flexure in member 1-4 contributes only to δ_c ; 4-5 contributes to δ_c and δ_d ; 5-2 contributes to δ_c and δ_f ; 5-6 contributes to δ_d and δ_f ; 6-3 contributes to δ_f only. The expedient of expressing y and the functions of x as moments due to unit loads at the reaction points of the transformed structure facilitates the mental process of fixing the proper limits of summation for

112 THEORY AND DESIGN OF DOUBLE-SPAN BRIDGE

the various terms in the equations which are the partial deflections contributed by flexure in the various members. The figure preceding Table II will assist in observing the proper limits. Numerical values for M_p , M_c , M_d , or M_f are entered in this table as positive or negative according to whether the assumed directions of C , D , and F would

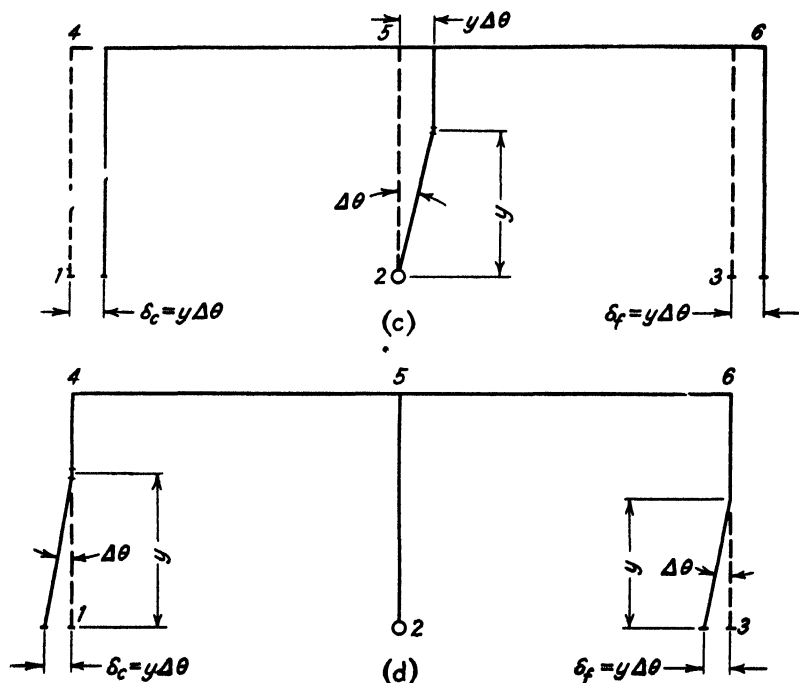


FIG. 48. (c and d).

produce positive or negative moment in the division s under consideration, as already explained. C , D , and F having been determined for any loading, the final reactions V_L , V_R , and H may be found by the simple laws of statics. In the following example of design, the two spans are equal; that is, $l_1 = l_2$.

The solution of the double-span frame may be approached by assuming the redundants differently. In

Fig. 49, for example, the transformed structure is assumed to be supported upon rollers at (1) and (3) and is without vertical support at (2). Member (2) is, however, held laterally at (2) as by vertical rollers, so that the structure will be stable under horizontal loads. The statically determinate reactions V_L , V_R , and H , and the redundants C , D , and F , are as shown. As before, the redundants are considered loads of unknown magnitude, and numerical values

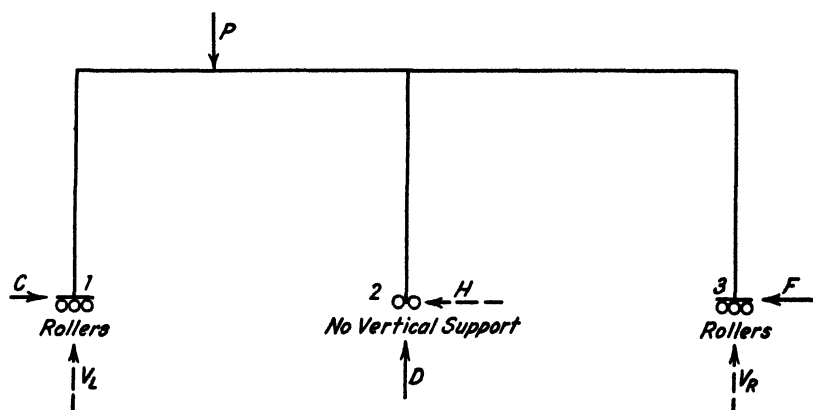


FIG. 49.

are derived that will satisfy the condition that δ_c , δ_d , and δ_f shall equal zero.

A number of other arrangements for the transformed structure are possible, some being shown in Fig. 50. The form of the equations will be alike for all systems. The system shown in Fig. 47 was selected because the numerical work involved in the solution is less than for most of the other systems.

In the following numerical example an influence load = 8 is assumed in deriving influence tables so the smallest moment M_p will equal unity and decimals will be avoided. The influence diagram is constructed for *unit* load by plotting $\frac{1}{8}$ the values for total moment as calculated in the tables.

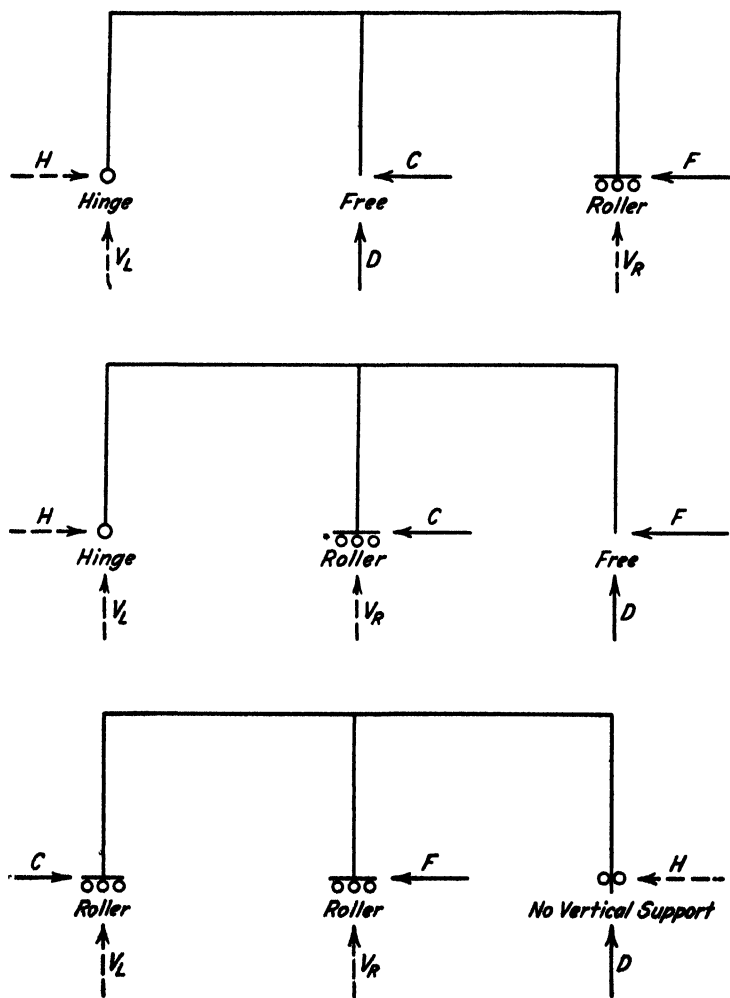


FIG. 50.

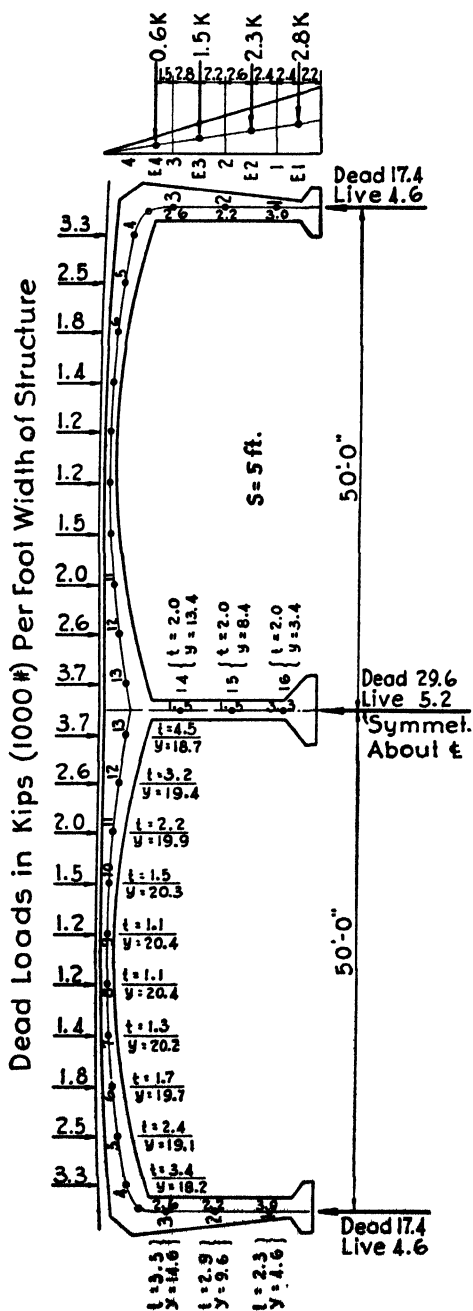


Fig. 51.

TABLE I.—PROPERTIES OF SECTIONS 1 FT. WIDE (FOOT UNITS) AND FRAME CONSTANTS.

z	Pt.	Depth f	I_c	A_s	$d = \frac{l}{2} - 0.16$	$I_o = nA_s d^2$	$I = I_c + I_o$	y	M_f	M_c	M_d	$\frac{M_f^2}{I}$	$\frac{M_c^2}{I}$	$\frac{M_d^2}{I}$	$\frac{M}{M_d}$
50	1R	2.3	1.01	0.083	0.99	.12	1.13	4.6	4.6	0	0	19	0	0	0
50	2R	2.9	2.03	0.167	1.20	.42	2.45	9.6	9.6	0	0	38	0	0	0
50	3R	3.5	3.58	0.167	1.59	.63	4.21	14.6	14.6	0	0	55	0	0	0
47.5	4R	3.4	3.27	0.167	1.54	.59	3.86	18.2	18.2	0	0	85	0	0	0
42.5	5R	4.1	4.15	0.167	1.04	.27	1.42	19.1	19.1	0	0	7.5	2	0	12
37.5	6R	4.7	4.41	0.139	0.69	.10	0.31	19.1	19.1	0	0	256	40	0	102
32.5	7R	4.3	4.18	0.083	0.49	.07	0.25	20.2	20.2	0	0	761	366	0	483
27.5	8R	4.1	4.11	0.174	0.39	.04	0.15	20.4	20.4	0	0	1,630	1,225	0	1,420
22.5	9R	4.1	4.08	0.139	0.59	.07	0.35	20.3	20.3	0	0	2,170	3,370	0	3,060
17.5	10R	4.5	4.28	0.139	0.94	.27	1.16	19.9	19.9	0	0	2,170	5,040	0	3,740
12.5	11R	3.2	2.72	0.083	1.44	.65	3.37	19.4	19.4	0	0	1,175	3,010	0	1,880
7.5	12R	2.0	0.67	0.083	2.09	1.36	8.95	18.7	18.7	0	0	341	1,210	0	642
2.5	13R	2.0	0.67	0.139	0.84	.15	0.82	13.4	13.4	0	0	42.5	111	535	244
0	14	2.0	0.67	0.139	0.84	.15	0.82	8.4	8.4	0	0	219	39	250	100
0	15	2.0	0.67	0.139	0.84	.15	0.82	3.4	3.4	0	0	86	0	0	0
0	16	2.0	0.67	0.139	0.84	.15	0.82	3.4	3.4	0	0	86	0	0	0
2.5	13L	2.0	0.67	0.083	2.09	1.36	8.95	18.7	18.7	0	0	219	39	250	100
7.5	12L	2.0	0.67	0.083	2.09	1.36	8.95	18.7	18.7	0	0	219	39	250	100
12.5	11L	3.2	2.72	0.083	1.44	.65	3.37	19.4	19.4	0	0	341	1,210	0	642
17.5	10L	4.5	4.28	0.139	0.94	.27	1.16	19.9	19.9	0	0	2,170	5,040	0	3,740
22.5	9L	4.1	4.08	0.139	0.59	.07	0.35	20.3	20.3	0	0	1,175	3,010	0	1,880
27.5	8L	4.1	4.11	0.174	0.39	.04	0.15	20.4	20.4	0	0	341	1,210	0	642
32.5	7L	4.3	4.18	0.083	0.49	.07	0.25	20.2	20.2	0	0	761	366	0	483
37.5	6L	4.7	4.41	0.139	0.69	.10	0.31	19.1	19.1	0	0	256	40	0	102
42.5	5L	4.1	4.15	0.167	1.04	.27	1.42	18.2	18.2	0	0	85	0	0	0
47.5	4L	3.4	3.27	0.167	1.54	.59	3.86	14.6	14.6	0	0	55	0	0	0
50	3L	2.9	2.03	0.167	1.20	.42	2.45	9.6	9.6	0	0	38	0	0	0
50	2L	2.3	1.01	0.083	0.99	.12	1.13	4.6	4.6	0	0	19	0	0	0
50	1L	2.0	0.67	0.083	2.09	1.36	8.95	18.7	18.7	0	0	219	39	250	100

2 10,364 | 29,976 | -319 | -11,682

By Symmetry:—

$$\sum \frac{M^2}{I} = \sum \frac{M_c^2}{I}$$

and

$$\sum \frac{M_f M_d}{I} = \sum \frac{M_c M_d}{I}$$

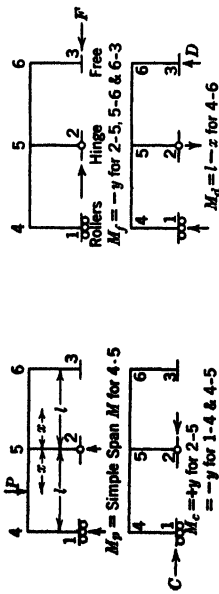


TABLE II

Influence Load 8 at Point 4L								Influence Load 8 at Point 5L							
Point	M_p	$\frac{M_c M_p}{I}$	$\frac{M_d M_p}{I}$	CM_c	DM_d	FM_f	Total Mom.	M_p	$\frac{M_c M_p}{I}$	$\frac{M_d M_p}{I}$	CM_c	DM_d	FM_f	Total Mom.	
1R						-1.0	-1.0						-2.6	-2.6	
2R						-2.1	-2.1						-5.5	-5.5	
3R						-3.2	-3.2						-8.3	-8.3	
4R					0.4	-3.9	-3.5					1.1	-10.4	-9.3	
5R					1.3	-4.2	-2.9					3.4	-10.9	-7.5	
6R					2.2	-4.3	-2.1					5.7	-11.2	-5.5	
7R					3.0	-4.4	-1.4					7.9	-11.5	-3.6	
8R					3.9	-4.4	-0.5					10.2	-11.7	-1.5	
9R					4.8	-4.5	+0.3					12.4	-11.7	+0.7	
10R					5.6	-4.4	+1.2					14.7	-11.6	+3.1	
11R					6.5	-4.3	+2.2					17.0	-11.4	+5.6	
12R					7.4	-4.2	+3.2					19.2	-11.1	+8.1	
13R					8.3	-4.1	+4.2					21.5	-10.7	+10.8	
14				9.4		-2.9	+6.5				+26.9		-7.7	+19.2	
15				5.9		-1.8	+4.1				+16.9		-4.8	+12.1	
16				2.4		-0.8	+1.6				+6.8		-1.9	+4.9	
13L	1	2	5	-13.1	8.2	3.6	-3.9	3	6	16	-37.6	21.5	-13.1	-10.8	
12L	3	17	38	-13.6	7.4	9	-3.2	9	52	113	-39.0	19.2	-8.0	-8.0	
11L	5	86	162	-14.0	6.5	2.5	-2.5	15	257	485	-40.0	17.0	-5.1	-5.1	
10L	7	406	649	-14.2	5.6	2.1	-1.6	21	1220	1950	-40.8	14.7	-	-	
9L	9	1295	1650	-14.3	4.8		-0.5	27	3670	4950	-41.0	12.4	-	-	
8L	11	1495	1650	-14.3	3.9		+0.6	33	4490	4950	-41.0	10.2	+2.2	+2.2	
7L	13	1050	910	-14.2	3.1		+1.9	39	3150	2730	-40.6	7.9	+6.3	+6.3	
6L	15	580	368	-13.9	2.2		+3.3	45	1740	1100	-39.6	5.7	+11.1	+11.1	
5L	17	229	90	-13.4	1.3		+4.9	51	685	269	-38.4	3.4	+16.0	+16.0	
4L	19	90	12	-12.7	0.4		+6.7	17	80	11	-36.6	1.1	-18.5	-18.5	
3L				-10.3			-10.3				-29.4		-29.4	-29.4	
2L				-6.7			-6.7				-19.3		-19.3	-19.3	
1L				-3.2			-3.2				-9.2		-9.2	-9.2	
Σ								-5180	Σ				16,574	Σ	
								5534					-15,350		

Either M_p or M_f hence $\Sigma \frac{M_p M_f}{I} = 0$ at all points.

TABLE II—Continued

Influence Load 8 at Point 6L										Influence Load 8 at Point 7L				
Point	M_p	$\frac{M_c M_p}{I}$	$\frac{M_d M_p}{I}$	CM_c	DM_d	FM_f	Total Mom.	M_p	$\frac{M_c M_p}{I}$	$\frac{M_d M_p}{I}$	CM_c	DM_d	FM_f	Total Mom.
1R	- 3.4	- 3.4	- 2.7	- 2.7
2R	- 7.2	- 7.2	- 5.6	- 5.6
3R	- 10.9	- 10.9	- 8.6	- 8.6
4R	+ 1.5	- 13.6	- 12.1	- 10.7	- 9.6
5R	4.3	- 14.2	- 9.9	1.1	- 11.2	- 8.0
6R	7.2	- 14.7	- 7.5	3.2	- 11.5	- 6.2
7R	10.1	- 15.1	- 5.0	5.3	- 11.8	- 4.5
8R	13.0	- 15.2	- 2.2	7.3	- 12.0	- 2.5
9R	15.9	- 15.2	+ 0.7	9.5	- 12.0	- 0.4
10R	18.8	- 15.2	+ 3.6	11.6	- 12.0	+ 1.8
11R	21.7	- 14.9	+ 6.8	13.7	- 11.9	+ 4.1
12R	24.6	- 14.5	+ 10.1	15.8	- 11.7	+ 6.4
13R	27.5	- 14.0	+ 13.3	17.8	- 11.4	+ 9.0
14	+ 41.3	- 10.0	+ 31.3	+ 49.3	20.0	- 11.0	+ 41.4
15	+ 25.9	- 6.3	+ 19.6	+ 30.9	- 4.9	+ 26.0
16	+ 10.5	- 2.5	+ 7.9	+ 12.5	- 2.0	+ 10.5
17L	5	- 10	27	- 57.6	27.5	- 25.1	7	15	37	- 68.8	20.0	- 41.8
18L	15	- 86	189	- 59.8	24.6	- 20.2	21	121	265	- 71.4	17.9	- 32.5
19L	25	- 429	806	- 61.3	21.7	- 14.6	35	600	1,130	- 73.2	15.7	- 22.5
20L	35	- 2,030	3,250	- 62.5	18.8	- 8.7	49	2,840	4,550	- 74.6	13.7	- 11.9
21L	45	- 6,110	8,250	- 62.9	15.9	- 2.0	63	8,560	11,550	- 75.0	11.6	- 0.4
22L	55	- 7,480	8,250	- 62.9	13.0	+ 5.1	77	10,460	11,550	- 75.0	9.5	+ 11.5
23L	65	- 5,250	4,550	- 62.3	10.1	+ 12.8	91	7,350	6,560	- 74.3	7.3	+ 24.0
24L	75	- 2,900	1,835	- 60.7	7.2	+ 21.5	65	2,510	1,590	- 72.5	5.3	- 2.2
25L	45	- 605	238	- 58.9	4.3	- 9.6	39	523	206	- 70.3	3.2	- 28.1
26L	15	- 71	10	- 45.0	1.5	- 39.6	13	61	8	- 67.0	1.1	- 52.9
27L	- 29.6	- 45.0	- 53.8
28L	- 14.2	- 29.6	- 35.3
29L	- 14.2	- 16.9
Σ	- 24,971	27,405	Σ	- 33,040	37,246

Either M_p or M_f hence $\sum \frac{M_p M_f}{I} = 0$ at all points.

TABLE II—Continued

Point	Influence Load 8 at Point 8L						Influence Load 8 at Point 9L							
	M_p	$\frac{M_c M_2}{I}$	$\frac{M_d M_p}{I}$	CM_c	DM_d	FM_f	Total Mom.	M_p	$\frac{M_c M_p}{I}$	$\frac{M_d M_p}{I}$	CM_c	DM_d	FM_f	Total Mom.
1R						-0.1	-0.1						+3.2	+3.2
2R						-0.1	-0.1						+6.8	+6.8
3R						-0.2	-0.2						+10.3	+10.3
4R						-0.3	-0.3						+12.8	+12.8
5R					-0.2	-0.3	-0.5					-1.7	-8.2	+11.1
6R					-0.6	-0.3	-0.9					-5.2	+13.4	+8.2
7R					-1.0	-0.3	-1.3					-8.8	+13.9	+5.1
8R					-1.5	-0.3	-1.8					-12.3	+14.2	+2.1
9R					-1.9	-0.3	-2.2					-15.8	+14.4	-1.4
10R					-2.3	-0.3	-2.6					-19.3	+14.4	-4.9
11R					-2.8	-0.3	-3.1					-22.8	+14.3	-8.5
12R					-3.2	-0.3	-3.5					-26.3	+14.0	-12.3
13R					-3.6	-0.3	-3.9					-29.8	+13.7	-16.1
14					-4.0	-0.3	-4.3					-33.3	+13.2	-20.1
15						-0.2	+47.7						+9.4	+46.8
16						-0.1	+29.8						+29.3	+29.3
17							+13.1						+2.4	+11.9
18							-61.6							
19					-4.0		-45.7					-33.3		-74.4
20					-3.6		-49.1					-54.1		-50.9
21					-3.2		-52.5					-56.3		-26.8
22					-2.8		-55.9					-58.5		-2.4
23					-2.3		-59.3					-60.7		+22.8
24					-1.9		-62.7					-62.9		+8.3
25					-1.5		-66.1					-65.1		+5.6
26					-1.1		-69.5					-67.3		-18.7
27					-0.6		-72.7					-69.5		-31.5
28					-0.2		-75.9					-71.7		-43.4
29							-79.1					-73.9		-40.7
30							-82.3					-76.1		-26.8
31							-85.5					-78.3		-12.8
32							-88.7					-80.5		
33							-91.9					-82.7		
34							-95.1					-84.9		
35							-98.3					-87.1		
36							-101.5					-89.3		
37							-104.7					-91.5		
38							-107.9					-93.7		
39							-111.1					-95.9		
40							-114.3					-98.1		
41							-117.5					-100.3		
42							-120.7					-102.5		
43							-123.9					-104.7		
44							-127.1					-106.9		
45							-130.3					-109.1		
46							-133.5					-111.3		
47							-136.7					-113.5		
48							-139.9					-115.7		
49							-143.1					-117.9		
50							-146.3					-120.1		
51							-149.5					-122.3		
52							-152.7					-124.5		
53							-155.9					-126.7		
54							-159.1					-128.9		
55							-162.3					-131.1		
56							-165.5					-133.3		
57							-168.7					-135.5		
58							-171.9					-137.7		
59							-175.1					-139.9		
60							-178.3					-142.1		
61							-181.5					-144.3		
62							-184.7					-146.5		
63							-187.9					-148.7		
64							-191.1					-150.9		
65							-194.3					-153.1		
66							-197.5					-155.3		
67							-200.7					-157.5		
68							-203.9					-159.7		
69							-207.1					-161.9		
70							-210.3					-164.1		
71							-213.5					-166.3		
72							-216.7					-168.5		
73							-219.9					-170.7		
74							-223.1					-172.9		
75							-226.3					-175.1		
76							-229.5					-177.3		
77							-232.7					-179.5		
78							-235.9					-181.7		
79							-239.1					-183.9		
80							-242.3					-186.1		
81							-245.5					-188.3		
82							-248.7					-190.5		
83							-251.9					-192.7		
84							-255.1					-194.9		
85							-258.3					-197.1		
86							-261.5					-199.3		
87							-264.7					-201.5		
88							-267.9					-203.7		
89							-271.1					-205.9		
90							-274.3					-208.1		
91							-277.5					-210.3		
92							-280.7					-212.5		
93							-283.9					-214.7		
94							-287.1					-216.9		
95							-290.3					-219.1		
96							-293.5					-221.3		
97							-296.7					-223.5		
98							-299.9					-225.7		
99							-303.1					-227.9		
100							-306.3					-230.1		
101							-309.5					-232.3		
102							-312.7					-234.5		
103							-315.9					-236.7		
104							-319.1					-238.9		
105							-322.3					-241.1		
106							-325.5					-243.3		
107							-328.7					-245.5		
108							-331.9					-247.7		
109							-335.1					-249.9		
110							-338.3					-252.1		
111							-341.5					-254.3		
112							-344.7					-256.5		
113							-347.9					-258.7		
114							-351.1					-260.9		
115							-354.3					-263.1		
116							-357.5					-265.3		
117							-360.7					-267.5		
118							-363.9					-269.7		
119							-367.1					-271.9		
120							-370.3					-274.1		
121							-373.5					-276.3		
122							-376.7					-278.5		
123							-379.9					-280.7		
124							-383.1					-282.9		
125							-386.3					-285.1		
126							-389.5					-287.3		
127							-392.7					-289.5		
128							-395.9					-291.7		
129							-399.1					-293.9		
130							-402.3					-296.1		
131							-405.5					-298.3		
132							-408.7					-300.5		
133							-411.9					-302.7		
134							-415.1					-304.9		
135							-418.3					-307.1		
136							-421.5					-309.3		
137							-424.7					-311.5		
138							-427.9					-313.7		
139							-431.1					-315.9		
140							-434.3					-318.1		
141							-437.5					-320.3		
142							-440.7					-322.5		
143							-443.9					-324.7		
144														

TABLE II—Continued

Influence Load 8 at Point 12L										Influence Load 8 at Point 13L					
Point	M_p	$\frac{M_c M_p}{I}$	$\frac{M_d M_p}{I}$	CM_c	DM_d	FM_f	Total Mom.	M_p	$\frac{M_c M_p}{I}$	$\frac{M_d M_p}{I}$	CM_c	DM_d	FM_f	Total Mom.	
1R	+ 2.9	+ 2.9	+1.0	+1.0	
2R	+ 6.0	+ 6.0	2.1	+2.1	
3R	+ 9.1	+ 9.1	3.2	+3.2	
4R	11.3	+ 9.9	4.0	+3.5	
5R	11.9	+ 7.6	4.2	+2.7	
6R	12.2	+ 5.1	4.3	+1.8	
7R	12.5	+ 2.5	4.4	+0.9	
8R	12.7	— 0.1	4.5	0.0	
9R	12.7	— 3.0	4.5	—1.0	
10R	12.6	— 5.9	4.5	—2.0	
11R	12.4	— 8.9	4.4	—3.1	
12R	12.0	—12.2	4.2	—4.3	
13R	11.6	—15.4	4.1	—5.4	
14	8.3	+17.5	2.9	+5.8	
15	5.2	+10.9	1.9	+3.7	
16	2.1	+ 4.4	+0.8	+1.5	
13L	—27.0	—22.8	—9.5	+5.4	
12L	—24.2	—13.5	—8.5	+4.3	
11L	—21.3	+10.1	—7.5	+3.2	
10L	—18.5	+ 6.6	—6.5	+2.1	
9L	—15.7	+ 3.3	—5.5	+1.1	
8L	—12.7	+ 0.3	—4.5	+0.1	
7L	—10.0	— 2.8	—4.4	—0.9	
6L	— 7.1	— 5.6	—3.5	—1.8	
5L	— 4.3	— 8.4	—2.7	—2.7	
4L	— 1.4	—10.9	—0.5	—3.5	
3L	—10.0	—10.0	—3.2	—3.2	
2L	— 6.6	— 6.6	—2.1	—2.1	
1L	— 3.1	— 3.1	—1.0	—1.0	
Σ		—13,933	17,799				— 3.1	Σ	—4,671	5,995					

Either M_p or M_f hence $\Sigma \frac{M_p M_f}{I} = 0$ at all points.

TABLE III

$$\left\{ \begin{array}{l} C \sum \frac{M_c^2}{I} + D \sum \frac{M_d M_d}{I} + F \sum \frac{M_c M_f}{I} + \sum \frac{M_c M_p}{I} = 0. \\ C \sum \frac{M_d M_c}{I} + D \sum \frac{M_d^2}{I} + F \sum \frac{M_d M_f}{I} + \sum \frac{M_d M_p}{I} = 0. \\ C \sum \frac{M_f M_c}{I} + D \sum \frac{M_f M_d}{I} + F \sum \frac{M_f^2}{I} + \sum \frac{M_f M_p}{I} = 0. \end{array} \right.$$

Solution of Equations:

Influence Load 8 of Point	4L	5L	6L	7L	8L	9L	10L	11L	12L	13L
Equations										
I. $10.364 C - 11.682 D - 319 F =$	5180	15,350	24,971	33,040	37,902	37,316	31,293	22,961	13,933	4671
II. $-11.682 C + 29,976 D - 11,682 F =$	-5534	-16,574	-27,405	-37,246	-44,304	-45,356	-39,064	-29,077	-17,799	-5995
III. $-319 C - 11,682 D + 10,367 F =$										
Dividing by Coefficient of C:										
I. $C - 1.127 D - 0.0308 F =$	0.500	1.481	2.409	3.188	3.656	3.600	3.019	2.215	1.344	0.451
II. $C - 2.566 D + F =$	0.474	1.419	2.346	3.188	3.793	3.883	3.344	2.489	1.524	0.513
III. $C + 36.62 D - 32.5 F =$										
Subtracting II from I:										
(a) $1.439 D - 1.0308 F =$	+0.026	+0.062	+0.063	+0.000	-0.136	-0.283	-0.325	-0.274	-0.180	-0.063
Subtracting II from III:										
(b) $39.19 D - 33.50 F =$	-0.474	-1.419	-2.35	-3.188	-3.790	-3.88	-3.344	-2.49	-1.524	-0.513
Dividing by Coefficient of D:										
(a) $D - 0.716 F =$	+0.018	+0.0431	+0.044	+0.000	-0.095	-0.197	-0.226	-0.190	-0.125	-0.043
(b) $D - 0.855 F =$	-0.012	-0.0362	-0.060	-0.0814	-0.097	-0.099	-0.085	-0.063	-0.0389	-0.013
Subtracting (b) from (a):										
$0.139 F =$	+0.030	+0.0793	+0.104	+0.0814	+0.002	-0.098	-0.141	-0.127	-0.0862	-0.030
$F =$	+0.217	+0.571	+0.747	+0.586	+0.014	-0.704	-1.014	-0.916	-0.620	-0.219
Substituting (a) $0.716 F =$	+0.156	+0.409	+0.535	+0.420	+0.010	-0.504	-0.726	-0.656	-0.444	-0.157
	+0.018	+0.043	+0.044	+0.000	-0.095	-0.190	-0.226	-0.190	-0.125	-0.043
	+0.174	+0.452	+0.579	+0.420	-0.085	-0.701	-0.932	-0.846	-0.569	-0.200
$D =$										
Substituting in II $2.566 D =$	+0.445	+1.160	+1.484	+1.078	-0.219	-1.800	-2.443	-2.173	-1.460	-0.515
$-F =$	-0.217	-0.571	-0.747	-0.586	-0.014	+0.704	+1.014	+0.916	+0.620	+0.219
	-0.474	+1.419	+2.346	+3.188	+3.793	+3.883	+3.344	+2.489	+1.524	+0.513
$C =$	+0.702	+2.008	+3.083	+3.680	+3.560	+2.787	+1.915	+1.232	+0.684	+0.217

Diagrams Showing Complete Reactions for Unit Load

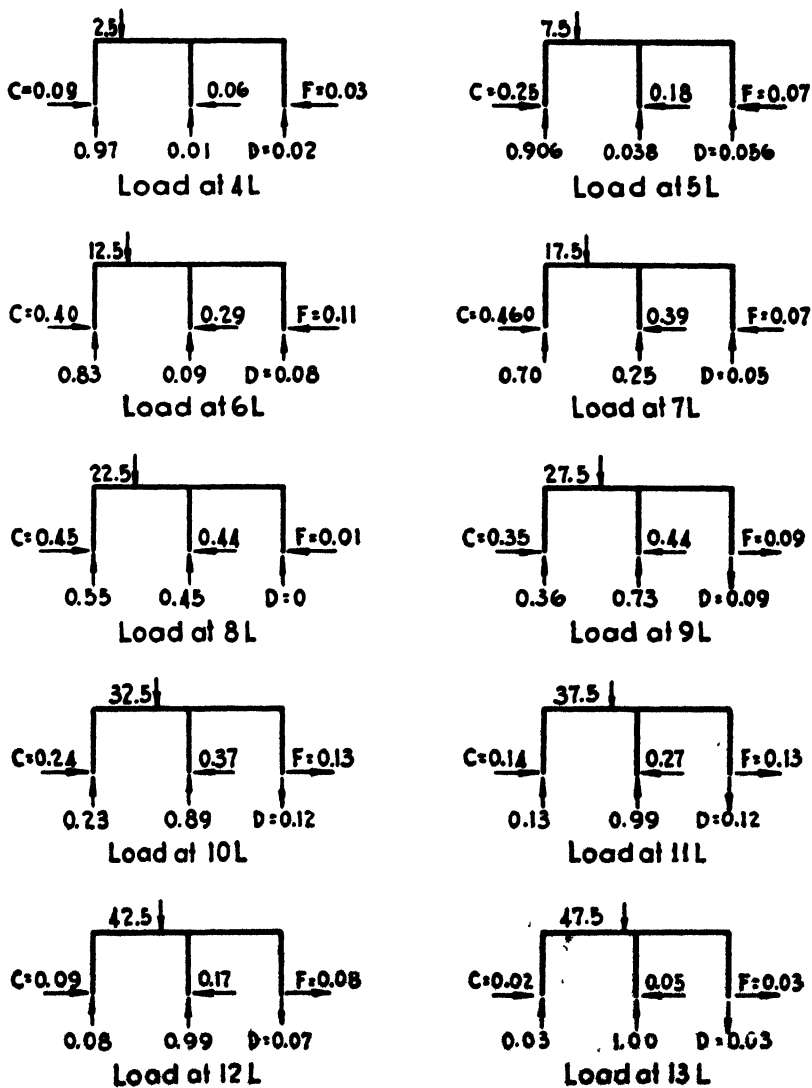


FIG. 52.

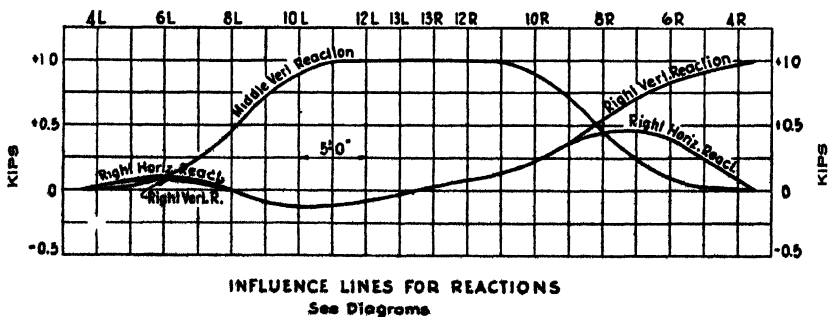
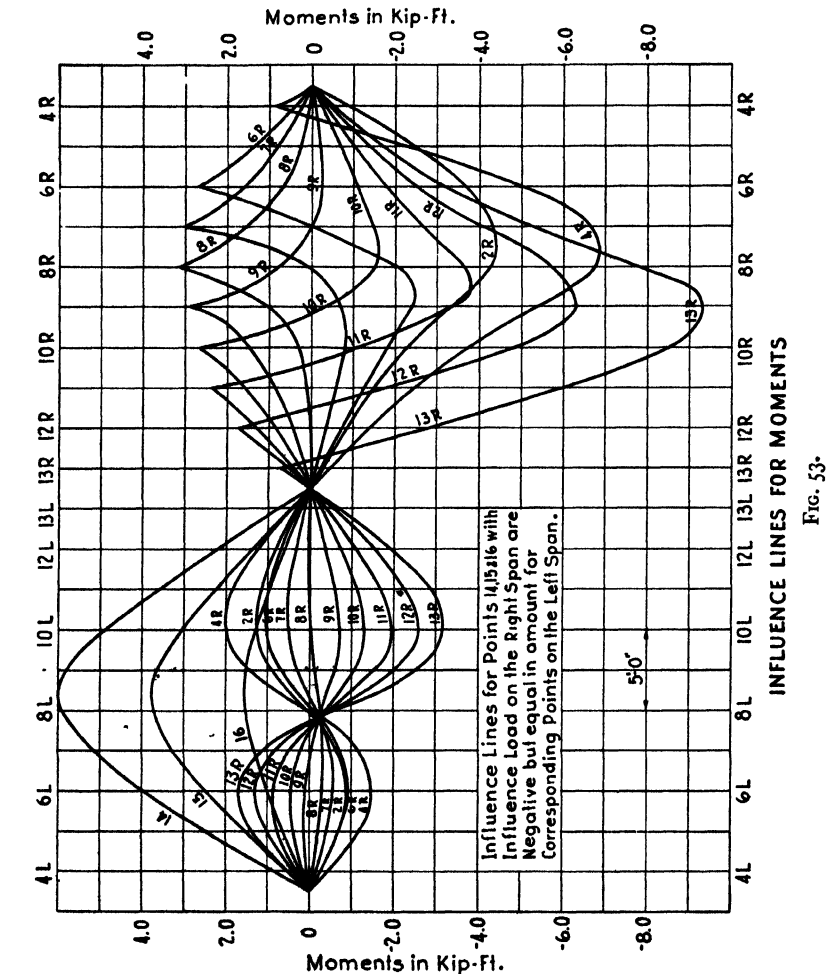


FIG. 54.

TABLE IV.—DEAD LOAD MOMENTS

Moment factors (*MF*) are scaled from the influence line diagram. The product of load and moment factor will give the actual dead load moment *M*.

Point	Load	Point 1R		Point 2R		Point 3R		Point 4R		Point 5R		Point 6R		Point 7R		Point 8R		Point
		<i>MF</i>	<i>M</i>	<i>MF</i>	<i>M</i>	<i>MF</i>	<i>M</i>	<i>MF</i>	<i>M</i>	<i>MF</i>	<i>M</i>	<i>MF</i>	<i>M</i>	<i>MF</i>	<i>M</i>	<i>MF</i>	<i>M</i>	
4L	3.3	-0.01	-0.03	-0.26	-0.86	-0.40	-1.32	-0.44	-1.45	-0.36	-1.19	-0.26	-0.86	-0.18	-0.59	-0.06	-0.20	4L
5L	2.5	-0.32	-0.80	-0.69	-1.73	-1.04	-2.60	-1.16	-2.90	-0.94	-2.35	-0.69	-1.73	-0.45	-1.13	-0.19	-0.48	5L
6L	1.8	-0.42	-0.76	-0.90	-1.62	-1.36	-2.45	-1.51	-2.72	-1.24	-2.24	-0.94	-1.70	-0.62	-1.12	-0.27	-0.49	6L
7L	1.4	-0.34	-0.48	-0.70	-0.98	-1.07	-1.50	-1.20	-1.68	-1.00	-1.40	-0.77	-1.08	-0.56	-0.78	-0.31	-0.43	7L
8L	1.2	-0.01	-0.01	-0.01	-0.01	-0.02	-0.02	-0.06	-0.07	-0.11	-0.13	-0.16	-0.19	-0.22	-0.26	-0.27	-0.32	8L
9L	1.2	+0.40	+0.48	+0.85	+1.02	+1.29	+1.55	+1.39	+1.67	+1.02	+1.22	+0.64	+0.77	+0.25	+0.30	-0.18	-0.22	9L
10L	1.5	+0.59	+0.88	+1.21	+1.82	+1.85	+2.78	+2.01	+3.02	+1.52	+2.28	+1.01	+1.52	+0.47	+0.71	-0.09	-0.14	10L
11L	2.0	+0.52	+1.04	+1.10	+2.20	+1.68	+3.36	+1.82	+3.64	+1.40	+2.80	+0.94	+1.88	+0.46	+0.92	-0.05	-0.10	11L
12L	2.6	+0.36	+0.94	+0.75	+1.95	+1.14	+2.96	+1.24	+3.22	+0.95	+2.46	+0.64	+1.66	+0.31	+0.81	-0.01	-0.03	12L
13L	3.7	+0.12	+0.44	+0.26	+0.96	+0.40	+1.48	+0.44	+1.63	+0.34	+1.26	+0.22	+0.81	+0.11	+0.41	.00	.00	13L
12R	3.7	-0.12	-0.44	-0.26	-0.96	-0.40	-1.48	-0.44	-1.63	-0.34	-1.26	-0.22	-0.81	-0.11	-0.41	+0.01	+0.04	12R
11R	2.6	-0.39	-1.02	-0.82	-2.13	-1.25	-3.25	-1.36	-3.53	-1.05	-2.72	-0.70	-1.82	-0.35	-0.91	+0.04	+0.10	11R
10R	2.0	-0.71	-1.42	-1.48	-2.96	-2.25	-4.50	-2.44	-4.88	-1.86	-3.72	-1.24	-2.48	-0.59	-1.18	+0.10	+0.20	10R
9R	1.5	-1.10	-1.65	-2.30	-3.45	-3.49	-5.24	-3.79	-5.69	-2.85	-4.28	-1.82	-2.73	-0.80	-1.20	+0.31	+0.47	9R
8R	1.2	-1.60	-1.92	-3.35	-4.02	-5.09	-6.11	-5.42	-6.50	-3.94	-4.73	-2.34	-2.81	-0.70	-0.84	+1.04	+1.25	8R
7R	1.2	-2.05	-2.46	-4.27	-5.12	-6.50	-7.80	-6.75	-8.10	-4.45	-5.34	-2.02	-2.42	-0.45	-0.54	+2.60	+3.12	7R
6R	1.8	-2.11	-2.96	-4.41	-6.20	-6.73	-9.45	-6.61	-9.30	-3.51	-4.93	-0.27	-0.38	+2.30	+3.20	+1.44	+2.02	6R
5R	2.5	-1.78	-3.21	-3.70	-6.68	-5.61	-10.14	-4.95	-8.93	-1.20	-2.16	+2.10	+3.80	+1.60	+2.80	+0.64	+1.16	5R
4R	3.3	-1.15	-2.88	-2.41	-6.03	-3.67	-9.18	-2.31	-5.78	+1.20	+3.00	+1.39	+3.48	+0.79	+1.98	+0.27	+0.68	4R
		-0.40	-1.32	-0.84	-2.78	-1.29	-4.26	+0.26	+0.86	+0.61	+2.01	+0.41	+1.35	+0.24	+0.79	+0.08	+0.26	
	Σ		-17.6		-37.7		-57.2		-49.1		-21.4		-3.7		+4.1		+6.9	

NOTE.—Average values of influence line ordinates over distance *s* are used for Point 4R, Load at 4R; Point 5R, Load at 5R, etc.

TABLE IV.—DEAD LOAD MOMENTS—Continued
 Moment factors (*MF*) are scaled from the influence line diagram. The product of load and moment factor will give the actual dead load moment *M*.

Point	Load	Point 9R		Point 10R		Point 11R		Point 12R		Point 13R		Right Vert. Reaction		Right Horiz. Reaction		Middle Vert. Reaction		Point
		<i>MF</i>	<i>M</i>	<i>MF</i>	<i>M</i>	<i>MF</i>	<i>M</i>	<i>MF</i>	<i>M</i>	<i>MF</i>	<i>M</i>	Factor	React.	Factor	React.	Factor	React.	
4L	3.3	+0.04	+0.13	+0.15	+0.49	+0.28	+0.93	+0.40	+1.32	+0.53	+1.72	+0.02	+0.07	+0.03	+0.10	+0.01	+0.03	4L
5L	2.5	+0.09	+0.23	+0.39	+0.98	+0.70	+1.75	+1.01	+2.53	+1.35	+3.3	+0.06	+0.15	+0.07	+0.18	+0.04	+0.10	5L
6L	1.8	+0.09	+0.16	+0.45	+0.85	+0.85	+1.53	+1.26	+2.26	+1.69	+3.05	+0.06	+0.14	+0.11	+0.20	+0.09	+0.16	6L
7L	1.4	-0.05	-0.07	+0.22	+0.31	+0.51	+0.71	+0.80	+1.12	+1.12	+1.57	+0.05	+0.07	+0.07	+0.10	+0.25	+0.35	7L
8L	1.2	-0.32	-0.38	-0.28	-0.46	-0.44	-0.53	-0.49	-0.59	-0.54	-0.65	0	0	+0.01	+0.01	+0.45	+0.54	8L
9L	1.2	-0.61	-0.73	-1.06	-1.27	-1.54	-1.85	-2.01	-2.41	-2.51	-3.01	-0.09	-0.11	-0.09	-0.11	+0.73	+0.88	9L
10L	1.5	-0.69	-1.04	-1.30	-1.95	-1.94	-2.91	-2.60	-3.90	-3.15	-4.73	-0.12	-0.18	-0.13	-0.20	+0.89	+1.34	10L
11L	2.0	-0.58	-1.16	-1.11	-2.22	-1.70	-3.40	-2.27	-4.54	-2.90	-5.80	-0.12	-0.24	-0.13	-0.26	+0.99	+1.98	11L
12L	2.6	-0.37	-0.96	-0.74	-1.92	-1.11	-2.89	-1.52	-3.95	-1.92	-4.98	-0.07	-0.18	-0.0	-0.21	+0.99	+2.60	12L
13L	3.7	-0.13	-0.48	-0.25	-0.93	-0.39	-1.44	-0.54	-2.00	-0.67	-2.48	-0.03	-0.11	-0.03	-0.11	+1.00	+3.70	13L
13R	3.7	+0.14	+0.52	+0.26	+0.93	+0.40	+1.48	+0.54	+2.00	+0.20	+0.74	+0.03	+0.11	+0.02	+0.07	+1.00	+3.70	13R
12R	2.6	+0.41	+1.06	+0.82	+2.13	+1.26	+3.27	+1.10	+2.86	-2.85	-7.40	+0.08	+0.21	+0.09	+0.23	+0.99	+2.60	12R
11R	2.0	+0.82	+1.64	+1.56	+3.12	+1.60	+3.20	+1.86	-7.26	-6.03	-12.06	+0.13	+0.26	+0.14	+0.28	+0.99	+2.60	11R
10R	1.5	+1.46	+2.19	+2.00	+3.00	-1.10	-1.65	-4.84	-7.63	-8.50	-12.75	+0.23	+0.35	+0.24	+0.36	+0.89	+1.98	10R
9R	1.2	+2.30	+2.76	-0.30	-0.36	-3.35	-4.02	-6.36	-7.63	-9.30	-11.46	+0.36	+0.43	+0.35	+0.42	+0.73	+0.88	9R
8R	1.2	+0.76	+0.91	-1.51	-1.81	-3.64	-4.37	-5.71	-6.85	-7.70	-9.24	+0.55	+0.66	+0.45	+0.54	+0.45	+0.54	8R
7R	1.4	-0.05	-0.07	-1.49	-2.09	-2.81	-3.94	-4.06	-5.70	-5.22	-7.32	+0.70	+0.98	+0.46	+0.63	+0.25	+0.35	7R
6R	1.8	-0.25	-0.45	-1.09	-1.96	-1.82	-3.28	-2.53	-4.56	-3.14	-5.66	+0.83	+1.50	+0.40	+0.72	+0.09	+0.16	6R
5R	2.5	-0.20	-0.50	-0.64	-1.60	-1.00	-2.50	-1.35	-3.38	-1.64	-4.10	+0.91	+2.27	+0.25	+0.62	+0.04	+0.10	5R
4R	3.3	-0.06	-0.20	-0.20	-0.66	-0.31	-1.02	-0.40	-1.32	-0.49	-1.62	+0.97	+3.20	+0.09	+0.30	+0.01	+0.03	4R
		+3.5		-5.3		-20.9		-45.7		-82.8		+9.5		+3.87		+23.36		

Dead Load Thrusts: Points 4R to 13R: Right Horizontal Reaction = 3.9 kips.

Point 3R: Right Vertical Reaction +1.3 = 10.9.

2R: 10.9 + 1.3 + 1.1 = +13.3.

1R: 13.3 + 1.1 + 0.8 = 15.2.

14: Middle Vertical Reaction + 0.75 = 24.1.

15: 24.1 + 1.5 = 25.6.

16: 25.6 + 1.5 = 27.1.

LIVE LOADING H20

Width of Roadway 40 ft.

Reduction of intensity of loading for 22 ft. width in excess of 18 ft.
 $= 40 - 18 = 22\%$

Use impact factor throughout for loaded length of one span, 50 ft

Impact $\frac{50}{30+50} = 25\%$ $1.25 \times 0.78 = \text{say } 1.0$. Use

wheel loads distributed over traffic lane width of 9 ft.

Concentrations per ft. width of bridge from 20 ton truck

$$\frac{32000}{9} = 3500^* \text{ and } \frac{8000}{9} = 900^*$$

$$\text{From 15 ton trucks } \frac{24000}{9} = 2700 \text{ and } \frac{6000}{9} = 700^*$$

Train load for calculating live load moments and thrusts from influence lines, as follows or reversed



TABLE V.—CONCENTRATED LIVE LOAD MOMENTS *M* AND NORMAL THRUSTS *N*

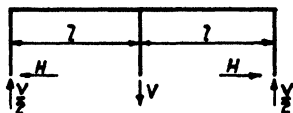
Moment Factors (*MF*) and Thrust Factors (*NF*) are read directly from influence line diagrams. The product of load and moment factor gives actual moments *M*, and product of load and thrust factor gives actual thrusts *N*

Load	Point 1R				Point 2R				Point 3R			
	<i>MF</i>	<i>M</i>	<i>NF</i>	<i>N</i>	<i>MF</i>	<i>M</i>	<i>NF</i>	<i>N</i>	<i>MF</i>	<i>M</i>	<i>NF</i>	<i>N</i>
3.5	+0.59	+2.06	-0.12	-0.42	-2.1	-7.35	+0.70	+2.45	-4.40	-15.4	+0.65	+2.3
0.9	+0.18	+0.16	-0.04	-0.0	-1.2	-1.08	+0.21	+0.24	-2.20	-2.0	+0.21	+0.2
2.7	-0.42	-1.13	+0.08	+0.22	-0.90	-2.4	+0.08	+0.2
0.7
Total	+2.2	-0.4	-9.6	+2.9	-19.8	+2.7
	-0.5	-0.4

Load	Point 3R				Point 4R				Point 5R			
	<i>MF</i>	<i>M</i>	<i>NF</i>	<i>N</i>	<i>MF</i>	<i>M</i>	<i>NF</i>	<i>N</i>	<i>MF</i>	<i>M</i>	<i>NF</i>	<i>N</i>
3.5	-6.7	-23.50	+0.70	+2.45	+1.95	+6.8	-0.13	-0.45	+2.0	+7.00	+0.25	+0.9
0.9	-3.8	-3.42	+0.16	+0.25	+0.65	+0.6	+0.05	+0.2	+1.5	+4.05	-0.12	-0.3
2.7	-1.4	-3.78	+0.08	+0.22	+0.80	+2.2	+0.10	+0.27	+0.5	+0.35	-0.04	-0.1
0.7
Total	-30.7	+2.9	+9.6	-0.1	+11.4	+0.6
	+2.0	+1.9

Load	Point 6R				Point 7R				Point 8R			
	<i>MF</i>	<i>M</i>	<i>NF</i>	<i>N</i>	<i>MF</i>	<i>M</i>	<i>NF</i>	<i>N</i>	<i>MF</i>	<i>M</i>	<i>NF</i>	<i>N</i>
3.5	+2.70	+9.4	+0.40	+1.4	-2.45	-8.6	0.40	+1.4	-0.8	-2.80	+0.28	+1.0
0.9	-1.00	-0.9	0.12	+0.1	-0.25	-0.22	+0.06	+0.1
2.7	+1.00	+2.7	-0.13	-0.3	-0.95	-2.6	0.08	+0.2	-0.65	-1.75	+0.11	+0.3
0.7	+0.40	+0.3	-0.05	-0.0
Total	+12.4	+1.1	-12.1	+1.7	-4.8	+1.4
	+1.3	+1.9

Temperature Stresses- Table VII



In equations for balanced earth pressure substitute $+\frac{Ect}{s}$ for $\sum \frac{M_e M_k}{l}$ (temperature rise) and 0 for $\sum \frac{M_e M_k}{l}$

$$I. 10020H + 5840V + \frac{Ect}{s} = 0.$$

$$II. 5840H + 3751V + 0 = 0$$

$$\frac{Ect}{s} = \frac{144 \times 2000 \times 0.000065 \times 35 \times 50}{5} = 655 \text{ (kip-ft. units for } 35^\circ \text{ rise in temperature)}$$

$$I. H + 0.589V = -0.065$$

$$II. \frac{H + 0.642V = 0}{0.059V = 0.065}$$

$V = 1.1$ and $H = -0.7$ for temperature rise of 35°

Mom. due to $H = Hy$. Mom. due to $V = V \frac{l-x}{2}$

Moments.

Point	1	2	3	4	5	6	7	8	9	10	11	12	13
y	4.6	9.6	14.6	18.2	19.1	19.7	20.2	20.4	20.4	20.3	19.9	19.4	18.7
$\frac{1}{2}(l-x)$	0	0	0	1.2	3.8	6.2	8.8	11.2	13.8	16.2	18.8	21.2	23.8
Hy	-3.2	-6.7	-10.2	-12.7	-13.4	-13.8	-14.1	-14.3	-14.3	-14.2	-13.9	-13.6	-13.1
$\frac{1}{2}V(l-x)$	+0	+0	+0	+1.5	+4.2	+6.8	+9.7	+12.3	+15.2	+17.8	+20.7	+23.9	+26.2
Total	-3.2	-6.7	-10.2	-11.4	-9.2	-7.0	-4.4	-2.0	+0.9	+3.6	+6.8	+9.7	+13.1

Normal Thrusts: Points 1, 2, 3; $N = +0.5$

Points 4 to 13; $N = +0.7$

Points 14, 15, 16; $N = -1.1$

For temperature fall of 45° Moments and Normal Thrusts will be of opposite sign and numerically $\frac{45}{35}$ x those calculated above.

Loading	Point 1R		Point 2R		Point 3R		Point 4R		Point 5R		Point 6R		Point 7R		Point 8R	
	M	N	M	N	M	N	M	N	M	N	M	N	M	N	M	N
Dead	-17.6	+15.2	-37.7	+13.3	-57.2	+10.9	-49.1	+3.9	-21.4	+3.9	-3.7	+3.9	+4.1	+3.9	+6.9	+3.9
Earth P.	+14.5		+17.7		+11.3		+3.3	+2.5	+1.3	+2.5	+0.4	+2.5	-0.6	+2.5	-0.8	+2.5
Sub-total	-3.1	+15.2	-20.0	+13.3	-45.9	+10.9	-45.8	+6.4	-20.1	+6.4	-3.3	+6.4	+3.5	+6.4	+6.1	+6.4
Live +	+2.2	-0.2	+4.6	-0.5	+7.0	-0.4	+9.6	-0.1	+11.4	+0.6	+12.4	+1.1	+12.2	+1.3	+11.1	+1.9
Live -	-9.6	+2.9	-19.8	+2.7	-30.7	+2.9	-31.0	+2.0	-20.8	+1.9	-12.1	+1.7	-4.8	+1.4	-1.2	+0.1
Temp. rise	-3.2	+0.5	-6.7	+0.5	-10.2	+0.5	-11.4	+0.7	-9.2	+0.7	-7.0	+0.7	-4.4	+0.7	-2.0	+0.7
Temp. fall	+4.1	-0.6	+8.6	-0.6	+13.1	-0.6	+14.7	-0.9	+11.9	-0.9	+9.0	-0.9	+5.7	-0.9	+2.6	-0.9
Max.Total +									+3.2	+6.1	+18.1	+6.6	+21.4	+6.8	+19.8	+7.4
Max.Total -	-15.9	+18.6	-46.5	+16.5	-86.8	+14.3	-88.2	+9.1	-50.1	+9.0	-22.4	+8.8	-5.7	+8.5		

Loading	Point 9R		Point 10R		Point 11R		Point 12R		Point 13R		Point 14R		Point 15R		Point 16R	
	M	N	M	N	M	N	M	N	M	N	M	N	M	N	M	N
Dead	+3.5	+3.9	-5.3	+3.9	-20.9	+3.9	-45.7	+3.9	-82.8	+3.9	+24.1		+25.6		+27.1	
Earth P.	-0.4	+2.5	+0.4	+2.5	+1.9	+2.5	+3.5	+2.5	+5.8	+2.5						
Sub-total	+3.1	+6.4	-4.9	+6.4	-19.0	+6.4	-42.2	+6.4	-77.0	+6.4	+24.1		+25.6		+27.1	
Live +	+10.8	+1.6	+10.7	+1.1	+10.3	+0.8	+8.2	+0.5	+6.0	+0.4	+24.2	+2.2	+15.0	+2.2	+6.2	+2.2
Live -	-3.4	+0.6	-10.0	+1.4	-20.4	+1.4	-31.5	+1.3	-44.4	+1.4	-24.2	+2.2	-15.0	+2.2	-6.2	+2.2
Temp. rise	+0.9	+0.7	+3.6	+0.7	+6.8	+0.7	+9.7	+0.7	+13.1	+0.7	-1.1		-1.1		-1.1	
Temp. fall	-1.2	-0.9	-4.6	-0.9	-8.7	-0.9	-12.5	-0.9	-16.9	-0.9	+1.4		+1.4		+1.4	
Max.Total +	+14.8	+8.7	+9.4	+8.2	-48.1	+6.9	-86.2	+6.8	-138.3	+6.9	+24.2	+25.2	+15.0	+26.7	+6.2	+28.2
Max. Total -			-19.5	+6.9							-24.2	+25.2	-15.0	+26.7	-6.2	+28.2

Table 1X
Calculation of Reinforcing Steel Area per ft. width, for revised final depths t . See Note below.

K ft.	Moment		N lbs.	$e \cdot N$ Inches	t Inches	d Inches	$e' = \frac{e \cdot d}{t - 2}$	$\frac{e'}{d}$	$K = \frac{N e'}{b d^2}$	f_c	f_s	Revised p	Revised A_s per ft. width	A_s'	$\frac{A_s'}{A_s}$
	ft. lbs.	inch lbs.													
1	-15900	-190000	18600	102	27	25	21.7	0.9	54						1
2	-46500	-558000	16500	39.8	32	30	47.8	1.6	73	550	18000	.0018	0.65		2
3	-86800	-1040000	14900	72.7	37	35	89.2	2.6	87	600	"	.0037	1.55		3
4	-107000	-1285000	14700	87.4	38	36	104.4	2.9	99	650	"	.0042	1.81		4
5	-109200	-1058000	9100	116.1	36.5	34.5	132.4	3.8	95	600	"	.0041	1.74		5
6	-22400	-601000	9000	66.7	27	25	78.2	3.1	94	620	"	.0041	1.23		6
7	-22400	-269000	8800	30.5	20	18	98.5	2.1	87	600	"	.0032	0.69		7
8	-21400	-257000	6800	57.8	15.5	13.5	43.6	3.2	136	800	"	.0025	0.54		8
9	-14800	-178000	8700	20.5	13.8	11.8	25.4	2.2	152	800	18000	.0050	0.70	1.0	9
10	-9400	-119000	8200	13.8	17.5	15.5	20.6	1.3	59	470	"	.0010	0.19		10
11	-19500	-234000	6900	53.9	17.5	15.5	40.7	2.6	98	650	"	.0039	1.53		11
12	-86200	-1035000	6800	152.0	34	32	93.6	4.5	111	700	"	.0035	1.45		12
13	-138800	-1660000	6900	241.0	48	46	263.0	5.7	69	520	"	.0036	2.00		13
14	-24200	-290000	115	24	22	21.5	21.5	1.0	94	630	"	.0007	0.19		14
15	-15000	-180000	26700	6.7	24	22	16.7	0.8	77	550	"				15
16	-6200	-75000	28200	2.7	24	22	12.7	0.6	62						16

Note that the thicknesses t used in the above table and for the actual structure are slightly less than was assumed in the foregoing design calculations. The dead loads and frame constants would be slightly different, but the error is negligible.

Calculation of reinforcement for Point 8:

Assume $k = 0.44$. Then $Kd = 4.9$, $jd = 11.2$, $\frac{A_s}{b d} = 9.61$, $f_s = 800 \times 15 \times \frac{6.9}{4.9} = 15400$, $f_s' = 800 \times 15 \times \frac{2.9}{4.9} = 7100$.

Moment to be carried = $N e' = 7400 \times 36.8 = 272000$

Moment of resistance = $12 \times 4.9 \times 400 \times 9.6 \times \frac{226000}{46000}$

To be carried by additional steel = $\frac{272000 - 15400 \times 36}{15400 \times 3.6} = 15400 \times 3.2 = 15400$

$A_s = \frac{46000}{15400 \times 3.6} = 0.7" \text{ say } 1.0"$

$A_s' = \frac{7100}{15400 \times 3.6} = 0.14"$

Note that smaller value for k would give larger A_s and smaller A_s' .

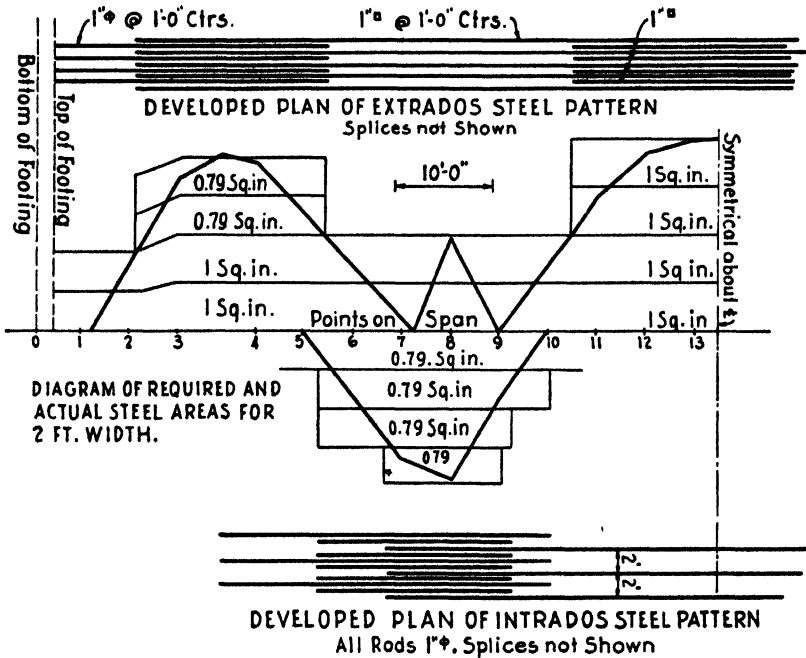
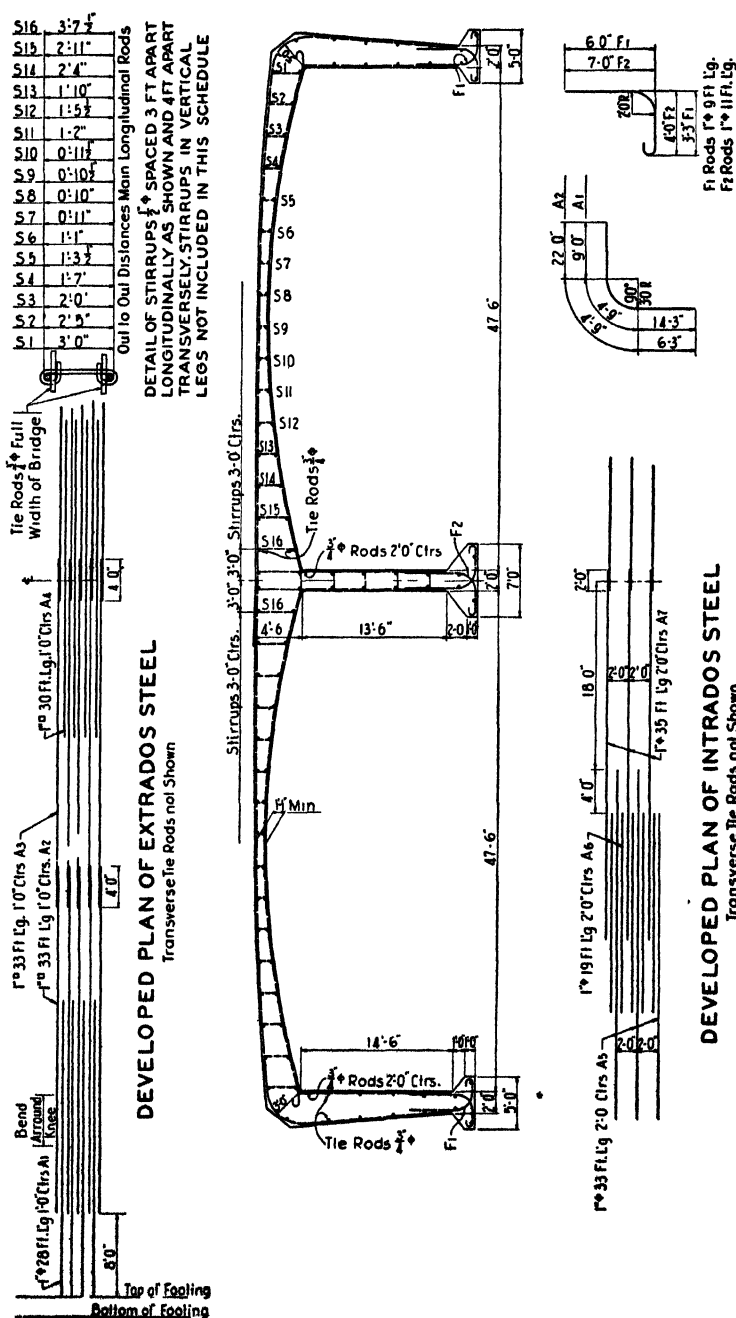


FIG. 55.



DEVELOPED PLAN OF INTRADOS STEEL

Transverse Tie Rods not Shown

FIG. 56.

Application of Double-Span Rigid-Frame Bridges

The illustration at the end of this chapter shows the adaptation of the double-span bridge to dual highways. The modern tendency to separate opposing traffic, wherever possible, by means of a separation strip, is bringing the construction of double-span bridges to the fore.

See Chapter XI for discussion in regard to rigid-frame bridges restrained at the footings.



14th Street grade separation on the Mount Vernon Memorial Highway in Virginia.
Courtesy of U. S. Bureau of Public Roads.

CHAPTER X

THE THEORY AND DESIGN OF SKEWED ARCH OR FRAME BRIDGE

General Discussion.—The design of skewed bridges is constantly assuming more importance as the needs of modern traffic are better appreciated. It is little short of criminal nowadays to permit crooked alignment of a through highway, approaching a bridge, in order to avoid skew in the structure; and many existing structures will have to be replaced in the near future in order to eliminate blind curves, originally introduced to permit the construction of a square bridge. A particular reason for avoiding skewed bridges of the solid barrel-arch type has been the fact that several failures convinced conservative engineers that the skew introduced certain forces that were not generally recognized. Some engineer mathematicians realized that the skew arch demanded special consideration, and for many years various attempts were made to solve the problem but without success.

The difficulty lay in the fact that they were dealing with forces in space whereas the edifice of structural analysis has been reared upon uni-planar mechanics. The practical engineer who risked a skewed arch design was accustomed to analyze a unit strip parallel to the main axis as he would a square arch element and assume that the skew arch was a composition of a number of such strips or elements. The error of such an assumption may be made apparent by a homely illustration. Cut from a piece of cardboard a skew slab *abcd* as indicated in Fig. 57, and support it upon two triangular scales or like supports along lines *e-f* and *g-h* so that the ends cantilever beyond the supports. Apply a load

in the middle. The acute corners will rise off the supports, showing that the load tends to travel the shortest distance to the supports and the slab deforms so that the elements of curvature are visibly perpendicular to the unsupported edges. Now, with the load still applied, press down on the

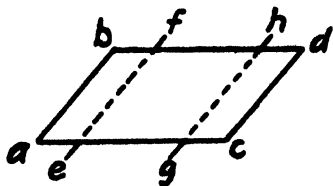


FIG. 57.

cantilevered ends of the cardboard until the slab is horizontal along the supports. The slab is so constrained that the elements of curvature are visibly parallel to the supported edges of the slab and the load is obviously traveling in the skew direction to the supports instead of in the shortest direction. The restraint introduced in the second case is an element of design which should be considered. Skew arch action is analogous.

If the fixed skew arch ring proper is adequately secured to abutments of sufficient mass to resist the skew effects, the loads will travel parallel to the skew; if not, incipient failure will cause the loads to travel a shorter distance to the abutments and complete failure may result. In the two-hinged skew arch the skew forces must be resisted at the hinges. In the skew rigid frame, the legs act as abutments for the top of the frame and are of sufficient mass so that usually little transverse reinforcement is required. In heavily skewed bridges of long span relative to width, the tendency of the acute corners to rise must be examined.

The general proposition may thus be stated as follows: The skew arch is a structure containing forces which cannot generally be made parallel to a single plane; they must therefore be analyzed in three dimensions instead of two as for the right arch. The skew of the structure introduces forces and moments which either do not exist at all in the right arch or are present in a small degree.

Before proceeding with the discussion, a system of reference axes for working in three planes will be adopted. As in a right arch, the horizontal axis perpendicular to the

abutments is called the X axis, and the vertical axis, the Y axis. The axis parallel to the abutment (not used for the right arch) is called the Z axis. Each axis is perpendicular to the other two and each of the three planes formed by the axes is perpendicular to the other two. The XZ plane which is the horizontal plane in which both the X and Z axes lie is perpendicular to the YZ plane and to the XY plane; the latter is the vertical plane perpendicular to the abutments, and the plane in which all forces and reactions in a right arch are assumed to lie. A moment couple about any particular axis lies in a plane parallel to the plane in which the other two axes lie.

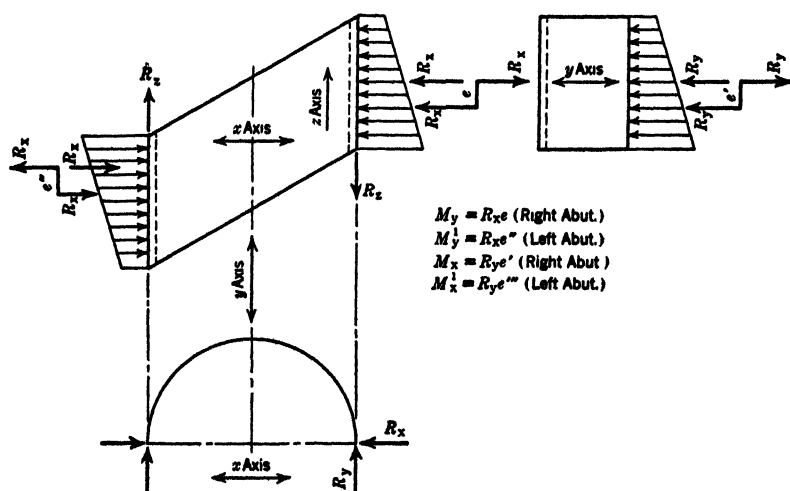


FIG. 58.

In Fig. 58 is represented a two-hinged skew arch with its reactions due to any load. The general directions of the X , Y and Z axes are shown, but the most convenient points of origin will be indicated later on. The total vertical reactions R_y are the same as for a simple beam of the same span, and of a width equal to the skew width of arch. The total horizontal reactions R_x are equal to each other

and depend upon the elastic and geometric properties of the arch. If the analysis of this arch is to be general, the assumption must be made that reactions R_y and R_z are not uniform along the abutments but in general as shown in Fig. 58; that is, variable and unsymmetrical about the center line of the abutment. This condition as to reaction R_z may be represented by placing reaction R_z at the center of the abutment and introducing a moment or couple M_y equal to $R_z e$ about the Y axis. Likewise the condition as to reaction R_y may be represented by placing reaction R_y at the middle of the abutment and introducing a moment or couple M_z equal to $R_y e'$ about the X axis. It is also seen that the two horizontal reactions R_z form a couple which tends to rotate the structure as a whole. To resist this tendency, the two cross shears R_y are called into play and form a couple which balances in part the moment produced by the two reactions R_z .

The moment M_z was illustrated by the cardboard skew slab experiment, in which the tendency of the acute corners to rise off the supports was shown. A moment reaction like M_z in Fig. 58 was required to resist this tendency.

In general terms the five reactions in a skew *two-hinged* arch are set up by the tendency of the unrestrained structure to deflect and rotate in all directions and in all planes when subjected to load. The abutments are free to rotate at the real or assumed hinges; therefore no resisting moments are set up to compensate. The tendency of the abutments to deflect along the X axis is resisted by reactions R_z (horizontal thrust as in the right arch) and the tendency to deflect along the Z axis is resisted by reactions R_y . The tendency of the abutments to rotate about the X axis is resisted by moment M_z and the tendency to rotate about the Y axis is resisted by moments M_y . The tendency of the abutments to deflect along the Y axis is resisted by reactions R_y .

Fixing the footings affects the skew arch in the same manner as it does the right arch; the tendency to rotate about the Z axis is resisted by a counter moment, and there

are therefore six reaction components instead of five as in the hinged structure.

The magnitude of the reactions for any given condition of loading is found by deflection calculations, applying the principles heretofore demonstrated, as will be shown in a numerical example.

Once the reactions are determined, the stresses existing at any section may be calculated from considerations of equilibrium. Reactions R_y and R_z produce moments, shears and thrusts in the vertical planes perpendicular to the Z axis—the stresses met with in the right arch. Reactions R_x produce shear parallel to the Z axis. Reaction moments M_y and M_z produce torsion in the vertical and horizontal portions of the arch, respectively. Reactions R_y with moment arms along Z axis and reactions R_z with moment arms along the Y axis produce torsion in the horizontal sections of the arch. Reactions R_x with moment arms along the Z axis produce torsion in the vertical sections of the arch. Torsion in the inclined sections of the arch is produced by combinations of all the torsion moments. The torsion moments in turn produce vertical shears in the YZ plane, which are small and may be neglected. They also produce horizontal shears parallel to the Z axis which must be combined with the shears due to reaction R_x . A moment about the Y axis is also developed by all the reactions and reaction moments parallel to the XZ plane. This moment, though large numerically, is resisted by the entire arch acting as a horizontal beam between reaction supports; the width of the arch is the depth of the beam, therefore the stresses produced are very small. This horizontal moment about the Y axis may then be neglected as far as the horizontal portion of the arch is concerned. In all cases, as in the analysis of any other structure, the external forces have their effect on the numerical values of the stresses outlined above.

The first complete solution for the reactions in a skew

fixed arch appeared as a paper by J. Charles Rathbun (then of the University of Washington) in the Transactions, 1924, of the American Society of Civil Engineers. His pioneer mathematical work was afterward verified by the classical three-dimensional deformeter analysis of Professor George E. Beggs of Princeton University. Subsequently Professor Rathbun extended his method of analysis to the two-hinged arch or frame bridge for the Westchester County Park Commission. Based upon this theory, several skew arch and frame bridges have been designed and built, up to 50 degrees skew. The following exposition of Professor Rathbun's theory is by Richard M. Hodges, designer for the Westchester County Park Commission.

Derivation of Equations.—It has been shown in the foregoing discussion that a skewed hinged arch or frame structure under load develops five reaction components at each abutment. As in the case of the double-span square-frame bridge, the supports are assumed to be so altered by the removal of redundant reactions that the structure becomes a simple span beam, as indicated in Fig. 59. In this case the redundant reactions are R_x , R_y , M_x and M_y , all at the right support, R_v being the simple span reaction. Because this transformed structure is statically determinate, the stresses in all parts of the structure due to any given loading may be found by the laws of static equilibrium. Likewise, the linear and angular deflections at the right support may be calculated. The redundant reactions are now assumed to be applied in such manner that the linear and angular deflections due to them are equal and opposite to the deflections in the transformed structure. In other words, the total resultant deflection in any direction at the right support with all forces acting is equal to zero. The fundamental general equations used in this derivation are mathematical expressions of the above statement.

This is the same general principle followed in finding the reactions for the double-span frame. Attention is called

to the general discussion of algebraic sign conventions in Chapter IV. The same convention of signs is used here as applied in the design of the fixed-end frame and the double-span frame.

In accordance with the convention of signs used in the foregoing work, all moments causing tension along the intrados are considered positive. In the case of the skewed frame, all moments about the z axis, corresponding to the moments occurring in rectangular structures, are governed by the same convention; but it is necessary to consider, in addition, moments about the v axis (the torsional moments) which also enter into the equations for the unknown reactions. The positive direction of moments about the v axis, and also the positive directions of all other forces and moments acting at P , are in the directions shown in Fig. 59. All redundant reactions at the right support are assumed to be directed as shown in the figure. Unit thrusts and couples are in each case assumed to act in the directions of the corresponding reactions.

All substitutions in the general deflection equations, to obtain the final equations, are made with due regard to the signs of the moments caused at P by the reactions acting as assumed, and by the direction of the external loading under consideration. In making numerical substitutions in the final equations, it is only necessary to take care of the proper signs of terms containing trigonometrical functions of the angle ϕ . After solution of the equations, the true directions of the reactions are established in each case by their signs. If positive they are in the directions originally assumed, and, if negative, they are in the opposite directions.

The internal stresses at any section (such as P , Fig. 59) may be represented for the sake of simplicity by a system of external forces and moments exerted by the portion of the arch to the left of the cut section on the portion of the arch to the right of the cut section. These forces and reactions must be such as to keep the portion of the arch

to the right of the cut section in equilibrium under the applied loading and the reactions at right support. The forces and moments representing the internal stresses at P are T_u , T_v , T_z , M_u , M_v , and M_z , acting along the three axes

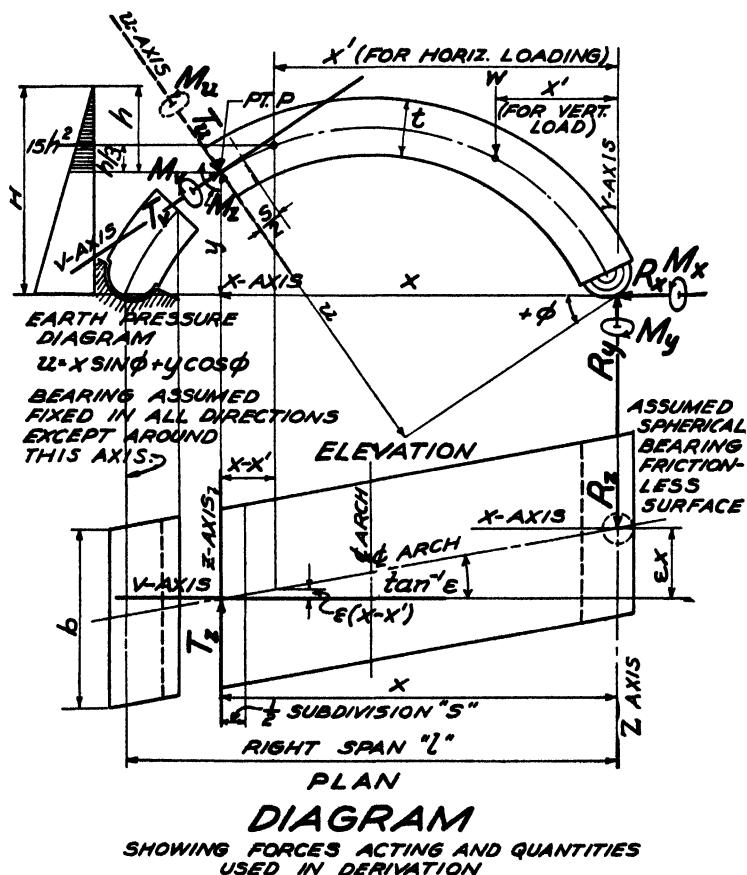


FIG. 59.

u , v and z perpendicular to each other and intersecting at P . As will be seen by referring to the figures, the axis v is tangential to the neutral surface at P and in plane perpendicular to the abutments; the axis u is perpendicular to the neutral

surface at P ; and the axis z is horizontal and parallel to the abutments. Axes u and v (while always remaining in a vertical plane) change in direction according to the location of P . Axis z is in the same direction for any location of P , and for the special case when P is at the right support, axis z becomes the line of action of reaction R_r .

The best way to avoid difficulty in skew arch analysis is to obtain, in the beginning, a clear idea of the various axes and the moments and forces acting. This can be done only by a close study of the figure.

The moment M_u and the thrust T_u are shown dotted, indicating that they exist, although they have been neglected in the computations.

The quantity $F = \frac{bt^3}{3.58}$, used in the calculations, is the factor of torsion; an empirical quantity which is analogous to the polar moment of inertia. For further information, the reader is referred to *Bulletin 3*, Faculty of Applied Science and Engineering, School of Engineering Research, University of Toronto. All other symbols and quantities used in the analysis and in the computations are defined in Fig. 59 and Table I.

The slide rule is sufficiently precise for all the numerical work in the following tables, excepting the solution of the simultaneous equations in Table II. Here it is advisable to use the calculating machine.

REACTIONS FOR TWO-HINGED SKEWED ARCH

By inspection of the diagram, general expressions may be written for M_r , M_u , M_z , T_r , T_u and T_z , respectively, in terms of the loading and the unknown reaction components. Since M_u and T_u may be neglected—see text—expressions for these quantities have been omitted.

For Vertical Loading as Indicated on Diagram

$$M_s = R_v x - W(x - x') - R_z y = M_0 - R_z y;$$

$$\begin{aligned} M_v &= R_z \sin \phi \epsilon x - R_z u + M_z \cos \phi - M_v \sin \phi \\ &\quad + R_v \cos \phi \epsilon x - W \cos \phi \epsilon (x - x'); \\ &= R_z \sin \phi \epsilon x - R_z u + M_z \cos \phi - M_v \sin \phi \\ &\quad + M_0 \cos \phi \epsilon; \end{aligned}$$

$$T_v = -R_v \sin \phi + W \sin \phi + R_z \cos \phi = V_0 \sin \phi + R_z \cos \phi;$$

$$T_s = R_s.$$

In which M_0 = moment for simple beam of right span l ;

In which V_0 = shear for simple beam of right span l .

The above equations for vertical loading can be made to apply to the horizontal earth pressure loading shown on diagram (30 lb./sq. ft./ft. depth) without rewriting by making the following substitutions:

For simple span moment M_0 in expression for M_s :
 substitute $R_v x - \underline{5h^3}$

For $M_0 \cos \phi$ in expression for M_v :
 substitute $R_v x \cos \phi - \underline{15h^2 \sin \phi (x - x')}$

For $V_0 \sin \phi$ in expression for T_v :
 substitute $-R_v \sin \phi - \underline{15h^2 \cos \phi}$

NOTE.—All terms underlined above are to be dropped in considering any point to the right of location of applied loading.

Derivation of Equations for Redundant Reactions

Consider the deflections at right support due to moments M_s and M_v at any section such as P in diagram. (Deflections due to M_s and to the thrusts T_s , T_v and T_v are comparatively small and may be neglected.)

Let M_z = moment at P about z axis due to all forces acting;

M_v = moment at P about v axis due to all forces acting;

$m_{v(x)}$ = moment at P about v axis due to unit thrust at right reaction along R_z ;

$m_{v(y)}$ = moment at P about v axis due to unit thrust at right reaction along R_z ;

$m_{v(ox)}$ = moment at P about v axis due to unit couple at right reaction along M_z ;

$m_{v(oy)}$ = moment at P about v axis due to unit couple at right reaction along M_v ;

$m_{z(x)}$ = moment at P about z axis due to unit thrust at right reaction along R_z ;

$m_{z(y)}$ = moment at P about z axis due to unit thrust at right reaction along R_z ;

$m_{z(ox)}$ = moment at P about z axis due to unit couple at right reaction along M_z ;

$m_{z(oy)}$ = moment at P about z axis due to unit couple at right reaction along M_v ;

G = shearing modulus of elasticity;

ϵ = tangent of the skew angle;

s = a division of the arch axis;

k = ratio of modulus of elasticity for direct stress to modulus for shear $= \frac{E}{G}$.

The total deflections at right support along the lines of action of each of the unknown reaction components, due to all forces acting, are equal, respectively, to zero.

That is:

$$\begin{aligned} \text{I. } & \frac{s}{G} \sum \frac{M_v m_{v(x)}}{F} + \frac{s}{E} \sum \frac{M_z m_{z(x)}}{I} = 0 \\ \text{II. } & \frac{s}{G} \sum \frac{M_v m_{v(z)}}{F} + \frac{s}{E} \sum \frac{M_z m_{z(z)}}{I} = 0 \\ \text{III. } & \frac{s}{G} \sum \frac{M_v m_{v(ox)}}{F} + \frac{s}{E} \sum \frac{M_z m_{z(ox)}}{I} = 0 \\ \text{IV. } & \frac{s}{G} \sum \frac{M_v m_{v(oy)}}{F} + \frac{s}{E} \sum \frac{M_z m_{z(oy)}}{I} = 0 \end{aligned}$$

Referring to Fig. 59 and to page 146:

$$M_v \text{ (for vertical loading)} = R_x \sin \phi \epsilon x - R_z i l \\ + M_x \cos \phi - M_v \sin \phi + M_0 \cos \phi \epsilon$$

$$M_z \text{ (for vertical loading)} = -R_x y + M_0$$

$$M_v \text{ (for horizontal loading)} = R_x \sin \phi \epsilon x - R_z u \\ + M_x \cos \phi - M_v \sin \phi \\ + [R_v x \cos \phi - 15 h^2 \sin \phi (x - x')] \epsilon$$

$$M_z \text{ (for horizontal loading)} = -R_x y + R_v x - 5 h^3.$$

$$m_{v(x)} = \sin \phi \epsilon x; \quad m_{v(z)} = -u; \quad m_{v(ox)} = \cos \phi; \quad m_{v(oy)} = -\sin \phi; \\ m_{z(x)} = -y; \quad m_{z(z)} = 0; \quad m_{z(ox)} = 0; \quad m_{z(oy)} = 0.$$

Substituting above values in equations I, II, III and IV, simplifying cancelling and collecting terms, the final equations are obtained as follows:

$$\begin{aligned} \text{I. } & R_x \left(\epsilon^2 \kappa \sum \frac{x^2 \sin^2 \phi}{F} + \sum \frac{y^2}{I} \right) - R_x \epsilon \kappa \sum \frac{ux \sin \phi}{F} \\ & + M_x \epsilon \kappa \sum \frac{x \sin \phi \cos \phi}{F} - M_v \epsilon \kappa \sum \frac{x \sin^2 \phi}{F} \\ & = -\epsilon^2 \kappa \sum \frac{M_0 \sin \phi \cos \phi x}{F} + \sum \frac{M_0 y}{I} \end{aligned}$$

$$\begin{aligned} \text{II. } & R_x \epsilon \sum \frac{ux \sin \phi}{F} - R_x \sum \frac{u^2}{F} + M_x \sum \frac{u \cos \phi}{F} \\ & - M_v \sum \frac{u \sin \phi}{F} = -\epsilon \sum \frac{M_0 u \cos \phi}{F} \end{aligned}$$

$$\text{III. } R_x \epsilon \sum \frac{x \sin \phi \cos \phi}{F} - R_z \sum \frac{u \cos \phi}{F} + M_x \sum \frac{\cos^2 \phi}{F} \\ - M_y \sum \frac{\sin \phi \cos \phi}{F} = - \epsilon \sum \frac{M_0 \cos^2 \phi}{F}$$

$$\text{IV. } R_x \epsilon \sum \frac{x \sin^2 \phi}{F} - R_z \sum \frac{u \sin \phi}{F} + M_x \sum \frac{\sin \phi \cos \phi}{F} \\ - M_y \sum \frac{\sin^2 \phi}{F} = - \epsilon \sum \frac{M_0 \sin \phi \cos \phi}{F}$$

Note that left-hand members of above equations apply to any loading. Right-hand members of equations as above given apply particularly to vertical loading, for which M_0 = simple span moment. For horizontal earth pressure use substitutions given on page 148. For temperature reactions substitute for right-hand members of equations I, II, III and IV, respectively, the terms:

$$+ \frac{Ectl}{s}; \quad - \frac{E\epsilon ctl}{\kappa s}; \quad 0; \quad \text{and } 0. \quad (t^\circ \text{ rise})$$

(c = coefficient of expansion)

Equations as given are in final form for numerical substitution. All summations are to be carried through entire arch. Summations in left-hand members of equations are constant summations; once made they will apply for all loadings. Summations in right-hand members are variable summations and must be made separately for each loading and each position of influence loads. All symbols and quantities are as shown in Fig. 59 and explained in text.

Design of Sections.—The method for designing sections explained in the following text is substantially that proposed originally by Professor Rathbun in 1926 and later explained in detail in his paper in *Proceedings, American Society of Civil Engineers* for April, 1931. The procedure can be readily understood by following through the tabulated calculations. Figure 65 shows the forces acting on any

cut section as found from the preceding analysis, and the transformation of these forces into directions parallel to the assumed directions of the two systems of reinforcement.

The transformed forces having been determined, the final step is to design the two reinforcement systems independently, using for each system the two forces acting in the direction considered. The forces used for the longitudinal system are the direct moment M_i and the direct thrust T_i . The forces used for the transverse system are the torsion moment M_i and the shear T_i . The longitudinal system is designed for flexure and compression in the same way as for a rectangular arch and needs no explanation. The transverse system is designed for a combination of torsional and direct shear in accordance with the method proposed by Professor Rathbun, which will be found clearly illustrated and explained in the tabulations. The general method may be briefly summarized as follows:

The direct transverse shear, at the location considered, is distributed parabolically across the width of the arch, and in the same way as vertical shear is distributed along the depth of a simple beam. The maximum intensity, three halves of the average unit shear, is at the center line of the arch and is constant throughout the depth.

The maximum torsional shear is found by Merriman's formula, $v = 9M_i \div 2bt^2$ for elongated rectangular shafts, which is used in this connection in preference to St. Venant's formula simply because it is more severe. The maximum torsional shears exist at the top and the bottom across the center line of the arch, and in opposite directions; the vertical distribution being triangular, as shown in diagram accompanying Table XIX. The direct shear and torsional shear acting across the center line of arch at the section considered are combined, and the capacity of the plain concrete (30 lb. per sq. in.) is deducted. Transverse reinforcement is then designed to take the remainder by a method analogous to that followed for designing vertical

stirrups for an ordinary concrete beam whose depth is the width of bridge and whose width is the depth of arch.

Figure 59 indicates the positive directions of M_i and T_i at any section. Whenever M_i and T_i are of the same sign they work together to cause shearing stress at the extrados and against each other in causing shearing stress at the intrados; and conversely, when they are of different sign they combine to cause shearing stress at intrados and oppose each other in causing shearing stress at the extrados. After making the transformation the same effects hold true for M_t and T_t .

This leads to the following rule, which is based on the positive directions of M_i and T_i as previously assumed:

(1) When v_i and v_t are of the same sign, add to obtain resultant shear at extrados and subtract to obtain resultant shear at intrados.

(2) When v_i and v_t are of different sign, add to obtain resultant shear at intrados and subtract to obtain resultant shear at extrados.

The algebraic sign of the *resultant* shear is not significant in view of the type of reinforcement used. Therefore in Table XVIII the signs are dropped as soon as they have served their purpose of determining the resultant shears top and bottom.

TABLE II.—SOLUTION OF SIMULTANEOUS EQUATIONS

Equations	VERTICAL UNIT LOAD AT POINT NO.			Earth Pressure Left	Temperature Stresses
	6R	8R	10R		
I. $+119.664 R_2 - 30.867 R_3 + 0.1341 M_2 - 0.5163 M_3$	$= +19.72$	$= +37.57$	$= +48.15$	$= +13039.0$	$= +1215.0$
II. $+11.561 R_2 - 43.735 R_3 + 1.418 M_2 - 0.2477 M_3$	$= -4.49$	$= -8.61$	$= -11.27$	$= -3298.0$	$= -336.0$
III. $+0.0502 R_2 - 1.418 M_2 + 0.0664 M_3 + 0$	$= -0.219$	$= -0.424$	$= -0.538$	$= -146.9$	$= 0$
IV. $+0.1934 R_2 - 0.2477 R_3 + 0 - 0.0090 M_3$	$= +0.0057$	$= +0.0078$	$= +0.0024$	$= -5.09$	$= 0$
Dividing each equation by its R_2 coefficient:					
I. $+R_2 - 0.2579 R_3 + 0.0011 M_2 - 0.0043 M_3$	$= +0.1648$	$= +0.3139$	$= +0.4023$	$= +108.95$	$= +10.15$
II. $+R_2 - 3.7830 R_3 + 0.1226 M_2 - 0.0214 M_3$	$= -0.3882$	$= -0.7449$	$= -0.9746$	$= -285.27$	$= -30.79$
III. $+R_2 - 28.2470 R_3 + 1.3227 M_2 + 0$	$= -4.3685$	$= -8.4382$	$= -10.7211$	$= -2926.59$	$= 0$
IV. $+R_2 - 1.2809 R_3 + 0 - 0.0465 M_3$	$= +0.0295$	$= +0.0466$	$= +0.0124$	$= -26.32$	$= 0$
Subtracting Equations II, III and IV, respectively, from Equation I:					
1. $+3.5231 R_3 - 0.1215 M_2 + 0.0171 M_3$	$= +0.5530$	$= +1.0588$	$= +1.3769$	$= +394.22$	$= +40.94$
2. $+27.9801 R_3 - 1.3216 M_2 - 0.0043 M_3$	$= +4.5333$	$= +8.7521$	$= +11.1234$	$= +3035.24$	$= +10.15$
3. $+1.0229 R_3 + 0.0011 M_2 + 0.0422 M_3$	$= +0.1353$	$= +0.2733$	$= +0.3899$	$= +135.27$	$= +10.15$
Dividing each equation by its R_3 coefficient:					
1. $+R_3 - 0.0345 M_2 + 0.0048 M_3$	$= +0.1569$	$= +0.3004$	$= +0.3906$	$= +111.83$	$= +11.61$
2. $+R_3 - 0.0472 M_2 - 0.0002 M_3$	$= +0.1620$	$= +0.3127$	$= +0.3974$	$= +108.44$	$= +0.36$
3. $+R_3 + 0.0011 M_2 + 0.0413 M_3$	$= +0.1323$	$= +0.2672$	$= +0.3812$	$= +132.24$	$= +9.92$
Subtracting Equations 2 and 3 respectively, from Equation 1:					
A. $+0.0157 M_2 + 0.0050 M_3$	$= -0.0051$	$= -0.0123$	$= -0.0068$	$= +3.39$	$= +11.25$
B. $-0.0316 M_2 - 0.0364 M_3$	$= +0.0246$	$= +0.0332$	$= +0.0094$	$= -20.41$	$= +1.69$
Dividing each equation by its M_2 coefficient:					
A. $+M_2 + 0.3925 M_3$	$= -0.4016$	$= -0.9685$	$= -0.5354$	$= +266.93$	$= +886.03$
B. $-M_2 - 1.0242 M_3$	$= +0.6910$	$= +0.9326$	$= +0.2640$	$= -573.31$	$= +47.48$

For coefficients of R_2 , R_3 , M_2 , M_3 , see Table I.

For unit vertical load substitutions, see Table III, IV & V.

For earth pressure substitutions, see Tables VI & VII.
For temperature substitutions, see Table VIII.

TABLE II.—SOLUTION OF SIMULTANEOUS EQUATIONS—Continued

Equations	VERTICAL LOAD AT POINT No.			Earth Pressure Left	Temperature Stresses
	6R	8R	10R		
Adding Equation A to Equation B: - 0.6317 M_y + M_y	= + 0.2894 = - 0.4581	= - 0.0359 = + 0.0568	= - 0.2714 = + 0.4296	= - 306.38 = + 485.01	= + 933.5 = - 1477.8
Substituting value of M_y in Equation A, and solving: ... M_x	= - 0.4016 = + 0.1798	= - 0.9685 = - 0.0223	= - 0.5354 = - 0.1886	= + 266.93 = - 190.37	= + 886.0 = + 580.0
Substituting values of M_x and M_y in Equation I and solving: ... R_e	= - 0.2218	= - 0.9908	= - 0.7040	= + 76.56	= + 1466.0
Substituting values of R_e , M_x and M_y in Equation I and solving: ... R_e	= + 0.1569 = + 0.0022 = - 0.0076	= + 0.3004 = - 0.0002 = - 0.0342	= + 0.3906 = - 0.0021 = - 0.0243	= + 111.83 = - 2.33 = + 2.64	= + 11.6 = + 50.5 = + 7.0
Substituting values of R_e , M_x and M_y in Equation I and solving: ... R_e	= + 0.1515	= + 0.2660	= + 0.3642	= + 112.14	= + 69.2
Substituting values of R_e , M_x and M_y in Equation I and solving: ... R_e	= + 0.1648 = - 0.0020 = + 0.0002 = + 0.0391	= + 0.3139 = + 0.0002 = + 0.0011 = + 0.0686	= + 0.4023 = + 0.0018 = + 0.0008 = + 0.0939	= + 108.95 = + 2.09 = - 0.08 = + 28.92	= + 10.1 = + 17.8 = - 1.6 = - 6.3
	= + 0.2021	= + 0.3838	= + 0.4988	= + 139.88	= + 20.0

For coefficients of R_e , R_e , M_x , M_y , see Table I.
For unit vertical load substitutions, see Tables III, IV & V.
For earth pressure substitutions, see Tables VI & VII.
For temperature substitutions, see Table VIII.

TABLE III.—VERTICAL INFLUENCE LOAD AT 6R

Point	Values for Substitution in Right-Hand Members of Equations I, II, III, IV (See Table II)						Final Moments and Thrusts ($R_x = +0.202$, $R_y = +0.152$, $M_x = -0.222$, $M_y = -0.460$)					
	$\frac{M_0 \sin \phi \cos \phi}{F}$	$\frac{M_0 \cos \phi}{F}$	$\frac{M_0 \sin \phi}{F}$	$\frac{M_0 \cos \phi}{F}$	$\frac{M_0 \sin \phi}{F}$	$\frac{M_0 \cos \phi}{F}$	$M_x = R_x \sin \phi - R_y \cos \phi + M_0 \cos \phi$	$M_y = M_0 - R_x y$	R_x	R_y	$T_x = -R_x \sin \phi + \sin \phi + R_x \cos \phi$	T_y
	$M_0 \text{ for Load } \frac{4.3}{13} = 3.02$	$\frac{M_0 \sin \phi \cos \phi}{F}$	$\frac{M_0 \cos \phi}{F}$	$\frac{M_0 \sin \phi}{F}$	$\frac{M_0 \cos \phi}{F}$	$\frac{M_0 \sin \phi}{F}$	M_x	M_y	R_x	R_y	T_x	T_y
1L	0	0	0	0	0	0	0	0	0	0	0	0
2L	0	0	0	0	0	0	0	0	0	0	0	0
3L	0	0	0	0	0	0	0	0	0	0	0	0
4L	0	0	0	0	0	0	0	0	0	0	0	0
5L	0	0	0	0	0	0	0	0	0	0	0	0
6L	0	0	0	0	0	0	0	0	0	0	0	0
7L	0	0	0	0	0	0	0	0	0	0	0	0
8L	0	0	0	0	0	0	0	0	0	0	0	0
9L	0	0	0	0	0	0	0	0	0	0	0	0
10L	0	0	0	0	0	0	0	0	0	0	0	0
11L	0	0	0	0	0	0	0	0	0	0	0	0
12L	0	0	0	0	0	0	0	0	0	0	0	0
13L	0	0	0	0	0	0	0	0	0	0	0	0
14L	0	0	0	0	0	0	0	0	0	0	0	0
15L	0	0	0	0	0	0	0	0	0	0	0	0
16L	0	0	0	0	0	0	0	0	0	0	0	0
17L	0	0	0	0	0	0	0	0	0	0	0	0
18L	0	0	0	0	0	0	0	0	0	0	0	0
19L	0	0	0	0	0	0	0	0	0	0	0	0
20L	0	0	0	0	0	0	0	0	0	0	0	0
21L	0	0	0	0	0	0	0	0	0	0	0	0
22L	0	0	0	0	0	0	0	0	0	0	0	0
23L	0	0	0	0	0	0	0	0	0	0	0	0
24L	0	0	0	0	0	0	0	0	0	0	0	0
25L	0	0	0	0	0	0	0	0	0	0	0	0
26L	0	0	0	0	0	0	0	0	0	0	0	0
27L	0	0	0	0	0	0	0	0	0	0	0	0
28L	0	0	0	0	0	0	0	0	0	0	0	0
29L	0	0	0	0	0	0	0	0	0	0	0	0
30L	0	0	0	0	0	0	0	0	0	0	0	0
31L	0	0	0	0	0	0	0	0	0	0	0	0
32L	0	0	0	0	0	0	0	0	0	0	0	0
33L	0	0	0	0	0	0	0	0	0	0	0	0
34L	0	0	0	0	0	0	0	0	0	0	0	0
35L	0	0	0	0	0	0	0	0	0	0	0	0
36L	0	0	0	0	0	0	0	0	0	0	0	0
37L	0	0	0	0	0	0	0	0	0	0	0	0
38L	0	0	0	0	0	0	0	0	0	0	0	0
39L	0	0	0	0	0	0	0	0	0	0	0	0
40L	0	0	0	0	0	0	0	0	0	0	0	0
41L	0	0	0	0	0	0	0	0	0	0	0	0
42L	0	0	0	0	0	0	0	0	0	0	0	0
43L	0	0	0	0	0	0	0	0	0	0	0	0
44L	0	0	0	0	0	0	0	0	0	0	0	0
45L	0	0	0	0	0	0	0	0	0	0	0	0
46L	0	0	0	0	0	0	0	0	0	0	0	0
47L	0	0	0	0	0	0	0	0	0	0	0	0
48L	0	0	0	0	0	0	0	0	0	0	0	0
49L	0	0	0	0	0	0	0	0	0	0	0	0
50L	0	0	0	0	0	0	0	0	0	0	0	0
51L	0	0	0	0	0	0	0	0	0	0	0	0
52L	0	0	0	0	0	0	0	0	0	0	0	0
53L	0	0	0	0	0	0	0	0	0	0	0	0
54L	0	0	0	0	0	0	0	0	0	0	0	0
55L	0	0	0	0	0	0	0	0	0	0	0	0
56L	0	0	0	0	0	0	0	0	0	0	0	0
57L	0	0	0	0	0	0	0	0	0	0	0	0
58L	0	0	0	0	0	0	0	0	0	0	0	0
59L	0	0	0	0	0	0	0	0	0	0	0	0
60L	0	0	0	0	0	0	0	0	0	0	0	0
61L	0	0	0	0	0	0	0	0	0	0	0	0
62L	0	0	0	0	0	0	0	0	0	0	0	0
63L	0	0	0	0	0	0	0	0	0	0	0	0
64L	0	0	0	0	0	0	0	0	0	0	0	0
65L	0	0	0	0	0	0	0	0	0	0	0	0
66L	0	0	0	0	0	0	0	0	0	0	0	0
67L	0	0	0	0	0	0	0	0	0	0	0	0
68L	0	0	0	0	0	0	0	0	0	0	0	0
69L	0	0	0	0	0	0	0	0	0	0	0	0
70L	0	0	0	0	0	0	0	0	0	0	0	0
71L	0	0	0	0	0	0	0	0	0	0	0	0
72L	0	0	0	0	0	0	0	0	0	0	0	0
73L	0	0	0	0	0	0	0	0	0	0	0	0
74L	0	0	0	0	0	0	0	0	0	0	0	0
75L	0	0	0	0	0	0	0	0	0	0	0	0
76L	0	0	0	0	0	0	0	0	0	0	0	0
77L	0	0	0	0	0	0	0	0	0	0	0	0
78L	0	0	0	0	0	0	0	0	0	0	0	0
79L	0	0	0	0	0	0	0	0	0	0	0	0
80L	0	0	0	0	0	0	0	0	0	0	0	0
81L	0	0	0	0	0	0	0	0	0	0	0	0
82L	0	0	0	0	0	0	0	0	0	0	0	0
83L	0	0	0	0	0	0	0	0	0	0	0	0
84L	0	0	0	0	0	0	0	0	0	0	0	0
85L	0	0	0	0	0	0	0	0	0	0	0	0
86L	0	0	0	0	0	0	0	0	0	0	0	0
87L	0	0	0	0	0	0	0	0	0	0	0	0
88L	0	0	0	0	0	0	0	0	0	0	0	0
89L	0	0	0	0	0	0	0	0	0	0	0	0
90L	0	0	0	0	0	0	0	0	0	0	0	0
91L	0	0	0	0	0	0	0	0	0	0	0	0
92L	0	0	0	0	0	0	0	0	0	0	0	0
93L	0	0	0	0	0	0	0	0	0	0	0	0
94L	0	0	0	0	0	0	0	0	0	0	0	0
95L	0	0	0	0	0	0	0	0	0	0	0	0
96L	0	0	0	0	0	0	0	0	0	0	0	0
97L	0	0	0	0	0	0	0	0	0	0	0	0
98L	0	0	0	0	0	0	0	0	0	0	0	0
99L	0	0	0	0	0	0	0	0	0	0	0	0
100L	0	0	0	0	0	0	0	0	0	0	0	0

Note.—Portion of table to left of double line was computed for the purpose of completing the substitutions in equations for reaction components (Table II).

Portion of table to right of double line was computed after the solution of equations.

TABLE V.—VERTICAL INFLUENCE LOAD AT 10R

[illegible]

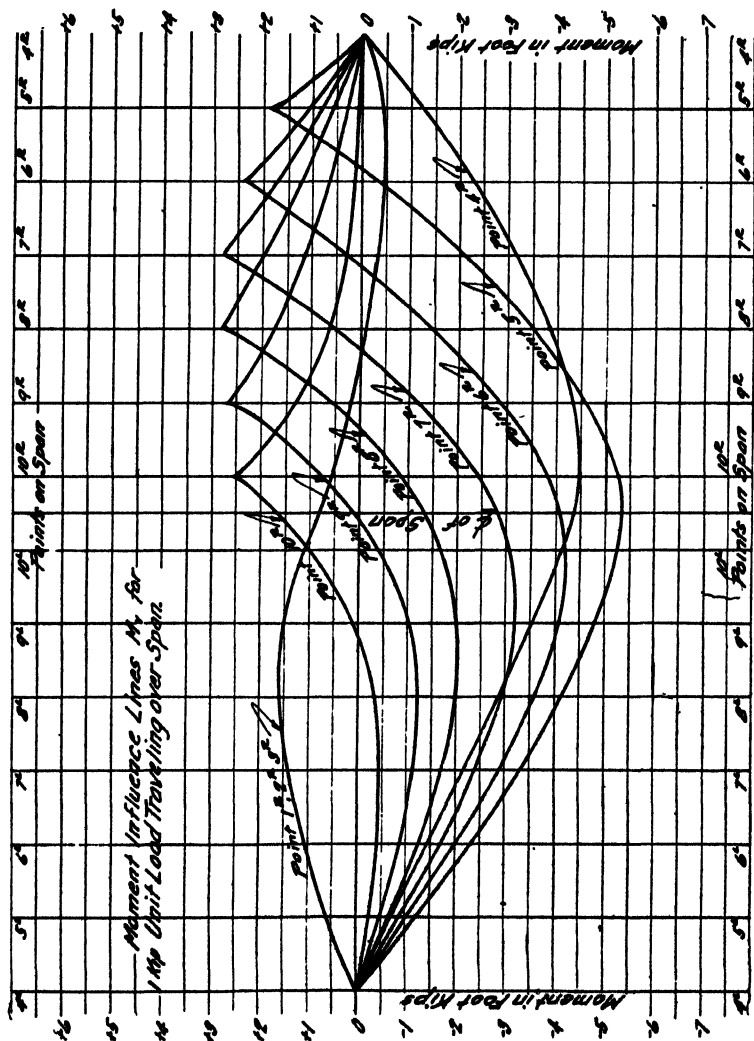


FIG. 61.

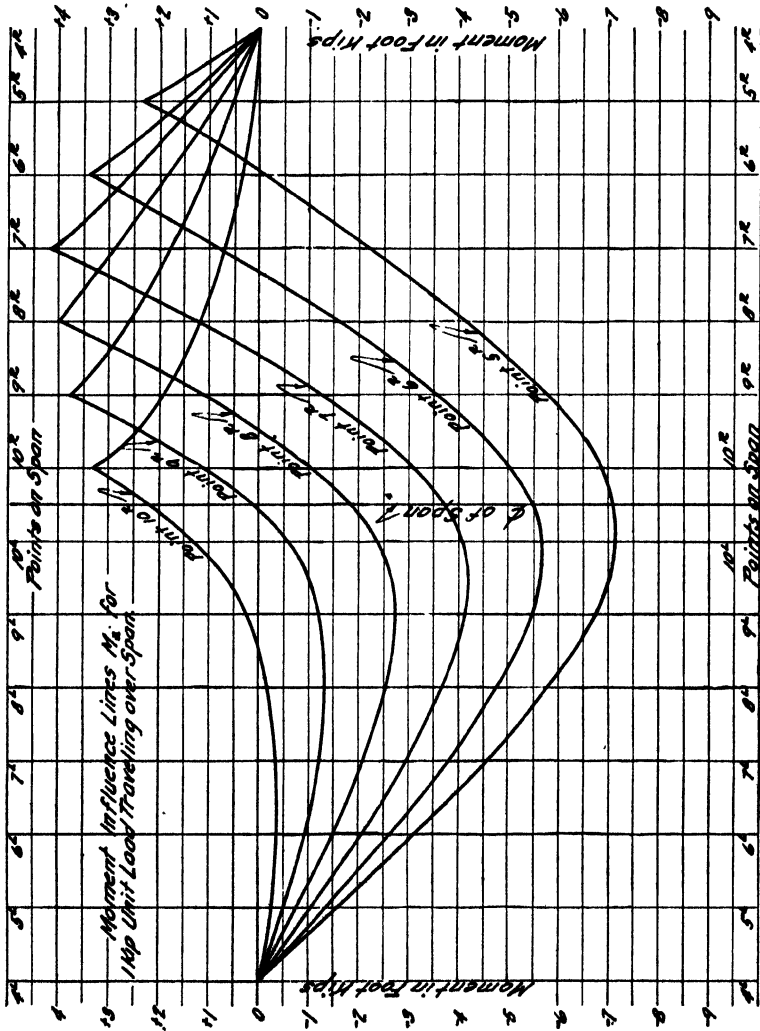


FIG. 62.

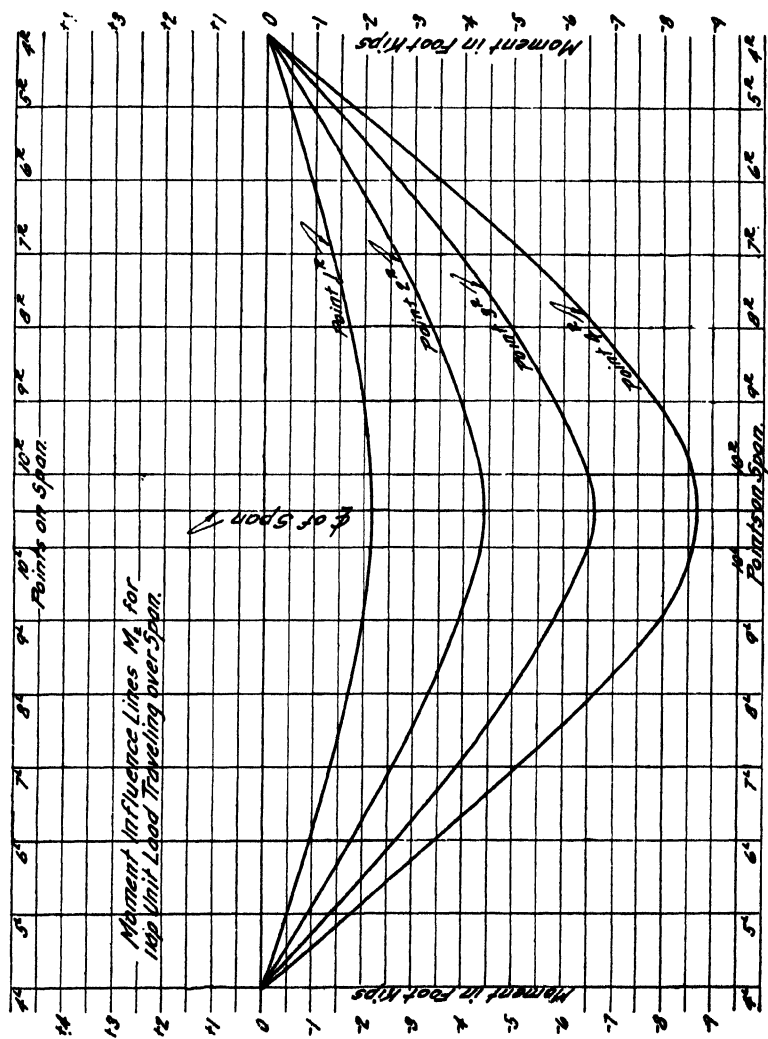


FIG. 63.

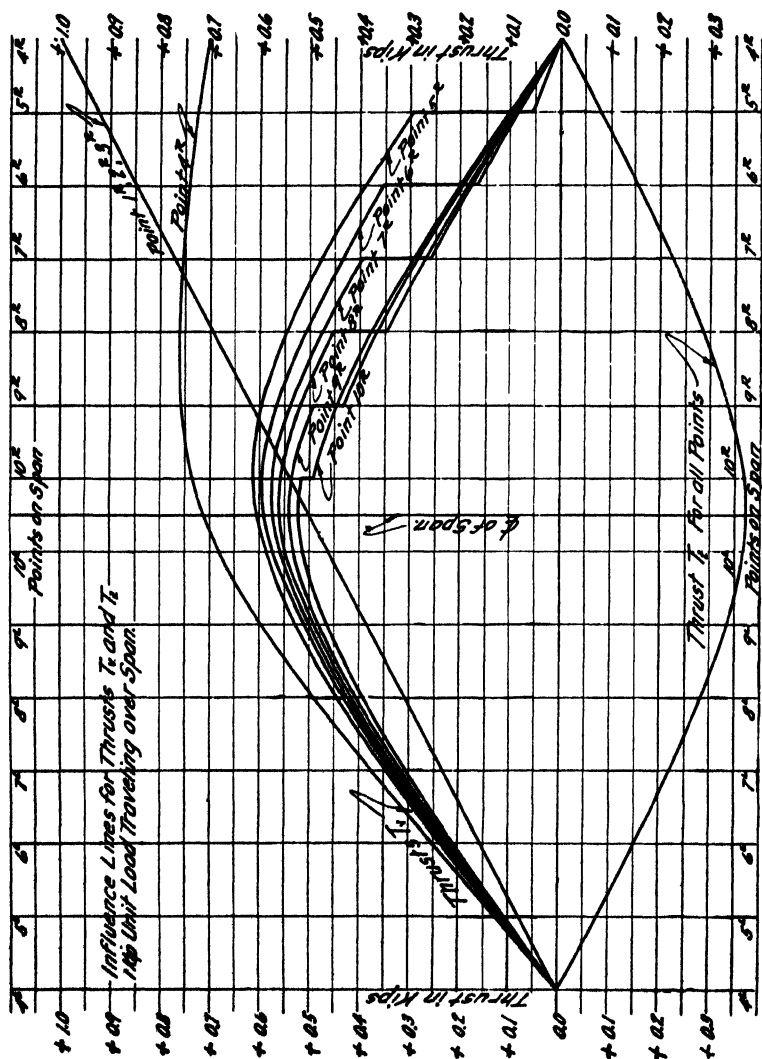


FIG. 64.

TABLE VI.—EARTH PRESSURE ON LEFT
QUANTITIES FOR SUBSTITUTION IN EQUATIONS (SEE TABLE II)

Point	$M_0 = R_y x - 5H^2$			$M'_0 = R_y \cos \phi x - 15H^2 \sin \phi (x - x')$			Right-Hand Members of Equations I, II, III, IV						Point
	$R_y x$	$5H^2$	M_0	$R_y \cos \phi x$	$15H^2 \sin \phi \times (x - x')$	M'_0	$\frac{M_0 \gamma}{I}$	$\frac{M'_0 \sin \phi}{F}$	$\frac{M'_0 \mu}{F}$	$\frac{M'_0 \cos \phi}{F}$	$\frac{M'_0 \sin \phi x}{F}$		
1R	0		0	0		0	0	0	0	0	0	1R	
2R	0		0	0		0	0	0	0	0	0	2R	
3R	0		0	0		0	0	0	0	0	0	3R	
4R	0		0	0		0	0	0	0	0	0	4R	
5R	+5.5		+5.5	+5.3		+5.3	0.2	-0.0009	+0.06	0.004	0.004	5R	
6R	+10.9		+10.9	+10.7		+10.7	1.0	-0.0028	0.26	0.015	0.024	6R	
7R	+16.4		+16.4	+16.2		+16.2	3.1	-0.0068	0.82	0.046	0.088	7R	
8R	+21.9		+21.9	+21.7		+21.7	8.4	-0.0130	2.18	0.119	0.224	8R	
9R	+27.3		+27.3	+27.2		+27.2	18.3	-0.0158	5.03	0.258	0.340	9R	
10R	+32.8		+32.8	+32.8		+32.8	30.7	-0.0112	8.75	0.433	0.289	10R	
10L	+38.3		+38.3	+38.3	Negligible	+38.3	35.7	+0.0131	10.93	0.504	0.394	10L	
9L	+43.7		+43.7	+43.6		+43.6	29.3	+0.0253	9.43	0.414	0.870	9L	
8L	+49.2		+49.2	+48.8		+48.8	18.8	+0.0292	6.53	0.266	1.130	8L	
7L	+54.7		+54.7	+54.0		+54.0	10.5	+0.0227	3.91	0.151	0.977	7L	
6L	+60.2		+60.2	+58.9		+58.9	5.6	+0.0156	2.31	0.082	0.738	6L	
5L	+65.6		+65.6	+63.7		+63.7	2.8	+0.0104	1.35	0.043	0.537	5L	
4L	+71.0		+71.0	+50.2		+50.2	1.8	+0.0156	0	0.016	0.870	4L	
3L	+71.0	+7.2	+63.8	0	0	0	1.5	0	0	0	0	3L	
2L	+71.0	+19.0	+52.0	0	0	0	1.6	0	0	0	0	2L	
1L	+71.0	+39.4	+31.6	0	0	0	1.1	0	0	0	0	1L	
Σ							+170.4	+0.0814	+52.77	+2.351	+4.547	Σ	
							+13632.0	+5.09	+3298.0	+146.9	+593.0		

* NOTE.—All figures to this point are based on earth pressure acting on a one-foot vertical strip of abutment. Resulting summations are therefore multiplied by 80 (skew width of bridge) before substituting in equations.

$$R_y = \frac{WH^2}{2} \cdot \frac{H}{55.9} = \frac{5H^3}{55.9} = 1.27 \text{ kips.}$$

TABLE VII.—EARTH PRESSURE ON LEFT

FINAL MOMENTS AND THRUSTS

$$R_x = +139.9 \quad R_y = +112.1 \quad M_x = +76.6 \quad M_y = +48.5$$

Points	$M_y = R_x \sin \phi \epsilon x - R_y \cos \phi - M_y \sin \phi + M'_{0\epsilon}$					$M_x = M_0 - R_{xy}$			$T_y = -R_y \sin \phi - 15k^2 \cos \phi + R_x \cos \phi$			T_z	Points
	$R_x \sin \phi \epsilon$	$R_x \cos \phi$	$M_y \sin \phi$	$M'_{0\epsilon}$	M_y	M_0^*	R_{xy}	M_x	$R_y \sin \phi$	$15k^2 \cos \phi$	$R_x \cos \phi$	T_y	
1R	0	0	-485	0	+485	0	602	-602	-101.6		0	+101.6	1R
2R	0	0	-485	0	+485	0	1204	-1204	-101.6		0	+101.6	2R
3R	0	0	-485	0	+485	0	1806	-1806	-101.6		0	+101.6	3R
4R	0	1360	-343	0	-963	0	2408	-2408	-72.0		98.8	+170.8	4R
5R	-109	1870	-113	+331	-1461	440	2560	-2120	-23.7		135.8	+159.5	5R
6R	-175	1930	-90	+669	-1271	870	2685	-1815	-18.9		137.1	+156.0	6R
7R	-208	1980	-72	+1013	-1027	1310	2780	-1460	-15.1		138.2	+153.3	7R
8R	-204	2050	-53	+1355	-770	1750	2850	-1100	-11.1		138.8	+149.9	8R
9R	-143	2180	-30	+1698	-519	2180	2910	-730	-6.2		139.4	+145.6	9R
10R	-73	2270	-13	+2050	-203	2620	2940	-320	-2.6		139.7	+142.3	10R
10L	+85	2440	+13	+2390	+99	3050	2940	+110	+2.6		139.7	+137.1	10L
9L	+229	2540	+30	+2720	+455	3490	2910	+580	+6.2		139.4	+133.2	9L
8L	+460	2740	+53	+3050	+793	3930	2850	+1080	+11.1		138.8	+127.7	8L
7L	+695	2920	+72	+3370	+1149	4380	2780	+1600	+15.1		138.2	+123.1	7L
6L	+959	3100	+90	+3680	+1524	4810	2685	+2125	+18.9		137.1	+118.2	6L
5L	+1313	3320	+113	+3980	+1934	5250	2560	+2690	+23.7		135.8	+112.1	5L
4L	+4310	5800	+343	+3140	+1361	5680	2408	+3272	+72.0		98.8	+26.8	4L
3L	+6100	6270	+485	0	-655	5110	1806	+3304	+101.6		0	-101.6	3L
2L	+6100	6270	+485	0	-655	4160	1204	+2956	+101.6		0	-101.6	2L
1L	+6100	6270	+485	0	-655	2530	602	+1928	+101.6		0	-101.6	1L

* NOTE.—Values of M_0 and M'_0 were obtained from Table VI and multiplied by skew width of bridge = 80'.

TABLE VIII.—TEMPERATURE STRESSES $\pm 50^\circ \text{F.}$

Values for substitution in equations (see Table II):

$$\frac{+E\epsilon t l}{s} = \frac{288,000 \times 0.000065 \times 50 \times 55.9}{4.3} = +1215 \text{ kips/square ft.}$$

$$\frac{-E\epsilon t l}{s} \left(\frac{\epsilon}{\kappa} \right) = -1215 \left(\frac{0.7813}{2.67} \right) = -356 \text{ kips/square feet}$$

$$M_y = -1478$$

$$M_x = +1466$$

$$R_z = +69.3$$

$$R_x = +20.0$$

Point	$M_v = R_z \sin \phi \epsilon x - R_x u + M_x \cos \phi - M_y \sin \phi$					$M_z = -R_x y$	T_v	T_z
	$R_z \sin \phi \epsilon x$	$R_x u$	$M_x \cos \phi$	$M_y \sin \phi$	M_v	$-R_x y$	$R_z \cos \phi$	R_z
1R	0	0	0	+1478	-1478	-86	0	$R_z = +69.3^x$
2R	0	0	0	+1478	-1478	-172	0	
3R	0	0	0	+1478	-1478	-258	0	
4R	0	838	1036	+1044	-846	-344	14	
5R	-16	1155	1425	+344	-90	-366	19	
6R	-25	1190	1436	+275	-54	-384	20	
7R	-30	1225	1448	+219	-26	-398	20	
8R	-29	1266	1455	+161	-1	-403	20	
9R	-21	1343	1462	+90	+8	-416	20	
10R	-11	1397	1466	+38	+20	-420	20	
10L	+12	1503	1466	-38	+13	-420	20	
9L	+33	1572	1462	-90	+13	-416	20	
8L	+66	1690	1455	-161	-8	-408	20	
7L	+100	1800	1448	-219	-33	-398	20	
6L	+137	1910	1436	-275	-62	-384	20	
5L	+188	2050	1425	-344	-93	-366	19	
4L	+617	3570	1036	-1044	-873	-344	14	
3L	+872	3870	0	-1478	-1520	-253	0	
2L	+872	3870	0	-1478	-1520	-172	0	
1L	+872	3870	0	-1478	-1520	-86	0	

TABLE IX.—DEAD LOAD MOMENTS M_r AND THRUSTS T_r

Moment factors (M. F.) are scaled from influence line diagram. The product of load and moment factor will give the actual dead load moment.

Point	Load	Point 1R, 2R, 3R		Point 4R		Point 5R		Point 6R		Point 7R		Point 8R		Point 9R		Point 10R		Point
		MF	M	MF	M	MF	M	MF	M	MF	M	MF	M	MF	M	MF	M	
1R	288	0	0	0	0	0	0	0	0	0	0	0	0	0	0	0	0	1R
2R	175	0	0	0	0	0	0	0	0	0	0	0	0	0	0	0	0	2R
3R	199	0	0	0	0	0	0	0	0	0	0	0	0	0	0	0	0	3R
4R	510	0	0	0	0	0	0	0	0	0	0	0	0	0	0	0	0	4R
5R	361	-0.4	-144	-1.3	-469	+1.8	+650	+1.1	+397	+0.8	+289	+0.6	+217	+0.3	+108	+0.1	+36	5R
6R	289	-0.4	-116	-2.3	-665	-0.3	-87	+2.3	+665	+1.7	+491	+1.2	+347	+0.7	+202	+0.1	+29	6R
7R	237	-0.3	-71	-3.2	-758	-2.1	-498	+0.3	+71	+2.8	+664	+2.0	+474	+1.1	+261	+0.3	+71	7R
8R	196	-0.1	-20	-3.9	-765	-3.5	-686	-1.5	-294	+0.5	+98	+2.8	+548	+1.8	+353	+0.6	+118	8R
9R	170	+0.2	+34	-4.3	-731	-4.6	-782	-2.9	-493	-1.2	-204	+0.5	+85	+2.7	+459	+1.3	+221	9R
10R	155	+0.6	+93	-4.5	-698	-5.3	-822	-3.8	-589	-2.4	-372	-0.9	-140	+0.7	+109	+2.5	+388	10R
10L	155	+1.1	+171	-4.1	-636	-5.3	-822	-4.2	-651	-3.1	-481	-1.7	-264	-0.4	-62	+1.0	+155	10L
9L	170	+1.5	+255	-3.5	-595	-4.8	-816	-4.1	-697	-3.2	-544	-2.0	-340	-1.0	-170	+0.1	+17	9L
8L	196	+1.6	+314	-2.8	-549	-4.1	-895	-3.6	-795	-2.9	-568	-2.0	-392	-1.2	-235	-0.3	-59	8L
7L	237	+1.4	+332	-2.2	-521	-3.3	-782	-2.9	-687	-2.4	-568	-1.7	-403	-1.1	-261	-0.4	-95	7L
6L	289	+1.1	+318	-1.4	-405	-2.3	-665	-2.0	-578	-1.7	-491	-1.3	-375	-0.9	-260	-0.4	-116	6L
5L	361	+0.6	+216	-0.7	-253	-1.2	-433	-1.0	-361	-0.9	-325	-0.7	-252	-0.5	-181	-0.2	-72	5L
4L	510	0	0	0	0	0	0	0	0	0	0	0	0	0	0	0	0	4L
3L	199	0	0	0	0	0	0	0	0	0	0	0	0	0	0	0	0	3L
2L	175	0	0	0	0	0	0	0	0	0	0	0	0	0	0	0	0	2L
1L	288	0	0	0	0	0	0	0	0	0	0	0	0	0	0	0	0	1L
Σ			+1382		-7045		-6548		-3922		-2011		-495		+323		+693	Σ

Thrust Factor for unit load at any point is constant throughout.

Hence T_r for all Points = Σ (Load \times Thrust Factor).

$$T_r = 2 \times [(361 \times .08) + (289 \times .15) + (237 \times .22) + (196 \times .29) + (170 \times .34) + (155 \times .37)].$$

$$T_r = 594K.$$

TABLE X.—DEAD LOAD MOMENTS M_z

Moment factors (MF) are scaled from the influence line diagram. The product of load and moment factor will give the actual dead load moment M .

Point	Load	Point 1R		Point 2R		Point 3R		Point 4R		Point 5R		Point 6R		Point 7R		Point 8R		Point 9R		Point 10R		Point
		MF	M	MF	M	MF	M	MF	M	MF	M	MF	M	MF	M	MF	M	MF	M	MF	M	
1R	288	0	0	0	0	0	0	0	0	0	0	0	0	0	0	0	0	0	0	0	0	1R
2R	175	0	0	0	0	0	0	0	0	0	0	0	0	0	0	0	0	0	0	0	0	2R
3R	199	0	0	0	0	0	0	0	0	0	0	0	0	0	0	0	0	0	0	0	0	3R
4R	510	0	0	0	0	0	0	0	0	0	0	0	0	0	0	0	0	0	0	0	0	4R
5R	361	-0.5	-180	-0.9	-325	-1.4	-505	-1.8	-650	+2.3	+830	+1.5	+541	+1.2	+433	+0.8	+289	+0.5	+180	+0.1	+36	5R
6R	289	-0.9	-260	-1.8	-520	-2.7	-780	-3.5	-1,010	-0.1	-29	+3.4	+983	+2.6	+751	+1.8	+520	+1.1	+318	+0.3	+87	6R
7R	237	-1.3	-308	-2.6	-616	-3.9	-945	-5.2	-1,232	-2.2	-321	+0.8	+100	+4.1	+972	+2.0	+687	+1.8	+426	+0.7	+166	7R
8R	196	-1.7	-333	-3.3	-647	-5.0	-980	-6.7	-1,313	-4.1	-804	-1.6	-314	+1.2	+235	+4.0	+785	+2.6	+510	+1.2	+235	8R
9R	170	-2.0	-340	-3.9	-664	-5.8	-987	-7.9	-1,343	-5.8	-987	-3.5	-595	-1.2	-204	+1.1	+187	+3.7	+630	+1.9	+323	9R
10R	155	-2.1	-326	-4.3	-667	-6.5	-1,007	-8.6	-1,333	-6.9	-1,070	-5.0	-775	-3.1	-480	-1.0	-155	+1.1	+170	+3.3	+512	10R
10L	155	-2.1	-326	-4.3	-667	-6.5	-1,007	-8.6	-1,333	-7.1	-1,100	-5.6	-868	-4.1	-636	-2.4	-372	-0.6	-93	+1.3	+202	10L
9L	170	-2.0	-340	-3.9	-664	-5.8	-987	-7.9	-1,343	-6.7	-1,140	-5.5	-935	-4.1	-697	-2.7	-458	-1.2	-204	+0.2	+34	9L
8L	196	-1.7	-333	-3.3	-647	-5.0	-980	-6.7	-1,313	-5.8	-1,140	-4.8	-941	-3.7	-726	-2.5	-490	-1.3	-255	-0.2	-39	8L
7L	237	-1.3	-308	-2.6	-616	-3.9	-945	-5.2	-1,232	-4.6	-1,090	-3.8	-900	-3.0	-711	-2.1	-497	-1.2	-284	-0.3	-71	7L
6L	289	-0.9	-260	-1.8	-520	-2.7	-780	-3.5	-1,010	-3.1	-895	-2.6	-751	-2.1	-607	-1.5	-433	-0.9	-260	-0.4	-116	6L
5L	361	-0.5	-180	-0.9	-325	-1.4	-505	-1.8	-650	-1.6	-577	-1.4	-505	-1.0	-361	-0.8	-289	-0.5	-180	-0.3	-108	5L
4L	510	0	0	0	0	0	0	0	0	0	0	0	0	0	0	0	0	0	0	0	0	4L
3L	199	0	0	0	0	0	0	0	0	0	0	0	0	0	0	0	0	0	0	0	0	3L
2L	175	0	0	0	0	0	0	0	0	0	0	0	0	0	0	0	0	0	0	0	0	2L
1L	288	0	0	0	0	0	0	0	0	0	0	0	0	0	0	0	0	0	0	0	0	1L
Z			-3,494		-587.8		-10,368		-13,762		-8,523		-4,870		-203.1		-226		+958		+1,261	Z

TABLE XI.—DEAD LOAD THRUSTS T ,Thrust factors (TF) are scaled from the influence line diagram. The product of load and thrust factor will give the actual dead load thrust T .

Point	Load	Point 1R		Point 2R		Point 3R		Point 4R		Point 5R		Point 6R		Point 7R		Point 8R		Point 9R		Point 10R		Point
		TF	T	TF	T	TF	T	TF	T	TF	T	TF	T	TF	T	TF	T	TF	T	TF	T	
1R	288	1.00	288	0	0	0	0	0	0	0	0	0	0	0	0	0	0	0	0	0	0	1R
2R	175	1.00	175	1.00	175	0	0	0	0	0	0	0	0	0	0	0	0	0	0	0	0	2R
3R	199	1.00	199	1.00	199	1.00	199	0	0	0	0	0	0	0	0	0	0	0	0	0	0	3R
4R	510	1.00	510	1.00	510	1.00	510	1.00	510	0	0	0	0	0	0	0	0	0	0	0	0	4R
5R	361	0.92	332	0.92	332	0.92	332	0.72	260	0.18	65	0.08	29	0.09	33	0.09	33	0.10	36	0.10	36	5R
6R	289	0.85	246	0.85	246	0.85	246	0.74	214	0.39	113	0.26	75	0.18	52	0.19	55	0.19	55	0.20	58	6R
7R	237	0.77	183	0.77	183	0.77	183	0.75	178	0.48	114	0.44	104	0.33	78	0.27	64	0.29	69	0.29	69	7R
8R	196	0.69	135	0.69	135	0.69	135	0.76	149	0.55	108	0.51	100	0.48	94	0.40	78	0.37	72	0.38	74	8R
9R	155	0.62	105	0.62	105	0.62	105	0.76	129	0.60	102	0.57	97	0.54	92	0.52	88	0.46	78	0.45	77	9R
10R	155	0.54	84	0.54	84	0.54	84	0.73	113	0.61	94	0.60	93	0.58	90	0.56	87	0.54	84	0.51	79	10R
11R	170	0.46	71	0.46	71	0.46	71	0.68	105	0.59	91	0.57	88	0.56	87	0.55	85	0.53	82	0.51	79	11R
12R	196	0.38	65	0.38	65	0.38	65	0.60	102	0.53	90	0.51	87	0.50	85	0.49	83	0.48	82	0.46	78	12R
13R	237	0.31	61	0.31	61	0.31	61	0.49	88	0.49	96	0.43	84	0.42	82	0.42	82	0.41	80	0.39	76	13R
14R	237	0.23	54	0.23	54	0.23	54	0.37	88	0.35	83	0.34	81	0.33	78	0.32	76	0.31	73	0.30	71	14R
15R	289	0.15	43	0.15	43	0.15	43	0.25	72	0.24	69	0.23	66	0.23	66	0.22	64	0.21	61	0.21	61	15R
16R	361	0.08	29	0.08	29	0.08	29	0.13	47	0.12	43	0.12	43	0.11	40	0.11	40	0.11	40	0.10	36	16R
17R	310	0	0	0	0	0	0	0	0	0	0	0	0	0	0	0	0	0	0	0	0	17R
18R	199	0	0	0	0	0	0	0	0	0	0	0	0	0	0	0	0	0	0	0	0	18R
19R	175	0	0	0	0	0	0	0	0	0	0	0	0	0	0	0	0	0	0	0	0	19R
20R	288	0	0	0	0	0	0	0	0	0	0	0	0	0	0	0	0	0	0	0	0	20R
Σ			2380		2292		2117		2063		1068		947		877		835		812		794	Σ

TABLE XII.—CONCENTRATED LIVE LOAD MOMENTS M_s AND NORMAL THRUSTS T_s

Moment Factors (MF) and Thrust Factors (TF) are read directly from Influence Line Diagrams. The product of load and moment factor gives actual moments M_s , and the product of load and thrust factor gives actual thrusts T_s . Note that the position of the load system must be the same as for maximum M_s moments (see Table XIII) since the latter controls in all cases.

Load	Point 1R, 2R, 3R, Load B at 101L				Point 4R, Load B at 101L				Point 5R, Neg., Load C at 6R				Point 5R, Pos., Load B at 5R				Point 6R, Neg., Load B at 8R			
	MF	M	TF	T	MF	M	TF	T	MF	M	TF	T	MF	M	TF	T	MF	M	TF	T
A	+1.6	+77	0.28	13	-2.8	-134	0.28	13	-3.3	-138	0.22	11	0	0	0.08	0	-3.2	-154	0.25	12
B	+0.8	+154	0.37	71	-4.4	-845	0.37	71	-5.1	-980	0.36	69	+1.9	0	0.0	15	-4.2	-807	0.37	71
C	-0.4	-14	0.08	3	-1.2	-43	0.08	3	-0.3	-11	0.16	6	0	0	0.0	0	0.0	0	0.0	0
D	0.0	0	0.0	0	0.0	0	0.0	0	0.0	0	0.0	0	0	0	0.0	0	0.0	0	0.0	0
Total +		+217		87				87				86		+365						
Total -						-1022				-1140						15		-961		83

Load	Point 6R, Pos., Load B at 6R				Point 7R, Neg., Load A at 7L				Point 7R, Pos., Load B at 7R				Point 8R, Neg., Load B at 91L				Point 8R, Pos., Load B at 8R			
	MF	M	TF	T	MF	M	TF	T	MF	M	TF	T	MF	M	TF	T	MF	M	TF	T
A	0.0	0	0.0	0	-2.5	-120	0.23	11	+0.4	+10	0.04	2	-1.6	-77	0.21	10	+0.0	+43	0.11	5
B	+2.4	+461	0.15	20	-3.2	-615	0.36	69	+2.8	+538	0.22	42	-2.0	-381	0.36	69	+2.8	+538	0.20	56
C	0.0	0	0.0	0	0.0	0	0.0	0	0.0	0	0.0	0	0.0	0	0.0	0	0.0	0	0.0	0
D	0.0	0	0.0	0	0.0	0	0.0	0	0.0	0	0.0	0	0.0	0	0.0	0	0.0	0	0.0	0
Total +		+461		20				80		+557		44						+581		61
Total -						-735								-461		79				

Load	Point 9R, Neg., Load C at 61R				Point 9R, Pos., Load B at 9R				Point 10R, Neg., Load B at 7L				Point 10R, Pos., Load B at 10R			
	MF	M	TF	T	MF	M	TF	T	MF	M	TF	T	MF	M	TF	T
A	-1.0	-48	0.18	9	+0.8	+38	0.20	10	-0.1	-5	0.04	2	+0.4	+10	0.25	12
B	-1.2	-230	0.33	63	+2.6	+499	0.35	67	-0.4	-77	0.22	42	+2.6	+499	0.37	71
C	0.0	0	0.0	0	0.0	0	0.0	0	0.0	0	0.0	0	0.0	0	0.0	0
D	0.0	0	0.0	0	0.0	0	0.0	0	0.0	0	0.0	0	0.0	0	0.0	0
Total +				72		+537		+77				44		+518		83
Total -		-178								-82						

TABLE XV.—FUNCTIONS OF ANGLE V

Point	$\cos \phi$	$\tan V = \frac{1}{\epsilon \cos \phi}$	Angle V	$\sin V$	$\cos V$	$\sec V$	$\sec^2 V$	Point
1	0	0	0	0	1.000	1.000	1.000	1
2	0	0	0	0	1.000	1.000	1.000	2
3	0	0	0	0	1.000	1.000	1.000	3
4	0.707	0.552	$28^\circ 55'$	0.483	0.875	1.142	1.305	4
5	0.972	0.759	$37^\circ 15'$	0.605	0.796	1.256	1.577	5
6	0.982	0.767	$37^\circ 30'$	0.609	0.793	1.260	1.589	6
7	0.989	0.773	$37^\circ 40'$	0.611	0.791	1.264	1.597	7
8	0.994	0.777	$37^\circ 50'$	0.613	0.790	1.266	1.603	8
9	0.998	0.780	$37^\circ 55'$	0.615	0.788	1.268	1.608	9
10	1.000	0.782	38°	0.616	0.788	1.269	1.610	10

ϕ (see Fig. 59). V = The projection of the skew angle on a plane tangent to the neutral surface at the point considered.

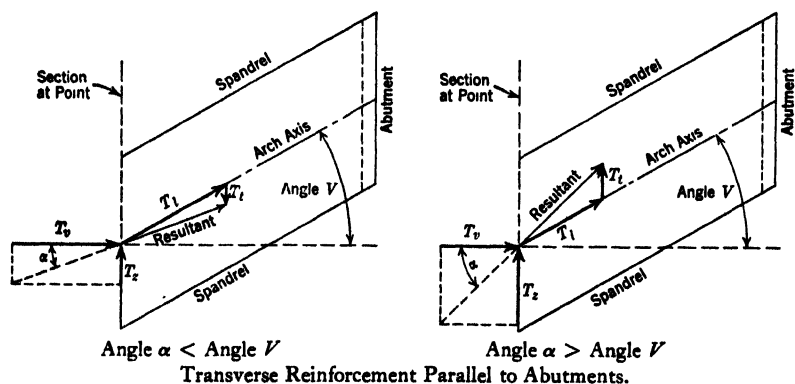


FIG. 65.—Transformation of Forces Acting on Cut Section as Calculated, to Forces Acting in Directions Desired for Design of Reinforcement.

Equations

$$T_t = T_v \sec V$$

$$T_z = T_v \tan V - T_t$$

$$M_t = M_z \sec V$$

$$M_z = M_t \tan V - M_t$$

The transformations of T_v and T_z only are indicated on the figures. M_v and M_z correspond vectorially to T_z and T_v , respectively; therefore their equations may be written down directly as shown.

Note that V is not the bridge skew angle, but its projection onto a plane tangent to the neutral surface at the point under consideration.

TABLE XVI.—TRANSFORMATION OF MOMENTS AND FORCES. TRANSVERSE STEEL PARALLEL TO ABUTMENTS

Point	M_s	M_v	T_v	T_s	$M_t = \frac{M_s}{M_s \sec V}$	$T_t = \frac{T_v}{T_v \sec V}$	$M_t = M_s \tan V - M_v$			$T_t = T_v \tan V - T_s$			Point
							$M_s \tan V$	M_v	M_t	$T_v \tan V$	T_s	T_t	
1	- 2,600	+ 2,929	2723	836	- 2,600	2723	0	+ 2929	- 2929	0	836	- 836	1
2	- 5,989	+ 2,929	2435	836	- 5,989	2435	0	+ 2929	- 2929	0	836	- 836	2
3	- 10,159	+ 2,929	2260	836	- 10,159	2260	0	+ 2929	- 2929	0	836	- 836	3
4	- 15,288	- 8,539	2461	974	- 17,500	2820	- 8450	- 8529	+ 79	1360	974	+ 386	4
5	- 9,898	- 7,316	1496	974	- 12,440	1880	- 7520	- 7316	- 204	1138	974	+ 164	5
6	- 6,239	- 4,688	1368	970	- 7,860	1720	- 4790	- 4688	- 102	1050	970	+ 80	6
7	- 3,239	- 2,654	1295	967	- 4,100	1643	- 2500	- 2654	+ 154	1000	967	+ 33	7
8	- 1,268	- 938	1247	966	- 1,605	1580	- 988	- 938	- 50	972	966	+ 6	8
8	+ 992	+ 114	1176	810	+ 1,256	1494	+ 772	+ 114	+ 658	914	810	+ 104	8
9	+ 1,996	+ 786	1172	826	+ 2,536	1482	+ 1560	+ 786	+ 774	914	826	+ 88	9
10	+ 2,147	+ 1,089	1167	832	+ 2,730	1486	+ 1677	+ 1059	+ 588	915	832	+ 83	10

NOTE.—All moments are in kip-feet (1000 ft.-lb.). All thrusts are in kips (1000 lb.). All quantities are for full width of bridge.

TABLE XVII.—DESIGN OF LONGITUDINAL REINFORCEMENT. TRANSVERSE REINFORCEMENT PARALLEL TO ABUTMENTS

Point	M_1 Full Width, Kip-Ft.	M_1 Full Width, Kip-In.	T_1 Full Width, Kips	m_1 One Foot Width, Kip-In.	t_1 One Foot Width, Kips	$e = \frac{m_1}{t_1}$ In.	t_1 In.	$d = t_1 - 2.5$ In.	$e' = e + \frac{t_1 - 2.5}{2}$ In.	$\frac{e'}{d}$	$K = \frac{t_1 e'}{bd^2}$	f_b Lb. per Sq. In.	f_b Lb. per Sq. In.	p	A_s per Ft. Square Width	Loca- tion Point
1	- 2,600	- 31,200	2723	- 512	44.7	11.4	32	29.5	24.9	0.9	106	18,000	670	Ex.
2	- 5,990	- 71,900	2435	- 1180	39.8	29.6	42	39.5	48.1	1.2	102	18,000	660	0.0017	0.81	Ex.
3	- 10,160	- 121,900	2260	- 2000	37.1	54.0	52	49.5	77.5	1.6	98	18,000	640	0.0027	1.61	Ex.
4	- 17,500	- 210,000	2820	- 3450	46.2	74.5	56	53.5	100.0	1.9	135	18,000	800	0.0044	2.83	Ex.
5	- 12,440	- 149,300	1880	- 2450	30.8	79.5	48	45.5	101.0	2.2	125	18,000	750	0.0047	2.56	Ex.
6	- 7,860	- 94,300	1720	- 1545	28.2	54.7	39	36.5	71.7	2.0	127	18,000	760	0.0045	1.97	Ex.
7	- 4,100	- 49,200	1643	- 807	26.9	30.0	32	29.5	43.5	1.5	112	18,000	700	0.0029	1.03	Ex.
8	- 1,605 + 1,256	- 19,300 + 15,100	1580 1494	- 316 + 248	25.9 24.5	12.2 10.1	27 27	24.5 24.5	23.2 21.0	0.9 0.9	84 71	18,000 18,000	590 525	0.0004 0.000	0.12 0	Ex. Int.
9	+ 2,536	+ 30,400	1482	+ 499	24.3	20.5	23	20.5	29.5	1.5	143	16,500	800	0.0038	0.94	Int.
10	+ 2,730	+ 32,800	1486	+ 538	24.4	22.0	21	18.5	30.0	1.6	178	10,000	800	0.0107	2.38	Int.

NOTE.—Ex. indicates extrados; Int. indicates intrados.

 m_1 and t_1 are obtained by dividing M_1 and T_1 by the square width of bridge (61 ft.).Note that thicknesses t finally used (to give convenient spacing of reinforcing rods) are slightly larger than originally assumed for analysis. The error involved is negligible and recalculation unnecessary.

TABLE XVIII.—TOTAL NET SHEARS FOR DESIGN OF TRANSVERSE REINFORCEMENT.
TRANSVERSE REINFORCEMENT PARALLEL TO ABUTMENTS

Point	Unit Shears due to Torsion				Unit Shears due to Direct Shears		Total Unit Shear $v_t \pm v_s$ Lb. per Sq. In.		Total Net Shear to be taken by Steel Lb. per Sq. In.		Point	
	M_t , Kip-Ft.	M_t , Kip-In.	I_s , In.	ϕ^2	$v_t = \frac{9M_t}{2bt^2}$ Lb. per Sq. In.	T_t Kips	$v_s = \frac{1.5T_t}{bt}$ Lb. per Sq. In.	Intrados	Extrados	Intrados v_2		Extrados v_1
1	-2929	-35,150	32	1024	∓ 171	-836	-44	127	215	97	185	1
2	-2929	-35,150	42	1764	∓ 100	-836	-33	67	133	37	103	2
3	-2929	-35,150	52	2700	∓ 65	-836	-27	38	92	8	62	3
4	+ 79	+ 948	56	3140	± 2	+386	+12	10	14	0	0	4
5	- 204	- 2,448	48	2300	∓ 5	+164	+ 6	11	1	0	0	5
6	- 102	- 1,224	39	1521	∓ 4	+ 80	+ 3	7	1	0	0	6
7	+ 150	+ 1,800	32	1024	± 9	+ 34	+ 2	7	11	0	0	7
8	+ 658	+ 7,900	27	729	± 54	+104	+ 6	48	60	18	30	8
9	+ 774	+ 9,240	23	529	± 87	+ 88	+ 6	81	93	51	63	9
10	+ 588	+ 7,060	21	441	± 80	+ 83	+ 7	73	87	43	57	10

NOTE.— b in above table = width of bridge in direction of transverse reinforcement = 75 ft.

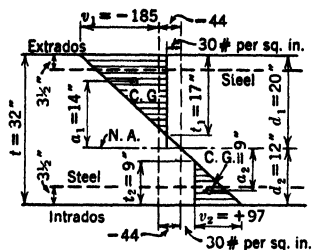
The concrete is assumed to carry its share of total shear at 30 lb. per sq. in.

Design of Transverse Reinforcement

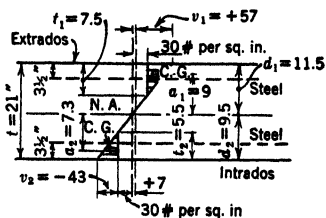
The shear distribution diagrams shown in the sketches accompanying Table XIX are drawn to scale for the points at the crown and near the footing and are typical of the diagrams for the remaining points. The direct shear is always small in comparison with the torsional shear, and it rarely occurs, as in the diagram for point 1, that the direct shear is greater than the amount of shear assumed to be taken by the concrete alone.

For practical purposes, the design throughout the width of this structure is based on the maximum shears which occur along the center line, and the steel is made the same top and bottom, being calculated for the moment about the neutral axis of the larger of the shear triangles.

Opinions differ as to the correct theory for the design of transverse reinforcement, but there seems to be little disagreement in the final results reached by the several methods proposed. A more rigorous analysis than that given here is unnecessary. The reader is referred to the paper by Professor Rathbun, and the discussions following, which appear in Volume 98 (1933) of the *Transactions* of the American Society of Civil Engineers: "An Analysis of Multiple Skew Arches on Elastic Piers."



Distribution at Point 1



Distribution at Point 10

TABLE XIX.—DESIGN OF TRANSVERSE REINFORCEMENT—RODS PARALLEL TO ABUTMENTS

Point	t_1 in.	Extrados						Intrados						Point
		v_1	t_1	d_1	$d_1 - 3.5$	a_1	A_s	v_2	t_2	d_2	$d_2 - 3.5$	a_2	A_s	
1	32	185	17.0	20.0	16.5	14.0	0.90	97	9.0	12.0	8.5	9.0	0.33	1
2	42	103	21.8	28.2	24.7	20.9	0.63	37	7.7	13.8	10.3	11.2	0.10	2
3	52	62	24.5	37.3	33.8	29.0	0.44	8	3.0	14.7	11.2	13.7	0.01	3
4	56	0	4
5	48	0	5
6	39	0	6
7	32	0	7
8	27	30	7.5	15.3	11.8	12.5	0.08	18	4.5	11.7	8.2	10.5	0.03	8
9	23	63	8.5	12.4	8.9	9.5	0.19	51	6.8	10.6	7.1	8.3	0.14	9
10	21	57	7.5	11.5	8.0	9.0	0.16	43	5.5	9.5	6.0	7.3	0.10	10

t_1 and t_2 are scaled from diagram for each point.

A_s = required transverse steel area in square inches per foot, width of bridge.

$$18,000 A_s (d_1 - 3.5) = \frac{v_1 t_1 a_1}{2} \times 12; \text{ or } A_s = \frac{1}{3000} \left(\frac{v_1 t_1 a_1}{d_1 - 3.5} \right).$$

Permissible Approximations

A study was begun by the Westchester County Park Commission under the direction of Richard M. Hodges to determine what approximations could be made to the exact analysis of skewed arch or frame bridges to reduce the amount of mathematical work; but the study was suspended before the procedure for proportioning the transverse reinforcement was completed. This appeared to be the only unsolved element of the problem. The author, however, feels warranted in making recommendations with respect to the design of concrete rigid-frame bridges up to about 25° skew. Within this limit the skew frame bridge may be designed as one without skew, having a span length equal to the skew span of the actual structure. Nominal transverse reinforcement, such as is used to position the longitudinal reinforcement and knit the structure together laterally, will be adequate to resist the relatively small torsional effects.

METHOD OF DESIGN OF SYMMETRICAL DOUBLE-SPAN SKEW FRAME BRIDGE

By PROFESSOR J. CHARLES RATHBUN
College of the City of New York

Let Fig. 68*a* represent a double-span skew structure symmetrical about a vertical axis. This can be analyzed for any system of loads provided that one is able to analyze the right span of this structure after certain changes are made in the central post.

First Step. Let us assume that for every load on the right span there is an equal load symmetrically located relative to the central vertical axis. From the nature of this arch every stress and every strain in one arch has its corresponding equal stress and strain in the other. In the central leg these either cancel each other or combine to double their value.

We can therefore obtain a complete solution by considering arch $ABCD$ of Fig. 68*b*, in which the loads, dimensions, and material are the same as in the right part of Fig. 68*a* with the exception of the leg AB .

As the vertical thrust and moment about the vertical (Y) axis from the two spans combine in the middle leg, the leg should be considered as having half its actual rigidity for such forces.

The two horizontal force components R_x and R_z of one span are canceled by those from the other, and the same is true for the moments about each of the horizontal axes. Therefore the middle leg should be assumed as infinitely rigid for the forces along, and moments about the X axis and Z axis.

With these changes in the properties of the section AB the arch $ABCD$ may be analyzed by the methods and formulas previously given in this chapter.

Second Step. Let us assume that the loading on the right span is the same but that the loads symmetrically opposite are negative or upward. The solution of this problem will give the same stresses in each arch except that those opposite each other are of opposite sign. This can easily be shown by revolving the structure a half revolution about its vertical axis of symmetry. This gives a complete reversal of stress. The solution indicated is the only one that will give this result.

At B and in the leg AB the vertical force and the moment about the vertical axis will be zero, owing to the fact that forces in one arch are opposite those in the other. However, the horizontal force and the moment about a horizontal axis (each represented by two components) mutually aid each other. This as before can be allowed for in the single arch $ABCD$ by making the section AB infinitely rigid to the first moment and force and of half the actual rigidity to the other two moments and two forces.

With these changes in the properties of AB , the arch,

ABCD can again be solved. The resulting stresses in the left arch will be the same except for change in sign.

Third Step. By combining the solutions of these two steps we have the analysis of the symmetrical two-span frame under an unsymmetrical load.

Fourth Step. In an actual bridge structure some loads (such as dead loads) are symmetrically placed and some are not. For the symmetrically placed loads, the procedure outlined as the "First Step" is to be followed. For the unsymmetrically placed loads the procedure outlined as the "First Step" is to be followed using a loading of one half the sum of the loading on the left and right spans. Then the procedure outlined under "Second Step" is to be followed using a loading of one half the difference of the loading on the left and right spans. One need solve for the forces and moments at *D* only. Adding the two results gives the reactions at the right abutment; while subtracting them gives those at the left. The stress analysis and design from this stage on is the same as previously explained in this chapter for the single-span structure.

It is to be noted that the signs of the reactions at the abutment of the left arch are taken when it is rotated into the position of *ABCD*.

The above solution may be followed for those special cases where the designer feels that the assumption of hinged abutments is unwarranted, by using the formulas and methods of paper 1542 of the 1924 *Transactions* of the American Society of Civil Engineers for the design of the sections *ABCD* of Fig. 68*b*.

The more general solution of this problem may be found in paper 1827 of the 1933 *Transactions* of the American Society of Civil Engineers. Here the unsymmetrical structure of two or more spans is analyzed by an entirely different method.

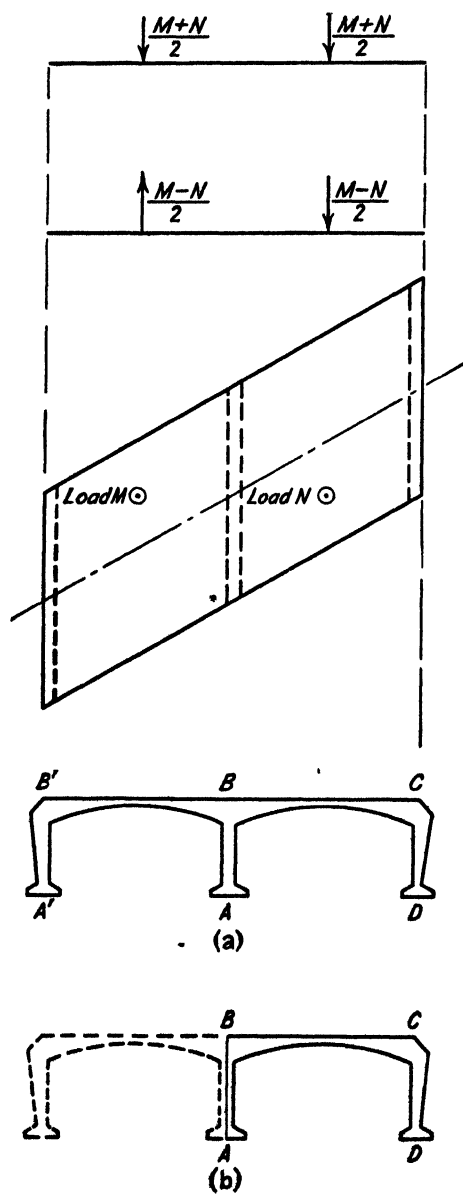


FIG. 68.

CHAPTER XI

PRACTICAL POINTS ON DESIGN AND CONSTRUCTION

DESIGN OF BRIDGES HAVING RESTRAINT AT THE FOOTINGS

Chapter IV as written for the first edition of this book contains some observations relating to the design of rigid-frame bridges without physical hinges at the footings. The results of recent experience, studies, and laboratory tests provide the basis for more definite recommendations for the design of this type of structure. The topic is therefore discussed at more length here as applying at least to both single-span and double-span structures, of the size that would be used for grade separation projects.

Concrete Frame Bridges

In Fig. 38, Chapter VI, a comparison was shown of total maximum moments for fixed-end conditions and for hinged-end conditions in a single-span concrete rigid-frame bridge. Excepting for the positive moment in the vertical leg the agreement is very close. It will also be noticed from the calculations for reinforcement that the only practical difference in the final result is that reinforcement is required at the inside face of the vertical legs for assumed fixed-end conditions. If the influence lines for both conditions are superimposed one upon the other it will be seen that, point for point, there is considerable divergence. Nevertheless the total effect of dead load, live load, earth pressure, and temperature change has been found to be nearly the same

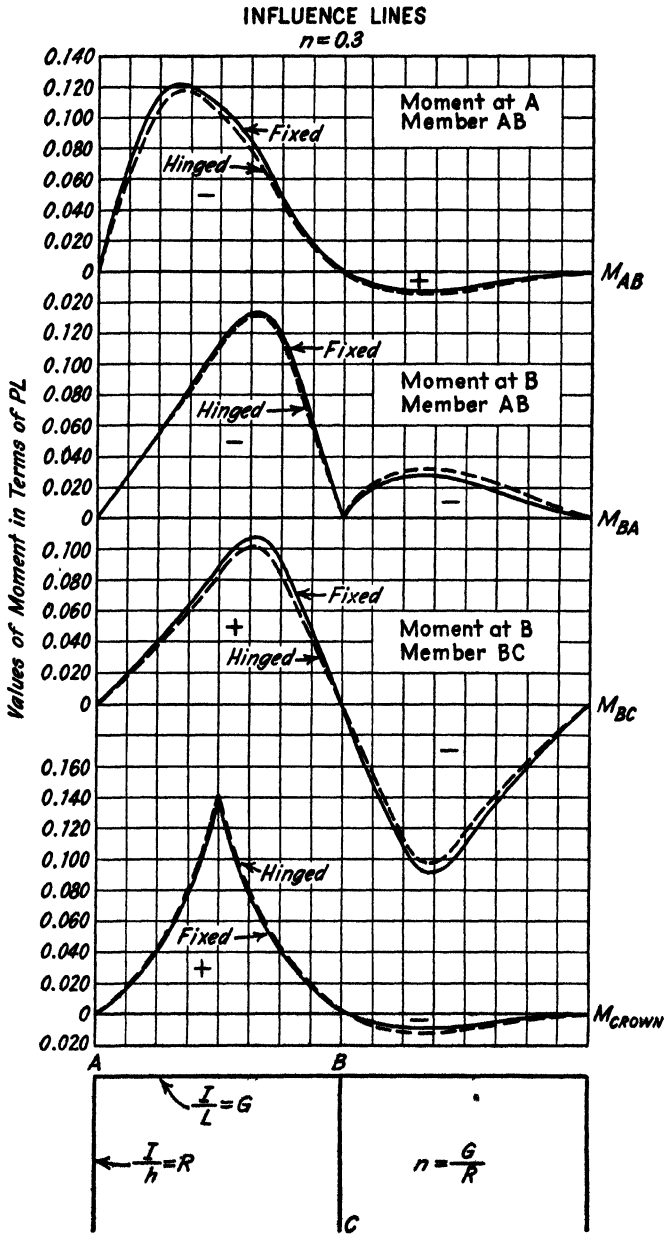
for fixed-end and hinged-end conditions for bridges of 40-ft. to 60-ft. span.

A few comparisons for assumed fixed-end conditions and hinged-end conditions in double-span concrete frame bridges have also been made which show close agreement except for the positive moments requiring reinforcement on the inside faces of the vertical legs. Figure 69 shows the results of one comparison for the critical moments.

In an actual bridge structure, the condition of complete fixity at the footings is rarely realized. For *assumed* hinge points at the middle of the base some calculated restraint may be introduced by an actual eccentricity of the reaction due to the bearing width of the footing on soil foundation or rock foundation; but this is of negligible amount as was explained in Chapter IV. With pile foundations it is possible that considerable restraint may be introduced by reason of the grip of the footings upon the piles which will necessitate reinforcement at the inside faces of the vertical legs. It is the opinion of the writer that even then it is unnecessary to design for the two extremes of hinged-end conditions and fixed-end conditions or to use physical hinges, which are expensive expedients and entirely superfluous except under extraordinary circumstances.

In laboratory tests made at the University of Illinois * on single-span concrete rigid frames with bases rigidly fixed by mechanical means, there was a discrepancy between the experimental results and the calculated fixed-end moment at the bases. No cracks were visible above the footings, but it was finally discovered that microscopic cracks had developed just above the footings—such cracks as would be no more damaging to the structure than those occurring in any flexural member at ordinary working stresses. Nevertheless this was sufficient materially to reduce the calculated end

* See "Tests on Rigid Frame Bridges" by Wilbur M. Wilson, Ralph W. Kluge in the American Concrete Institute *Journal*, May-June, 1938, and *Bulletin* 308 of the University of Illinois Engineering Experiment Station.



Courtesy of Gordon L. Jeppesen, University of Illinois.

FIG. 69.

moments. It thus appears that in an actual structure very small angular changes at the footings due to the elasticity of the soil or to very small yield of piles will be sufficient to minimize restraint at the footings so that it will act like a structure with hinge points near the middle of the base. For concrete rigid-frame bridges of the size usually required for highway grade separation, a calculation for assumed hinged-end conditions only will be adequate, and a good guess can be made of the amount of reinforcement on the inside faces of the vertical legs that will provide for all probable contingencies. The analysis made in Chapter VI for a single-span bridge will be a good guide.

Steel Rigid-frame Bridges.—Steel rigid-frame bridges have been treated in different ways.

1. When very good soil conditions were encountered so that the footings were comparatively narrow (in the longitudinal direction of the bridge), the bases of the girders were anchored to the concrete footings and hinge points were assumed at the bottom of the footing near its center line.

2. When soil conditions required comparatively wide footings and the vertical legs of the girders were embedded in concrete, with the cut-off walls for retaining the approach fill placed in front of the vertical legs of the girders, the bases of the girders were set upon lead plates in pockets formed by angles securely anchored to the concrete footing. Hinge points were assumed, for design purposes, to be at the middle of the girder bases. After the girders were set all interstices in the pockets were filled with bituminous material and added insurance against collection of water was provided by weep holes from the pockets. This arrangement is preferable to the use of pin bearings, which would not be open to inspection after construction.

3. When soil conditions required comparatively wide footings and the vertical legs of the girders were to be permanently exposed, with the cut-off walls for retaining the

approach fill placed back of the vertical legs of the girders, physical hinges (usually of the pin variety) were placed at the bases of the girders.

4. Steel frame bridges have been designed and constructed for fixed-end conditions when for particular reasons massive footings had to be built, the anchorages at the bases of the girders being designed for the calculated fixed-end moment.

The choice of any one of these expedients will depend upon the foundation conditions, the relative cost of fixed-end anchorage or pin bearings for any particular bridge, and the preferences of the designer.

Secondary Effects in Design.—Recommendations are sometimes made to allow, in the design of concrete structures like those illustrated in this book, for such secondary effects as shrinkage and restraint of "side-sway." Plastic yield is also a secondary effect as certain as that of shrinkage but not usually recognized as an element of design. The combined effect of shrinkage, plastic yield, and restraint of side-sway in the structures we are considering is uncertain and not of great importance. In the opinion of the writer all these secondary effects may be neglected unless the designer is governed by specifications to the contrary. The neglect of them is less serious than the neglect of other factors that we are not accustomed to worry about, such as the position of the live load laterally that would give maximum calculated stresses in an arch-like structure. This point is discussed further on. Design calculations are necessarily more or less of a convention for arriving at reasonable proportions for a bridge, which is not a laboratory specimen, so that it will carry expected loads at safe unit stresses and give good service. The simpler these calculations are, the better. Monumental structures may require more accuracy in design than small ones because certain secondary effects may be more pronounced relative to the principal effects. Secondary effects are discussed here so

that the reader may understand their implications and not be disturbed by differences in practice.

Shrinkage.—As the concrete in a structure ages, shrinkage will occur. Its effect will be equivalent to that due to a drop in temperature, but it will be less in a heavily reinforced structure than in one with light reinforcement. A shrinkage coefficient of 0.0002 is sometimes used, which will have a calculated effect equivalent to a drop in temperature of about 30° . The effect of shrinkage, however, will be modified by plastic yield. The two effects are concomitant, and one cannot properly be considered as an element of design without the other. In like manner the effect of seasonal change in temperature will be modified by plastic yield. It is true that over a period of several years plastic yield diminishes until it practically disappears and its relieving effects decrease; but during this period the structural quality of the concrete is improving. Working stresses are based upon the qualities of concrete at an age of 30 days when plastic yield is fully effective.

Finally all calculated stresses are derived by neglecting the considerable amount of tension in the concrete that remains over part of the section of flexural members at the stage of working stresses. This is as it should be, the point to this discussion being that there is a range of uncertainty of structural action so that minor differences in practice are of little significance.

Plastic Yield or Flow.—Under sustained loads, such as the dead loads, the concrete in a structure will be subject to continued deformation up to a certain limit. This structural change of the concrete will result in a lowering of the neutral axis of a flexural member and a readjustment of the internal stresses on a cross-section. Although the modulus of elasticity of the concrete itself may stay practically constant after the curing process is complete, the effect of plastic flow upon the deformations of the structure and upon the redistribution of stress on a cross-section is

as though the modulus of elasticity of the concrete had decreased. For this reason the structures in this book were designed for a modular ratio $n = E_s \div E_c = 15$, although the tests on the field control cylinders of concrete showed a value of $E_c = 3,000,000$ or more. The current specifications of the American Association of State Highway Officials specify a design value of $n = E_s \div E_c = 10$, and it is recommended that this be observed in the design of new structures for the sake of uniformity in practice. A considerable difference in the assumed value of the modular ratio will make little difference in the final design of the structure, so that the effect of plastic flow as an element of design may ordinarily be neglected. For further discussion of this topic the reader is referred to a paper by F. E. Richart, R. L. Brown, and T. G. Taylor in the *Journal of the American Concrete Institute*, January-February, 1934, "Effect of Plastic Flow in Rigid Frames of Reinforced Concrete."

"Side-Sway."—If the live loads upon a symmetrical structure like that shown in Fig. 28, Chapter V, are symmetrically placed each side of the crown, it is obvious that the bending and deflections of the members will also be symmetrical about the crown and that the top of the frame will not move longitudinally relative to the footings. If the live loads are unsymmetrically placed, as for example a single line of loads across the bridge at point 8R of Fig. 28, the bending and deflections will be unsymmetrical about the center of the span; and the top of the frame, unless restrained by other forces, will move longitudinally with respect to the footings; in other words, it will have a horizontal deflection.

If this deflection is restrained by external forces, additional stresses will be set up in the structure. It is doubtful whether any considerable restraint to side-sway in an actual bridge structure will be provided by the development of passive earth pressure at the ends of the frame. Tests on

one of the bridges built by the Bronx River Parkway Commission indicated that the elasticity of ordinary soil was sufficient to prevent any appreciable amount of piling up of passive earth pressure, due to flexure in the structure. Expansion joints in the roadway pavement at the ends of the bridge should be adequate to prevent restraint that might otherwise be developed. If a portion only of the width of the bridge is loaded, the unloaded portion will restrain side-sway in the loaded portion; but the load itself will be distributed laterally and the stresses in the longitudinal strip under the load will be less than if the strip is calculated as an independent unit.

Even if side-sway were fully restrained the results would be of little consequence, partly because live-load stresses are a small part of the total and partly for the following reasons. For the condition of live loading causing *maximum* stresses at the critical sections (the knee and the crown) the tendency to sway is very slight; and at other points where eccentric live loading for the maximum stresses does cause appreciable tendency to sway, the concrete sections have excess capacity. Any calculation for restraint of side-sway is therefore of little practical value. As a matter of academic interest, however, the method of calculation is explained.

Calculation of Restraint of Side-Sway.—The influence table following Fig. 28 in Chapter V shows “total moments” for an influence load of $13/4$ at any particular point.

The horizontal deflection at the crown will be $\frac{s}{E} \sum \frac{My'}{I}$,

in which y' is measured from the point at which the deflection is being calculated; that is, $y' = 18.2 - y$ in Fig. 28. If “side-sway” is prevented by a force H' acting horizontally at one end of the frame the calculated horizontal deflection at the crown due to it must be equal and opposite to that due to the vertical load at 8R. To find its coefficient, assume tentatively $H' = 1$. Horizontal components of

the reactions for $H' = 1$ may be calculated in the same manner as were the horizontal components for earth pressure at one end of the frame. Vertical components of the reactions are due to the overturning effect of $H' = 1$. Total moments M' may then be calculated for all divisions, and the crown deflection will be $\frac{s}{E} \sum \frac{M'y'}{I}$. From the two equations for deflection there is derived

$$H' = \frac{\sum \frac{My'}{I}}{\sum \frac{M'y'}{I}}.$$

It is to be noted that analysis by the moment-distribution method infers that side-sway does *not* occur, and a correction is necessary to determine stresses under the condition that the structure is free to sway. Despite the apparent inconsistency involved, it is the writer's opinion that, if analysis is made by the method explained in this book, correction for restraint may be neglected; and if analysis is made by the moment-distribution method, correctional stresses resulting from freedom to sway may also be neglected. Restraint is probably partial, and the effect of either restraint or sway in bridges is negligible, for reasons explained heretofore; except perhaps in unsymmetrical structures having legs of quite different length.

Placement of Live Load.—The accepted convention for calculating live-load stresses in a slab or arch-like structure which is continuous for its full width is to assume that the maximum stress that is produced on any portion carrying a traffic lane will be that produced by the direct loads upon the lane. As a matter of fact, the eccentric application of live loads to one side only of the roadway will increase the stresses at the edge of the bridge due to the direct application of the load, the principle being analogous to that of the eccentrically loaded column. In general, the maximum

stresses at the edge of the bridge will occur when the outer two-thirds of the roadway is loaded; and, if considered in design, this would result in a progressive strengthening of the sections from the center line of the bridge to the outer edges. This is a point that appears to have escaped the attention of bridge engineers, but there is good reason against revising our conventions of design with respect to the use of live load to agree with theory.

We have a clear case of expediency to consider: whether to design the structure for extreme but occasionally probable conditions of loading within conventional limits of stress, or to design for ordinarily expected conditions and permit the conventional working stresses to be exceeded for the extreme conditions. The usual conventions of design as to loading and working stresses do result in structures that perform good service; therefore we may conclude that they represent the usual wear and tear upon the structures very well and that it is unnecessary to assume conditions that would result in abnormalities of proportion.

If any specific recommendation may be made, the writer would suggest that, in designing bridges of the barrel type, the provision of the specification permitting reduction of intensity of live load for the wider bridges be ignored. This provision is intended to allow for the effect of supposed dispersion of traffic upon wider roadways. Ignoring this reduction will automatically provide in some degree for the effect of eccentricity of the reduced loading. This recommendation has not been followed in the design calculations contained in this book, but the specification for loading has been followed literally.

Intrados Curves.—The rigid-frame bridges illustrated in this book were built without fillets at the inside corner of the knee. Bridges have been built with fillets, but the compounding of the fillet curve and the circular segment curve of the top present a less pleasing appearance. Compound intrados curves are usually unsatisfactory.

By referring to the tests on knee specimens and rigid-frame-bridge models described in Chapter XIV, it will be seen that very high stress concentrations exist, under load, at the sharp corners of the unfilleted specimens. When these specimens were tested to destruction, however, failure did not occur on the sections at the corner but on sections some distance from the corner where the stress condition was more like that existing in a beam. The only exception was for knees having abnormally high percentages of steel reinforcement. Failure at the point of high stress concentration had to be induced deliberately. The Columbia University tests described in the first edition of this book and the University of Illinois tests described in Chapter XIV of this edition demonstrated beyond all reasonable doubt that the unfilleted knee is safe in the construction of structures like rigid-frame bridges.

The significance of localized high concentration of compressive stress such as exists at the sharp corner of a knee specimen is not yet known. The reason why such specimens do not fail at the corner may be that the compression at the corner is a confined stress. Compressive forces come in from all directions—along each leg and radially toward the corner from the curved band of reinforcing rods.

In a so-called compression test of a concrete cube the specimen really fails by shearing along inclined planes, indicating a comparatively low apparent compressive value. A flat plate, however, would show much higher compressive resistance. Another analogy is afforded by calculated shear. Higher working stresses are allowed for punching shear than for shear used as a measure of diagonal tension in a concrete beam. The designer should not impair the appearance of his structure in order to minimize the stress concentration at the knee.

Proportions for Analysis.—Experience with this type of structure has been too limited to establish general rules for proportioning, preliminary to analysis. A rough guide for a

single-span concrete solid section frame bridge carrying a separate roadway pavement and designed for H20 loading is as follows:

Make the thickness at the knee (t in inches) $= 4 + \frac{S}{14.5}$

and the crown thickness $= 4 + \frac{S}{53}$, in which S = the clear span length in inches. The depth at the knee may be decreased at the expense of an increase in thickness at the crown, and vice versa; but no general rule can be given.

For a double-span concrete solid section frame bridge the thickness at the knee may be assumed as $4 + \frac{S}{17}$ and the thickness at the face of the vertical leg may be assumed as $15 + \frac{S}{15}$. The crown thickness will be about the same as for the single-span structure. The final design need not agree exactly with these approximate proportions assumed for analysis. Observe the sample calculations.

Construction Joints.—In construction it is convenient to pour the footings as the first operation. The cantilever portions of the footing are reinforced by means of bent rods shown in typical plan Fig. 33, which are crossed in the footing and carried above the footing about 3 or 4 ft. as a splice to the main rods in the vertical legs which are set up as a second operation after completion of the footings. Effective keyways should be provided in the tops of the footings to bond the vertical legs thereto.

The third operation is the casting of the vertical legs. It is convenient in pouring to make construction joints at the tops of the vertical legs, stepped and keyed, as shown in the typical plan (Fig. 33). The top of the frame may be poured monolithic or in two or more longitudinal sections.

It is of the utmost importance that all construction joints be thoroughly cleaned, picked and broomed to

remove all laitance and expose clean aggregate before making the succeeding pour.

Expansion Joints.—In structures not faced with arch ring stones it has been the practice of the Westchester County Park Commission to provide expansion joints between the approach retaining walls and the structure proper, so that the frame is free of all other construction. In structures faced with stone arches, provision is preferably made for carrying the large thrust of the stone arch directly into the approach walls and in such cases expansion joints between the frame and approach walls are avoided, or placed back of the point where the thrust may be considered as reaching the ground. The superincumbent masonry of the walls and parapets will bring the thrust quickly to the foundations, and back of this point expansion joints may be provided in the walls if desired. It is realized that inter-action between the frame proper and the stone arch will disturb the calculated stresses in both, but if both units are designed to be separately self-supporting no concern need be felt over this condition of affairs.

Anchoring of Stone Arch Facing.—It has been the practice of the Commission to securely anchor each individual arch ring stone of stone-faced bridges to the concrete frame by means of two steel anchors embedded in the joints, and hooked into drill holes in the bed face of the stones. These anchors project into the concrete frame which is poured after setting up the stone arch on falsework.

Secondary Reinforcement.—"Distributing" rods, tie-rods and stirrups are used in addition to the calculated main reinforcement. "Distributing" rods are used in the stone-faced structures only, when expansion joints between the approach retaining walls and structure proper are omitted immediately back of the frame. This is to prevent the formation of cracks in the corners of the frame where it abuts against the approach walls. The distribut-

ing rods are about five or six in number, about 1 sq. in. in section, hooked at each end and are placed in the extrados at the knee. *Transverse tie-rods* about $\frac{3}{4}$ in. in diameter and about 3 ft. on centers top and bottom serve to hold the main reinforcement in place and to tie the structure together, preventing any formation of cracks due to possible uneven supporting action of the soil. *Stirrups* hooked over the top and bottom mainrods or transverse tie-rods, as shown on the typical plan Fig. 33 serve to hold the top and bottom systems of reinforcement securely in place. They are not required as calculated shear reinforcement.

Footings.—In designing pile foundations, in particular, in which piles are driven through soft material offering little lateral resistance, the direction of the reactions should be determined for all probable cases; dead load with active earth pressure; dead and live load with active earth pressure; and possibly dead load with excess earth pressure equal to twice ordinary active pressure; dead and live load with excess earth pressure. If the direction of the reactions depart far from the vertical, battered piles should be used so that they will properly carry the inclined loads coming upon them.

CHAPTER XII

GENERAL NOTES ON RIGID-FRAME BRIDGES

Rigid-frame bridge construction in the United States was first applied to some of the grade separations between the parkways of Westchester County, New York, and intersecting streets and highways. The rigid-frame type was evolved to overcome the difficulties encountered where the distance between the two roadway grades was restricted and where street excavation for the abutments of an arch bridge would have been expensive. The type was so well adapted to its purpose that, in addition to about ninety built in Westchester County from 1922 to 1933, about four hundred were built elsewhere in the United States up to 1939. Rigid-frame bridge construction is advancing rapidly abroad so that nearly every country in the world now has its examples. Many have been built to carry heavy railroad traffic.

The rigid-frame bridge has its varieties. The sample calculations given in this book for concrete bridges are for the solid or barrel type, because it is predominant for grade separation structures. In Westchester County a few concrete bridges of ribbed construction have been built, but the best example is that shown in this chapter. The outstanding example of cellular construction is in Seattle, Washington. In this chapter several varieties are illustrated.

Figure 70 shows a solid-section or barrel-type concrete frame bridge with an elliptical intrados, of which several were built in Westchester County. The elimination of massive abutments necessary for a fixed arch proved to be an economy, and the elliptical opening, permitted by the conditions controlling the grades of the intersecting road-

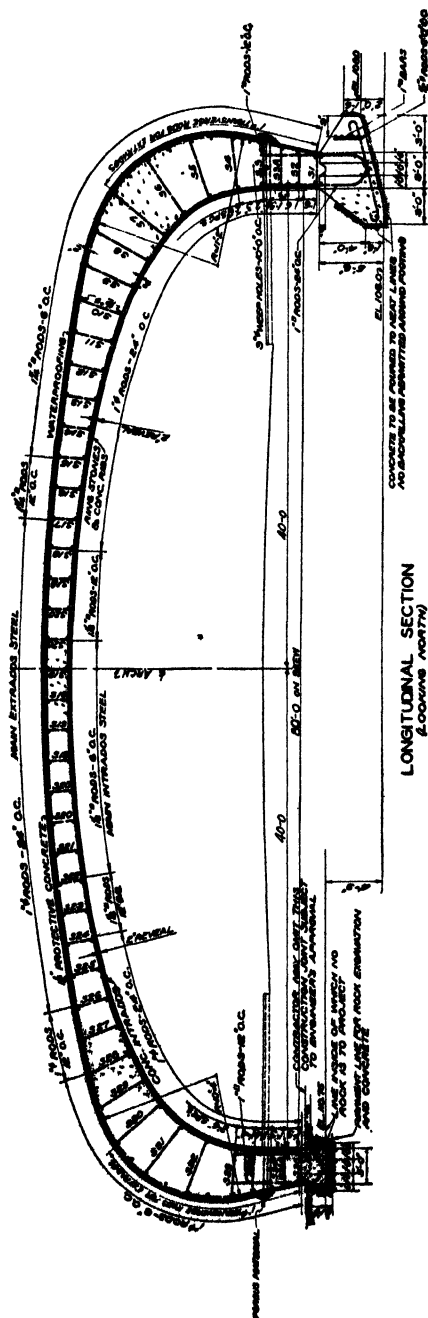


FIG. 70.

ways, was a pleasing variation among the other frame bridges on the parkways.

Figure 71 illustrates ribbed construction. This con-



FIG. 71a.

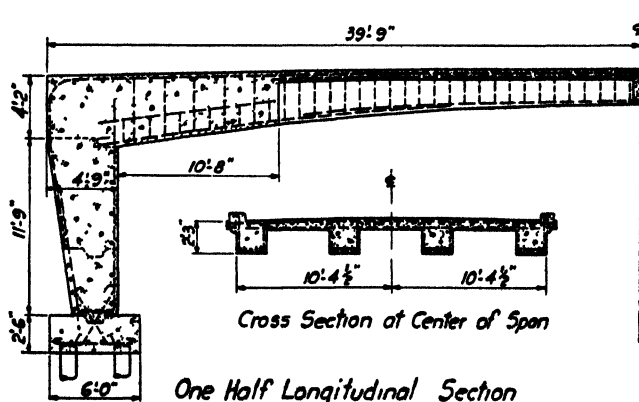


FIG. 71b.

Krape Park Bridge, Freeport, Illinois

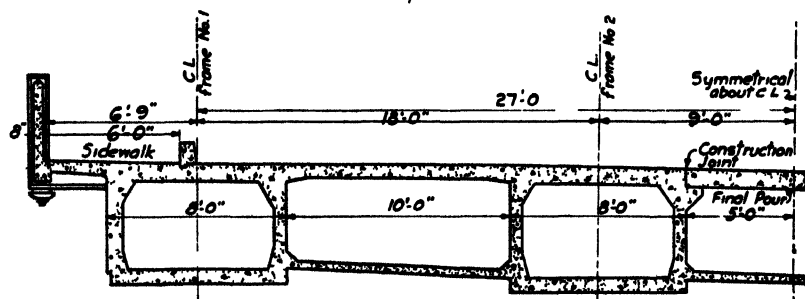
struction in mid-span reduces the dead-load bending moments throughout the structure, and for long spans the saving in materials may offset the increased cost of formwork and the fabrication and placement of steel reinforce-

ment. The bridge itself, designed by Mogens Ipsen, is a beautiful example of modernistic treatment which at the same time avoids the bizarre.

Figure 72 illustrates cellular construction. The bridge is



FIG. 72a.



Cross Section of the Box Girders at the center of the 175'-0" Span

FIG. 72b.

Schmitz Park Bridge, Seattle, Washington. 175-ft. span
Courtesy of the City of Seattle.

in Schmitz Park, Seattle, Washington, and was designed in the office of the city engineer. A full description appears in the *Engineering News-Record* for June 24, 1937.

Figure 73 shows the type of construction of a through

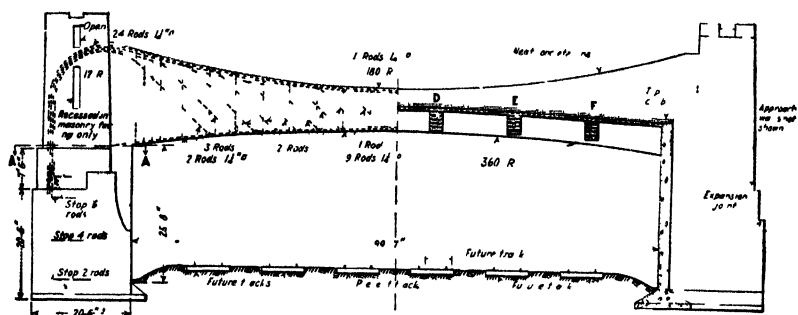


FIG. 73.



FIG. 74.—The Herval Bridge, Brazil. Built by the firm of Emilio Baumgart; Rolf Schjodt in charge of design. Middle span 224 ft. End spans 88 ft.



FIG. 75.

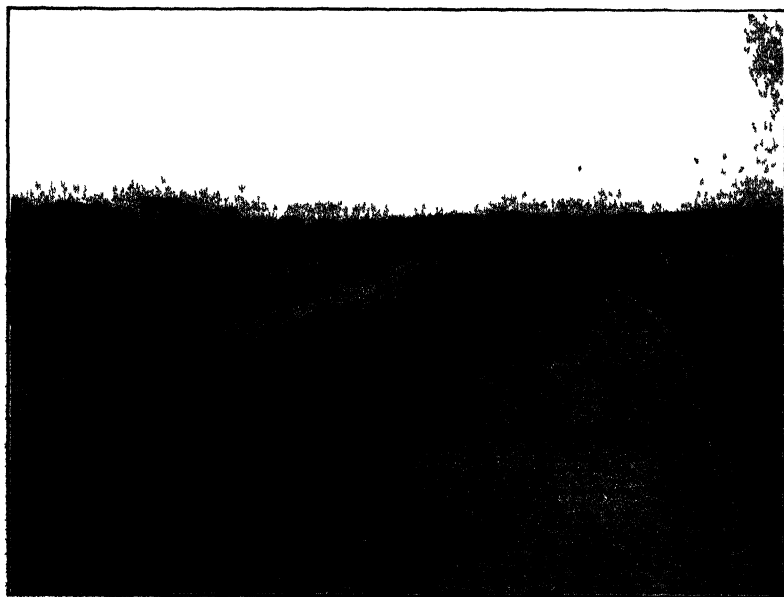


FIG. 76.

girder bridge, consisting of two concrete rigid-frame girders carrying a floor system of transverse floor-beams and a deck slab. The bridge carries the Bronx River Parkway over the New York Central Railroad tracks at Valhalla, N. Y., and it is a good example of what should not be done along the lines of bridge architecture. Contrasted with this is the Herval Bridge at Ste. Catharina, Brazil, shown in Fig. 74, which is also through girder construction with cross-beams between the girders to carry the floor slab. Its slender proportions and simplicity of line and detail produce a beautiful effect. The middle span is 224 ft. and end spans about 88 ft. A full description of the bridge and its construction appears in the *Engineering News-Record* of August 6, 1931.

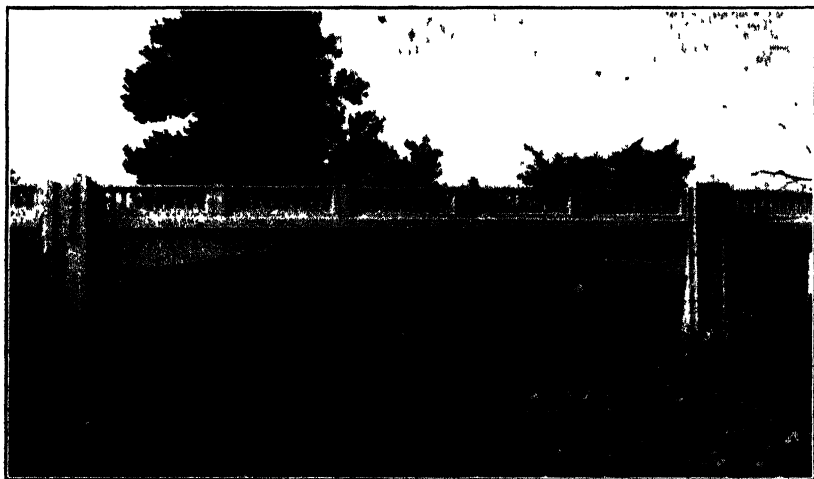
Figures 75 and 76 illustrate the advantage of the arch-like structure over the through girder or truss type in providing an unobstructed roadway over the structure. Both bridges are modern and were built to carry a highway over a railroad right-of-way, the total width of roadway being the same for both. The width of roadway was such that a middle truss was necessary for the through bridge. This constitutes an obstruction in a highway that is not divided by a continuous separation strip, as on a dual highway.

A few good examples of rigid-frame bridges finished in concrete are shown as a conclusion to this chapter. They are expressions of certain fundamental principles of architectural design, which are clearly and concisely explained in a booklet by the Portland Cement Association, "Architectural Design of Concrete Bridges." These principles alone cannot be applied by a novice to produce a beautiful bridge. A *good* architect has something to contribute in addition to the application of certain rules of thumb. Nevertheless the structural designer should know what principles of architectural design cannot be violated without resulting in a structure that is a positive offense to the eye.

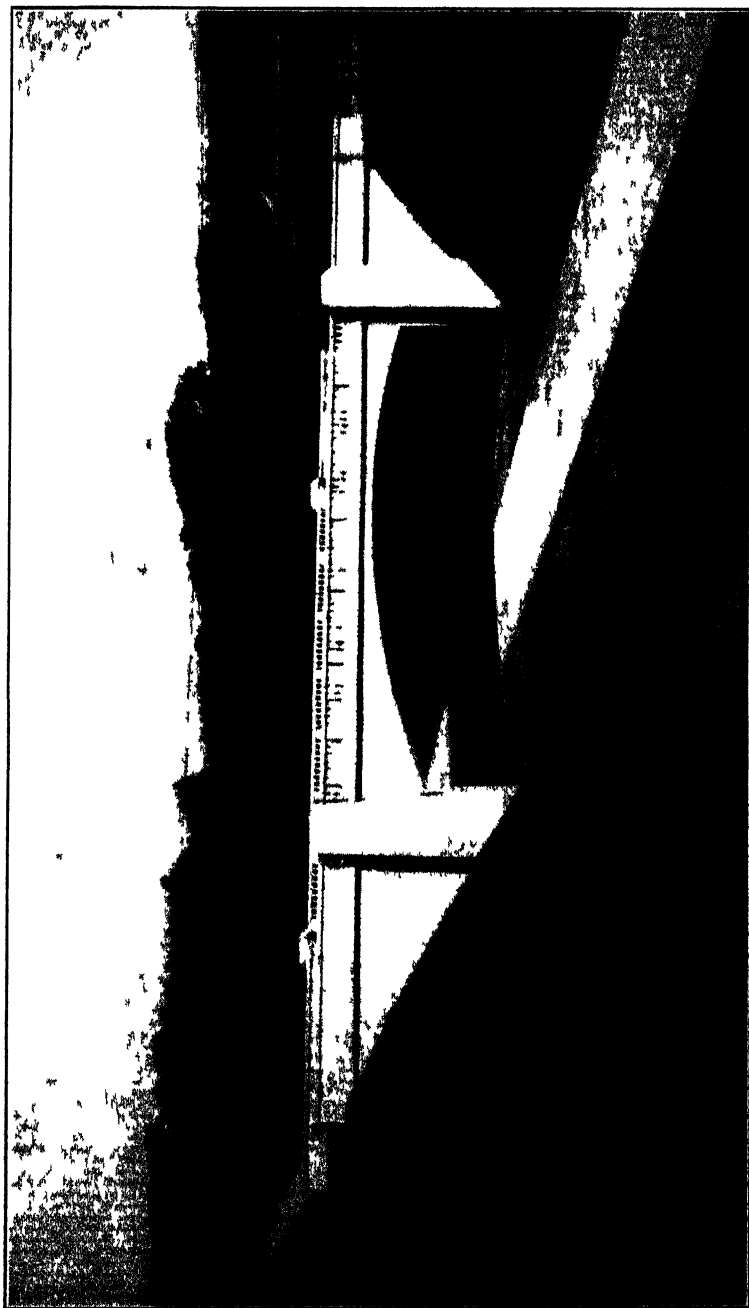
The rigid-frame bridge has now become a recognized

type, better adapted than any other for a particular set of conditions. It solves the problem, for example, when the distance between the roadways above and below is restricted, or when the length of approaches is an item of importance. In some instances the rigid-frame type has been selected when another type (such as the "rainbow" arch, in which the thrust closely follows the axis) would have been a better solution. The engineer should base his selection upon sound engineering principles.

The selection of barrel, ribbed, or cellular construction will depend upon the size of the structure and the relative cost of materials, fabrication and placement of reinforcement, and formwork. No general rules can be given.



Findlay-Delphos Road Bridge, Putnam County, Ohio. 50-ft. span
Courtesy of the Portland Cement Association



Bridge carrying Six Mile Road over Middle Rouge Parkway, Wayne County, Michigan. Span 60 feet
Courtesy of the Portland Cement Association

CHAPTER XIII

DEFORMETER ANALYSIS

For Rigid Frame Bridges of High Indeterminacy

By PROFESSOR GEORGE E. BEGGS
Princeton University

FOREWORD BY THE AUTHOR

The mathematical methods explained in this book have been found to be rapid and easily applied in the designing room, for structures which are indeterminate to the third or fourth degree. The analysis of the skew arch or frame is more complicated but this is a problem by itself. The Westchester County Park Commission has not had occasion to build more than one double-span frame bridge for fixed-end conditions and only two triple-span frame bridges for free-end conditions. Mathematical methods have therefore not been systematized for such highly indeterminate structures. In such cases a different method of attack is used, namely the deformer method of Professor George E. Beggs of Princeton University, who will discuss the method in this Chapter.

DISCUSSION BY PROFESSOR BEGGS

Figure 77 illustrates the principle underlying the determination of the reactions for a statically indeterminate structure fixed at the footings by measuring relative displacements in a flat model of the structure. It is desired to find the reaction at *B*, say, due to an assumed load *P* acting as shown. The model is fixed at *A*, *C* and *D*. Move point *B* vertically a known amount d_1 without permitting rotation. Measure carefully the corresponding deflection.

d_2 in the direction of application of the assumed load P . Then it may be shown that $Vd_1 = Pd_2$, the equation giving the relation between the vertical component V of the reaction and any load P in terms of relative displacements.

Restore the model to its unstrained position. Move B horizontally a known amount d_3 again without permitting rotation. Measure again the corresponding displacement d_4 and the equation $Hd_3 = Pd_4$ gives the relation between the horizontal component H of the reaction and any load P in terms of relative displacements.

Restore the model as before. Rotate point B without permitting other motion, and measure the rotation d_5 and displacement d_6 . Then $Md_5 = mPd_6$ in which m is the

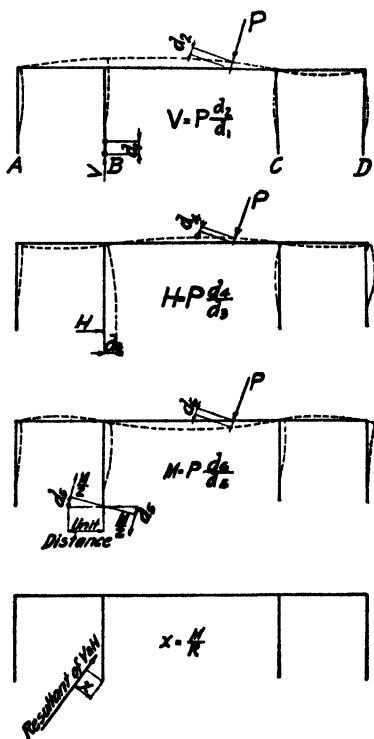


FIG. 77.



2 PAIRS OF GAUGE PLUGS OF TWO DIFFERENT SIZES PRODUCE PURE RELATIVE VERTICAL MOTION OF THE GAUGE BARS "m" AND "n".



SHEAR PLUGS PRODUCE PURE RELATIVE HORIZONTAL MOTION OF THE GAUGE BARS "m" AND "n".



MOMENT PLUGS OF DIFFERENT DIAMETERS PRODUCE PURE RELATIVE ROTATION BETWEEN "m" AND "n".

FIG. 78.

scale ratio of the model.

Having now H , V and M , the amount, direction and point of application of R_B may be found as indicated in Fig. 77. In the same manner the reactions at A , C and D may be determined for a given load P . Proceed in like

manner for assumed load at other points in order to deter-

mine the influence lines for the structure by means of which reactions for any system of loading may be found.

The arbitrarily imposed displacements at reaction points of the model are accomplished by means of deformer gages capable of producing very small deflections with an accuracy to 1-40,000 of an inch, and the corresponding small displacements at the points of application of the assumed loads are measured by means of filar micrometer microscopes. The principle of the deformer gages is illustrated in Fig. 78. Bar *m* is fastened to the board on which the model is mounted and the reaction point of the model is fastened to the movable bar *n* which is held against

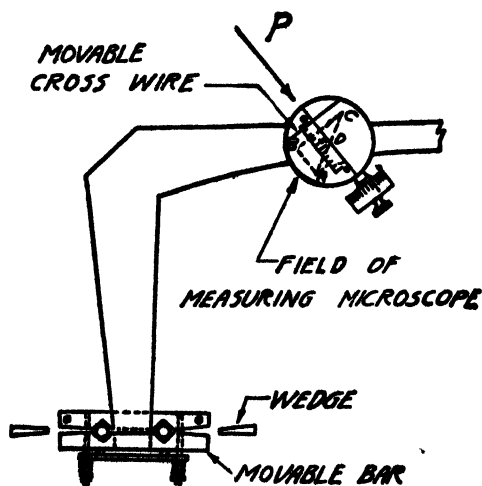


FIG. 79.

the gage plugs by means of a spring connection between *m* and *n*. In the unstrained position of the model, normal plugs are in place. These may be removed by spreading the bars *m* and *n* by means of small wooden wedges. To produce a known vertical displacement of the reaction point the normal plugs are removed and smaller diameter

plugs of like size are inserted. A reading on a reference point on the model at the point of application of the assumed load is then taken by means of the micrometer in the field of the measuring microscope (Fig. 79). The small plugs are then removed from the deformer gages and the larger diameter plugs are inserted, the difference in diameter of the small and large plugs being the known vertical displacement. A second reading is then taken on the reference point at the point of application of the assumed

load by means of the micrometer microscope and the difference of the two readings gives the displacement at the load.

Horizontal displacements at the reaction points are produced by means of rectangular plugs as indicated in the middle line of Fig. 78. Rotation of the reaction point is produced by interchanging a small-size plug and a large-size plug in the sockets of the deformer gages as indicated in the lower line of Fig. 78.

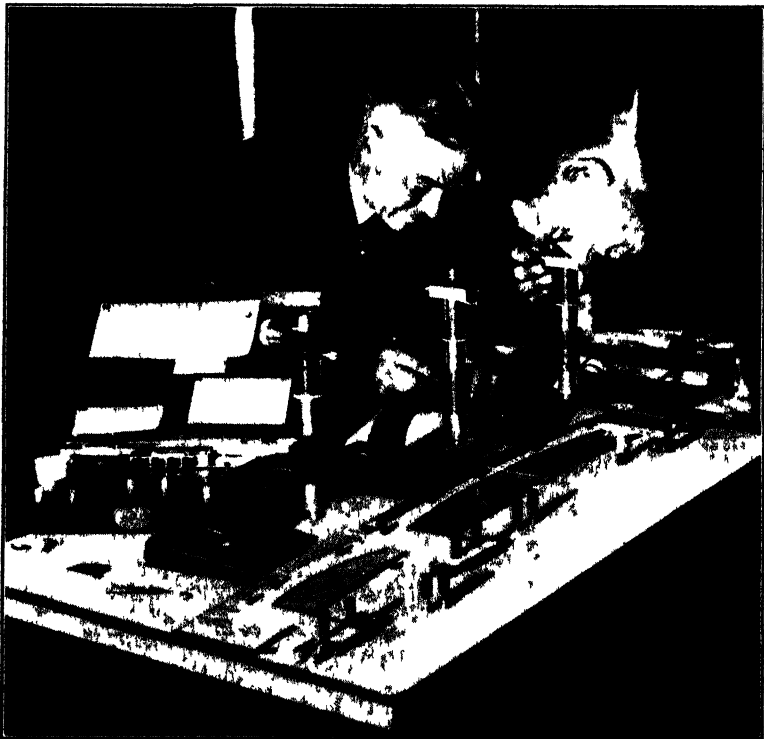


FIG. 80

Figure 80 shows the set-up of the deformer apparatus over a model of one of Mr. Hayden's rigid-frame bridges designed for the Westchester County Park Commission.

The models used in the investigations may be of cellu-

loid or pasteboard so cut that the width at any section is proportional to the cube root of the gross moment of inertia of the corresponding section of the structure. Three-dimensional structures such as ribbed frames having T-shaped sections may thus be analyzed by means of two-dimensional models, the only restriction being that the forces analyzed must be uniplanar.

In order that the displacements in the celluloid or pasteboard models may be unaffected by frictional resistance, the models rest on small steel ball-bearings supported on plate glass. Small steel weights (shown in Fig. 8o) hold the models against the ball-bearings and prevent warping of the models.

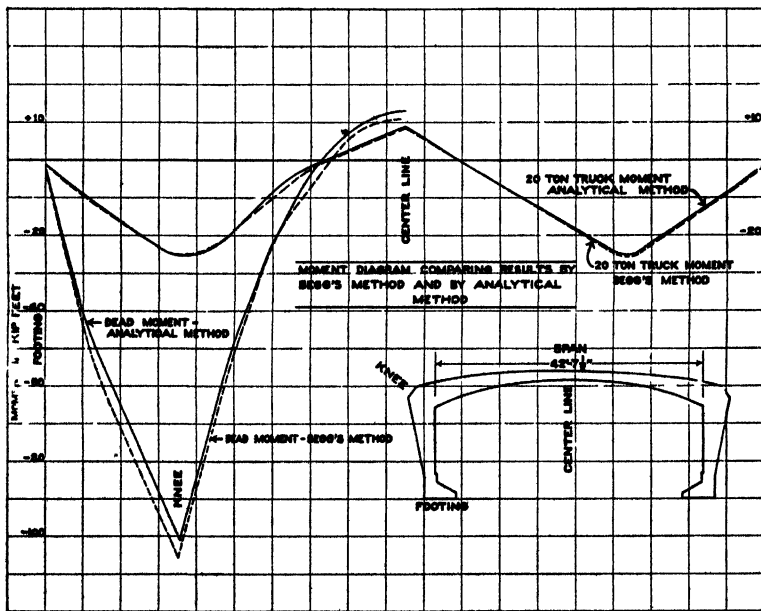


FIG. 81.

It is to be noted that no actual loads are applied to the model, the process being only the measurement of related displacements, the ratio of which is the ratio of load to reaction component. Models cut from homogeneous mate-

rials may be relied upon to give results that are substantially correct as applied to structures of such composite materials even as reinforced concrete. The approximation involved is no greater than is involved by the application of mathematical methods of analysis, in which the elastic properties are calculated for gross moments of inertia of the uncracked sections thus assuming practical homogeneity. The reliability of theory based on such assumptions has been verified by numerous tests such as those of Abe (University of Illinois Bulletin 107) and the government tests of Slater (*Proceedings*, American Concrete Institute, 1919) on constant-section frames. Stresses are, of course, calculated on the cracked section.

A comparison of analysis by deformeter and by mathematical methods for a small rigid-frame structure is shown in Fig. 81. The agreement is seen to be very close.

CHAPTER XIV

RESEARCH IN RIGID-FRAME BRIDGES

By **HAROLD E. WESSMAN**

Professor of Structural Engineering, New York University

The increasing use of steel and reinforced-concrete rigid-frame bridges in recent years has been accompanied by a series of investigations which have enhanced knowledge of this type of structure. Most of the research has focused attention on the knees, points where the usual beam analysis fails to provide a satisfactory picture of stress conditions. Other studies, however, such as those at the University of Illinois on full-size reinforced-concrete ribs have given insight into the validity of the elastic theory of analysis for the structure as a whole.

The practicability of the design of the first structure built by the Bronx Parkway Commission in 1922 was questioned, chiefly because of unknown stress conditions at the knee. In a curved beam, the unit stress is greater at the concave surface than it is on the convex side at the same section. The neutral axis does not coincide with the gravity axis but approaches the inner surface as the curvature increases. In a structural member such as a rigid-frame bent, with a sharp re-entrant angle at the knee, a high stress concentration tends to develop at the inside corner. Research to date indicates that this is not serious enough to endanger the safety of the structure.

It is important before discussing any tests to sound a note of warning. The treatment in this chapter must necessarily be brief, and readers are advised to scrutinize carefully the references for detailed information about test data. It should be kept in mind that what is so often referred to

in reports as "measured stress" is actually "measured strain." Measured strains below the yield point in steel members or steel reinforcing may be converted quite accurately into corresponding stresses, barring errors in gage readings. But measured strains in concrete give little clue to the corresponding stresses because of plastic flow and the variation of modulus with load and with time.

Some of the earliest tests on knee details were made at Columbia University in 1922 by A. H. Beyer and W. T. Krefeld. These tests are fully described in the *Engineering News-Record* for January 18, 1923. Six reinforced-concrete L-shaped or knee models $10\frac{1}{2}$ in. thick, 18 in. wide, and 7 ft. high were tested. As the load increased, tension cracks developed in the concrete, beginning at the outside surface and reaching almost to the re-entrant corner. The apparent neutral axis moved inward close to the corner, indicating a high compressive unit stress in that region. There was no compression failure, however, and the tests demonstrated the safety of the sharp-cornered detail. The effect of filleted corners was also studied, and it was found that fillets tend to reduce the local stress concentration.

Photoelastic tests were also made at this time in the Physics Laboratory of the Massachusetts Institute of Technology by T. H. Frost and D. B. Sayre. Two celluloid models, one with square corners and one with a filleted knee, were tested in polarized light. The shift of the neutral axis and the effect of the fillet in reducing the stress concentration at the inside corner were again demonstrated.

Field tests were also made by the Bronx Parkway Commission on two reinforced-concrete model frames 3 ft. wide with a clear span of 10 ft. and a height of 4 ft. The rib depth at the crown was $3\frac{1}{2}$ in., and the depth at the knee $10\frac{1}{2}$ in. Each model supported a concentrated load of 13 tons at the center of the span, with calculated unit stresses of 79,000 lb. per sq. in. in the steel reinforcement and 4,900 lb. per sq. in. in the concrete. These stresses were calculated

on the assumption that the flexure formula was valid for these high stresses.

University of Illinois Tests.—The first tests on reinforced-concrete rigid frames at the University of Illinois were made by Mikishi Abe during the World War. The purpose was, primarily, to study the cross-frames of concrete ships. These tests are reported in *Bulletin* 107 of the Engineering Experiment Station and will not be discussed here.

A rather extensive investigation relating particularly to rigid-frame bridges has been made in recent years, however, under the sponsorship of the Portland Cement Association. Part I of this investigation, published in 1938 in *Bulletin* 307 of the University of Illinois Engineering Experiment Station, is entitled "Tests of Reinforced Concrete Knee Frames and Bakelite Models," by F. E. Richart, T. J. Dolan, and T. A. Olson. Part II, also published in 1938, is entitled "Laboratory Tests of Reinforced Concrete Rigid Frame Bridges," by W. M. Wilson, R. W. Kluge and J. V. Coombe.

The tests of knee frames reported in Part I were planned "to determine the moment-resisting capacity and the elastic properties of the corner portion of a rigid frame, using various types of fillets and arrangements of reinforcement." Twenty-four frames, twelve different types with two of each type, were tested to failure at 28 days. Eight other frames, representing four different types, were held under a sustained load of 12,400 lb. for 1 year and 5 months in order to observe the effect of plastic flow on strains, rotations, and deflections. The load was then removed to observe the elastic recovery before the frames were tested to failure.

Figure 82 illustrates the type of specimen and the manner of loading for both the rapid and sustained tests. Each leg of the knee frame is 6 ft long. The depth of the leg on the unfilleted specimens at the sections adjacent to the re-entrant corner is 16 in. All frames were 12 in. wide, and all frames, except one pair, had 1 per cent of steel tensile reinforcement, an amount which required a calcu-

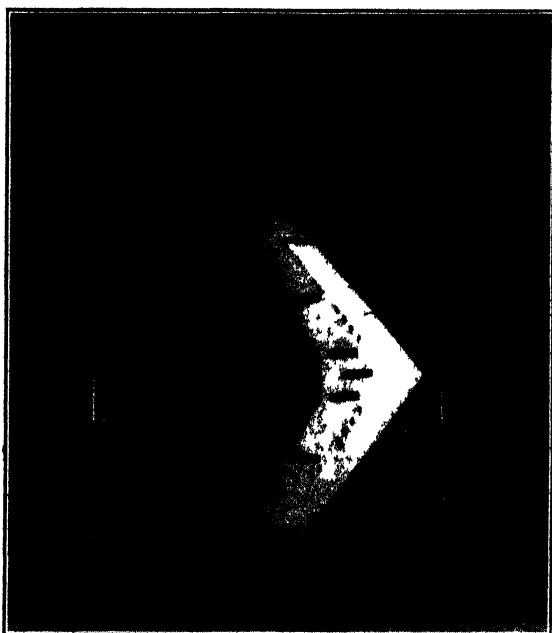


FIG. 82.—Test Frames Under Rapid and Sustained Loading
Courtesy of University of Illinois Engineering Experiment Station

lated load of 12,400 lb. in order to develop working stresses. Three per cent of tensile reinforcing was used in one pair of frames in order to insure a compression failure at the knee. Variety in the types tested was obtained by using compression reinforcing in some frames and by having two sizes of 45° fillets and two sizes of circular fillets.

In the rapid loading tests "cracking began in all of the frames at a load of about 10,000 lb., and most of the frames failed initially by exceeding the yield point of the tensile reinforcement." A secondary crushing occurred in some of the frames, but the only well-defined compression failure occurred in the two frames having the high percentage of tensile steel. This failure occurred near the re-entrant corner, but at relatively high loads, loads which were more than four times as much as the load giving normal computed working stresses.

Specimens with fillets showed a marked increase in strength over those with sharp corners. Even though it is recognized that fillets tend to reduce local stress concentrations, the increase in strength was probably due to the fact that the fillets reduced the moment-arm of the applied load and also increased the depth of the section where failure occurred.

As noted previously, only one pair of frames had enough tensile reinforcing to develop a definite compression failure; consequently, it is not possible to determine from these tests any definite relations between ultimate strength, local stress concentrations at the re-entrant corner, and fillets. It must also be kept in mind that the knee frames in these tests behave somewhat differently from a rigid-frame bridge. Adding a fillet to the knee frame causes a decrease in moment at the corner section due to a given applied load. Adding a fillet to a rigid-frame bridge may cause an increase in the moment at the corner section due to a given load. There is a change in the distribution of positive and negative moments. Nevertheless, there is no question but that

fillets reduce local stress concentrations. This has been beautifully demonstrated by photoelastic tests.

The eight frames which were kept under sustained loading for 1 year and 5 months showed very definite time yield effects. Deflections, rotations, and concrete strains increased greatly over those measured when the load was first applied. But, when the frames were finally tested to destruction, they showed little variation in ultimate strengths from those of the corresponding frames tested at 28 days. Of most significance in these tests was the effect of compressive reinforcing in reducing plastic yielding to practically one-half of that occurring in corresponding frames with no compression steel.

Photoelastic tests on Bakelite scale models of the knee frames are also reported in Part I of the University of Illinois investigation. Figure 83 shows the fringe photographs for seven models. Each fringe or black band represents a locus of points having the same difference of principal stresses, or, in other words, the same intensity of maximum shearing stress. In the frames with sharp inside corners, a large number of fringes converge at the corner, indicating high stress concentrations in this region. Fringe photographs of frames with fillets indicate a reduction in localized stress intensities.

Part II of the University of Illinois Investigation is significant by virtue of the size of specimens tested. Figure 84 presents the details of Specimen 1. It is practically a full-size slice $1\frac{1}{2}$ ft. wide from a highway bridge with a span of 48 ft. One other specimen was also tested. It differed from Specimen 1 only by the addition of shear reinforcement, consisting of $\frac{1}{2}$ -in. round looped stirrups spaced on 12-in. centers in the deck and legs.

Specimen 1 was tested, both with bases fixed and bases hinged, to determine whether the actual behavior of the structure conformed to the action anticipated from calculations based on the elastic theory. Specimen 2 was built

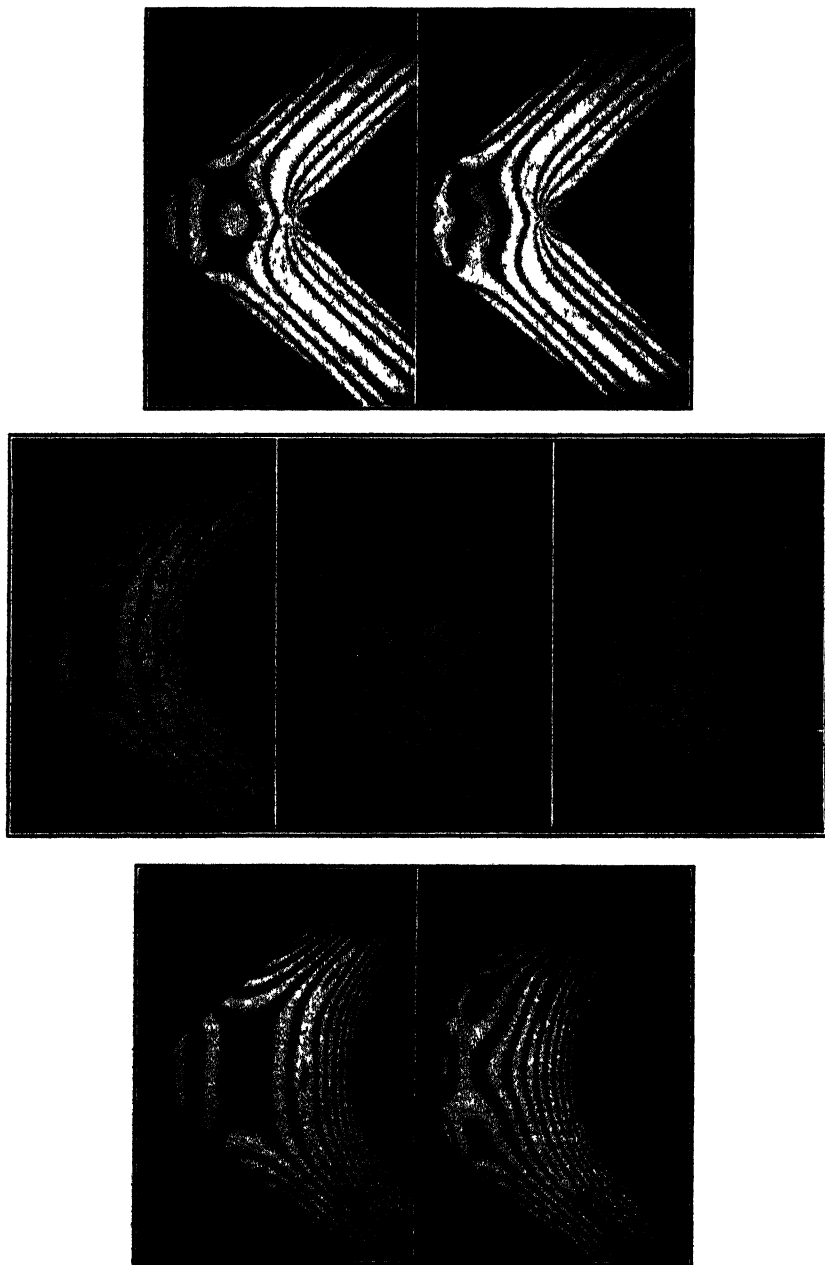


FIG. 83.—Fringe Photographs of Bakelite Knee Frame Models
Courtesy of University of Illinois Engineering Experiment Station

primarily for use in the study of time yield effects in concrete upon a rigid-frame bridge. It was also tested, however, for certain elastic constants, such as the reaction components, M , H and V , at each base due to a horizontal displacement of 0.10 in., without any settlement or rotation. Components were also determined for a settlement of 0.10 in. and then for a rotation of 0.001 radian. These

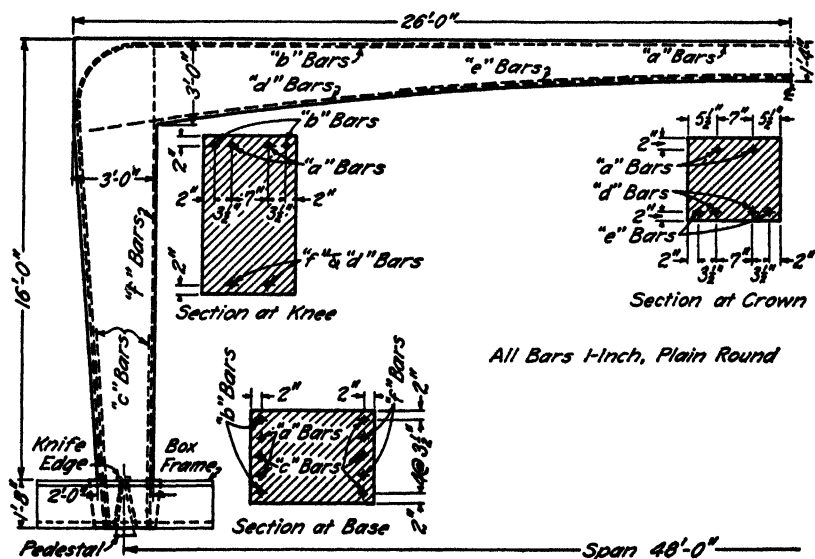


FIG. 84.—Details of Rigid-Frame Bridge

Courtesy of University of Illinois Engineering Experiment Station

tests were made because similar tests for Specimen 1 produced values having considerable variation, particularly in the moment at the base in the fixed structure. In both specimens, however, experimental values of M , H and V due to arbitrary displacements or rotations differed materially from values calculated by the elastic theory. A small microscopic crack near the base was subsequently detected near the base of one leg of Specimen 2. Further tests and studies indicated that cracks, too small to be detected with the naked eye, will affect the elastic behavior of reinforced-

concrete structures such as these *when subjected to foundation displacements*. On the other hand, *final moments due to loads* at sections governing the design of the structure were not appreciably affected by cracks.

Influence lines for crown moment calculated by the elastic theory agreed quite closely with those obtained experimentally, both with the structure free to sway and with sway prevented. There was also good agreement at the knee when the structure was free to sway. With sway prevented, however, maximum influence ordinates determined experimentally for moment at the knee are approximately 50 per cent greater than when sway is allowed. In a symmetrical structure this would not change dead-load moments but might increase live-load moments appreciably. However, it takes only a very small sway, 0.01 to 0.02 in., to reduce the moment to that corresponding to the free condition.

Design loads corresponding to the axle loads, including impact, of a 20-ton truck distributed over a 9-ft. width of roadway were subsequently placed on Specimen 1. The larger load was applied at the center of the span and the smaller one 14 ft. from the center. The moment at the crown obtained with the bases hinged was 15 per cent less than that calculated by the elastic theory. When the bases were fixed, the actual value was 14 per cent less than the theoretical value. These differences, though not very large, may seem somewhat puzzling, in view of the fairly good agreement obtained for the influence lines. It must be kept in mind, however, that the reactions due to a 20-ton truck load acting upon a statically indeterminate, reinforced-concrete structure may not be exact multiples of the reactions caused by unit loads acting upon the structure in the same positions. The influence lines were computed, of course, from the effects of unit loads. Moreover, the final crown moment is obtained by getting a difference of values. A small error in one of the values consequently results in a

much larger error in the final answer. For the hinged bent, the following equation expresses the crown moment:

$$M_c = M_s - Hy_c,$$

where M_c is the final moment at the crown, M_s is the "simple-span" moment at the same point, H is the horizontal thrust, and y_c is the ordinate to the crown. An error of 1 per cent in H may result in an error of 15 per cent, or even more, in the value for M_c , depending upon the relative magnitude of the two terms on the right-hand side of the equation.

At the knee, with bases hinged, the design loads gave a moment 3 per cent greater than that from the elastic theory. When the bases were fixed the values coincided.

Finally, Specimen 1 was loaded to destruction, by adding increments of load corresponding to design live loads. Five live loads and a fraction had been placed when the structure failed abruptly in shear near the quarter point at a section where the moment was very small. There was no evidence of impending failure at the sharp re-entrant corner at the knee, even though tension cracks beginning at the outside surface extended to within 3.5 in. of the inside face.

Specimen 2 was also finally tested to destruction, but not until it had been subjected to time yield tests. The effect of temperature was studied over a period of 462 days. The tests indicated that time yield or plastic flow in the concrete reduces temperature stresses somewhat during the first two or three years, but that the amount of reduction gradually decreases as the structure becomes older. The effect of gradual spreading of the bases was also studied. The span subject to the design live load was increased by increments of $\frac{1}{4}$ in. with 7-day intervals between increments until a total spread of 4 in. was recorded. Again, it was noted that time yield appreciably reduced the stresses caused immediately after each displacement of the bases.

The span length was then maintained at a value 4 in.

greater than normal, while the structure was tested to failure. In spite of the severe initial punishment, the frame carried a maximum of five live loads. Failure, when it occurred, was due to steel at the knees being stressed beyond the yield point. The resulting yielding enhanced the deflection at the crown where the steel had also passed the yield point. The failure was not abrupt like that of Specimen 1, thus demonstrating the value of the shear reinforcement in giving a tougher structure.

Of interest are the recommendations relative to design appearing at the end of *Bulletin* 308, Part II, of the University of Illinois Investigation. They are quoted here in full.

(1) An analysis of a reinforced concrete rigid frame bridge by the elastic theory gives values for the moment, thrust, and shear on any section which are accurate enough for purposes of design if the analysis is based on the following assumptions:

(a) The stress-strain relation for the concrete has the same value at all sections and at all stresses.

(b) The moment of inertia is for an uncracked section.

(2) The variations in the modulus of elasticity of the concrete that may be expected in a field structure will not have an appreciable effect upon the stresses due to loads.

(3) Restraining the deck of a rigid frame bridge so as to prevent longitudinal sway due to eccentric loads on the deck does not increase the maximum live-load moment at the crown, but does increase the live-load moment at the knee somewhat. But, since the dead load causes no sway and the dead-load moment at the knee is greater than the live-load moment, the resultant moment is not greatly affected. Provision should be made to prevent the structure from being subjected to an active longitudinal horizontal force at the end of the deck due to an expanding road slab or other similar cause.

(4) For a rigid frame bridge of the type tested, a flexural failure at the knee will cause the structure to collapse; a flexural failure at the crown may injure the roadway, but so long as the deck retains its ability to resist shear and thrust, the structure will not collapse nor will the moment be greatly affected at other sections; a flexural failure at the base will not appreciably affect the moment due to load at other sections, nor will it cause the structure to collapse if the base retains its capacity to resist shear and thrust; a small increase in thickness at the knee will

result in a considerable increase in the flexural strength of the knee. For these reasons an approximate determination of the moments at the crown and bases is satisfactory for purposes of design, but it is highly desirable to make ample provisions to resist the shear at these points. Because the moment at the knee is affected by the restraint against sway and is therefore somewhat uncertain, because extra flexural strength of the knee can be obtained with so little cost, and because a flexural failure of the knee is so serious, it is good engineering sense to design the knee for a moment somewhat greater than the moment computed by the elastic theory for structures free to sway.

(5) Variation in the angular restraint of the bases does not appreciably affect the resultant moments (resultant of the dead-load, live-load, temperature, and shrinkage moments) at the knee and crown. But because, for a structure of a given height, the moments at the bases due to shrinkage and temperature changes increase with the span and become excessive for long spans, hinged bases are definitely advantageous for long spans and are not disadvantageous, except possibly for cost, for short spans,

(6) Shear reinforcement added to the tenacity of the reinforced concrete rigid frame bridges tested, thereby increasing the deformation to which they could be subjected without failure.

(7) Deformation stresses of considerable magnitude have no great effect upon the load-carrying capacity of a concrete member properly reinforced for longitudinal and shearing stresses.

Photoelastic Analysis of Stress States.—The photoelastic method of stress analysis is now definitely recognized as a useful aid in securing valuable information about stress states at sections of a structure not susceptible of pure mathematical analysis. Briefly, the method consists of passing polarized light through loaded transparent models of structural units, and then scanning or taking pictures of the resulting image in order to evaluate the bands or fringes in terms of definite stress intensities. If a white light source is used, the fringes are colored red, green, yellow, etc. If a monochromatic light source is used, the fringes will be alternately black and white. Each fringe is proportional to the difference of principal stresses. The optical phenomenon of double refraction constitutes the fundamental basis for the procedure.

The method may be explained briefly by referring to Fig. 85, which illustrates the optical train in the Photoelastic Laboratory of the College of Engineering of New York University.

Unit 1 is the light source, here a mercury lamp. The light is passed through a filter making it monochromatic. The light, after being passed through lenses which are incor-



FIG. 85.—Photoelastic Laboratory at New York University

porated in unit 1 to make the emerging rays parallel, strikes the polarizing lens, unit 2 in the train. Before striking the lens, the rays are vibrating in all planes. After passing through the polarizer, however, they vibrate only in one plane, corresponding to the principal axis of the lens. The path of vibration or displacement is commonly portrayed as a sine curve. The plane-polarized beams of light then encounter the loaded, transparent model which is set up in the loading frame, unit 3. The model is usually made from

polished Bakelite and has the outline of the particular structural unit to be analyzed. In Fig. 85, a model of a rigid-frame bridge may be discerned. Loading frames of various types are used. This particular frame is a universal frame adaptable to a variety of loading conditions.

When a polarized beam of light strikes a point of the model under stress, the beam is resolved into two components vibrating in planes perpendicular to one another and coinciding with the directions of the two principal stresses existing at the point. The rays are retarded in passing through the model, and the relative retardation is expressed by the equation:

$$R = k(P - Q),$$

where k is an optical constant depending upon the thickness and kind of material used for the model, and P and Q are the principal stresses at the point. When P and Q have different values, the two rays emerge out of phase. The rays then pass through the analyzer, unit 4 in the optical train, whose principal axis is set at 90° to that of the polarizer. Components of the two rays parallel to this axis are passed, and they emerge, vibrating in one plane, but still out of phase. This phase difference causes an interference which manifests itself in bands of different colors, or in alternate light and dark bands, which are directly proportional to $P - Q$. Continuous dark bands or areas connect points of equal values of $P - Q$.

Unit 5 is a projection lens assembly for focusing the image on the ground-glass plate of unit 6, a camera without a lens. Unit 6 may be replaced by a screen upon which a large image may be projected for demonstration or lecture purposes.

A single continuous fringe, see Fig. 86, connects points which have the same value for the difference of principal stresses. The fringe is consequently called an "isochromatic." Since, in a two-dimensional stress system, the

maximum shearing stress is equal to one-half the difference of principal stresses, isochromatics are also loci of maximum shearing-stress intensities.

When a model is loaded gradually, a succession of fringes will be formed or will pass through a particular point or region under observation. The fringes, or dark bands, are counted in order of occurrence and are termed first order, second order, third order, etc. Each order corresponds to a definite value of the difference, $P - Q$ such as 350 lb. per sq. in. Hence, if five fringes or orders have passed a certain point, the value of $P - Q$ for that point is 1750 lb. per

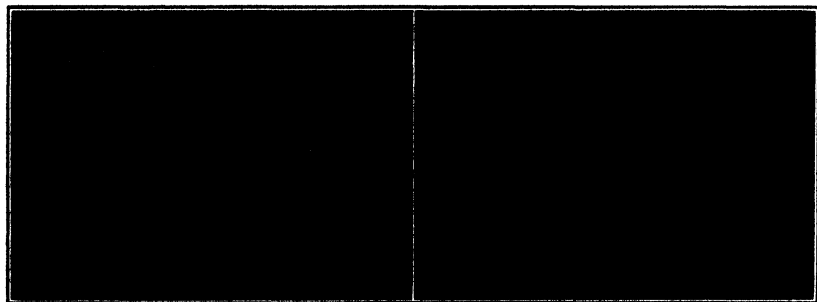


FIG. 86.—Fringe photographs of Rigid-Frame Bridge Models. Half of model with sharp corner shown on the left; half of model with filleted corner shown on the right

sq. in. If the point is located on a free boundary, the actual stress is 1750 lb. per sq. in., because then Q or one of the principal stresses is 0.

In many engineering problems, only the edge or boundary stresses are wanted. These may be quickly determined, since usually one principal stress is zero or has a relatively small value. Interior stresses are more difficult to obtain, inasmuch as the photoelastic method gives $P - Q$, the difference of principal stresses. In order to obtain separate values for P and Q , it is necessary to find $P + Q$ and then solve the two equations simultaneously. Although a number of methods are available for getting $P + Q$, they will not be described here. Suffice it to say, none of them is

absolutely satisfactory. They require the exercise of extreme care in order to achieve accurate results.

The preceding discussion has brought out the significance of fringes or "isochromatics." It may be noted that the dark bands are formed by the complete extinguishing of light at a series of points. This occurs when the relative retardation is an integral number of wave lengths of the light used. But other black bands will also appear which are not isochromatics. They are due to the fact that the directions of the principal stresses at some points coincide with the directions of the principal axes of the polarizer lens and the analyzer lens. The light is extinguished then, because the analyzer cannot pass components of a beam which meets it in a plane at 90° to its axis. These dark spots are called "isoclinics" because all points covered by these dark areas have the same directions for principal stresses.

In order to avoid confusion in distinguishing between "isochromatics" and "isoclinics," two quarter wave plates are added to the optical train. One of these may be seen in Fig. 85 attached to the polarizer unit. The other is mounted on the analyzer unit. The picture shows them swung out of line. When placed in line, they remove the isoclinics or directional effects completely. A thorough analysis of a stress state requires the evaluation of isochromatics for a definite loading; the determination of directions of principal stresses at all points by plotting isoclinics for different orientations of the axes of the polarizer and analyzer, keeping them, however, always at 90° to one another; and then the determination of the value of $P + Q$ at all points by one of several possible methods. The separate values of the principal stresses may then be calculated.

Figure 86 shows fringe photographs of two rigid-frame bridge models made in the Photoelastic Laboratory at New York University with the aid of Geo. B. Stevens, graduate assistant in civil engineering. One has a sharp, re-entrant

corner at the knee, and the other has a filleted inner corner. Two concentrated loads, symmetrical about the center line, were applied to the models. Stresses along the inner and outer surfaces of each model are plotted in Fig. 87. The maximum compressive stress in model 1 is at least 3180 lb. per sq. in. at the re-entrant corner. The fringes were so

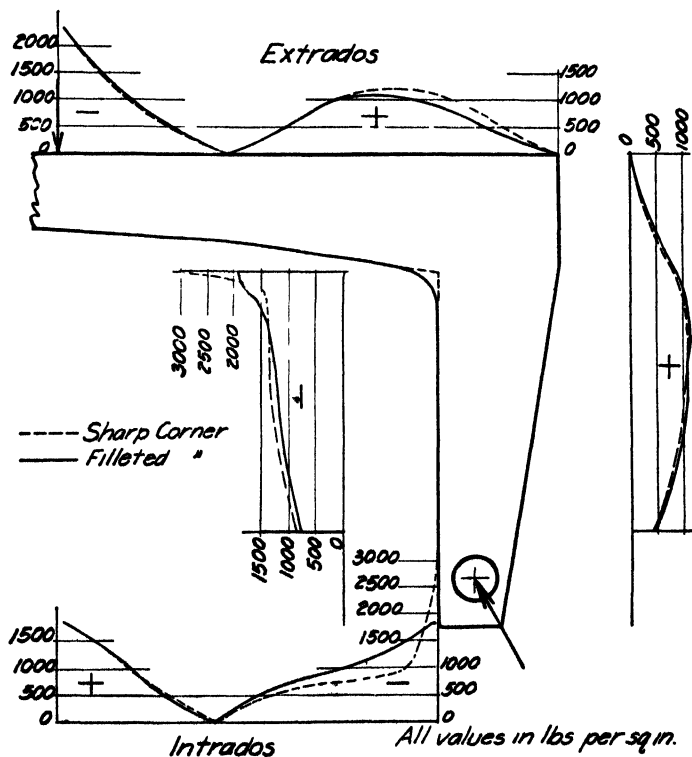


FIG. 87.—Edge Stresses in Rigid-Frame Bridge Models

close together that it was impossible to count them accurately. The maximum stress in model 2 is 1850 lb. per sq. in. This tends to illustrate the effect of the fillet. It must be kept in mind, however, that practical considerations make the square corner preferable in an actual reinforced-concrete or steel bridge.

National Bureau of Standards Tests.—In cooperation with the American Institute of Steel Construction, a number

of tests on steel knee frames were made by the National Bureau of Standards at the Washington Laboratory. The tests were made primarily to determine stress states in the flanges and web at the knee for working loads. Subsequently, the frames were loaded to destruction in order to determine failure characteristics and give more information on comparative behavior of different types of rigid knees. Detailed discussions of the tests may be found in *Research Papers* RP 1130, RP 1161, and RP 1224, National Bureau of Standards.

Three full-size specimens were tested. Specimen 1 is pictured in Fig. 88. It is a fabricated girder with a sharp re-entrant corner at the knee. Each flange consists of 2 angles 6 in. by 6 in. by $\frac{3}{8}$ in. The web plate is $\frac{3}{8}$ in. thick. The depth at the section adjacent to the knee is 3 ft. $4\frac{1}{2}$ in. There were stiffeners at the knee in line with the flange angles, but no diagonal stiffeners were used. Reinforcing plates were bolted to the outside corner, and tests were made with and without the plates.

Specimen 2 was also a fabricated girder, but instead of a sharp inside corner a curved flange of large radius was used. Flanges consisted of 2 angles 4 in. by 4 in. by $\frac{1}{2}$ in. The web plate was also $\frac{3}{8}$ in. thick. Crimped, bolted, radial stiffeners at the corner were used at first and then removed in a subsequent test. The outside corner was initially reinforced with a bent plate and clip angles, which were also removed in a subsequent test.

Specimen 3 was a welded girder frame with a sharp, re-entrant corner at the knee. Figure 89 illustrates both the manner of testing and the details of the frame. The flanges are 10 in. wide and $\frac{3}{4}$ in. thick. The web is $\frac{3}{8}$ in. thick, except at the ends of the legs under the loading shoes, where it was made $\frac{5}{8}$ in. thick. A diagonal stiffener was welded across the corner. The legs of specimen 3 were approximately 11 ft. long, those of specimen 2 approximately 10 ft., and those of specimen 1 about 12 ft. in length. Depths at the knee also

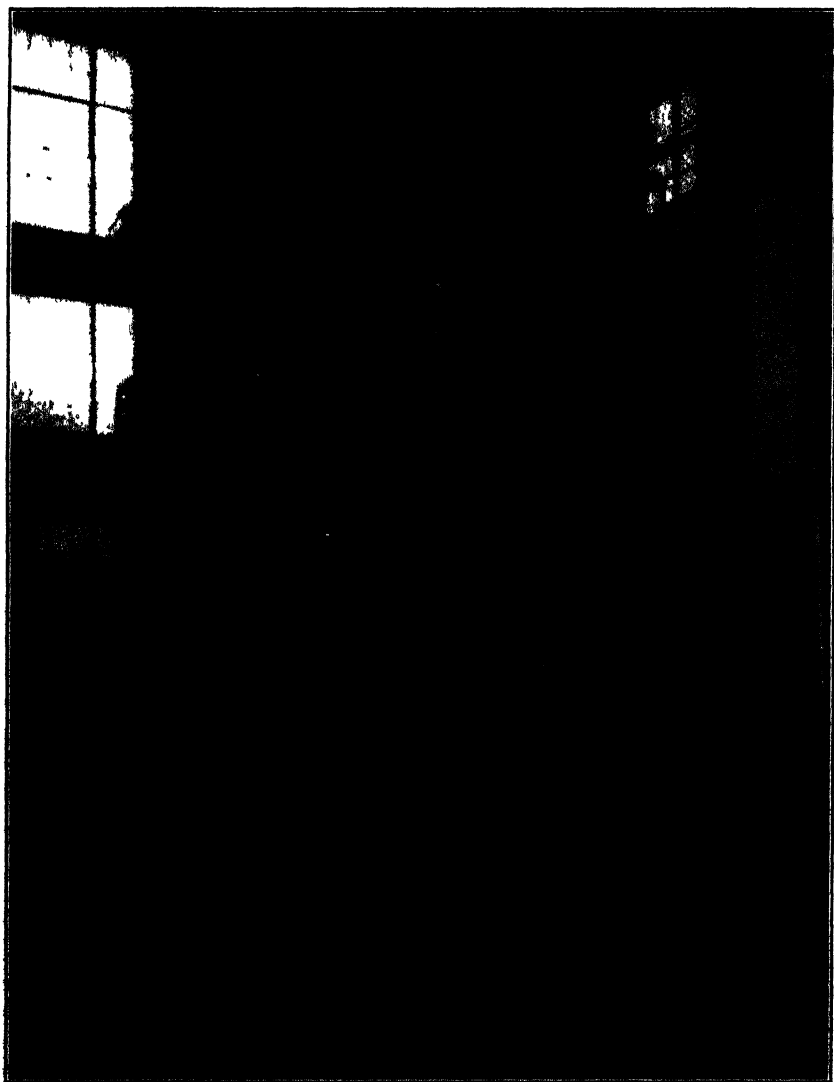


FIG. 88.—Riveted Knee Frame in Testing Square with Line
Courtesy of F. H. Frankland, Chief Engineer, American Institute of
Steel Construction

differed in each specimen; hence, they are not directly comparable.

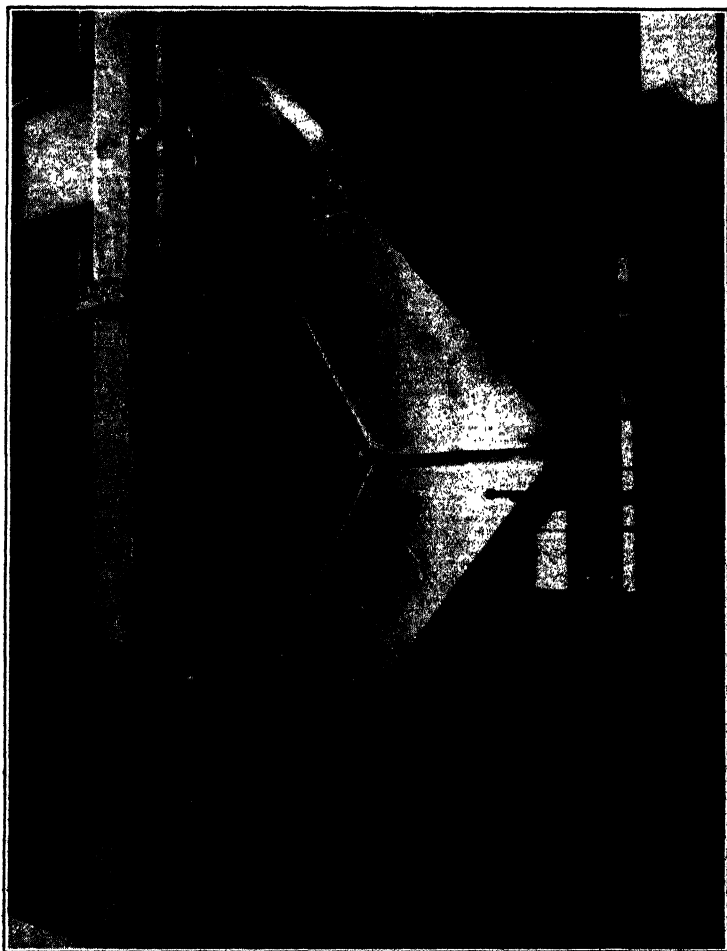


FIG. 89.—Welded Knee Frame under Test

Courtesy of F. H. Frankland, Chief Engineer, American Institute of Steel Construction

Numerous strain gage readings were taken on each specimen. Rosette patterns, each consisting of four intersecting gage lines 2 in. long, inclined at 45° to each other, were spotted at many points on the web at the knee and at

sections near the knee. See Fig. 88. Strain readings were also taken at different points on the flanges. Principal stresses and their directions were then computed from the measured strains. In every specimen, diagonal compression stresses in the web at the knee were relatively low. Maximum compression stresses in the flange at the re-entrant corner in specimen 1 were not excessive, in general being less than computed values. For the test load of 75 kips, which was 10 per cent higher than the design load calculated to produce a maximum compressive stress of 18,000 lb. per sq. in., the data indicate an actual stress slightly more than 18,000 lb. per sq. in. in the inner flange at the knee. Stresses in the compression flange of specimen 2, the filleted specimen, also seemed to be lower than computed values. In the welded specimen, compression stresses at the re-entrant corner seemed to be slightly greater than the computed values. In every specimen, stresses at the outside corner of the knee were quite small.

The three specimens were finally loaded to failure. The design loads corresponding to a calculated compression stress of 18,000 lb. per sq. in. and the ultimate loads are shown in the following table:

TABLE I

Specimen	Design Load, lb.	Maximum Load, lb.
1	67,900	168,000
2	56,800	72,000
3	73,800	153,600

Failure occurred in every specimen by sidewise deflection of the inside corner accompanied by buckling of the compression flange at the knee. There was also some buckling of the web in specimen 3. Table I indicates that the filleted specimen was the weakest. Relative performance, however, cannot be based on the data in Table I. It must be remem-

bered that the width of flange for specimen 1 was $12\frac{3}{8}$ in., and that for specimen 3 was 10 in., whereas for specimen 2, the filleted specimen, it was only $8\frac{3}{8}$ in. The specimens were not designed to have the same buckling resistance.

The tests indicate that knee details, like that of specimen 1, which are preferable from a fabricating standpoint, are also satisfactory from a structural viewpoint. A rectangular knee section, stiffened along the sides, did not develop any weakness. Moreover, it was shown that diagonal or radial stiffeners were not necessary. It is not good engineering, however, to generalize on the basis of these few tests. It must be kept in mind that the knee sections tested were not deep sections. Small strain readings do not always indicate absence of danger. In buckling failure, a slight increase of load may cause large deformations. Long-span girders with deep sections may need intermediate stiffeners in addition to stiffeners along the sides of the rectangular area at the knee. On the other hand, the behavior of specimen 1 gives confidence in the use of that type for girders not having radically different proportions.

Lehigh University Tests.—Two riveted-steel rigid frames were tested in 1938 at Lehigh University by Inge Lyse and W. E. Black in cooperation with the American Institute of Steel Construction. One of the frames was fabricated with knee sections approximately square and with sharp re-entrant angles at the inside corners; the second was constructed with curved inner fillets and straight outside flanges. Both frames were tested as two-hinged structures, chiefly to determine whether the stress states in the corners were similar to those obtained in the knee frames tested at the Bureau of Standards in Washington. Slippage of foundations and accuracy of the conventional theory of analysis and design were also investigated.

The frames were considered to be one-quarter-size models of imaginary prototypes with 72-ft. spans. Frame 1 had a

span of 18 ft. 8½ in., center to center of pins, and a rise of 6 ft. ½ in. to the center of the crown section. Frame 2 had a span of 18 ft. 7½ in. and a rise of 6 ft. The top member of frame 1 was constructed with a depth which varied from 6 in. at the crown to 15½ in. at the knee. The legs varied in width from 8½ in. at the base to 15½ in. at the knee. The top member of frame 2 had a constant depth of 6 in. from the crown to the knee section. The legs had a width of 7½ in. The depth at the knee section was variable, owing to the inner flange being curved to a radius of 2 ft. 3 in. In both frames, a web plate 5/32 in. thick was used. Each flange of frame 1 consisted of two angles 2 in. by 2 in. by 3/16 in., whereas in frame 2, each flange had two angles 2 in. by 2 in. by ¼ in. No special reinforcing, such as stiffeners or a thickened web plate, was provided at the knees in either frame.

Each frame was loaded at 2 points, 5 ft. 4 in. apart, and symmetrical with respect to the center of the span. Measurements were taken with an initial total load of 1000 lb. and with a final load of 13,000 lb. The differences consequently gave values corresponding to a total working load of 12,000 lb. Strains at a number of points on the web plate at the knee were measured with Huggenberger tensometers having 1-in. gauge lengths. Three-line strain rosettes were used. Strains on the surface of the flange angles, both at the heel and at the toe of each angle, were also observed. Most of the measurements were taken in the region at the knee, but flange strains at mid-span and various other points were also observed in order to permit a complete study of the behavior of the models. Stress states were then calculated, plotted and compared with computed stresses. Theoretical values in the web plate at the square knee were determined by the method of analysis developed at the Bureau of Standards.*

* "Strength of a Riveted Steel Rigid Frame Having Straight Flanges," by A. H. Stang, Martin Greenspan, and W. R. Osgood. *Journal of Research of the National Bureau of Standards*, Vol. 21, September 1938, p. 294.

Values determined experimentally were in general agreement with theoretical values. The maximum shear in the web of the square knee did not exceed 10,000 lb. per sq. in., for loads which gave a maximum compression stress of 24,000 lb. per sq. in. in the flange of the girder adjacent to the re-entrant corner. The compression stress in the flange of the column adjacent to the inner corner was 17,000 lb. per sq. in. The diagonal compression in the center of the web at the knee was also less than 10,000 lb. per sq. in. At the re-entrant corner, diagonal compression stresses were about 14,000 lb. per sq. in., but this was in a region of lateral support.

Stresses in the web plate of the frame having a curved fillet were also low. The maximum diagonal compression stress was approximately 10,000 lb. per sq. in. On the other hand, the compression stress in the flange angles at the knee was high, amounting to 27,000 lb. per sq. in. at a section near the beginning of the corner fillet. It is interesting to note that there was considerable difference between the stresses at the toe and at the heel of the angles. The preceding value of 27,000 lb. per sq. in. occurred at the heel of the angle. The corresponding stress in the toe at the same section was slightly more than 16,000 lb. per sq. in., thus indicating a decided variation in stress over the cross-section of the flange. There was a tendency for the outstanding legs of the curved flange angles to deflect inward, as the result of the radial component of compression caused by the curvature. This local yielding undoubtedly contributed to the stress concentration at the heel. Radial stiffeners milled to bear on the flange, or cover plates on the curved flange, might cause a different stress distribution. This matter was not investigated, however, in these tests.

The stress concentrations which developed at the sharp re-entrant angle of the square knee were, in the opinion of the investigators, due principally to imperfect bearing at the intersection of the compression flanges. It was found

that tight bearing did not exist in the frames as fabricated. There were small gaps at the ends of the flange angles, which were filled with shims tack-welded in place. This produced tight bearing only along the outstanding legs of the girder flange angles.

One interesting recommendation of the investigators relative to design of square knee-frames is as follows: "The horizontal and vertical sections through the inside corner of the knee are critical sections with respect to normal stresses. Apply the usual formula for flexure and direct stress to the horizontal section. On the vertical section, assume that the flange angles carry all the moment and thrust in the girder."

The last sentence of this recommendation reflects the type of fabrication of the test specimen. The vertical section was the one along which the splice was made between the top girder and the column leg. No definite web splice was provided at this section. If a definite web splice is provided in actual design, the web will undoubtedly assist the flange angles in carrying part of the moment and thrust.

The investigators also recommended that the web at the knee be designed to take a total horizontal shear equal to the tension in the top flange of the girder. In other words, the horizontal area along the top of the web at the knee, and likewise the number of rivets connecting the web to the flange, must be sufficient to develop the tensile strength of the flange where it intersects a vertical section through the inside corner of the knee.

In the curved knee, the investigators recommended that a square piece of the web above the neutral axis of the corner be investigated. Two sides of this square would coincide with the outside flange angles. The inside corner of the square would be defined by a point located one-quarter of the distance from the inside flange along the radial diagonal through the external corner of the knee. It was recommended that the square piece be investigated for the boundary forces introduced by the outside tension flanges

and by the bending and shearing forces along the inside edges.

It was found, as might be expected, that normal stresses upon radial sections of the curved knee did not exhibit a linear relationship. The neutral axis did not coincide with the centroidal axis, but was close to the curved compression flange. In the specimen tested, it was about one-fourth of the distance from the compression flange to the exterior corner along a radial diagonal section. Experimental values for compressive stresses in the curved flange were generally higher than computed values. The investigators recommend a method of reducing section moduli and moments of inertia within the curved knee in order to produce better agreement. The method is not included here because, on the basis of this one test, its general applicability is questionable.

Designers of rigid frames have wanted to know more about the uncertain stress states at the knees. They have also been interested, however, in the validity of the conventional methods of analysis for determining redundant reactions. In the two specimens tested, it was found that good agreement existed between horizontal reactions computed by conventional methods of analysis and those determined experimentally for both the square and the curved knee frame.

The preliminary report of the Lehigh University tests was kindly furnished to the writer by Mr. F. H. Frankland, Chief Engineer of the American Institute of Steel Construction.

CHAPTER XV

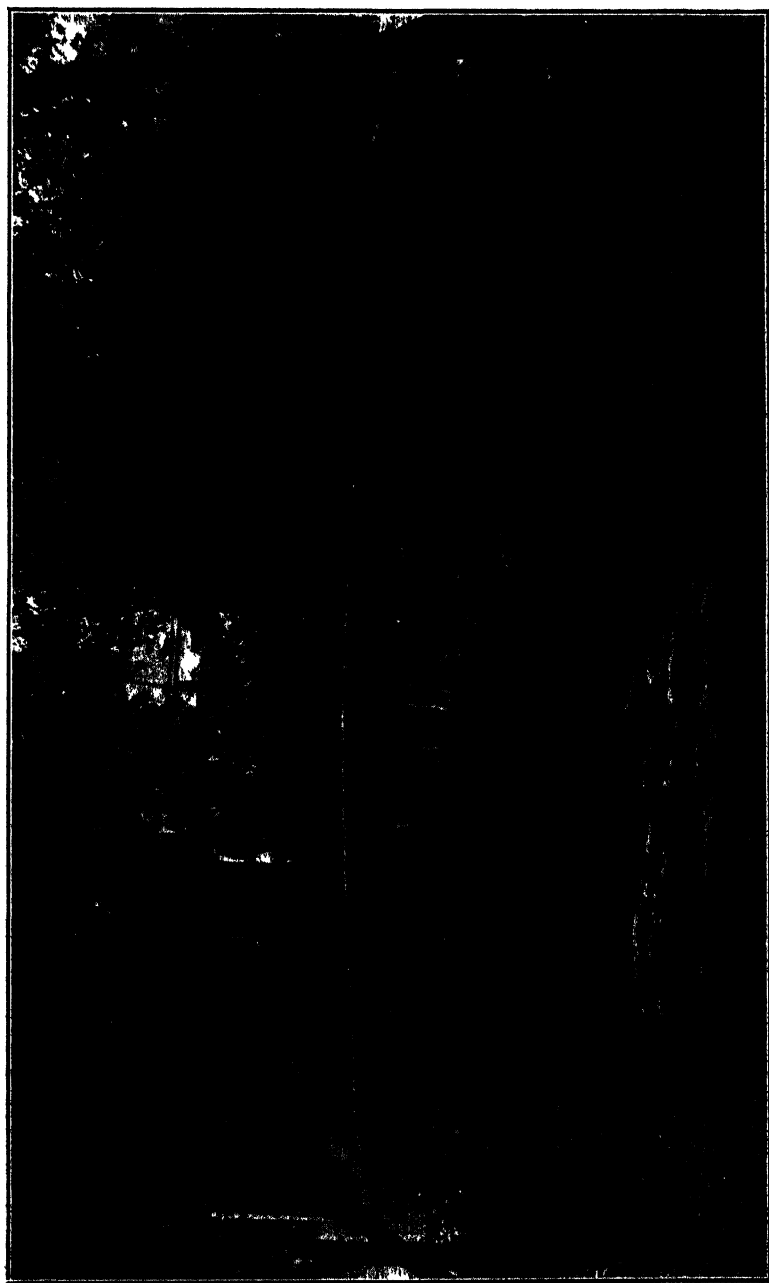
THE ARCHITECTURE OF SHORT-SPAN BRIDGES

By GILMORE D. CLARKE

Fellow, American Society of Landscape Architects
Landscape Architect, Westchester County Park Commission

The development of bridge construction constitutes an important element in the extension of communication and transportation and has been, from its earliest inception, one of the most important factors in human progress and the spread of civilization. Among the earlier civilizations, the Chinese evolved arch forms embodying a distinctively picturesque architectural treatment, but with no thought of adaptability for wheeled traffic. Later, and doubtless after the lapse of centuries, the Romans effectively developed the arch principle and extended its application to multiple arches supporting roadways and aqueducts, some of which still stand as monuments of skillful architectural and engineering design. The Greeks contributed practically nothing to the art of bridge building because their largest unit of construction was the stone or timber lintel with inherent limitations of span. The bridges built in Europe during the Middle Ages, particularly by peoples having old established governments and cultures, were characterized by distinctive architectural treatment.

Bridge building in America, on the other hand, has just as naturally reflected the pioneer conditions of life in the youngest of the great nations, engrossed, during its first century of growth, in conquering the wilderness and employing strictly utilitarian necessities for developing lines of communication and natural resources. With the progress



Bronx River Parkway Bridge at Tuckahoe, N. Y.—Westchester County Park System

that has now been made in such development and the resulting accumulation of wealth, there is developing the trend, characteristic of the growth of all civilized nations, toward a higher culture and more wholesome artistic standard for public works. The time has arrived when serious attention must be given to bridges as one of the most essential and important classifications of such works.

The problem before us today is to be able to build bridges which will endure, employing modern methods and materials, and at the same time giving them charm and beauty. This does not mean that we should attempt merely to imitate the designs of old bridges; we should rather build structures having individual architectural beauty, appropriate to their environment and to the materials used, instead of types that are purely utilitarian. Bridges designed with beauty of line and mass and having simplicity and refinement of detail will endure longer than structures lacking artistic conception.

“If you get simple beauty, and naught else,
You get about the best thing God invents.”

Robert Browning.

In all architectural study, we must go back to the beginning and study the art of the past, that we may, by seeing what has been done, profit by both good and bad examples. After all, ancient masonry bridges from a structural standpoint are not radically different from modern bridges of the same type. The only difference between the modern arch of reinforced concrete and the ancient arch of stone is that the modern structure may be constructed more economically, is less limited by restrictions, and may reach much longer spans than stone arches. The test of time will doubtless prove that concrete is no better than stone, in fact it may not be as long-lived, but we are forced to use it for the sake of economy in construction.

Bridges have played an important part in history and

have often been the center in battles, at one time defended, at another destroyed to prevent the advance of the enemy. As a result, many of the old structures have been either entirely destroyed or remain standing in part, serving no purpose save as reminders of the grim events of the past. Probably the most famous of these old bridges is the Pont St. Benezet over the River Rhone at Avignon, built by St. Benezet between the years 1177 and 1185. This magnificent old structure occupies the site of an old Roman bridge and some of the stone used may have been part of the older structure. The Pont St. Benezet no longer reaches across the Rhone since all but four arches and the tomb of the friar architect, St. Benezet, have been destroyed. The chapel has withstood the ravages of flood and battle, although a number of the arches were destroyed, rebuilt, and destroyed a second time. The bridge originally consisted of 21 arches, not built straight across the river, but pointed "V" shape up stream to resist floods and to serve as a more favorable means of protection against attacks of enemy infantry and cavalry.

Bridges are not only a measure of the historical development of peoples, but of their artistic development as well. They are among the oldest existing structures built by man and many remain as monuments to the engineering and artistic development of departed races. The ancient aqueduct, the Pont du Gard, which crosses the valley of the Gard near Remoulins, France, built by the Romans about 19 A.D. stands today the most famous and handsome of Roman monuments, a stirring tribute to the engineering and artistic genius of a race of builders. The fortified Pont Valentre over the River Lot at Cahors, a twelfth century French masterpiece, is one of the most interesting of the older bridges; the Puente de Alcantara at Toledo, Spain, is notable among fortified bridges. Originally Roman, it was rebuilt in the thirteenth and again in the seventeenth centuries. Bridges and rivers were inseparable and were

dominating influences upon towns and cities. When we think of Rome and the Tiber we remember the venerable old bridges which span that historic stream; Venice brings to mind the "Canale" and the Rialto; Florence gives us the Arno and the Ponte Vecchio; and so on.

Let us consider Paris, a city divided by the river Seine, where there exists today an almost complete historical and technical exhibit of the gradual development of bridge construction. The Seine is not a wide stream and there was every inducement to build many structures to provide for communication between the two parts of the city. There probably does not exist in any city of the world a group of bridges having the combined artistic merit of the 32 bridges which make the 24 crossings of the Seine within the city of Paris. It is doubtful if an ugly bridge would have stood the test of time; as a matter of fact it is believed that at least two-multiple-span suspension bridges, so common in France, were erected over the Seine and later replaced by arched bridges, torn down doubtless because they did not possess the artistic merit indicative of the French capital. It is of peculiar interest to note that "until the end of the 18th century all masonry bridges in Paris were built with semi-circular arches; from 1787 to 1852 all had segmented arches, and after that time, beginning with the new Pont Notre Dame, all had elliptical arches."*

In old bridges, little importance was given to the clearance under the structure, or "free-way" as it was called. The Romans built as many piers as were necessary to provide for semi-circular arches without consideration of the use of the waterway, often giving little thought to flood requirements. Restriction of the free-way in many old bridges resulted in washing away piers or in the undermining of abutments. To provide more free-way the "Corne de Vache" and openings in the abutments and

* "Bridges of Paris," Carl L. Rimmel, "The Military Engineer."

piers were resorted to. Later the flatter arch, both elliptical and segmental, were developed, the most daring design being the series of long flat segmental arches in Perronet's Pont de la Concord in Paris. Commerce demanded still more river-way and the next development in bridge design was the use of iron. The iron bridge was adaptable for use on longer spans than was possible with the stone arch and with the rapid expansion of civilization steel bridges were fabricated by the thousands without regard for appearance. The result is what we find throughout the length and breadth of the United States today, thousands of ugly beam, truss, and cantilever bridges over rivers, highways and railroads, which in time must be replaced, not entirely because of the effects of deterioration, but because people require something to satisfy their growing sense of the artistic. For a time it was thought that iron would replace stone even for short-span bridges, but now I feel sure that stone in modern bridges is destined to continue, because of the possibilities of its use in conjunction with reinforced concrete and with steel and iron.

Engineers have often pointed out that many, in fact most, of the old bridges were designed and built by engineers without the aid of architects. The designers, however, were both engineer and architect in one. When the old bridges were built, the science of engineering had not developed to the extent that it has today. "The balancing of the arch and the founding of its abutments were long practiced before they were reduced to something approaching scientific exactness. A good example of the haphazard method of building was a bridge built at Pont-y-pridd, in South Wales, by William Edwards less than 200 years ago. It was first built as a three-span arch, but soon after its completion was washed away by a flood. The builder then thought it would be better as a single span of 140 ft., although this was a larger span than had been attempted anywhere since the days of the Romans. The shape of

the arch was determined solely by the sweep of a pair of compasses, with the result that in its turn it fell down. The builder could see as it fell that the crown was pushed upwards by the great weight over the haunches. In rebuilding it, he introduced relieving openings to reduce this weight, and on the third occasion the bridge was successfully built. It remains to this day. It was a case where the first bridge failed by lack of knowledge of foundations, and the second bridge by lack of knowledge of the theory of balancing an arch, which is entirely a matter of its shape in relation to the load placed upon it. Finally both errors were corrected by experience gained in their observation, and not by deduction from elements as is the scientific practice of today.”*

The Pont Neuf or New Bridge, the oldest in Paris, begun in 1578 and completed in 1604, was more fortunate in that it was in continuous use until 1848 before the first repairs were made.

“The piers rested on timber platforms, which, although laid directly upon the sand, were, when the bridge was constructed, about three inches below the river bed. In 1885 one of the piers settled to such an extent that longitudinal fissures over a half meter wide appeared in the roadway. Investigation showed that the upstream half of the pier had been undermined, and that, since the construction of the bridge, the bed of the river had been lowered more than three meters so that in some cases it was below the pier footings. The repairs included the rebuilding of half the pier and half the adjoining arches.”†

It appears, therefore, that the bridge builders prior to the beginning of the nineteenth century might have better been called “architects” than “engineers,” since too little attention was paid to the purely structural requirements, although they doubtless utilized all of the available information of their day. In the case of the Pont Neuf,

* “Bridges,” by Sir E. Owen Williams, K. B. E., B. S. C., M. Inst. C. E. Journal of the Royal Institute of British Architects.

† “Bridges of Paris,” Carl L. Rimmel, “The Military Engineer.”

the builders can probably not be held responsible in the same manner as the builder of the bridge at Pont-y-pridd, since the former structure stood for almost 250 years before repairs became necessary.

How are we moderns to design bridges which approach models of perfection in every respect? Scientific research in engineering has taught the use of steel, and of steel and concrete in combination, probably the most economical types of construction for bridges. The exacting methods necessary to design the modern bridge structure require that the engineer devote his entire professional activity to master the science of structural design. The mind of the engineer is trained and disciplined to the working out of difficult computations and formulas. It is not reasonable to expect a mind, trained to the exactness of the engineer's, to possess at the same time a full knowledge and appreciation of those esthetic principles necessary to obtain a pleasing mass, a harmonizing of materials of construction, a continuity or flow of outline, rhythm in expressing several units in a larger mass, and with all, unity and simplicity to express the use for which a structure is intended.

In designing a bridge the best results are doubtless obtained when engineer and architect, each appreciating the limitations of the other, combine efforts to produce a bridge, structurally sound and esthetically pleasing. Few bridges have been constructed within recent years by engineers alone which would not have been more attractive, and not necessarily more expensive, had an architect been consulted as the design progressed. It is neither desirable nor sufficient for an engineer to design a bridge and then pass it on to the architect, who may apply decoration to either cover up structural members, which are neither pleasing nor artistic to the eye, or add decoration which only serves to distract from the structural honesty of the structure. Neither should the reverse order be practiced;

the architect may design a bridge pleasing in every way but not adaptable for good structural design. The ideal way is for engineer and architect to collaborate from the start; the result is more likely to possess those principles of good design which the representatives of both professions are able to contribute together toward a resultant work unified in structural soundness and artistic worth.

There has never been a time when collaboration has been more vital to the development of the works of man. Centuries ago the varied fields of endeavor in the arts and engineering were often accomplished by single practitioners. Michelangelo was an architect, engineer, painter and sculptor. Now each profession is in itself so complex that it is in turn divided into special branches, so that there are engineers who specialize in the design of bridges, or roads, or sewers; architects who specialize in school, or church, or apartment house design; and landscape architects who specialize in estate, or park design, or city planning. This specialization has been brought about by reason of the fact that our lives are short and modern civilization has developed to the extent that one individual must specialize upon one single phase, rather than attempt to master a whole profession, in order to be proficient in a limited but highly specialized field. The result is that we must be more proficient collaborators. This does not mean that one art or one scientific pursuit must be subservient to another, for an architect would never for one moment admit, for example, that the engineer should dominate in the field of house planning. On the other hand, there are collaborative problems in engineering which are unquestionably dominant, and here the architect must willingly recognize that fact. We must all learn to weigh the importance of our contributions, of our competence to contribute to the solution of any given problem. The leadership in a collaborative problem is not an easy one. That question is very often, usually, in fact, settled by the client. He may decide wisely

and he may not. Nevertheless, each collaborator can make as valuable and as generous a contribution whether assuming the dominant position in the scheme or not. Collaboration is dependent upon the collaborators being tactful, reasonable, and respectors of each other's opinions.

Three rules may be given for the guidance of collaborators. These I believe are essential to the success of any enterprise where representatives of more than one profession are involved and if satisfactory results are to be obtained. First, the collaborators must keep each other informed as to the development of each one's plans, since what one does or plans to do may affect the work of the other. Second, each collaborator must keep posted upon what the others are doing or plan to do and must personally assume the entire responsibility for suggestions for the improvement of the plans of the others, merely, however, in the capacity of consultant, whenever this is possible. This is especially true when the work of others relates closely to his own. Third, when one or the other of the collaborators is concerned about any particular phase of the problem which vitally concerns the resultant design, if after discussion and careful consideration they cannot agree, then the difference should be clearly set forth to the client, who will make the final decision.

The vast expansion of our systems of railroads and highways has called for the construction of many bridges, and since the development of structural steel, the large majority are purely utilitarian with no thought given to the esthetic principles of design. The reason for this was the speed and economy which appeared to be necessary and the more or less temporary nature of many of the structures. Practical pioneers in railroading and in highway development were not interested in the appearance of structures so long as they were structurally sound. There were exceptions, of course, but the exceptions were few. As a people, we were satisfied with the many ugly structures on highway

and railroad; but gradually we became sensitive to things out of harmony with nature, things which irritate those who have benefited by contact with the fine arts. The pioneering days of opening up vast new and unexplored regions are over and we are taking time for consideration of the beautiful in our surroundings.

In spite of this new artistic consciousness on the part of the people, many railroad and highway engineers con-

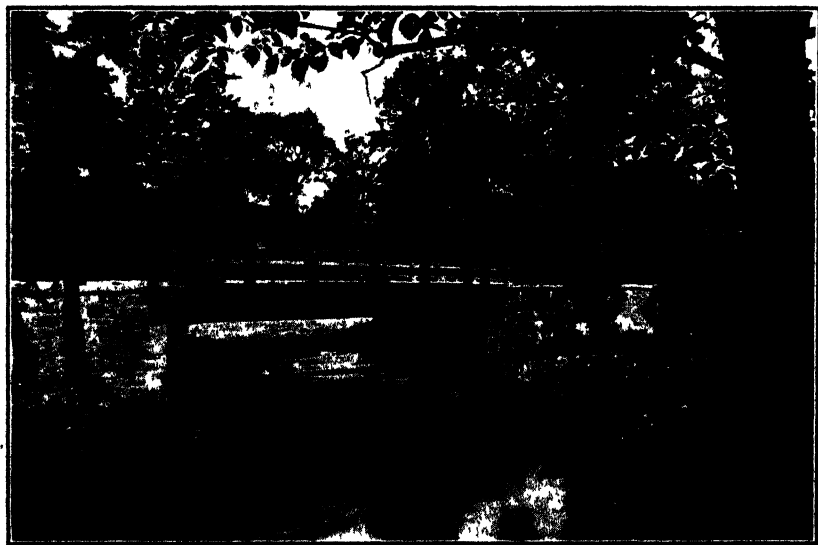


FIG. 1.—Bronx River Parkway Bridge—Westchester County Park System
(Concrete "T" beam construction, timber faced)

tinue to perpetrate upon a tolerant public, monstrosities which offend even the uncultured layman. One notable exception is the Pennsylvania Railroad, which has built many beautiful bridges, probably because artistic structures have become an asset to the railroad business. When wood and stone were the only materials for construction, bridges were, on the whole, most satisfactory in appearance. With the advent of structural steel and reinforced concrete, many ugly utilitarian structures were designed by engineers, principally because it was possible to build

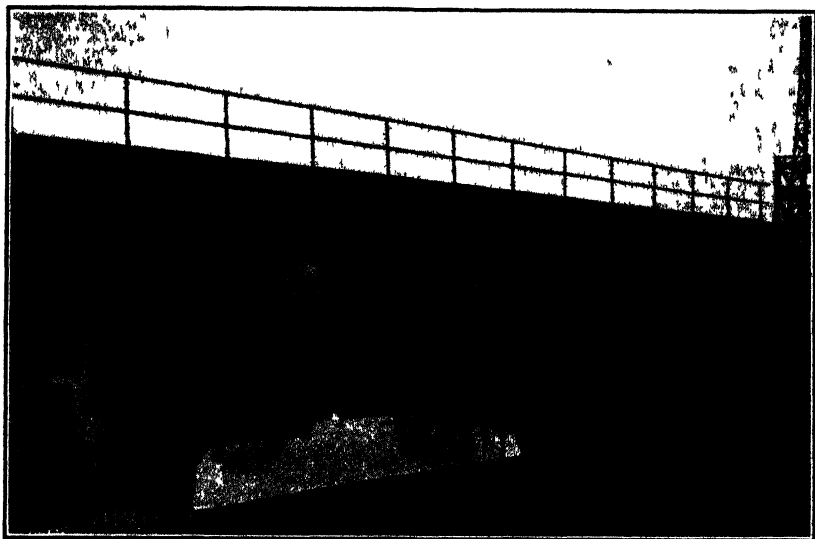


FIG. 2.—Plate Girder Bridge. (Compare with Fig. 1)



FIG. 3.—Reinforced Concrete Slab Bridge. (Compare with Fig. 1)

bridges quickly and cheaply. Only recently has the possibility for the extended use of these materials been worked out with a view toward learning how they may be used artistically. Concrete, steel beam, or girder used without the application of imagination as to their latent possibilities resulted in commonplace, ugly structures. Add the imaginative ideas of the engineer seeking for something better to replace the stereotype designs of the last fifty years and immediately it becomes possible to develop structures having a wide range of possibilities from the standpoint of architectural as well as engineering design without increasing the cost, and in many cases even reducing the cost over the commonplace design. The "rigid-frame" design in both steel and reinforced concrete made possible the development of interesting and beautiful bridges in places where normally the ordinary flat beam or girder bridges would have been used.

It is not intended to leave the impression that steel or reinforced-concrete beam or girder bridges are not subject to satisfactory artistic treatment. On the contrary, it is possible to treat them most satisfactorily and to make them artistic and pleasing, more particularly for relatively short spans and for the smaller structures where, in addition, the wood beam will be continued in use.

Let us now consider a few of the more important principles which should guide designers of bridges:

Fitness and beauty of design must be developed together. For a structure to be fit it must appear strong enough to fulfill the purposes for which it is built and at the same time be simple and honestly portray the materials which go to make it up. We should strive for honesty in design and construction. By that is meant to allow a structure to appear what it is intended to be. For example, concrete looks better, when, in the finished structure, it shows that it was poured. Our so-called "modern" architecture lends itself particularly well to the use of concrete since there are

no wide overhanging mouldings or cornices and the finished product appears as though it came out of a mould. Wood or steel forms are necessary, in most cases, to hold the concrete in the shape it is to have finally. Why not, therefore, permit the marks of these forms to be exposed since they tell the story of the mode of construction? More often these markings look better than a treated surface if the construction of the forms is the subject of careful planning. Many of the bridges illustrated in this volume are of rigid-frame reinforced-concrete construction with stone facing. The stone facing does not take away from the frankness of

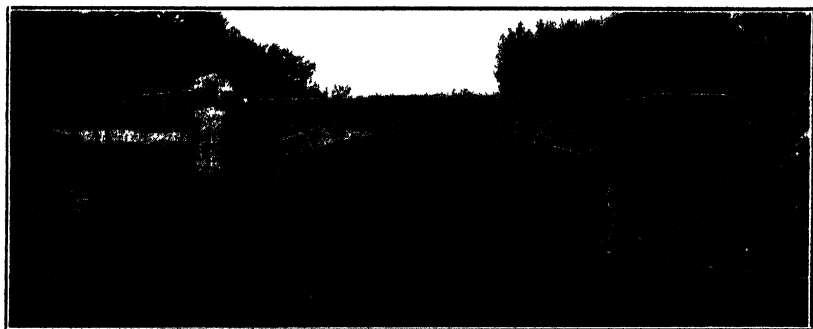


FIG. 4.—Boston Post Road Bridge over Cross County Parkway, Rye—Westchester County Park System

the design since the stone serves to protect the exposed faces of the bridge from the elements and at the same time aids in bringing the structure into closer harmony with its surroundings. This is more particularly true in a terrain where natural rock outcrops abound; in sections where there is no native rock, exposed concrete may be more economical and may be designed to be in keeping with the surroundings, for example, along the parts of the seashore where sand is the only natural building material.

Recently, we have listened to a controversy between the advocates of this demand for structural honesty in the case of the great new suspension bridge across the Hudson River between Manhattan Island, New York City, and New

Jersey, to date the longest single suspension span ever built. The tall structural steel piers stand as huge monuments to engineering genius. In their fabrication the architect had no concern but they are nevertheless impressive in their simple design reaching skyward to hold the suspension cables which reach across the waters of the Hudson River. The plans call for encasing these steel towers with stone, so that when the bridge is completed the cables will, in effect, be supported by immense piles of granite. The advocates of the naked steel piers are strong in denouncing the policy of the designers to cover up the steel with stone. On the other hand, the designers defend the adopted policy and state that the granite protects the steel and gives the piers a finer proportion. In a notable book on the general subject of bridges ("Bridges," by Charles S. Whitney) the author says, "A stone covering for steel or concrete may sometimes be proper to protect it from the elements or to provide a harmonious architectural treatment. Obviously, its use could be abused if stone work were constructed only as a sham serving no structural purpose. It is no more necessary for us to see the material inside of a bridge than it is to look through the bark of a tree." We cannot settle this difference of opinion here; the example has served to bring an important matter to the attention of all those interested in bridge design. Let us hope that the controversy will bring engineers and architects closer together rather than widening the gap between the two professions.

Beauty is only a relative attribute. A bridge may be beautiful to some, ugly to others. Again a bridge may be beautiful by night, ugly by day; this may be caused by overdone decoration, which is lost to view at night, leaving only the outline silhouetted against the sky; still another argument for simplicity in design. A simple structure graceful in outline, expressing at the same time unity in design, will usually be pleasing and therefore beautiful.

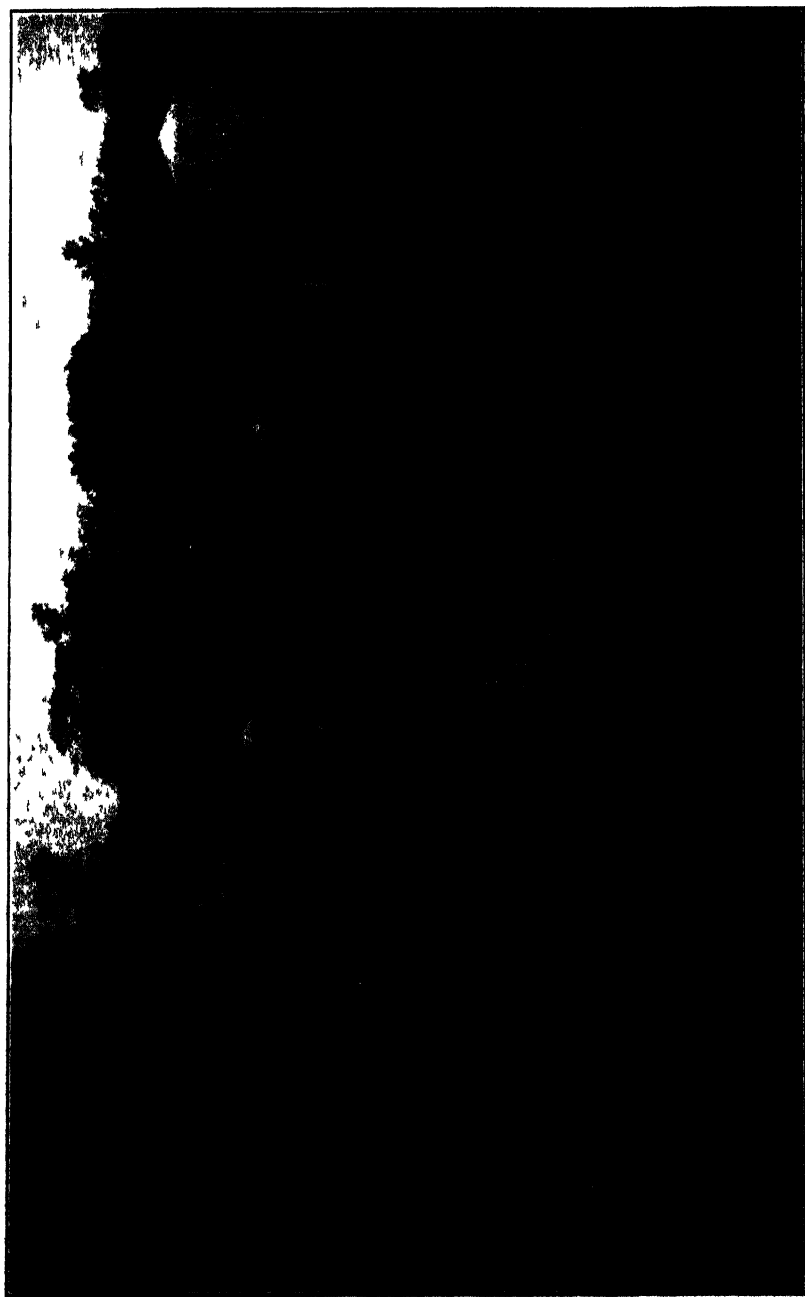


FIG. 5.—Park Avenue Bridge on the Bronx River Parkway.

Unity in design is a most important factor. In designing a particular bridge having five steel arch spans, with one of the end spans a single lift bascule, the architect felt that it was important to have the structure possess unity and to that end decided that it was necessary to plan the bascule differently than is customary. The bridge between Glen Island Park (Westchester County Park System, N. Y.) and the mainland, illustrated here, shows five similar steel arches, the highest and longest the bascule span, the others gradually decreasing in width and in height above the water as they approach the last span. The five spans of the bridge give the whole structure a feeling of unity since the similar arches carry a certain definite rhythm over the spanned space. Ordinarily, the bascule span would have been a flat girder, quite possibly curved at the hinged end; if thus planned the unity of the structure would have been lost.

A structure must be *suitable*, it must fit well into its surroundings. Bridges in the environment of cities may be formal in design with a refined use of materials and of course planned in harmony with the surrounding structures. Bridges in the country and in parks may take on a more rustic aspect and naturally there are degrees of this fashioned treatment. The more rugged the scenery and surroundings, the more rustic may the bridge be. It should never be so dominant a part of a picture that it does not leave one with the impression that it is a part of the earth it is built upon. A bridge, more than any other structure built by man, should harmonize with its surroundings and become a suitable part of a large composition. To bring a structure, no matter what it may be, (a house, a bridge, a church, or a monument) into a close relation with the surroundings, is as important as the design itself. The greatest works of architecture, the Parthenon, St. Peter's in Rome, the great cathedrals of Europe, are not in themselves alone, beautiful. These

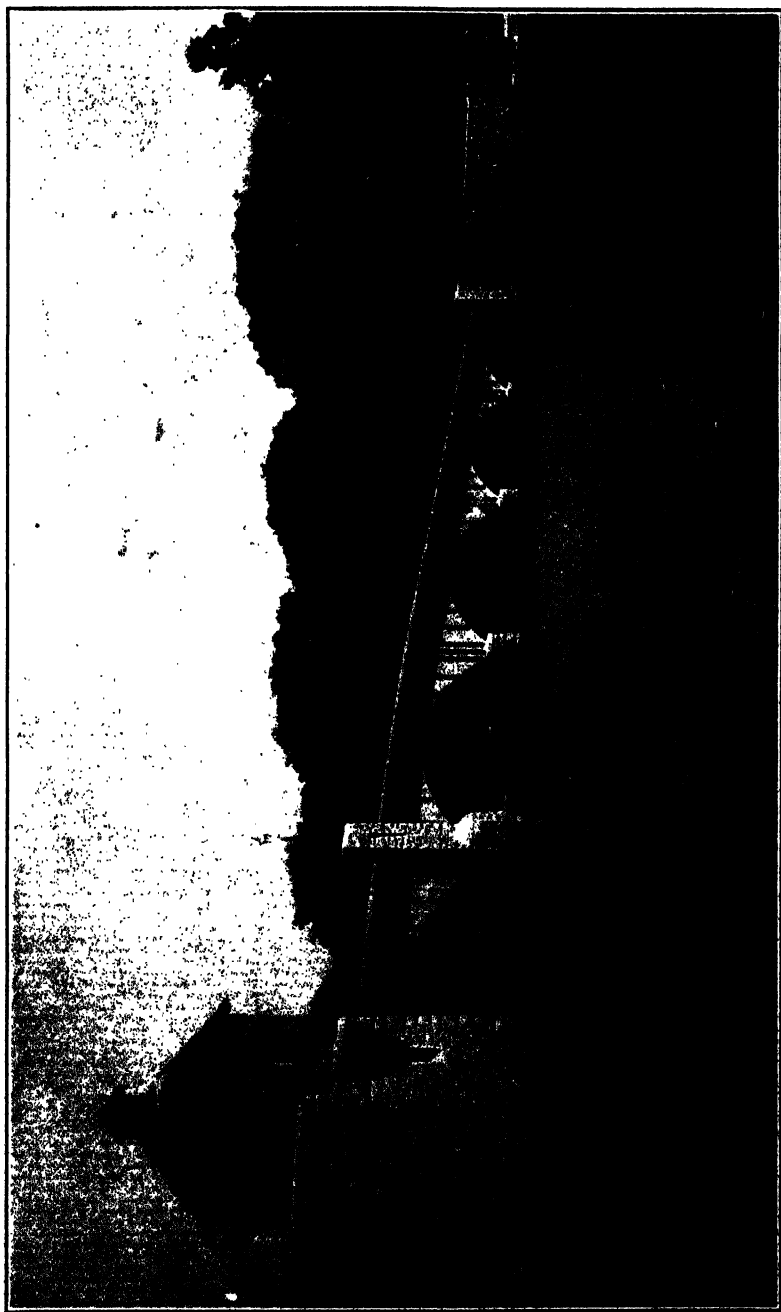


FIG. 6.—Glen Island Park Bridge—New Rochelle, N. Y.—Westchester County Park System
(Steel cantilever construction. The first span on the left is a single leaf bascule.) Waddell & Hardesty, Consulting Engineers for bascule span.

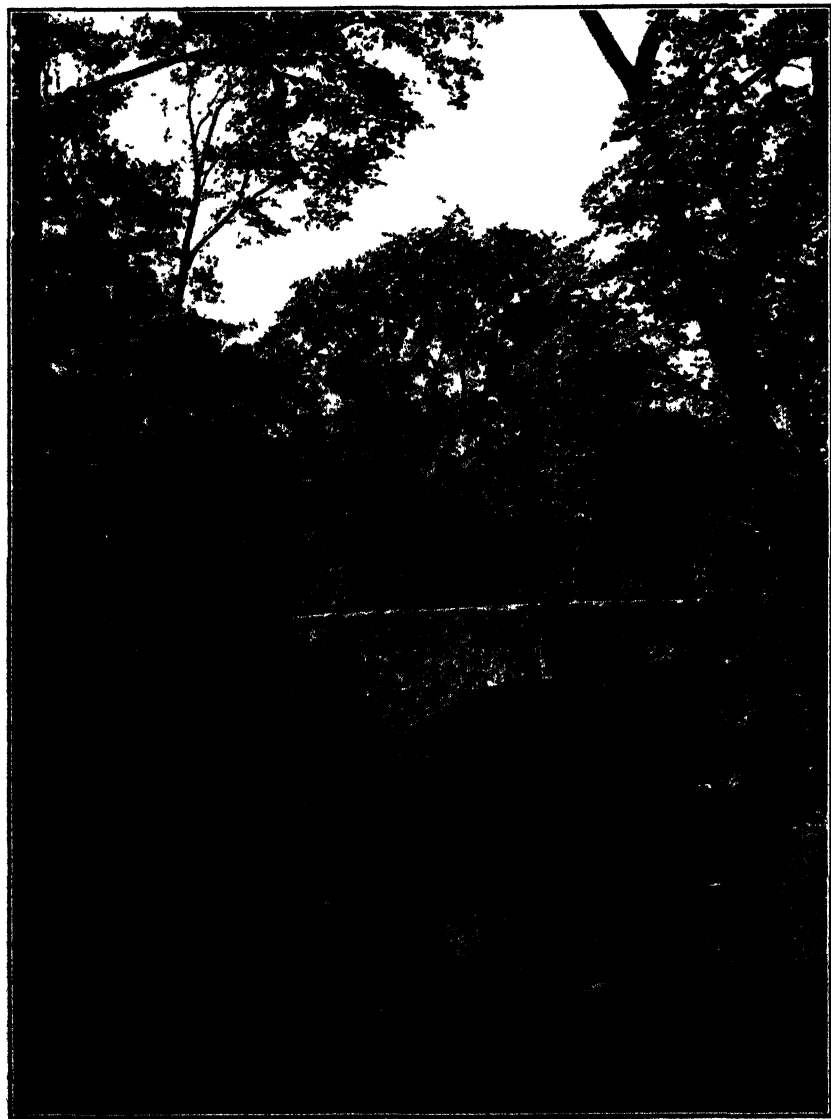


FIG. 7.—Bronx River Parkway Bridge—Westchester County Park System
C. W. Stoughton, Architect. (Concrete "T" beam construction with stone arches)

great monuments are parts of a landscape, part of larger artistic compositions from which they cannot be dissociated. To bring structures, and bridges more particularly, into close harmony and relation with their surroundings is, in the broader sense, the contribution which the artist makes to the field of design. It requires skill in the arrangement of architectural forms, and of the landscape as they relate to the big broad and unified compositions of nature and the works of man.

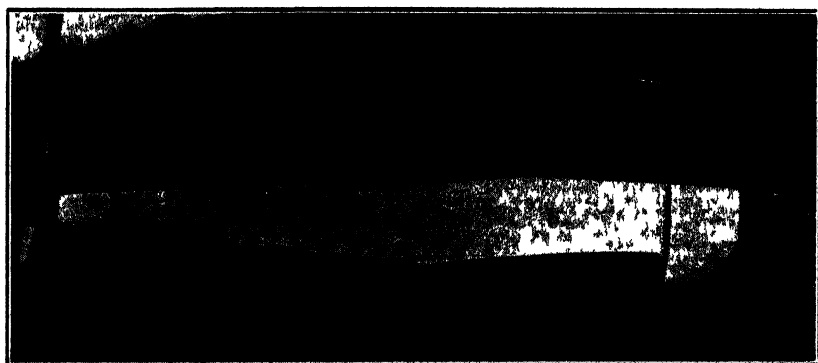


FIG 8—Highway Bridge, Constructed in 1929
(Compare with Fig 7, a "T" beam bridge of about same span)

The bridge has most simple requirements, but a single purpose, namely, to carry traffic. It should reflect those simple requirements in its design by being simple in plan and elevation, expressing conditions of the site as concerns the type of surroundings and the condition of the soil. It makes a difference whether the bridge is designed for mountain gorge or meadow stream, urban street or woodland road, rockbound shore or sandy beach. The problem for the designers is to find that one single structure, which will most admirably fit all the conditions of the site so that it satisfies the requirements of traffic, of waterway, of flood, and other conditions peculiar to each particular structure.

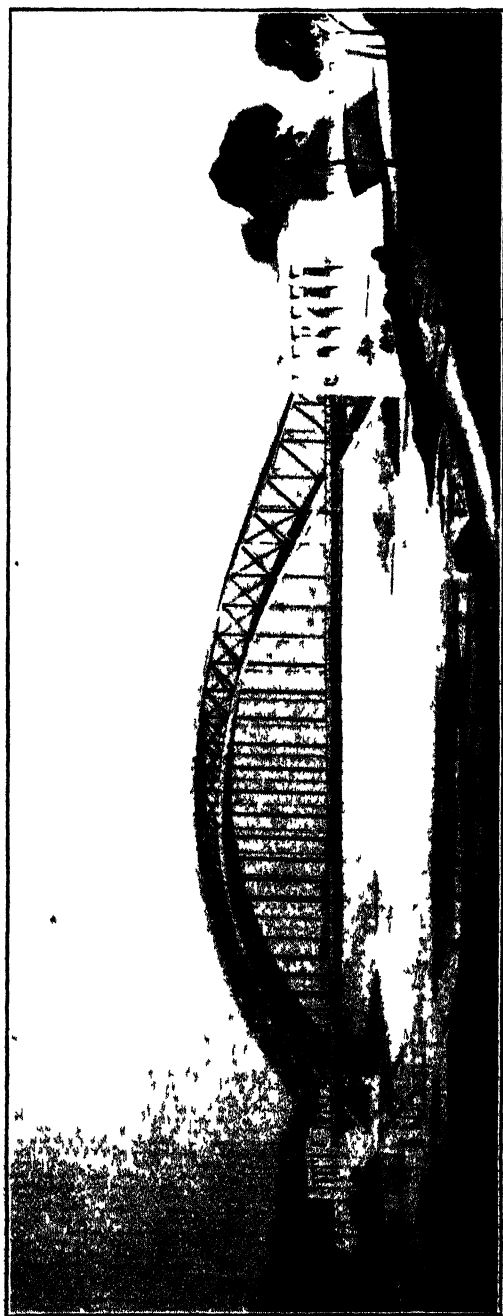
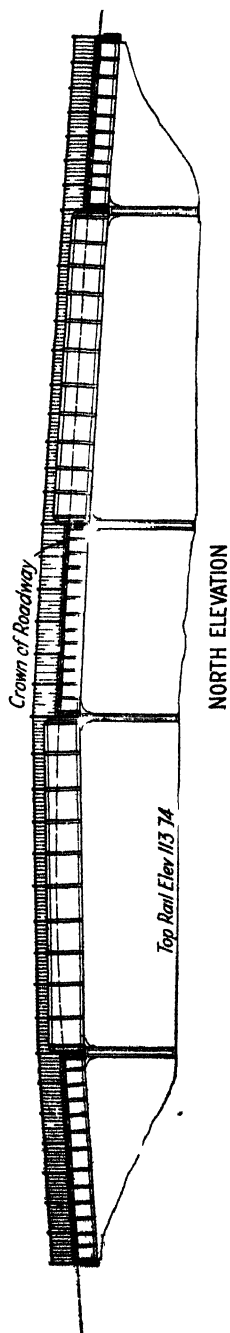


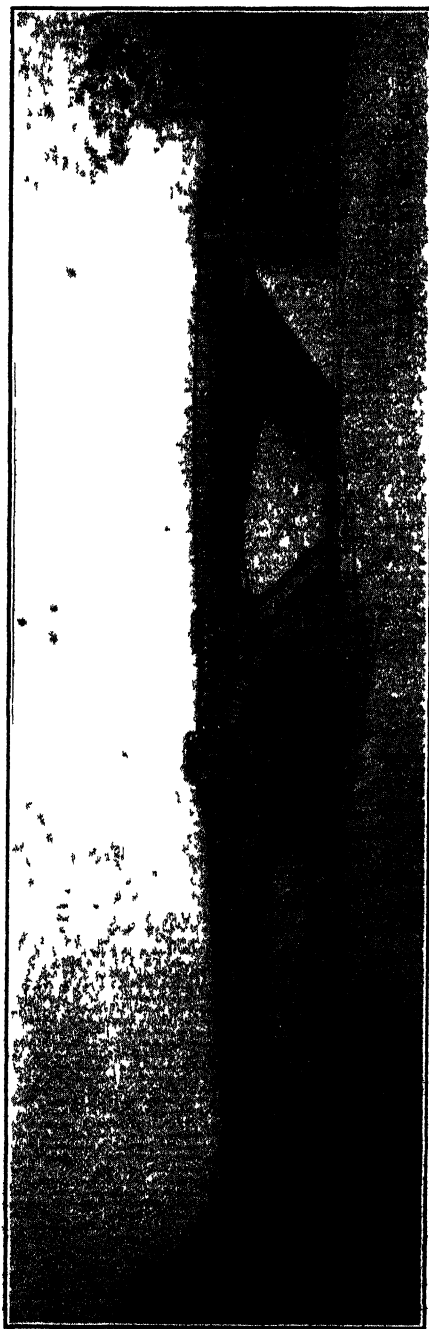
FIG. 9.—Bronx Parkway Extension Bridge over Croton Lake. (Span 750 Feet.) Westchester County Park System
C. F. Loyd, Architectural Designer
Office of Landscape Architect, W. C. P. S.
Howard C. Baird, Consulting Engineer
Jay Downer, Chief Engineer

The illustrations in this volume of bridges in which the engineer and architect collaborated from the beginning should prove the value of collaborative effort.

In closing this brief chapter, I want to pay tribute to Mr. Arthur G. Hayden, author of the other chapters in this volume, an engineer who has always fully appreciated the value of the architect in collaboration. To him must go the credit for the engineering design of nearly all of the bridges illustrated in this volume, some of rigid frame, some of other types of design. In each case the architect imposed restrictions or limitations and each time he has solved the particular special problem so as to retain the spirit of the original design as the architect intended. If this chapter merely serves to emphasize the importance of collaborative effort in this age of specialization, it will have served well.



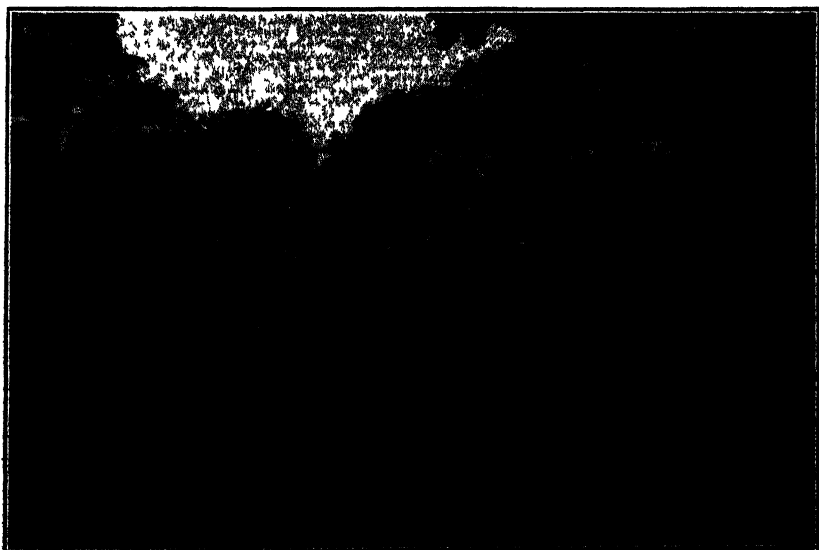
Bridge Proposed by Railroad Company for Odell Avenue, Yonkers, N. Y.



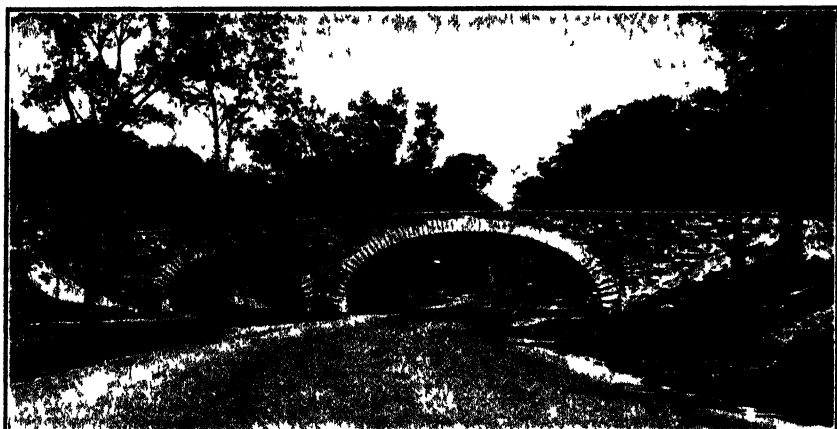
Odell Avenue Bridge, Yonkers, N. Y.—Saw Mill River Parkway—Westchester County Park System
Concrete rigid frame, stone faced, 62-foot arch, over parkway Steel rigid frame, 80-foot arch, over railroad



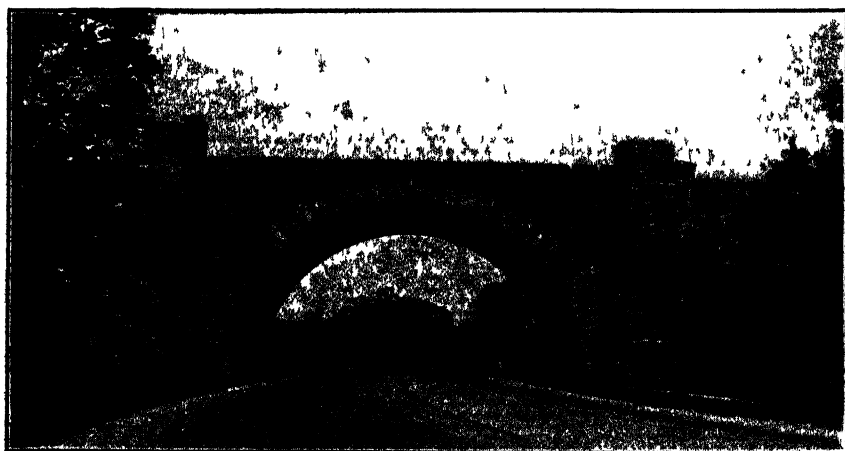
The Fenway—Boston Metropolitan Park System. Olmsted Bros., Landscape Architects



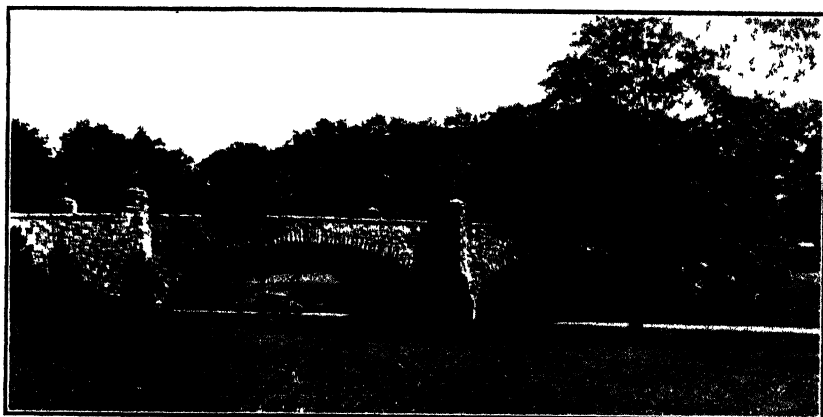
The Fenway—Boston Metropolitan Park System. Olmsted Bros., Landscape Architects



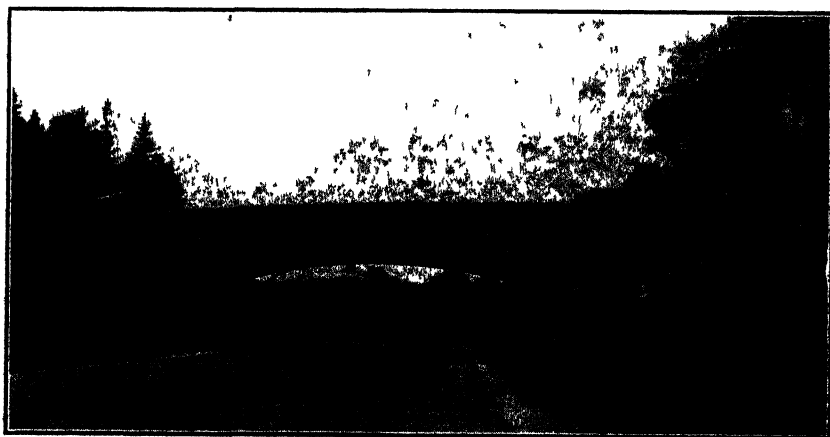
Mill Road Bridge, Hutchinson River Parkway—Westchester County Park System



Bridge Over Hutchinson River Parkway for N. Y., N. H. & H. Railroad
Westchester County Park System



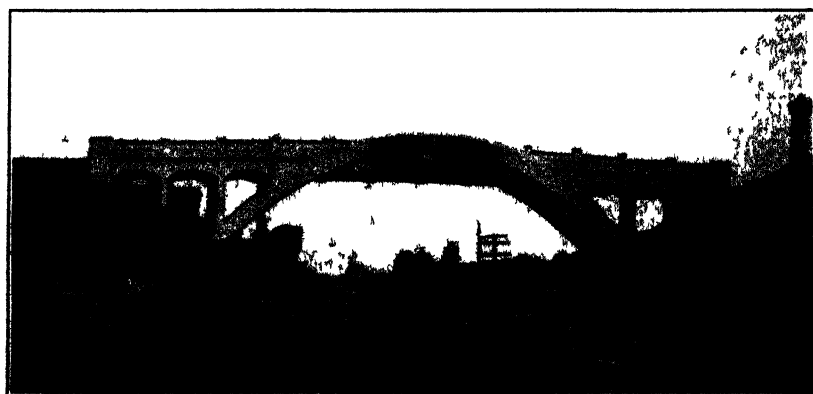
Colonial Heights Bridge—Bronx River Parkway—Westchester County Park System
Bowdin & Webster, Architects



Wilmot Road Bridge over Hutchinson River Parkway. (Rigid Frame)
Westchester County Park System



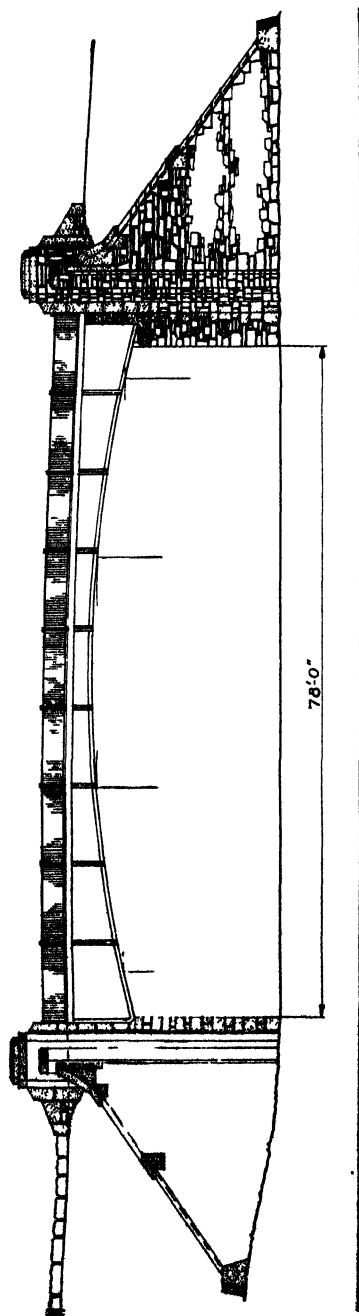
Railroad Bridge Constructed in 1929
(Compare with rigid frame bridge of similar span on page 265)



A Rigid-Frame Bridge Would Have Been More Economical
(Compare with rigid-frame bridge on page 265)

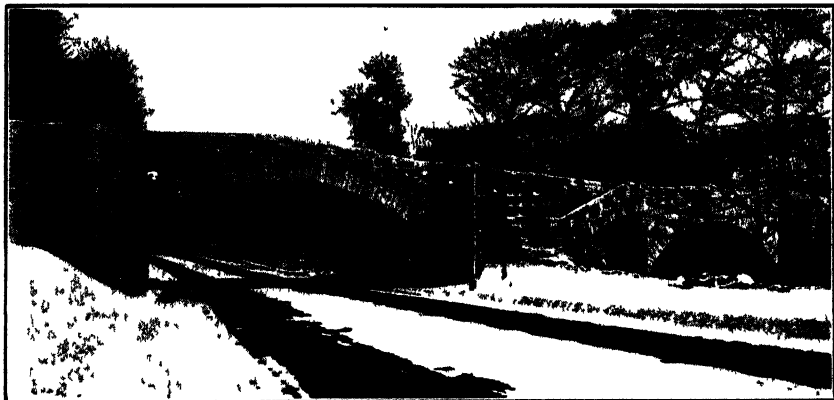


Bridge Carrying Bronx Parkway Extension over New York Central Railroad at Mt. Pleasant. A steel rigid-frame structure. Awarded First Prize by American Institute of Steel Construction as the best short-span steel bridge erected in the United States during year 1929

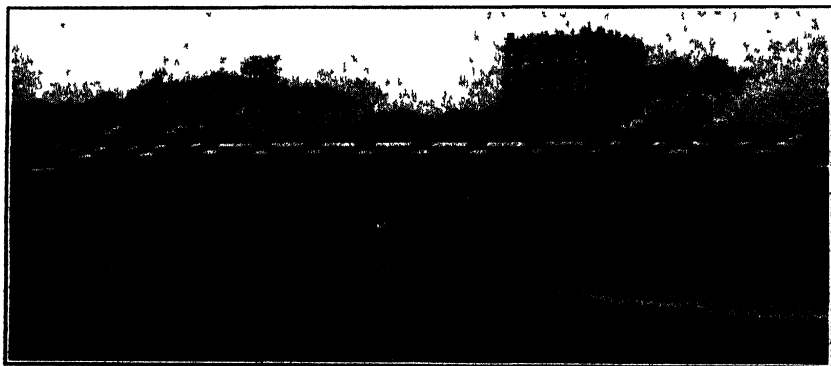


NORTH ELEVATION

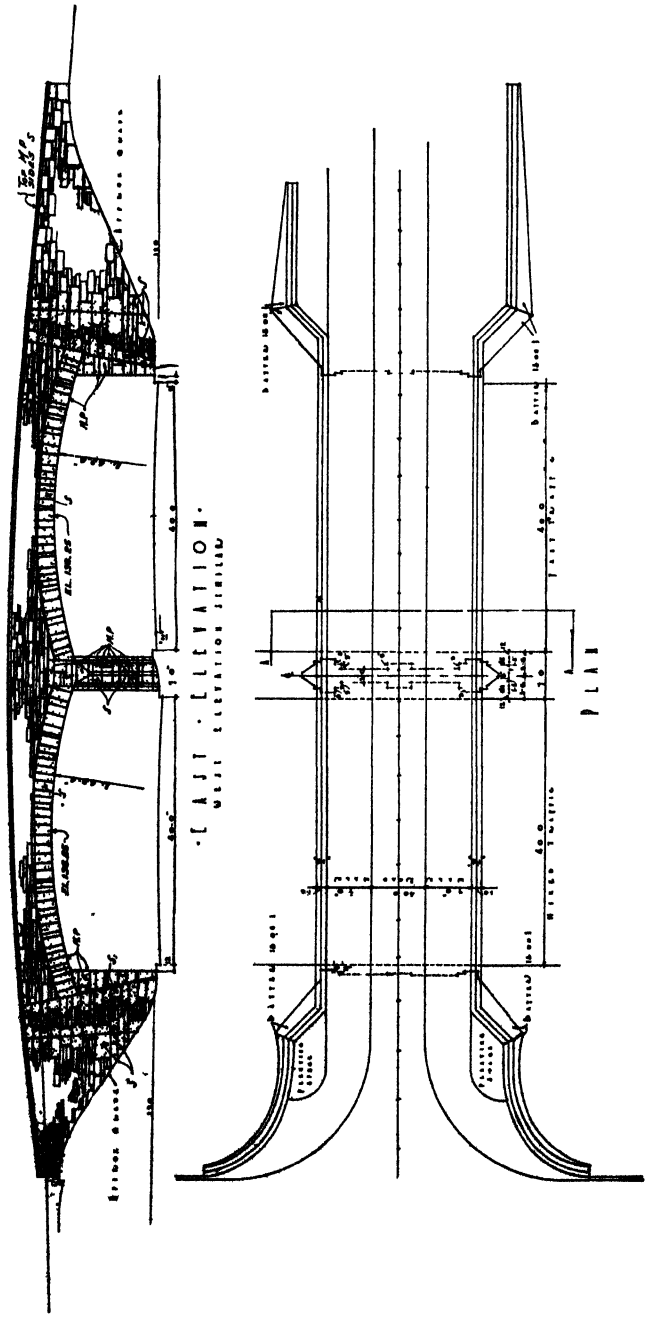
A grade separation structure, with highway passing over the railroad. Note economical design of wing walls. Design prepared for New York Central Railroad by Westchester County Park Commission.



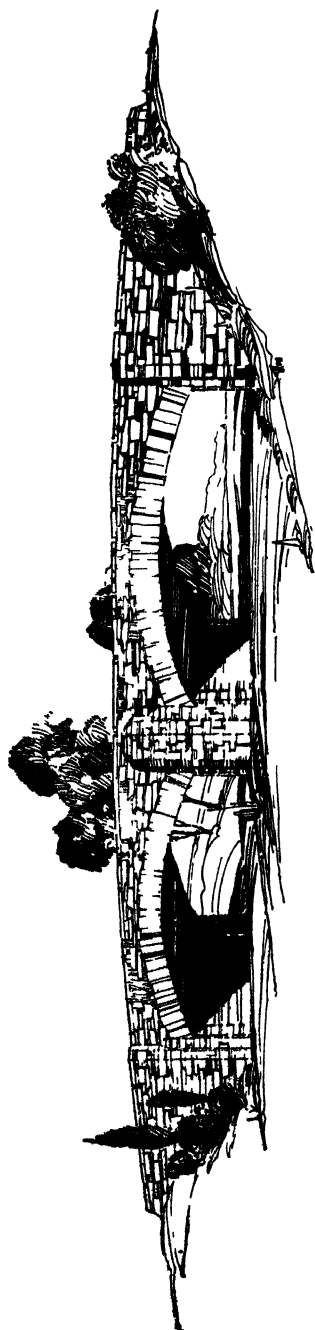
Bridge at Scarsdale—Bronx River Parkway—Westchester County Park System
C. W. Stoughton, Architect



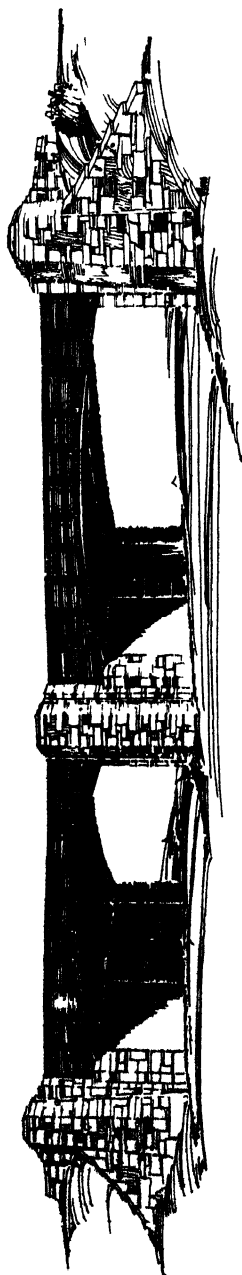
North Avenue Grade Separation, Lincoln Park, Chicago
(Concrete beam construction. Compare with rigid-frame designs on page 269)



Bridge on Cross County Parkway, Mt. Vernon, N. Y.—Westchester County Park System



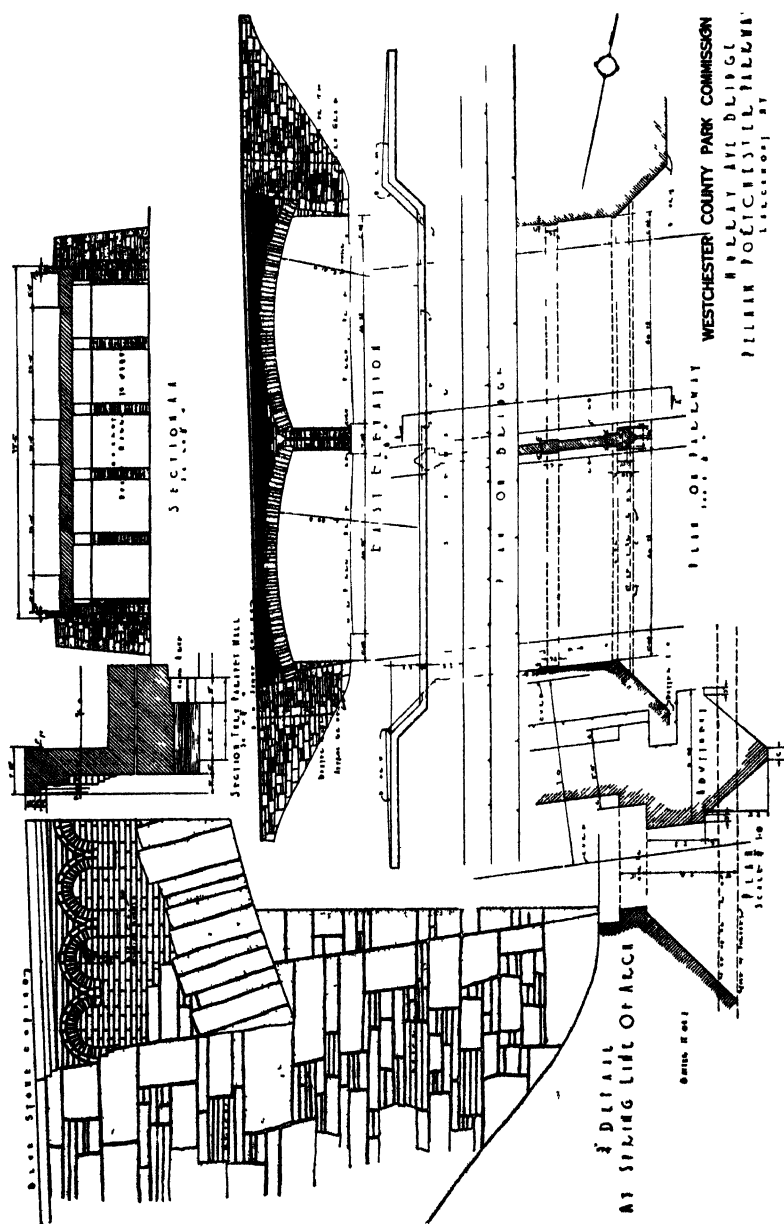
Fourteenth Street Bridge—Mt. Vernon Memorial Highway, Washington, D. C. (Rigid frame construction)
 Gilmore D. Clarke & Clinton F. Loyd, Architects. J. V. McNary, Designing Engineer, U. S. Bureau of Public Roads



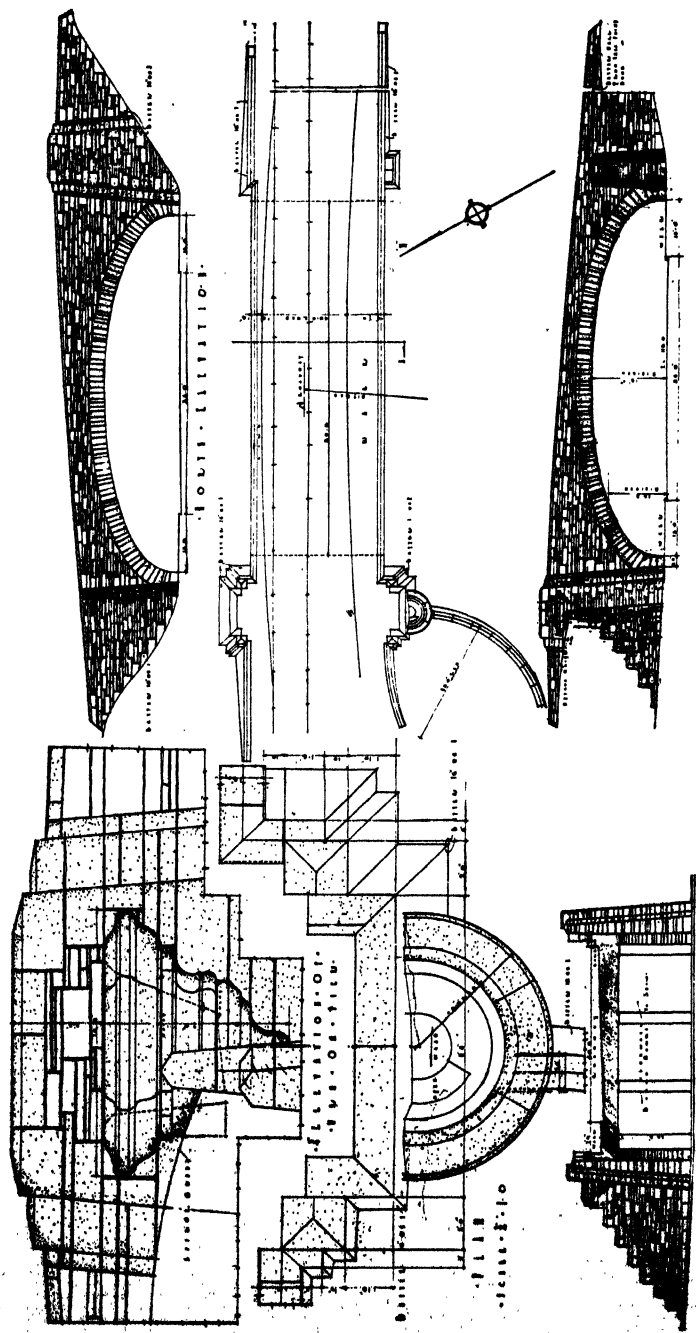
R. F. & P. Railroad Bridge—Mt. Vernon Memorial Highway, Washington, D. C. (Plate girder construction)
 Gilmore D. Clarke & Clinton F. Loyd, Architects. J. V. McNary, Designing Engineer, U. S. Bureau of Public Roads



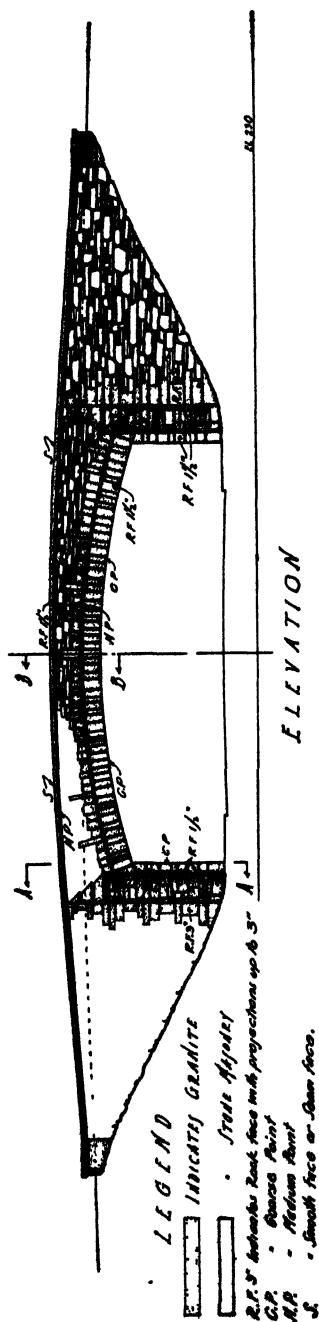
West Street Bridge—Hutchinson River Parkway—Westchester County Park System

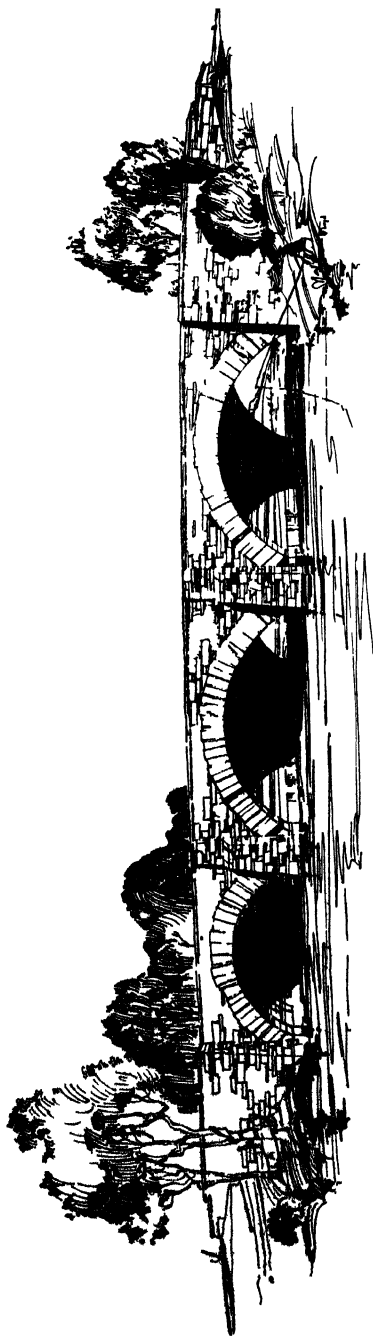


Double Arch Rigid Frame Bridge Constructed in 1929 on the Pelham-Portchester Parkway in Larchmont, N. Y.
Westchester County Park System



Bridge for the Cross County Parkway in Yonkers, N. Y.—Westchester County Park System.



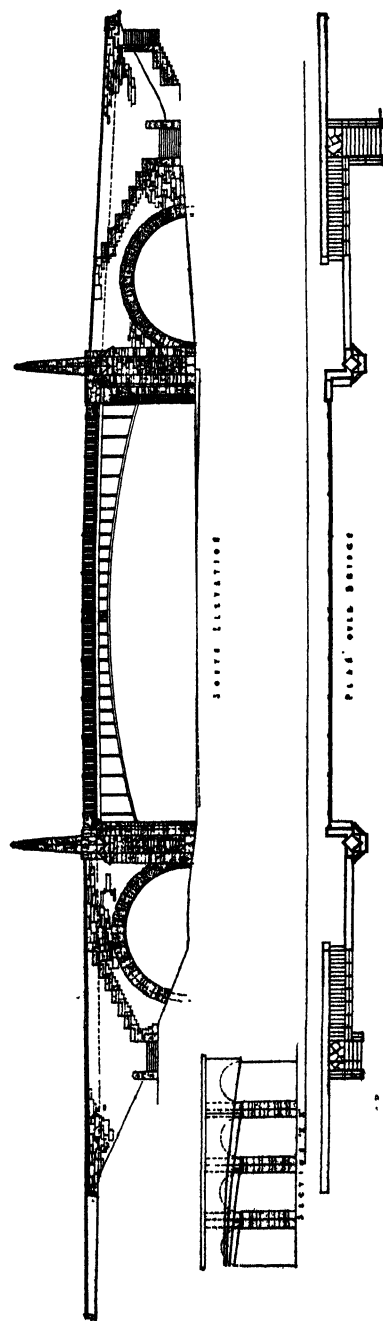


Hunting Creek Bridge—Mt. Vernon Memorial Highway, Washington, D. C. (Multiple span arch construction)
 Gilmore D. Clarke, & Clinton F. Loyd, Architects. J. V. McNary, Designing Engineer, U. S. Bureau of Public Roads



Wellington Underpass—Mt. Vernon Memorial Highway, Washington, D. C. (Rigid frame construction)
 Gilmore D. Clarke, & Clinton F. Loyd, Architects. J. V. McNary, Designing Engineer, U. S. Bureau of Public Roads

Cross County Parkway Bridge Over Central Park Avenue, Yonkers, N. Y.—Westchester County Park System



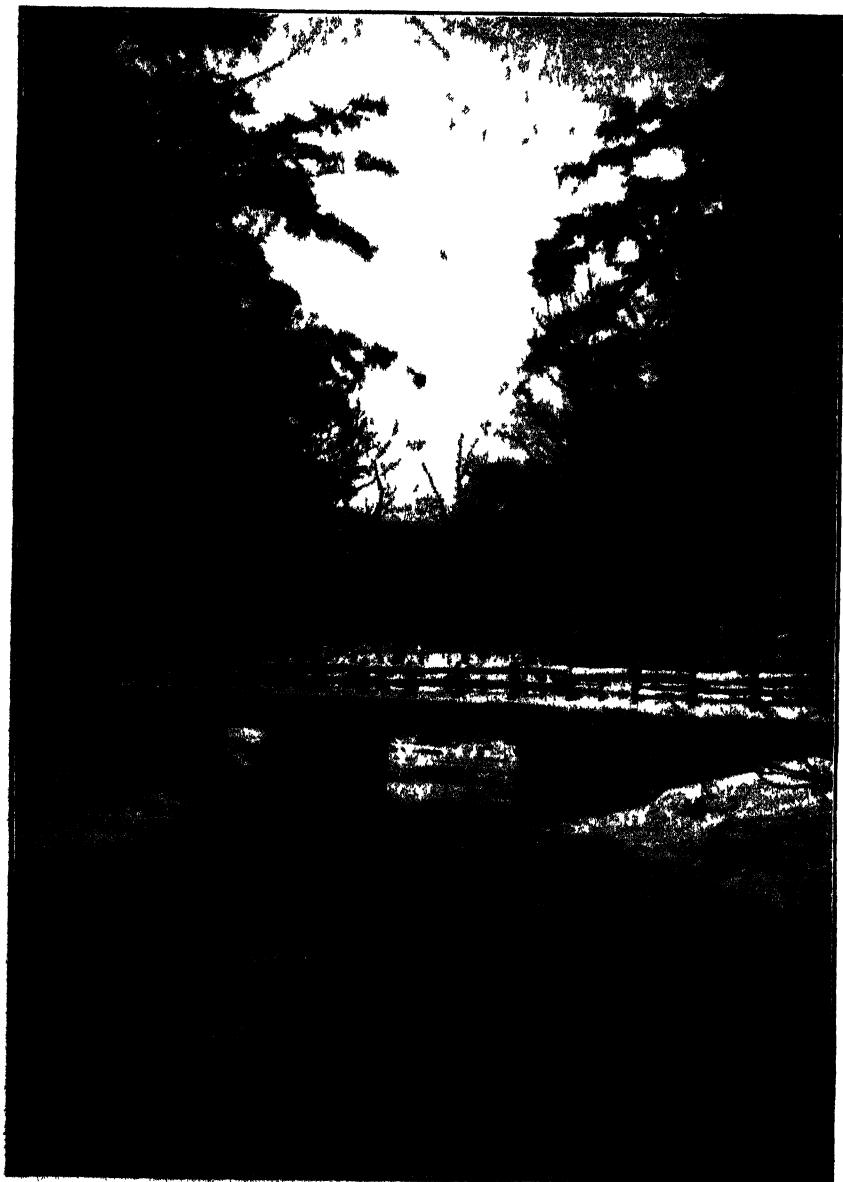
Central Park Avenue is a 100-foot street and it was necessary to provide 80 feet of pavement. Central span is 84 feet wide, steel rigid frame. The small end arches are for the sidewalks. The piers extending above the parapet walls terminate with lighting fixtures and are on but one side of the structure.



New Rochelle Road Bridge (Rigid Frame).—Hutchinson River Parkway—Westchester County Park System.



Woodland Place Viaduct, White Plains, N. Y.—Bronx River Parkway, Westchester County Park Commission.
Guy Vroman, Consulting Engineer. Palmer & Hornbostle, Consulting Architects



Garth Woods, Bronx River Parkway—Westchester County Park System

C. E. Wheeler, Architectural Designer

Double-span reinforced concrete "T" beam bridge. Abutments are faced with native stone. Concrete beam is faced with large timbers which have been adzed and treated with a wreathed gray stain.

APPENDIX

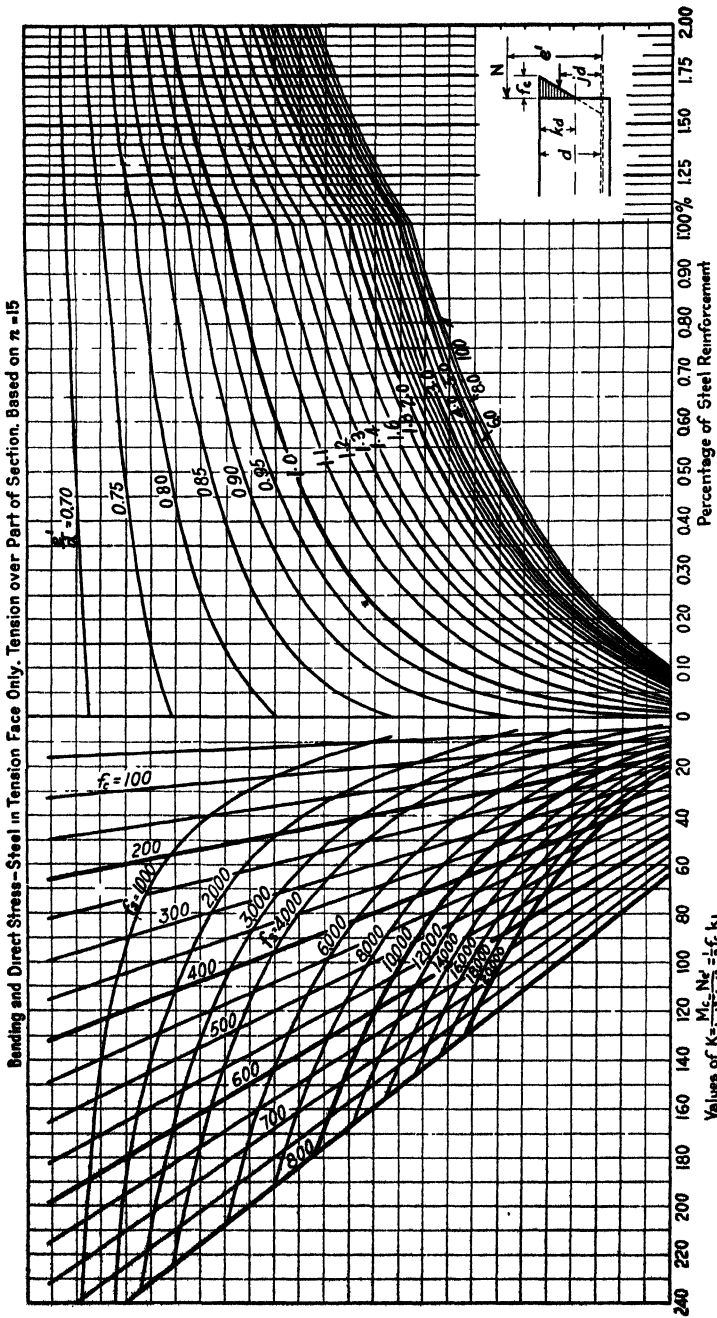
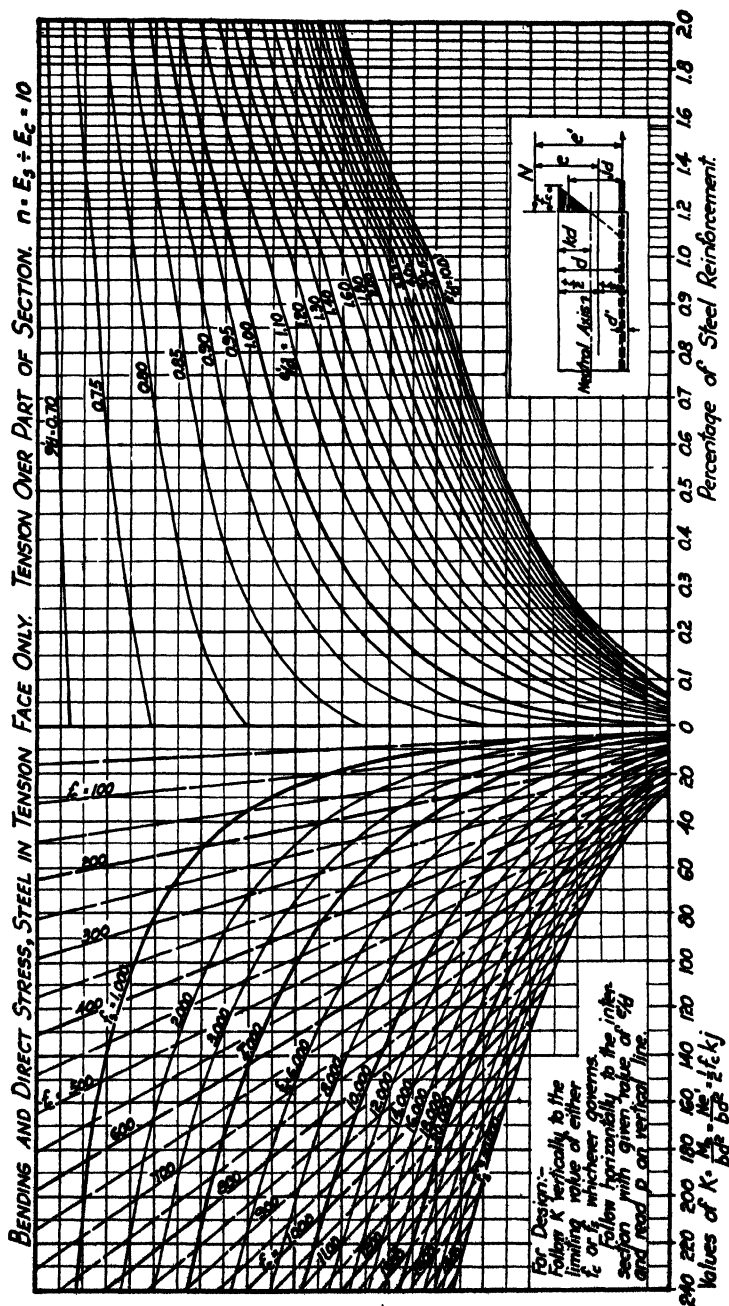


Fig. 87.



LIVE LOADS AND UNIT STRESSES

The live loadings now being used in the design of these bridges by the Westchester County (New York) Park Commission which first built them are as specified for steel highway bridges by the American Railway Engineering Association and the American Association of State Highway Officials.

Highway Concentrated Loads.—Motor trucks of various weights, all with 14 ft. wheel base and 6 ft. gage, eight-tenths of the total weight being on the rear axle and two-tenths on the front axle. Trucks in train are assumed to be a distance apart of 30 ft. from rear axle of preceding truck to front axle of following truck. Truck train loads consist of one heavier truck, the tonnage of which designates the load class, preceded and followed by any number of lighter trucks, each being three-quarters the weight of the heavier truck.

H 20 train load includes one 20-ton truck and any number of 15-ton trucks.

H 15 train load includes one 15-ton truck and any number of 11½-ton trucks.

H 10 train load includes one 10-ton truck and any number of 7½-ton trucks.

Traffic lanes are assumed 9 ft. wide and bridges having widths not in even multiples of 9 ft. are assumed to be loaded over their entire width with a load per foot of width equal to one-ninth of the load of one traffic lane. Trains of trucks over the width of the bridge are all assumed to be headed in the same direction. The wheel concentrations of these trains will have a lateral distribution and in the solid barrel arch-like type of structure under consideration it is assumed that the weight of each row of wheels across is uniformly distributed on a line over the width of bridge so that the load per foot of width will be one-ninth of an axle load. For example, each longitudinal strip one foot wide of a solid barrel arch is assumed to be loaded with a concentration of $\frac{32,000}{9}$ = say 3600 lb. from the rear axle of a 20-ton truck.

and $\frac{8000}{9}$ = say 900 lb. from the front axle. No longitudinal distribution of wheel loads is assumed.

Reduction of Traffic Intensity for Wide Bridges.—For bridges over 18 ft. wide, the above loads are reduced 1 per cent for each foot of width in excess of 18 ft. up to a maximum reduction of 25 per cent for bridges 43 ft. width and over.

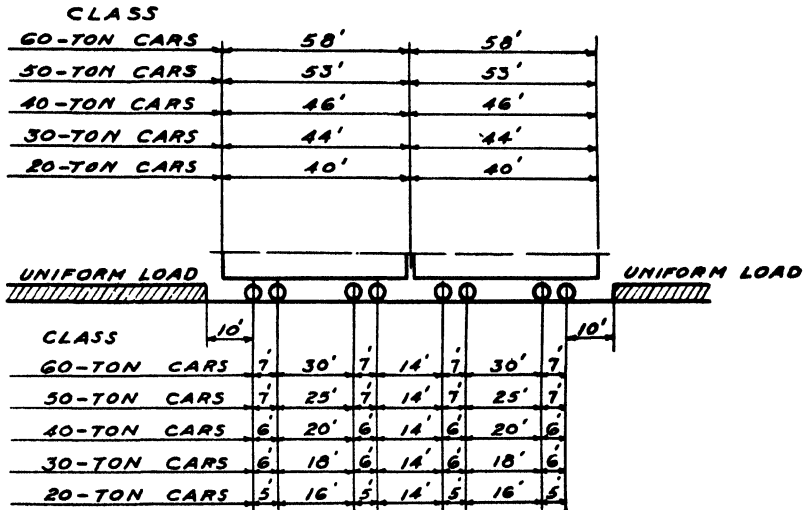


FIG. 88.

Equivalent Uniform Loading.—The following uniform loadings equivalent to the above concentrated loadings are specified by the A. R. E. A. and A. A. S. H. O. to be used for loaded lengths of 60 ft. or over. The figures given are for a uniform load per linear foot of traffic lane (9 ft. wide) and the concentrated excesses to be used in addition to the uniform load are to be considered as uniformly distributed on a line across the lane and are to be placed on the span so as to produce maximum stress at the point under consideration.

H 20 Unif. 640 lb. per lin. ft.	{	18,000 lb. for moment
Excess concentration		26,000 lb. for shear

H 15 Unif. 480 lb. per lin. ft.	{	13,500 lb. for moment
Excess concentration		19,500 lb. for shear

$$\begin{array}{l} \text{H 10 Unif. 320 lb. per lin. ft.} \\ \text{Excess concentration} \end{array} \left\{ \begin{array}{l} 9,000 \text{ lb. for moment} \\ 13,000 \text{ lb. for shear} \end{array} \right.$$

Correction for widths of roadway not in even multiples of 9 ft. and allowance for reduction of traffic intensity in the case of wide bridges are as for the concentrated train loads.

(Only the concentrated train loads will be used in this work since the influence line method is used throughout and there would not be the same saving of labor by the use of the equivalent uniform loading that there is in the stress calculation for truss members.)

Electric Railway Loadings.—The standard electric car loadings shown in Fig. 88 are recommended by the A. R. E. A. and A. A. S. H. O. unless otherwise specified by the interested electric railroad company. The loading consists of two cars on each track preceded and followed by a uniform load (without concentrated excess) corresponding to the class of highway loading specified in the preceding paragraph. Electric railway traffic lanes are assumed to be 10 ft. wide. Highway bridges carrying electric railway traffic should be designed for either of the following conditions whichever governs. (a) The highway loading of the appropriate class specified on any portion of the roadway including the electric car lanes. (b) The electric railway loadings on the car tracks and the highway loading on the remaining traffic lanes.

Sidewalk Loads.—Sidewalk loads, as recommended by the A. R. E. A. and A. A. S. H. O., for steel highway bridges, varying in intensity according to the width of sidewalk and the loaded length producing the maximum stress in the member under consideration, will not be used here. In the solid barrel type of structure treated in this book, it is more practical to carry the reinforcement calculated for the roadway section across the entire width of bridge including sidewalks, than to design the sidewalk sections separately. For the steel rigid-frame girder structure it is preferable, in designing the fascia girders, to use a flat load of say 80 lb. per square foot of sidewalk than to vary the intensity according to the critical loaded lengths of the various points.

Impact.—The specifications of the A. R. E. A. and A. A. S. H. O. for steel highway bridges provide for an allowance due to impact, vibration, etc., from the live loads, excepting the sidewalk loads. This

allowance is a fraction of the live load stress calculated as $I = \frac{50}{L + 150}$

in which L is the critical loaded length for the member under consideration. For the type of structure treated of in this book, varying the impact factor according to the critical loaded length of the point under consideration is an unnecessary refinement. L will therefore be defined,

here as the clear span of the structure and a single impact factor used for all points for which stress is calculated. For the sake of brevity, the live-load concentrations will be increased by the amount of impact allowance before applying them in design.

Allowance for Temperature Change.—Stresses induced in indeterminate reinforced-concrete structures by *seasonal* change in temperature are less in proportion than for steel structures, on account of gradual relief of temperature stresses due to the phenomenon known as “time yield” in the concrete. This fact accounts for the difference in temperature range specified for steel and for concrete structures.

Metal Structures:

Moderate climate, from 0° to $+120^{\circ}$ F.

Cold climate, from -30° to $+120^{\circ}$ F.

The rise and fall in temperature is to be figured from an assumed mean temperature.

Concrete Structures:	Temperature	Temperature
	Rise	Fall
Moderate climate.....	30° F.	40° F.
Cold climate.....	35° F.	45° F.

Unit Stresses for Concrete Structures.—The Joint Code is followed and allowable working stresses are given for a grade of concrete that will show a compressive strength of 2000 lb. per sq. in. in standard cylinder tests when the concrete is 28 days old. For other grades of concrete the allowable stresses would be in proportion to the indicated compressive strength.

Extreme fiber stress in compression (due to bend-

ing or combined bending and direct stress)....	800 lb. per sq. in.
Shear.....	60 lb. per sq. in.
Bond: for plain bars.....	80 lb. per sq. in.
for deformed bars.....	100 lb. per sq. in.
Tension in steel reinforcement.....	18,000 lb. per sq. in.

Standard specifications usually permit an increase of 25 per cent in unit stresses for arch ribs when temperature and rib-shortening effects are included, if such effects amount to more than 25 per cent of the total stresses without them.

NOTE.—Since publication of this book, the impact factor and allowance for temperature change, specified by the American Association of State Highway Officials, have been revised.

